CHARACTERIZATION OF CRUSHED PORTLAND CEMENT CONCRETE RUBBLE AGGREGATE FOR URBAN ROADS

A Thesis Submitted to the College of

Graduate Studies and Research

in Partial Fulfillment of the Requirements

for the Degree of Master of Science

in the Department of Civil and Geological Engineering

University of Saskatchewan

Saskatoon

By

Colin Michael Wandzura

PERMISSION TO USE

In presenting this thesis in partial fulfillment of the requirements for a Postgraduate degree from the University of Saskatchewan, the author has agreed that the Libraries of this University may make it freely available for inspection. The author has further agreed that permission for copying of this thesis in any manner, in whole or in part, for scholarly purposes may be granted by the professor or professors who supervised the thesis work or, in their absence, by the Head of the Department or the Dean of the College in which the thesis work was done. It is understood that any copying, publication, or use of this thesis or parts thereof for financial gain shall not be allowed without the author's written permission. It is also understood that due recognition shall be given to the author and to the University of Saskatchewan in any scholarly use which may be made of any material in this thesis.

Requests for permission to copy or to make other use of material in this thesis in whole or part should be addressed to:

Department of Civil & Geological Engineering

57 Campus Drive

University of Saskatchewan

Saskatoon, Saskatchewan, SK S7N 5A9

Canada

ABSTRACT

The City of Saskatoon is responsible for maintaining approximately 1,100 km of roads including locals, collectors, arterials, and freeways. With the aged state of the road infrastructure, increasing budget constraints limit the City's ability to maintain existing road infrastructure to an acceptable level of service and to construct new road infrastructure. The infrastructure demands related to urban growth within the City of Saskatoon have caused a shrinking aggregate supply and increasing aggregate demand. In turn, growing demand and dwindling resources for aggregate are resulting in rapid increases to road construction costs. Aggregate sources are a non-renewable resource in Saskatchewan. Therefore, road designers do not have an endless supply of quality aggregates. With limitations of the road building industry and the foreseeable economic growth projected for the City of Saskatoon, it is reasonable to expect that the unit costs of providing conventional pavement structures will continue to increase in Saskatoon.

Presently, the primary conventional road building materials include well graded granular base material, subbase, crushed rock and a wearing surface of either conventional hot mix asphalt concrete (HMAC) or Portland cement concrete (PCC). To ensure long term pavement performance, quality aggregate sources are needed in all road design structural layers. Recent years have seen an increased need for substructure drainage systems, therefore increasing the need for high quality crushed rock.

City of Saskatoon, like other urban centers, generates significant stock piles of concrete rubble annually. The primary objective of this research was to compare PCC material properties to those of conventional granular materials under realistic field state conditions. The second objective of this research was to validate the economic feasibility of using recycled PCC material within City of Saskatoon road structure through test section design and field test sections' structural performance.

Conventional and mechanistic material characterization was completed for recycled PCC well graded base course and recycled PCC drainage rock derived from PCC rubble, as well as conventional City granular base and drainage rock aggregates from typical City of Saskatoon stockpiles. Conventional testing completed on the samples included physical properties as required by COS aggregate specifications. Micro-Deval testing was also completed to compare

the mechanical breakdown of the aggregates tested. Based on the results of the conventional tests performed, the recycled PCC well graded base and the recycled PCC drainage rock were found to meet COS base and drainage rock specifications, respectively.

The recycled PCC well graded base material, recycled PCC drainage rock, COS granular base, and recycled PCC well graded base stabilized with different percentages of cement and slow setting type one (SS-1) asphalt emulsion were the research materials mechanistically tested. These materials were mechanistically tested using triaxial frequency sweep characterization to derive the mechanistic material constitutive relations across all the materials. Five repeat samples were gyratory compacted and tested at room temperature using the rapid triaxial testing. To characterize climatic durability, all the samples were moist cured for 28 days, characterized using the rapid triaxial test; then vacuum saturated and then characterized again using the rapid triaxial test. The mechanistic properties measured for the PCC material showed better climatic durability compared to those measured for the virgin aggregates, particularly after climatic durability testing.

Prior to vacuum saturation, the conventional COS granular base had a peak dynamic modulus of 457 MPa. Under the same testing conditions, recycled PCC well graded base unstabilized had a stiffness of 1081 MPa; the stabilized PCC samples with two percent cement had a dynamic modulus of 1542 MPa. The radial micro strain and Poisson's ratio were reduced for well graded PCC materials both unstabilized and stabilized compared to the conventional COS granular base. The conventional granular base had a peak radial micro strain of 194 compared to the untreated recycled PCC well graded base peak radial micro strain of 54 at the same testing parameters of low stress state at a testing frequency of 10 Hz prior to vacuum saturation. The conventional COS granular base samples failed under high deviatoric stress state at a 0.5 Hz testing frequency prior to vacuum saturation, whereas the PCC materials survived all testing frequencies and stress states. However, after vacuum saturation, the unstabilized recycled PCC well graded base samples failed under high stress state under a 10 Hz testing frequency.

To validate field structural performance, two road structures within the City of Saskatoon were used as test sections in which recycled PCC drainage rock was used as a structural drainage layer. The first test section was constructed in the east bound lane of Marquis Drive, and the second was completed at the University of Saskatchewan. Prior to construction of both the

Marquis Drive and North Road test sections, both sections were tested for peak surface deflections using the heavy weight deflectometer. Segment 1 of Marquis Drive had an average pre construction surface deflection of 1.85 mm under a primary weight limit. Section 1 of North Road had an average pre construction surface deflection of 1.17 mm under primary weight limit. After construction was complete on both test sections using recycled materials including a PCC drainage layer, HWD testing showed post construction peak deflections were significantly lower than the deflections measured pre construction.

Recycled PCC well graded base material performed well in mechanistic laboratory analysis. However, the material was not field tested in this research. Mechanistic laboratory and field analysis indicated that recycled PCC drainage rock aggregates met structural performance requirements.

The capital cost analysis showed that using recycled PCC drainage rock can reduce the overall cost of road rehabilitation projects when compared to using conventional virgin aggregates, particularly crushed drainage rock. The Marquis Drive section had a cost savings of $89,000, and the University of Saskatchewan section had a cost savings of $75,800 when recycled materials were used in lieu of virgin aggregates to rehabilitate the pavement structure. In addition, no PCC was disposed of in the landfill, saving the City of Saskatoon tipping fees and extending the life of the landfill.

This research showed that the crushed PCC rubble is both technically and economically feasible to use as high quality aggregates in City of Saskatoon streets. Based on the findings of this research, the City of Saskatoon should pursue the use of recycled PCC rubble aggregates in urban road construction.

ACKNOWLEDGEMENTS

During the preparation of this thesis, the author was fortunate to receive assistance from several dedicated engineers, professors, researchers, family members, and friends.

The City of Saskatoon's assistance funding the project and its willingness to recognize the value in using alternative aggregate sources in the construction of new rehabilitation of the existing road infrastructure is greatly appreciated. The successful completion of this research project would not have been possible without the continued guidance and encouragement received from the author's research supervisor, Dr. Curtis Berthelot. The author would also like to thank the advisory committee for their input: Dr. Kerry Mazeruk, Dr. Gordon Sparks, Dr. Amin Elshorbagy.

The achievement of a Master of Science degree is the author's largest and most challenging professional undertaking, requiring enormous supplies of patience and motivation. The author extends gratitude to his family and friends who, over the years, continued to grant patience, understanding, support and encouragement. The author especially thanks Diana and parents Lorne and Sharon for their love and support.

TABLE OF CONTENTS

LIST OF FIGURES

LIST OF TABLES

LIST OF ABBREVIATIONS

AASHTO- American Association of State Highway and Transport Officials

ACPA - American Concrete Pavement Association

ASTM - American Society for Testing and Materials

CBR - California bearing ratio

COS - City of Saskatoon

FHWA - Federal Highway Administration

GP - Poorly graded

GW - Well graded

HMAC - Hot mix asphalt concrete

HWD - Heavy weight deflectometer

L.A. - Los Angeles

NAPA - National Asphalt Pavement Association

NCHRP - National Cooperative Highway Research Program

NPV - Net present value

OG - Open graded

PCC - Portland cement concrete

RATT - Rapid triaxial test

RAP - Reclaimed asphalt pavement

RCA - Recycled concrete aggregate

SHRP - Strategic Highway Research Program

SMHI - Saskatchewan Ministry of Transportation and Infrastructure

SS-1 - Slow setting type 1 emulsion asphalt

USCS - United Soil Classification System

U.S. - United States

CHAPTER 1 INTRODUCTION

In recent decades, many Canadian urban centers have experienced steady and continual growth (Statistics Canada 2012). This growth has resulted in an increase of new infrastructure construction and the rehabilitation of existing road infrastructure within urban centers. Given this growth, aggregate supply needs in many Canadian cities have increased while the supply of quality aggregate has steadily decreased, particularly around urban centers located in the glaciated central plains region of North America (Berthelot et al. 2007, 2010A). Dwindling quality aggregate supply along with infrastructure expansion and renewal poses a significant problem for both provincial road agencies as well as municipal agencies across Canada (Berthelot et al. 2010B, 2010C).

The City of Saskatoon (COS) is responsible for maintaining approximately 1,100 km of roads, including local roads, collector roads, arterial roads, and freeways (COS 2009A). Budget constraints limit the City's ability to maintain existing aged road infrastructure and construct new road infrastructure. Urban growth within the Saskatoon area is a typical example of increasing aggregate demand in urban regions and shrinking aggregate supply (Berthelot et al. 2010B). A growing demand for aggregate has resulted in increasing road construction costs (Berthelot et al. 2007). Along with increased road construction costs, in service road infrastructure performance has reduced due to the increased truck traffic associated with increased construction and urban growth. This is particularly the case for thin paved local urban streets (Thomas et al. 2007, Thomas 2008).

As the City of Saskatoon expands, new neighbourhoods are being developed and constructed on all available land on the outskirts of the City limits. The location of these new neighbourhoods may have great appeal for housing developers, but the City of Saskatoon has been faced with many challenges when constructing roadway infrastructure due to poor subgrade conditions in many of the new neighbourhoods, such as Briarwood and Rosewood for example (Guenther 2010). During the development stage, the land is cleared and sloughs are filled with general fill. City of Saskatoon roads are comprised of subgrade preparation, subbase, granular base and a wearing surface of either conventional hot mix asphalt concrete (HMAC) or Portland cement concrete (PCC). Quality aggregate sources are needed in all design structural layers of

roads which raises concerns with regards to where additional aggregates will come from once Saskatchewan has exhausted quality aggregate pits (SMHI 2001-A).

Building roads on these marginal subgrades has led to the susceptibility of substructure moisture issues, causing failures in the road substructure due to weakening of subgrade (Guenther et al. 2010). Given the high fines found in typical City granular base materials, these granular bases tend to absorb water over time, further weakening the roads' structural integrity. Saskatchewan's freeze thaw cycles can further damage the road structure by causing subgrade fines to migrate into the base layer (Berthelot et al. 2002). The City of Saskatoon has addressed such concerns by installing drainage layers using crushed rock within some of its road structures.

As Saskatoon exhausts the natural aggregate pits within close proximity to the City limits, quality aggregates are being transported in excess of 100 kilometers away from the City of Saskatoon limits, from locations such as Wakaw, Dundurn, and Langham. These long haul distances result in higher costs and often lower quality aggregate (Berthelot et al. 2007).

Many urban centers, including the City of Saskatoon, generate significant volumes of Portland cement concrete (PCC) rubble resulting from infrastructure renewal (Berthelot et al. 2010A). Portland cement concrete rubble is generated from utility cuts and repairs, old driveway slabs, demolished buildings, and sidewalks, as seen in Figure 1.1. Traditionally, PCC rubble has been disposed of in landfills, stockpiled, or crushed for use as a low-quality backfill. Over the past five years, the City of Saskatoon generated approximately 100,000 tonnes of concrete rubble from public works projects alone (Guenther 2010). In the past, the City of Saskatoon has treated crushed PCC rubble aggregate as a low value fill material. Since the material has been considered low value fill, little effort has been put into sorting and processing the PCC rubble piles. The stockpiled concrete rubble material is highly contaminated with deleterious materials, resulting in low value product quality.

The concept of using recycled materials in road structures is not new and its use has been well documented by the National Asphalt Pavement Association (NAPA 2007). However, recycled materials commonly used in pavement design and rehabilitation focus on reclaimed hot mix asphalt concrete (HMAC), also known as reclaimed asphalt pavement (RAP). RAP is used in many jurisdictions in HMAC and cold mixes (Horvath 2003, Karlsson and Isacsson 2006).

There has been minimal research in the use of reclaimed PCC rubble as a structural granular layer in road construction or rehabilitation.

Figure 1.1 Typical Concrete Rubble Piles

In an effort to improve the end product value of stockpiled Portland cement concrete rubble materials, the City of Saskatoon piloted the use of impact crushing technology to accommodate larger pieces of concrete rubble, to remove reinforcing steel by magnetic extraction, and to generate PCC materials which met City base aggregate and crushed rock gradations.

The City of Saskatoon has limited experience with both recycled and reclaimed Portland cement concrete materials in many road applications because recycled materials have traditionally not been allowed as a building material in road construction (COS 2009B). There is a need to determine the technical and economic feasibility of reclaimed Portland cement concrete rubble as a structural layer in City of Saskatoon's pavement structures and field state conditions.

1.1 Importance of Research

Greater demands have been placed on transportation infrastructure renewal as well as improved sustainability of new road construction affiliated with urban expansion. It is important

to demonstrate that recycled Portland cement concrete aggregates are viable for City of Saskatoon road construction for the following reasons:

- Using crushed PCC materials would provide municipal agencies with an alternate solution to supply limitations and increasing costs associated with high quality conventional aggregates for the building and maintenance of existing road infrastructure.
- By reclaiming PCC rubble materials, the City of Saskatoon will reduce the amount of high value virgin aggregate required, thus reducing overall aggregate costs and truck traffic damage on existing infrastructure due to reduced aggregate haul.
- The City of Saskatoon's supply of PCC rubble will likely increase as the City experiences both growth and infrastructure renewal.
- Using PCC reused in a pavement structure will divert the material from the landfill.
- Recycling and reusing Portland cement concrete in road construction encourages sustainable infrastructure, which is a desirable aspect in a society that is focused on "green" initiatives (Transport Canada 2009).

1.2 Research Objectives

The goal of this research was to validate the use of crushed Portland cement concrete rubble in City of Saskatoon road structures. Sub-objectives of this research were:

- To compare PCC material properties to those of conventional granular materials under realistic field state conditions; and
- To validate the economic feasibility of using recycled PCC material within City of Saskatoon road structures through test section design and field test section structural performance.

1.3 Research Hypothesis

The hypothesis of this research was that crushed Portland cement concrete is technically feasible as a granular base course and drainage layer to be used in City of Saskatoon road structures.

1.4 Scope

This research considered City of Saskatoon open graded (OG) drainage PCC rock and well graded (GW) PCC rubble crushed from 2009 to 2010 stockpiled at the City of Saskatoon Nicolson Yard. Open graded drainage PCC rock was characterized for use as a drainage layer in reconstructed pavement structures. GW PCC aggregate was characterized for use as a base layer in reconstructed pavement structures.

Conventional laboratory testing was conducted according to COS granular base and crushed rock specifications (COS 2009B). Additional conventional laboratory testing included Micro-Deval and fine aggregate angularity testing.

GW PCC materials were chemically stabilized systems with different concentrations of Type 10 cement and a slow setting (SS-1) emulsion. Five (5) repeat samples or each stabilization system were tested.

Mechanistic laboratory characterization was performed using the rapid triaxial frequency sweep testing across four load frequencies and four stress states representative of the field state truck load spectra currently experienced by roads in Saskatoon.

City of Saskatoon field test sections were designed and constructed by the City of Saskatoon. A road model developed by PSI Technologies Inc. was used to model the strain response of the field test sections.

1.5 Methodology

The following project elements and tasks were employed in this research.

- Project Element 1: Background investigation and literature review
  - Task 1: Review literature pertaining to using recycled concrete as aggregate alternatives in base and drainage layers and general material property requirements from specifications, research reports, and journal articles.
  - Task 2: Review conventional material specifications for the City of Saskatoon. Review material specifications for jurisdictions that have used PCC as an aggregate alternative.

- Task 3: Review literature as to the processing and end product uses of recycled PCC rubble, including design, construction processes, and quality control and assurance.
- Task 4: Review literature pertaining to mechanistic laboratory tests related to base course material characterization.
- Task 5: Review literature pertaining to the measurement of deflections of road structures using heavy weight deflectometer in City of Saskatoon and other jurisdictions.
- Task 6: Review of continuum mechanistic road modeling principals.

- Project Element 2: PCC rubble processing review and material sampling
  - Task 1: Sample from COS Nicolson Yard PCC rubble pile and sample conventional COS granular base and crushed rock.
  - Task 2: Sample crushed PCC aggregates processed and stockpiled by the City of Saskatoon including the recycled PCC drainage rock and recycled PCC well graded base course.
- Project Element 3: Conventional physical laboratory characterization of PCC and conventional granular materials
  - Task 1: Classification of soils and soil-aggregate mixtures for highway construction purposes (ASTM D3282).
  - Task 2: Standard test methods for particle-size distribution of soils using sieve analysis (ASTM D6913).
  - Task 3: Uncompacted void content of fine aggregate (ASTM C1252).
  - Task 4: Organic content of the base aggregate (ASTM 2974).
  - Task 5: Determining the percentage of fractured particles in course aggregate (ASTM D5821).
  - Task 6: Laboratory compaction characteristics of soil using standard effort (600 kN-m/m^3) (ASTM D0698).

- Task 7: California Bearing Ratio of in place soils (ASTM D1883).
- Task 8: Standard test method for resistance of fine aggregate degradation by abrasion in the Micro-Deval apparatus (ASTM D7428).

- Project Element 4: Mechanistic characterization of PCC materials and conventional granular materials
  - Task 1: Stabilization analysis of five repeat samples of unstabilized conventional granular base, recycled PCC drainage rock and recycled PCC well graded base aggregate unstabilized and stabilized with: two percent cement, two percent SS-1 emulsion, one percent cement with one percent SS-1 emulsion, three percent cement, three percent SS-1 emulsion, and 1.5 percent cement with 1.5 percent SS-1 emulsion.
  - Task 2: Compact five repeat samples using gyratory compaction SHRP Level 1 criteria (AASHTO TP4). Moist-cure for 28 days.
  - Task 3: Pre-climatic conditioning, triaxial frequency sweep mechanical characterization on gyratory compacted well graded PCC samples at test temperatures of 20°C; frequency range of 0.5 Hz to 10 Hz; and deviatoric stress states representative of field state load conditions.
  - Task 4: Determine climatic durability of repeat well graded PCC samples using vacuum saturation testing.
  - Task 5: Post climatic conditioning, triaxial frequency sweep mechanical characterization of gyratory compacted, vacuum saturated well graded PCC samples at test temperatures of 20°C; frequency range of 0.5 Hz to 10 Hz; and deviatoric stress states representative of field state load conditions.
  - Task 6: Evaluate and compare material constitutive properties including dynamic modulus, Poisson's ratio, phase angle, and radial micro-strain for each PCC sample and stabilization system; include graphical analysis.
  - Task 7: Compare recycled PCC well graded base and PCC drainage rock to conventional City of Saskatoon granular base properties.

- Project Element 5: Field test section construction quality assurance and structural asset management
    - Task 1: Summarize constructed field test sections using recycled PCC drainage rock inside drainage layers, or as a structural layer within a pavement structure under COS field state conditions.
    - Task 2: Summarize quality control results from the field test sections.
    - Task 3: Measure the primary surface deflection response of the road structure using heavy weight deflectometer.
    - Task 4: Compare structural primary responses to predict primary responses using PSIPave3D^{TM} and the heavy weight deflectometer.
- Project Element 6: Economic evaluation and overall benefits of PCC aggregates
    - Task 1: Quantify the capital cost benefits of using PCC in City of Saskatoon field state conditions by comparing the construction costs of using PCC recycled aggregate versus conventional materials.
    - Task 2: Discuss the social benefits of using PCC aggregates in City of Saskatoon field state conditions.
    - Task 3: Discuss the environmental benefits of using PCC in City of Saskatoon field state conditions by evaluating the reduction in transportation needed to transport the PCC recycled aggregate material versus the conventional materials and also the landfill disposal cost savings.
- Project Element 7: Summary, conclusions and future research.

1.6 Layout of Thesis

Chapter One provides the introduction and the significance of the work performed in this research including the research goal, objectives, scope, and methodology pertaining to this work, along with the layout of the thesis. Chapter Two will summarize the literature review conducted pertaining to the thesis topic, along with background information. Chapter Three will summarize the process of the PCC rubble, and the conventional laboratory characterization methods used by road agencies to characterize the research materials. Chapter Four summarizes the conventional

laboratory characterization results of the crushed Portland cement concrete aggregates as well as conventional granular materials. Chapter Five will report the mechanistic laboratory characterization results from the mechanistic triaxial frequency sweep characterization of the PCC derived aggregates as well as granular materials. Chapter Six reports the field construction, end product heavy weight deflection, and PSIPave3D™ modeling results. Chapter Seven summarizes the economic benefits of using PCC in the City of Saskatoon field state conditions. Chapter Eight presents the summary, conclusions and future recommendations based on the results of this research.

CHAPTER 2 BACKGROUND AND LITERATURE REVIEW

This chapter provides background information pertaining to the use of Portland cement concrete (PCC) as an aggregate alternative for road construction. The history of recycling PCC and how the use of PCC as an aggregate for roads has evolved over the past several years will be presented. Currently the City of Saskatoon aggregate specifications for base aggregate and drainage rock will be reviewed. A comparison of physical properties of PCC and virgin aggregates used as structural layers within a pavement structure is presented. The physical properties of PCC and virgin aggregates sources using typical conventional testing methods will be discussed. Background information pertaining to mechanistic material characterization will also be discussed in the content of applied mechanistic road design.

2.1 Recycling Portland Cement Concrete Background and History

Portland cement concrete (PCC) is a composite building material composed of aggregate, water, and cement (Cement Association of Canada 2003). PCC is used in a variety of infrastructure structural applications including buildings, roads, overpasses, sidewalks, medians, driveways, houses, dams, and bridges, for example. The lifespan of a structure constructed with PCC depends on its use and application. For example, PCC interstate highways in the United States are estimated to have a lifespan of 50 years whereas buildings constructed with PCC over 100 years ago are still standing (Weiland et al. 2010). At the end of any PCC building's or road's lifespan, the question of what to do with the PCC rubble generated in the demolishment arises.

Recycling Portland cement concrete rubble on a large industrial scale was first performed and well documented after the Second World War in Britain and Germany (Nixon 1976). Rubble material was retrieved from city buildings that were destroyed by aerial bombing as well the demolition of war fortifications, and was processed and used in fill and new concrete applications (Nixon 1976). The use of recycled PCC as an aggregate alternative garnered very little research interest until 30 years later when it was realized that the amount of virgin aggregate would become limited (Nixon 1978). Since then, research efforts in several countries have demonstrated sufficient success in the development and use of construction waste such as PCC as an aggregate alternative.

In 1985, within the European Economic Communities, it was estimated that 50 million tonnes of PCC materials were generated each year (Hansen 1985). The United States and Japan generated 60 million tonnes of concrete rubble per year. At this point in time, much of the PCC material was treated as waste; only 10 to 12 million tonnes of the demolished concrete was recycled and reused as unstabilized base or subbase in highway construction (Hansen 1985).

In 2000, it was estimated that the United States recycled 150 million tonnes of PCC material annually (Rathje et al. 2006). The United States established incentives for waste concrete processing sites to promote the use of recycled aggregate. Most of the recycled concrete is used as fill material (FHWA 2008). Within the United States, the three main processors of concrete rubble include natural aggregate producers, contractors, and recycling centers. Of all the concrete rubble recycled in a total of 41 states, 50 percent of the processing was conducted by the natural aggregate producers, followed by 36 percent by contractors and 14 percent by recycling centers (FHWA 2008).

Japan has researched concrete recycling for 25 (Hansen 1992). In 1990, approximately 48 percent of Japan's concrete debris was processed and recycled. However, by the year 2000, the percentage of recycled concrete increased to 96 percent, due to the implementation of a recycling program for concrete waste in 1992, followed by the implementation of "quality specifications for reusing materials from demolished concrete for construction works" (Hansen 1992).

According to the Federal Highway Administration (FHWA) (2007), the United Kingdom consumed approximately 330 million tonnes of aggregates for PCC construction activities in 1989, of which only 10 percent was recycled concrete. However, since then, England alone in 2001 consumed 200 million tonnes of aggregate, of which 25 percent of the material used was recycled PCC materials (FHWA 2007). Both England and Scotland make up for two thirds of recycled aggregates processed out of concrete demolition materials in the United Kingdom.

Canada has been recycling concrete for approximately thirty years; the primary use for recycled PCC in Canada is as a subbase material for road construction (Cement Association 2003). Sorenson (2010) commented that compared to the rest of the world, Canada does very little concrete recycling. In Canada, 11 million tonnes of construction waste is generated every year (Cement Association 2003). As seen in Figure 2.1, the majority of the construction waste is

non-recyclable waste that is most likely landfilled. A smaller portion of construction waste, 21 percent or 2.31 million tonnes, is concrete rubble that can be recycled – however, it is not all recycled and reused; the amount of concrete that is actually reused is considered insignificant (Cement Association 2003).

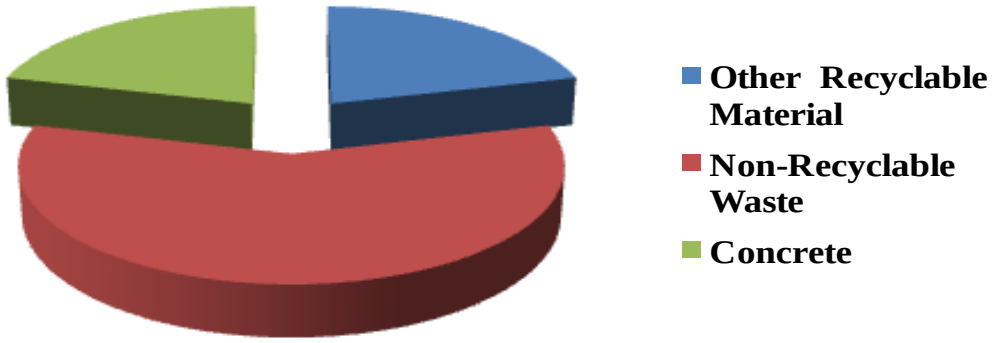

Figure 2.1 Construction Waste Generated in Canada (reproduced from Cement Association 2003)

Provinces within Canada have been recycling PCC in a variety of ways. A company in British Columbia is now using recycled PCC to build paving stones (Sorensen 2010). The cities of Saskatoon and Regina located within Saskatchewan have been using recycled PCC as fill material. The City of Regina recycles concrete at its landfill and allows local contractors to purchase processed and crushed PCC aggregate to reduce the costs of recycling the rubble. The cities of Saskatoon, SK and Camrose (in Alberta) have a fee-based disposal area in their landfills. The fees collected recover the costs associated with the operation, maintenance and overhead of the disposal site similar to the City of Regina; however, the material is solely used for city public works projects (City of Camrose 2011). The City of Edmonton, Alberta has been using recycled, crushed PCC as a fill and subbase material for years.

Out of all the provinces and territories, Ontario, followed by Quebec, Alberta and Saskatchewan, recycled the most tonnes of concrete per province in 2005. Ontario recycled a total of 434,000 tonnes of concrete, and Quebec recycled 190,000 tonnes (Holcim 2010). The primary use of the concrete out of all the provinces was as a low quality backfill material.

Portland cement concrete rubble is typically generated through the demolition of Portland cement concrete elements and is then crushed to a gradation appropriate for the intended use of

the recycled concrete material. In road construction, the most common use of recycled PCC is as a fill or subbase material. Recycled PCC has also been used in some jurisdictions as a base material, as an aggregate for concrete cement road surfaces, and as an aggregate for hot mix asphalt concrete surfaces.

2.2 Crushing Portland Cement Concrete Rubble

Figure 2.2 illustrates a PCC rubble stockpile. The PCC stockpile pictured here shows various sized rubble material retrieved from demolished roads, buildings, and sidewalks, for example. PCC stockpiles are typically contaminated with reinforcing steel, soil, fines material, granular base, bituminous asphalt concrete, and debris.

PCC materials are hauled to a processing plant or stockpile location where rubble stockpiles can be sorted, processed, and prepared for crushing. At the central processing plant, reclaimed PCC is typically subjected to primary and secondary jaw and cone crushers. Concrete rubble is first fed into a primary crusher that breaks the reinforcing steel from the concrete debris and crushes the rubble into a particle size. Removal of reinforcing steel is accomplished by an electromagnetic separator while the material is being transferred to the secondary crusher. The secondary crusher further breaks down the particle sizes to the desired gradation.

Impact crushers offer many advantages when it comes to crushing both virgin and recycled materials. With the introduction of impact type crushers in 1984, mobile processing plants have been able to reduce the two jaw and cone crushers' setup into one single impact crusher, therefore reducing the size of the plants, allowing onsite recycling, reducing emissions, and also increasing efficiency (Hansen 1985, Rathje et al. 2006). By processing recycled PCC rubble through an impact crusher, the aggregate being produced can be tailored to different grain size distributions, producing multiple materials at once. Furthermore, an impact crusher has the ability to generate increased fracture faces on individual aggregate particles. Screening the crushed material reduces fines content and improves crushed materials' gradation.

Figure 2.2 Typical Contaminated Concrete Rubble

Figure 2.3 Visual Angularity Comparison between Typical Base Course Aggregate (Left), and Well Graded PCC Material (Right)

Figure 2.3 compares the angularity achieved from a virgin base course aggregate and a crushed PCC material. The virgin base course aggregate was crushed using a conventional jaw and cone crusher. The PCC base aggregate was crushed using an impact crusher. The PCC aggregate crushed with the impact crusher has particles with more fractured faces than the virgin

base material's particles. This improves compaction and aggregate interlock of PCC for the use in road construction.

2.3 Uses of Recycled Portland Cement Concrete in Road Construction

In road construction, the most common use of recycled PCC is as a fill or subbase material. Figure 2.4 illustrates the end-uses of recycled, crushed PCC in the United States (U.S) (Kelly 1998, Rao et al. 2006). The breakdown of Figure 2.4 primarily focuses on the construction aggregate needed in road construction and rehabilitation (Kelly 1998).

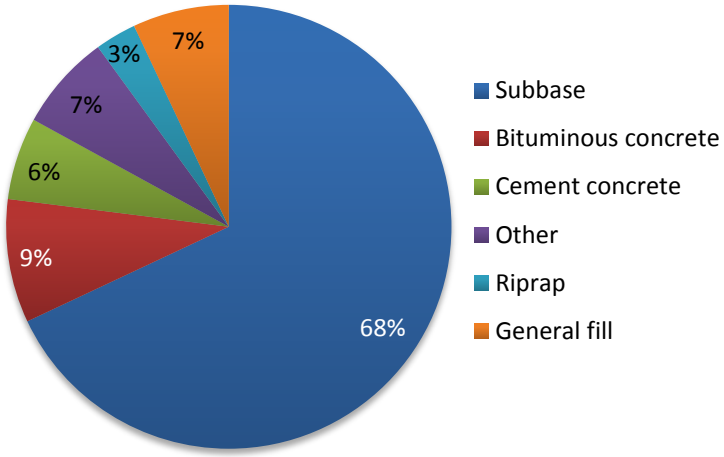

Figure 2.4 The End Uses of Crushed Portland Cement Concrete (reproduced from Kelly 1998)

For road construction applications, crushed Portland cement concrete has also been used in some jurisdictions as a base material, as an aggregate for concrete cement road surfaces, and as an aggregate for hot mix asphalt concrete surfaces. Figure 2.5 depicts a typical road structure, including wearing surface, base layer, and subbase layer, all on top of subgrade. The following sections describe the uses of recycled PCC in various road construction applications.

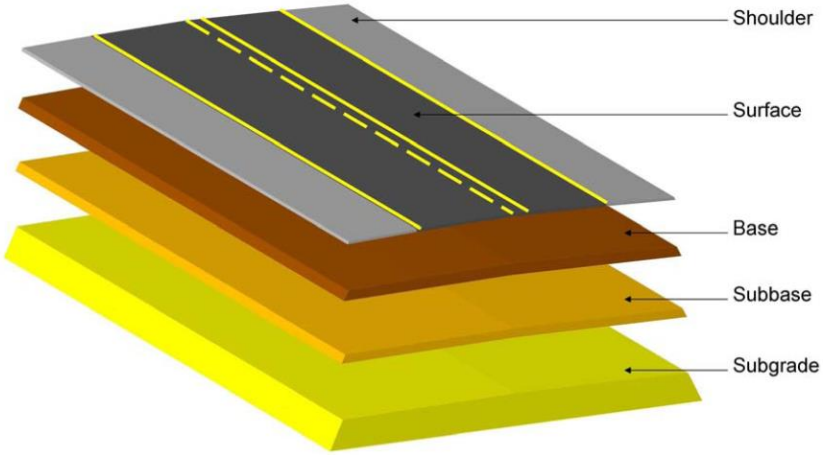

Figure 2.5 Typical Road Structure Cross Section (Soares 2005)

2.3.1 Recycled Portland Cement Concrete as a Subbase and Drainage Layer Material

The most common use for crushed PCC rubble in most countries is as a subbase material within a road structure (Hansen 1985). The purpose of the subbase layer is to keep the subgrade dry and distribute strains in the road structure. Subbase materials are typically composed of crushed, unbound aggregate with a typical top size of 25 mm, which is often referred to as a drainage layer. The purpose of a drainage layer is to provide a free draining strain distribution layer within a road structure susceptible to moisture infiltration and wetting-up issues. (COS 2009B).

Crushed PCC material is used in subbase layers because it has been shown to perform well, provide economic savings, and conserve natural resources (ACPA 2008). The Federal Highway Administration (FHWA) found that 38 states in the United States in 2004 used PCC as a subbase material. In 1989, the Ministry of Ontario transportation adopted open graded drainage layers using conventional drainage rock on major road ways, which included the drainage layer emptying into a drainage collector and finally an outlet system. The City of Saskatoon has also used drainage layers in some of road structures to mitigate moisture issues. Substructure drainage systems are used to mitigate marginal subgrade conditions, high water tables, and climatic conditions including excess moisture, spring thaw, and freeze-thaw cycles.

The high angularity and rough textured particle properties of Portland cement concrete when properly crushed and graded allows the PCC material to interlock and act as a drainage layer (Kazmierowski and Marks 1999, ACPA 2008). Due to the nature of crushing, small amounts of fine particles and dust can sometimes cling to coarse PCC aggregate. Studies have shown the amount of dust generated through the crushing process and leachate that is processed is not harmful to the environment (ACPA 2008, Staton 2006).

Chemical stabilization of subbase layers has been shown to improve the behaviour of road structural layers (Graymont Cement 2010, Little and Nair 2009). Stabilizers such as lime, cement, asphalt oil, and fly ash are often used to chemically stabilize subbase materials. The primary benefit of the stabilized subbase is that it provides a strong uniform structural layer. Secondary benefits of using a stabilized subbase are that it resists the pumping of fine material into the upper layers of the road structure during high moisture contents and allows the use of substandard recycled materials – for example, recycled material that is contaminated with other building materials (ACPA 2008). With regards to PCC materials, strengtheners such as cement and asphalt may improve the performance of a PCC subbase or drainage layer with regards to uniformity, stiffness, and fines content behaviour.

2.3.2 Recycled Portland Cement Concrete as a Base Material

Base materials may also be produced from Portland cement concrete rubble (Ooi et al. 2011, PSI Technologies 2010). In many studies, the performance of recycled PCC in a base layer has been comparable to that of virgin granular aggregate (ACPA 2008, Ooi et al. 2011). Gradation specifications for crushing base course material are stricter when compared to subbase and are typically well graded, with fines content less than twelve percent (COS 2009B). Other than those used in the surface course, base aggregates are considered high quality to ensure pavement durability and performance. Portland cement concrete materials have not been used in COS road base layers

2.3.3 Recycled PCC in Cement Concrete

Portland cement concrete materials can also be used as an aggregate in cement concrete road surfaces (FHWA 2007). The process of using recycled PCC as the sole aggregate or in percentage amounts of aggregate in new concrete was first introduced in the early 1940s. The first uses for cement concrete containing recycled PCC included roads, sidewalks, curbs and

gutters (ACPA 2008). Currently, the European Union uses cement concrete made of PCC for the bottom lift of a two lift cement concrete pavement road structure (FHWA 2007).

Multiple studies have been conducted to evaluate the ability to use concrete containing recycled PCC as the aggregate source. One of the first evaluations was done in the early 1970s; it concluded that the matrix bond between aggregate mortar matrix bond was reduced between 55 and 88 percent of the strength when compared to conventional aggregate. This research concluded that cement concrete made with recycled PCC aggregate was not recommended for structural uses (Frondiston 1977). Similar results were also observed and published in a paper by Department of Civil Engineering of Serbia; observations made showed that cement concrete prepared with recycled PCC as an aggregate had reduced material properties and performance when compared to 100 percent virgin aggregates (Malsev et al. 2010).

Similar findings were also published stating that producers of concrete can add up to 30 percent PCC aggregate without seeing a change in concrete properties (Limbachiya et al. 2000). All findings concluded that concrete made from recycled PCC is not recommended for structural applications where large deformations are expected and where harsh environmental conditions exist (Malsev et al. 2010); however, additives such as polymer and stainless steel reinforcing mesh on top of rebar did aid in the concrete's flexural strength (Limbachiya et al. 2000).

2.3.4 Recycled Portland Cement Concrete in Hot Mix Asphalt Concrete

Portland cement concrete materials have also been used as an aggregate in hot mix asphalt concrete (HMAC) road surfaces in a small capacity (FHWA 2007). The American Concrete Pavement Association (ACPA) found that the angularity and rough texture of crushed PCC aggregates provided stability and surface friction. The disadvantage of using Portland cement concrete aggregate in hot mix is that the PCC material is highly absorptive (Malsev et al. 2010). PCC aggregates have been shown to absorb more asphalt cement than conventional virgin aggregates or reclaimed asphalt pavement, resulting in an increased requirement for asphalt binder and further cost. Also, the use of PCC rubble derived aggregates in HMAC may lead to aggregate swelling in freeze thaw field state conditions due to calcium carbonate or chalky material released during the crushing process (Berthelot et al. 2011).

2.4 Physical Properties of Crushed PCC and Virgin Aggregates

Differences in the physical properties between crushed Portland cement concrete and virgin aggregates are influenced by the cement mortar which binds the aggregate together (Kelly 1998). The old mortar is composed of different materials compared to the materials found in virgin aggregates, which changes the physical properties of crushed PCC.

The specific gravity of crushed Portland cement concrete is typically lower than that of virgin aggregate. The specific gravity of crushed PCC averages between 2.3 and 2.4, and the specific gravity of virgin aggregate averages between 2.5 and 2.6 (Chan and Poon 2005). Water absorption percentages between the two materials are different. The cement mortar component of crushed concrete rubble produces more fines than natural aggregate which causes a much higher water absorption percentage in recycled Portland cement concrete. The water absorption percentage ranges between 4.0 percent for coarse crushed PCC and 7.6 for fine crushed PCC. The water absorption percentage for course virgin aggregate is 3.9 percent, and the percentage for sand is 0.4 percent (Nixon 1978).

The City of Saskatoon currently employs material specifications for road construction materials. Saskatchewan road agencies have traditionally relied on internally developed aggregate specifications, which are primarily based on past experience (Anthony 2007). Using conventional empirical test methods on conventional aggregate sources provides reliable data; however, these tests were not developed for recycled materials.

2.4.1 Grain Size Distribution

Grain size distribution influences a pavement layer's performance because it affects the particle on particle contact and the ability to dissipate stress within the system. The gradation of the material is important because it influences the stability, permeability, durability, friction resistance, and resistance to moisture damage of the aggregate (Haddock 2000). Figure 2.6 illustrates the base material and crushed rock gradation envelope specification for the COS (COS 2009B)

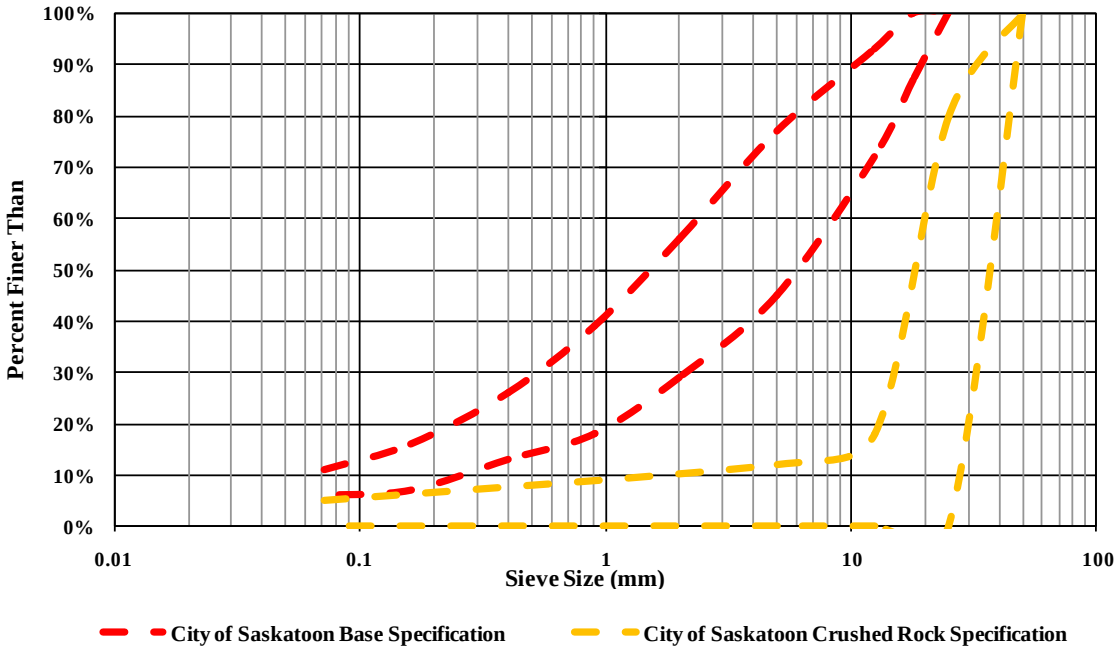

Figure 2.6 COS Base Course and Drainage Rock Grain Size Distribution Specification (COS 2009B)

2.4.2 Aggregate Angularity

The structural performance of a base course is directly related to the angularity of the fine and coarse aggregate, as it has an effect on aggregate interlock (NCHRP 2001). Aggregates with rounded rocks are not desired because the shear strength of the material is reduced (Roberts et al. 1996). Higher angularity of the aggregate leads to greater interlock and higher strength of material within a road structure. Most of the aggregate contained within the glacial aggregate deposits have no fractured faces. The only method of obtaining aggregate fractured faces is to crush and process larger source aggregate fraction through a crusher to achieve proper fracture and particle size. Figure 2.7 illustrates round aggregate retrieved from an aggregate pit on the right and mechanically crushed aggregate on the left. The number of fractured faces increases when the material is processed using a crusher.

Figure 2.7 Comparison of the Effects of Mechanically Crushing Aggregate, Mechanically Crushed (Left) and Natural Aggregate (Right) (Stone City 2010)

There are two types of aggregate angularity: coarse angularity is dependent on the number of fractured faces aggregate has of sizes greater than 5mm (COS 2009B), and fine angularity is dependent on the air voids of loosely compacted aggregate less than 2.36 mm (ASTM C1252).

2.4.2.1 Coarse Aggregate Angularity

Coarse angularity is determined by measuring the percentage of the aggregate particles with one or more fractured faces as specified in ASTM D5821 Using the material retained on the 5 mm sieve (greater than 5 mm in size), the numbers of aggregates with fracture faces are counted. The City of Saskatoon base coarse and drainage rock specifications require a fracture percentage of at least 50 percent (COS 2009B).

2.4.2.2 Fine Aggregate Angularity

Fine aggregate angularity is measured by calculating the percent of air voids present in a loosely compacted aggregate that passes the 2.36 mm sieve (ASTM C1252). A picture of the apparatus used to determine the fine angularity is illustrated in Figure 2.8. The fine aggregate of a given gradation is poured into a cylinder with the use of a funnel. The filled cylinder is weighed, and the amount of voids in the sample is computed using the volume of the cylinder

and the specific gravity of the dry aggregate. As the amount of volumetric voids increases, the aggregate becomes more angular (Roberts et al. 1996). This test does not account for particles that have cubical shape, which is often represented by PCC aggregate. With cubical material, its void content is low; however, it has a near 100 percent fractured face value.

Figure 2.8 Fine Angularity Apparatus (Durhamgeo.com 2012)

2.4.3 Organic Content

Most of the aggregate contained with the glacial aggregate deposits includes a certain percentage of organics. Primarily, the organics are found within the binder or fine clay that composes the lower end of the gradation curve. High levels of organics reduce the plasticity of the binder, therefore reducing the strength of the granular base material (NCHRP 2001).

ASTM D2974 describes the procedure for determining organic content. The organic content of granular base material is determined by taking a sample of the material and placing it inside an ignition oven. The oven is set at 440 degrees Celsius, which allows the organic material to be burnt off. The difference in masses both prior and post burn off determines the organic content.

The COS specifications for granular base aggregates also included a maximum allowable limit of organics allowed in the aggregate overall and below the 5 mm sieve size (COS 2009B). The COS specifications allow for a maximum of three percent organic fines by weight passing through the 5 mm sieve, and a maximum of one percent organic content overall for granular base materials. To determine the organic contents of both the conventional COS granular base and the recycled PCC well graded base material ASTM D2974 was followed. There is no COS specification limit for organic fines pertaining to COS crushed rock.

2.4.4 Standard Proctor Compaction Method

Standard Proctor compaction was developed by R.R. Proctor in 1933 as a method to determine the relationship between the optimum moisture content and dry density of the sampled soil (ASTM D0698). ASTM defines soil as "natural occurring fine- or coarse-grained soils, or composite or mixture of natural soils, or mixtures of natural and processed soils or aggregates such as gravel or crushed rock" (ASTM 0698). The standard Proctor compaction is designed for determining the compaction characteristics of unbound aggregates. The requirements for a standard Proctor test include a 943 cubic centimeter mold, with the soil being compacted in three layers at 25 blows per layer within the mold with a 2.49 kg hammer from a drop height of 30 centimeters. Figure 2.9 illustrates the automated Proctor hammer.

Figure 2.10 displays the increased compaction effort for modified Proctor compaction compared to standard Proctor compaction. The modified Proctor compaction method was developed during the Second World War to simulate larger compaction effort in construction of military airports. The requirements for a modified Proctor test include a 943 cubic centimeter mold, with the soil being compacted in five layers at 25 blows per layer within the mold with a 4.53 kg hammer from a drop height of 45 centimeters (ASTM 2009). Currently the modified Proctor can be used in projects where the loading experience on the area is high — for example, an industrial plant or warehouse. The COS does not specify the modified Proctor compaction method. When a modified Proctor is specified, the material is compacted to only 95 percent of optimum and the moisture content is two to three percent lower (Ping et al. 2003).

Figure 2.9 Automated Proctor Hammer

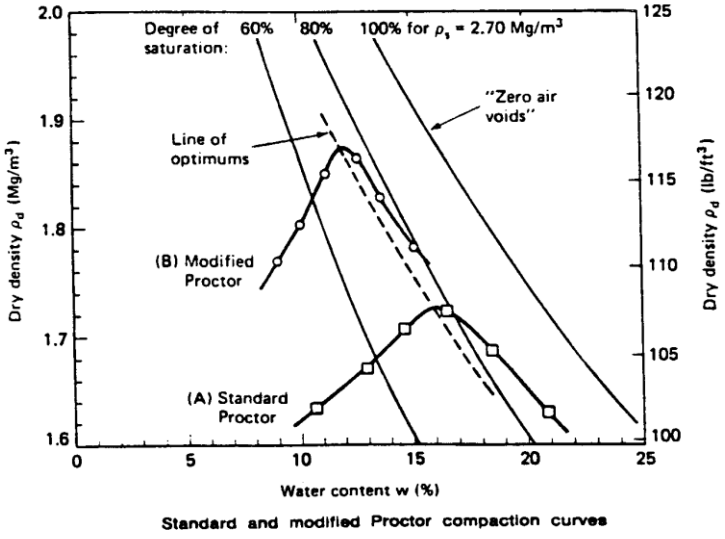

Standard and modified Proctor compaction curves

Figure 2.10 Standard and Modified Proctor Compaction Curves (Berthelot 2007)

Studies have shown that bound materials such as PCC and reclaimed asphalt pavement do not respond well to impact compaction (PSI Technologies 2010, Woosung 2006).

Furthermore, PCC materials are comprised of low mineral fines which resist impact compaction. Impact crushed PCC materials are highly fractured and have reduced fines content, resulting in an increased compactive effort required for 100 percent compaction.

2.4.5 Gyratory Compaction Method

The gyratory compaction method offers an alternative to the Proctor compaction method. The gyratory compactor was developed by the Corps of Engineers during the Second World War. The Texas highway department was one of the first agencies to adopt this style of compaction (Huber 1996). The gyratory uses a kneading process that simulates the action of compaction equipment during the construction process (Huber 1996). The gyratory compactor has the ability to compact not only bound materials like asphalt, but also unbounded naturally occurring aggregates and soils. The ASTM standard for gyratory compaction is ASTM D3387. Figure 2.11 displays a picture of a gyratory compactor.

Figure 2.11 Gyratory Compactor

A study conducted by the Department of Transport of Minnesota found that gyratory compaction better emulated field compaction when compared to standard Proctor compaction (Woosung 2006). Field density measurements of compacted reclaimed asphalt pavement base layers indicated that dry density and optimum moisture calculations determined by using the gyratory better correlated than those determined by the standard Proctor testing method (Woosung 2006). Other researchers have also indicated that during repeat samples and variable parameters that the gyratory compaction method ensures uniform continuum-type samples compared to the standard Proctor type compaction (Abdo et al. 2006, Berthelot et al. 2007, Berthelot et al. 2009D).

2.4.6 California Bearing Ratio

California Bearing Ratio (CBR) characterization is widely used by road agencies worldwide to provide a relative measure of strength and moisture durability across various road materials for structural design purposes. The test itself is a penetration test in which the pressure is measured to penetrate a soil sample with a plunger of a certain area. The measurement obtained from that soil is then divided by the pressure obtained of equal penetration of a crushed rock sample (Chan and Poon 2005). CBR testing can be conducted in the unsoaked or in the soaked condition.

The COS specifies that once the material has been compacted to 100 percent of the maximum dry density using the Proctor compacted style method, the CBR shall be a minimum value of 65 with a penetration of 0.1" or 0.2", whichever is greater (COS 2009B). The COS specification does not specify a CBR minimum peak strength value for crushed rock aggregates (COS 2009B).

2.4.7 Micro-Deval Abrasion Resistance

Traditionally, the Los Angeles (L.A.) abrasion and impact test has been widely used by many agencies to measure the degradation resistance of course material. However, in recent years, the L.A. abrasion test has been criticized for the lack of correlation with field performance (Rangaraju and Edlinski 2008, Raducanu 2002). Developed in France in the 1960s, the Micro-Deval has been used primarily in Canada and now in the United States. The government of Ontario has done extensive research and studies on the Micro-Deval and found that the Micro-Deval is a better indicator of aggregate quality than other degradation tests such as the L.A

abrasion test. A further study by the National Cooperative Highway Research program reinforced the argument by stating that the Micro-Deval gave a better indication of predicting field performance than the L.A abrasion test (Rangaraju and Edlinski 2008).

The Micro-Deval test is used worldwide to measure the durability and abrasion of aggregate (British Standards 2011). The Micro-Deval test method is used to simulate and measure the breakdown of the aggregate under abrasive forces of heavy wheel loads which aggregate layers experience during the construction processes. These heavy forces can break the aggregate down over time and change its gradation.

Currently the City of Saskatoon does not test for abrasion resistance or degradation of the granular base and drainage rock aggregates. The reason why the COS does not recognize abrasion resistance as a concern is that the aggregate pits are typically glacial alluvial pits by nature which generally exceed the minimum aggregate abrasion specification (Guenther et al. 2010). Degradation and abrasion is important because as a material experiences applied strains in the field, the material may experience degradation and abrasion which may result in the material breaking down. Base course aggregates that have high degradation or little resistance to abrasion can result in increased pavement distresses including rutting. Materials with high degradation can start breaking down during the construction process. There are numerous situations where the aggregate is subjected to heavy loads, such as the compaction equipment used in compaction of the base, or the trucks that are delivering the material to site (Rangaraju and Edlinski 2008). The National Cooperative Highway Research Program (NCHRP) performed a study in comparing the Micro-Deval test to the L.A abrasion test. It was found that the Micro-Deval showed closer correlation to field performance of the aggregates than that of the L.A Abrasion and that a loss of less than 18 percent indicated that material had good resistance to abrasion and degradation (White et al. 2006, Rangaraju and Edlinski 2008).

2.4.8 Vacuum Saturation

Vacuum saturation is a test method that is used to simulate moisture susceptibility in field state conditions. When an aggregate is completely saturated, the testing environment represents the worst case scenario for aggregates used as a structural layer contained within a road structure (Williamson and Weyers 2007). Vacuum saturating compacted coarse aggregate specimens aims at removing all the entrapped air within the sample matrix. By applying the vacuum source, it

forces water into the effective pores of the coarse aggregates. The benefit of using vacuum saturation is that the test is not affected by the nominal maximum aggregate size, gradation or mineralogy of the source. The test has also been effective on non-aggregate sources such as steel slag and crushed concrete (Beale and Zhanping 2008).

2.4.9 Mechanistic Rapid Triaxial Test

The triaxial approach to testing materials was originally developed in 1930 for soils testing (Holtz and Kovacs 1981) and has been adapted in various forms to other materials testing. Triaxial material testing is used by the road industry to characterize all types of road materials (Berthelot et al. 2003, 2005). The use of the rapid triaxial apparatus allows for the ability to quantify the fundamental mechanistic properties of materials in response to dynamic loading (Berthelot 1999, Crockford et al. 2002, Pellinen and Witczak 2002). The rapid triaxial test (RATT) replaced the conventional triaxial testing of road materials because of its abilities to handle full-size gyratory compacted samples, which are defined as samples that are 150 mm tall and have a radius of 150 mm. With the RATT being able to handle the full size samples, it allows researchers to characterize materials much more efficiently and therefore characterize a high number of samples using continuum mechanistic specifications.

The RATT cell consists of a cylindrical chamber which is able to accommodate standard gyratory compacted samples. The sample is contained within RATT cell by a pneumatic confinement bladder with six linear variable differential transducers mounted axially around the sample (Berthelot et al. 2003). Through the use of the RATT cell, unconventional road materials such as PCC can be characterized. Using the RATT cell to characterize road materials instead of the CBR method, the RATT cell is better able to simulate applied stresses as experienced in the field (Berthelot et al. 2010C). Properly characterizing road materials is vital for structural design of a road. A photo of the RATT cell can be seen in Figure 2.12.

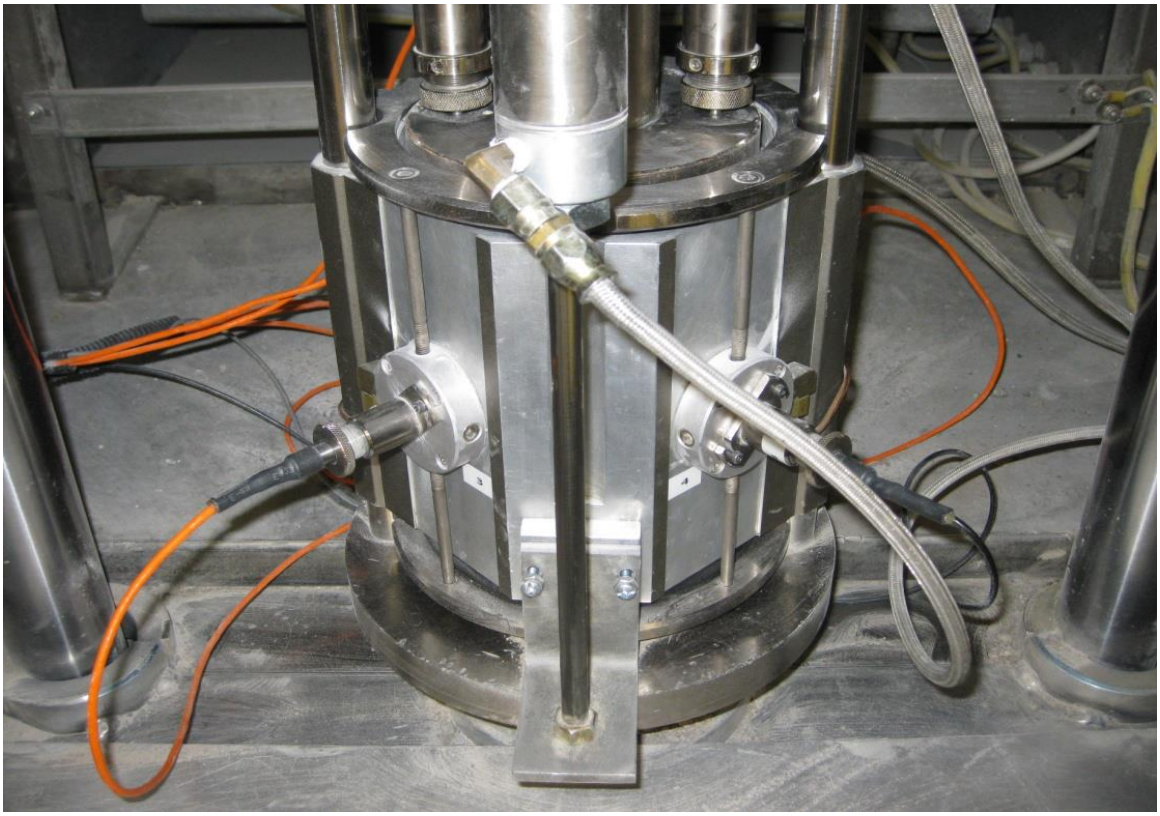

Figure 2.12 Rapid Triaxial Cell

The rapid triaxial test is a simple test, meaning that a material's properties can be determined directly from measurements with no inverse analysis or empirical relationships (Lytton 2000, Osman 2005). Using the rapid triaxial test also allows the user to measure the effects of multiaxial stress states on a material (Berthelot et al. 2002). The rapid triaxial test has also proven to be precise with little coefficient of variation, meaning multiple users have run repeat samples with little variation in results, across different materials (Anthony 2007, Berthelot 1999, Xu 2008).

When an aggregate sample is tested using the RATT cell, the sample is subjected to dynamic axial loading. The load is applied in a sinusoidal wave form, with continuous confinement by a pressure controlled pneumatic filled bladder. By applying a confinement pressure it better represents the multi axial stress state typical of applied field state conditions typically found within a road structure without premature failing of the sample (Brown et al. 2004). The applied and confinement pressures can be seen as illustrated in Figure 2.13. Without

confinement, compression tests do not provide the realistic field state conditions needed for mechanistic road modeling (Sotil et al. 2004).

Given the empirical nature of the California bearing ratio test for characterizing unbound aggregates, as well as limited empirical evidence of performance in the field of recycled PCC materials in Saskatoon, triaxial frequency sweep characterization using the RATT cell was conducted in this research (Berthelot et al. 2008). Using the RATT cell for mechanistically characterizing material properties related to material response to dynamic loading has been proven to provide reliable information (Berthelot et al. 2003, Crockford et al. 2002, Xu 2008).

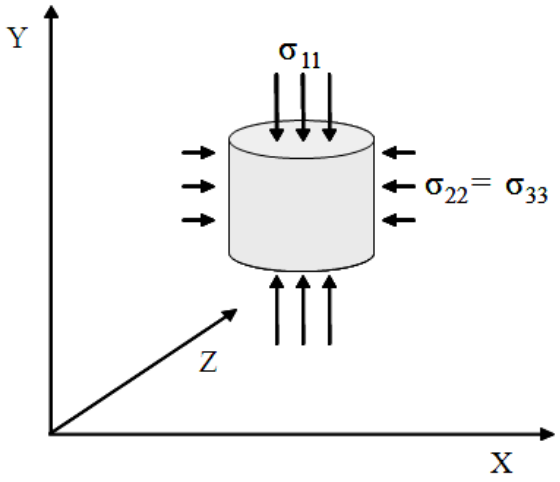

Figure 2.13 Applied Stress within Rapid Triaxial Test Cell (Berthelot 2007, Class Notes CE 867)

With the advancement of modern computers and full feedback controlled software, the RATT cell is fully feedback controlled. The software allows for the capability of applying loads at various frequencies with multiple combinations of axial and radial stress states (Berthelot 1999, 2009D). With the enclosure of the RATT cell, the user also has the ability to characterize materials across temperatures at which the loads are applied. The equipment measures the strains both radial and axial resulting from the loading combinations which allows for the determination of elastic and visco-elastic material properties (Berthelot et al. 2003). These properties include Complex Modulus (E*), Dynamic Modulus (E_D), Poisson's Ratio (v) and the Phase angle of the material.

2.4.9.1 Complex and Dynamic Modulus

The complex modulus can be defined as the ratio of the magnitude of the sinusoidal stress applied to the sample and the magnitude of the sinusoidal strain that is the outcome from the applied stress (Pellinen and Witczak 2002). The relationship between applied stress and strain is expressed in Equation 2.1.

$$E^* = \frac{\sigma}{\varepsilon} = \frac{\sigma_{11p} e^{i\omega t}}{\varepsilon_{11p} e^{i(\omega - \delta)}} \qquad \textbf{Equation 2.1}$$

Where:

E* = Complex Modulus (Pa)

σ = Applied stress (Pa)

ε = Strain response to applied stress (μm/μm)

σ_{11p} = Peak stress applied in the X_1 coordinate direction (Pa)

ω = Angular load frequency (radians per second)

t = Load duration (seconds)

ε_{11p} = Peak strain response in X_1 coordinate direction (μm/μm)

δ = Phase angle (radians)

The stiffness of a material is characterized by the complex modulus. A high stiffness modulus result occurs from a low strain in the material given the applied stress on the material. The dynamic modulus for linear elastic materials, E_D, may be described as a measure of the absolute value of the complex modulus or the peak stress to peak recoverable strain during material response. The primary purpose for measuring the dynamic modulus is to quantify the stress-strain relationships in a structural layer under an applied load. For an elastic material, the phase angle is zero meaning that the applied stress results in instantaneous strain. With the phase angle equalling zero the equation 2.6 is reduced and the dynamic modulus, E_D, is equal to the absolute value of the complex modulus, E*, as expressed in Equation 2.2 (Berthelot 1999).

$$E_D = \left|E^*\right| = \frac{\sigma_{11p}}{\varepsilon_{11p}} \qquad \textbf{Equation 2.2}$$

2.4.9.2 Phase Angle

The phase angle is used to characterize the relative viscoelastic effects of the material under dynamic loading within the RATT cell. A viscous material is defined as material which has a phase angle of 90 degrees. A non viscous or purely elastic material shows instantaneous strain with the applied stress resulting in a phase angle of zero as seen in Figure 2.14. The equation for phase angle can be found in Equation 2.3.

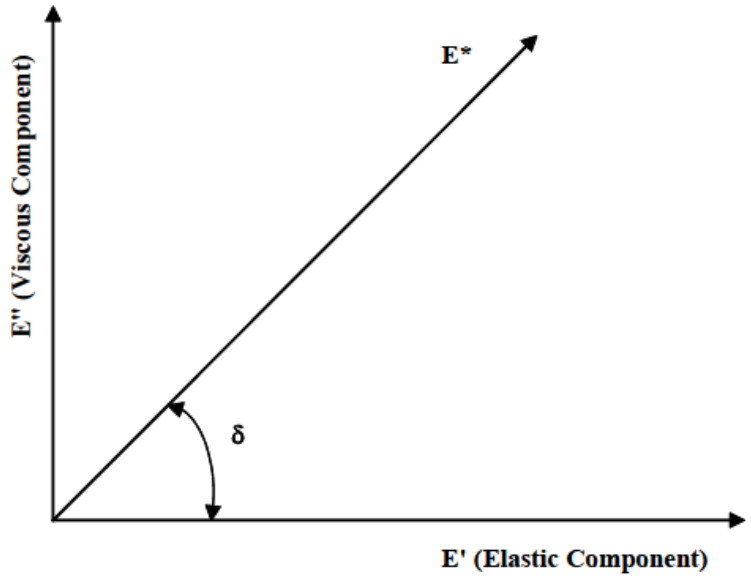

Figure 2.14 Phase Angle and Complex Modulus (Berthelot 2007)

$$\delta = \frac{t_i}{t_p}(360^0) \qquad \textbf{Equation 2.3}$$

Where:

δ = Phase Angle (degrees)

t_i = time lag between a cycle of sinusoidal stress and a cycle of strain (sec)

t_p = time for a stress cycle (sec)

2.4.9.3 Poisson's Ratio

Poisson's ratio is defined as the linear relationship of a lateral strain to an axial, which results from an applied load in the axial direction. The material property is used to characterize the multi-axial strain behavior of a material and for the structural modeling of roads. Poisson's ratio can be an important measure of the mechanistic properties of a road material. Due to the significance of the mechanic behaviour, it can influence the performance of the road structure. Poisson's ratio can be expressed as seen in Equation 2.4 (Berthelot 1999).

$$v_{11}(t) = \frac{\varepsilon_{22}(t)}{\varepsilon_{11}(t)} = \frac{\varepsilon_{33}(t)}{\varepsilon_{11}(t)} \qquad \textbf{Equation 2.4}$$

Where:

υ = Poisson's ratio in X1 coordinate direction

ε_{11} = Strain in X1 coordinate direction (axial)

ε_{22} = Strain in X2 coordinate direction (radial)

ε_{33} = Strain in X3 coordinate direction (radial)

2.4.10 Review of City of Saskatoon Aggregate Specifications

City of Saskatoon aggregate specifications for granular base and crushed rock are based on ASTM testing procedures. COS specifications for conventional granular base material include:

- The material must be well graded meet gradation bandwidth specifications (COS 2009B).
- At least 50 percent of the material greater than the 5 mm sieve must have at least one fractured face (COS 2009B).
- Organic content of material passing the 5 mm sieve must not be greater than three percent, and an overall organic content of one percent by weight (COS 2009B).

- Material compacted to 100 percent of the maximum density as determined by the standard Proctor test must have a minimum CBR of 65 in the unsoaked condition at either 0.1" or 0.2" penetration (COS 2009B).

COS has also developed a material specification for the crushed rock. Crushed rock is in drainage layers. The crushed rock must meet the following COS specifications:

- The material must be composed of fragments of durable rock, free from undesirable quantities of soft or flaky particles (COS 2009B).
- The material must meet a drainage rock gradation bandwidth specification (COS 2009B).
- At least 50 percent of the material greater than the 5 mm sieve must have at least one fractured face (COS 2009A).

2.5 Numerical Road Structural and Performance Predictions Modeling

With the advancements in computer mechanics technology, great achievements have been made in the ability to model road structures. The first road models were developed to predict and calculate different components within the road structure. Computer modeling programs were developed to compute the soil and pavement temperature conditions (FROST), the resilient modulus and Poisson's ratio (TRANS-FORM), stresses and strains in the pavement system (NELAPAV) and cumulative damage associated with traffic loading (CUMDAM) (Bigl and Berg 1996).

In a study conducted by the Department of Transportation in Minnesota, the information produced by the above four models was then inputted into another computer model called CRREL. The program was used to predict pavement performance, as shown in the below flow chart. The researchers were able to change conditions like the temperature or load configuration and see how the road structure would behave.

With the level of technology used at the time of the study, the model was able to provide useful information, and to provide a new tool in pavement and road structure design. However, the performance predictions were not able to simulate representative field state conditions and the outputted data was highly variable (Bigl and Berg 1996).

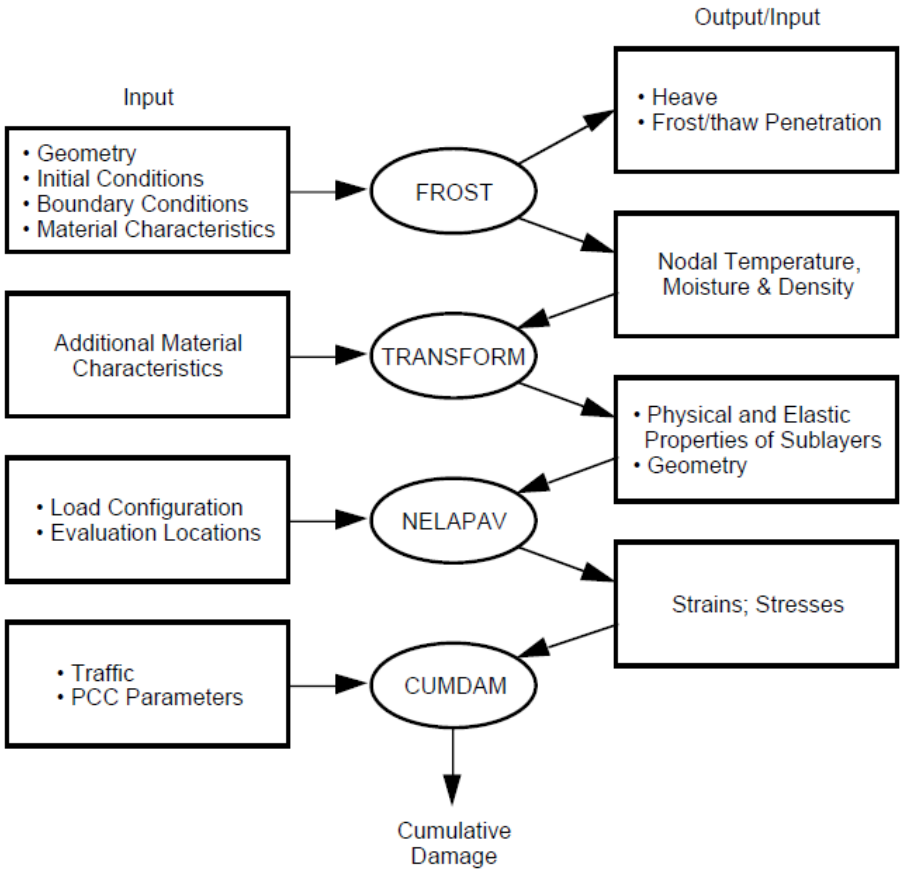

Figure 2.15 Flow Chart of Computer Models (Bigl and Berg 1996)

Since the development of computational mechanics structural assessment modeling programs, great advancements have been made with computer modeling. By using technology like the rapid triaxial test, mechanistic material properties such as Poisson's ratio and dynamic modulus are now inputted into the modeling program to represent the different materials found within the road. With larger computing power and memory capacity, the ability to examine how the structural layer acts on the particle scale has become reality. The ability to model the road at this scale results in the ability to observe how each layer of a road structure reacts to an applied load, therefore greatly increasing the accuracy of the model. The development of non-destructive testing equipment, primarily the heavy weight deflectometer (HWD), has allowed the ability to simulate different loading, and measurement of the structural deflections based on the applied load. The deflections predicted by the model can now be validated by the data collected by the HWD. The latest numerical models when compared to the HWD results are within five percent, making the accuracy of the model much greater than its earlier versions.

Early road structure failures are not uncommon within the first few years after construction, and also the need for a more comprehensive mechanistic pavement design model have been recognized (Berthelot et al. 2009C, Osman 2005). However, despite effort by researchers and road agencies to enhance and accept the mechanistic part of pavement design, no satisfactory comprehensive alternative to the empirical approach has been found (Osman 2005).

Advancements in road modeling have been made over the past couple of years, during which accurately predicting road structure performance has become a reality. The limitation of previous work has been the proper characterization of road materials, road geometry and loading rates. In prior road models, the road structure has been treated as a two dimensional structure, in which the material is considered homogeneous and only linear elastic and static loading is experienced (Erkens et al. 2002). These assumptions lead to inaccurate prediction using the model, because structural layers within a road actually experience non linear and viscoelastic loading. In order to properly model traffic loading, three dimensions are needed to characterize the road structure. Modeling programs such as PSIPave3D^{TM} use a finite element code which breaks the road structure into a mesh of nodes. Each of the nodes has a mechanistic material property in which a portion of the load is applied to the node, similar to how different areas of a pavement road experience different loading under moving traffic. A simplified breakdown can be seen in Figure 2.16.

The processing capability of computers will always be the limiting factor of using applied computational mechanics to analyze and develop road structures. There is a balance between the time spent using a program, and the amount of useful information that is gained during the time spent. The time period allotted for the design of a road structure is the limitation with which an engineer/designer has to work when using pavement analysing software (Lytton 2000).

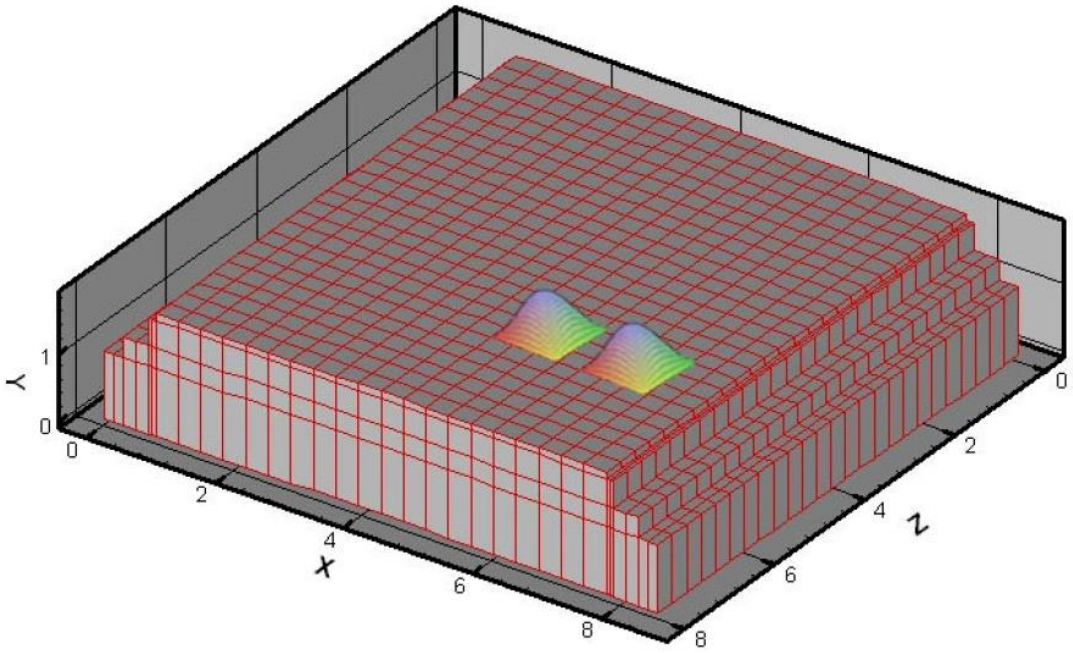

Figure 2.16 Loading of Pavement in Three Dimensions (Soares 2005)

2.6 Chapter Summary

The initial recycling of Portland cement concrete was first performed on a large and well documented scale after the Second World War in Britain and Germany. Material was used from city buildings that were destroyed by the aerial bombing, as well as the demolition of war fortifications. The use of recycled PCC as an aggregate alternative prompted very little research interest until recently when the possibility of limited quantities of quality aggregates was becoming a reality.

Canada as a country does very little concrete recycling when compared to the rest of the developed industrialized countries. Canada has been recycling concrete for approximately thirty years, with the primary uses including subbase material for road construction. However, with increasing pressures brought on by society to be environmentally responsible, the continuing research advances in technology will provide the ability to use recycled material as a high value aggregate alternative.

Most of the aggregate reserves that supply the Saskatoon's material demand require an average haul distance of 100 km from the outer City limits or greater for delivering aggregate to construction sites. The aggregate haul distances are estimated to increase for some areas by as much as 30 percent in the next fifty years.

The properties that define the City of Saskatoon base course and drainage rock specifications are primarily physically based with empirical correlation to performance. These include gradation analysis, course aggregate angularity, standard Proctor, and California bearing ratio.

Using mechanistic computational mechanics to characterize road materials instead of the CBR has enabled researchers to better simulate applied stresses as experienced in the field. Properly characterizing road material constitutive properties is vital for mechanistic structural design of a road. With the advancement in technology and the utilization of mechanistic laboratory material characterization such as the RATT cell, the ability to model and simulate the structural behavior of road structures is becoming a reality. It was not until recent advances in computational engineering mechanics for road primary response modeling, that road designers have been able to model different road structure designs, including the use of unconventional materials, and evaluate their structural performance without actually building the road.

CHAPTER 3 PROCESSING AND CRUSHING OF RECYCLED PORTLAND CEMENT CONCRETE AND CONVENTIONAL PIT RUN MATERIALS

The materials used in this research include City of Saskatoon (COS) reclaimed Portland cement concrete (PCC) and pit run granular material. To achieve material gradations applicable for pavement layers, both PCC and pit run materials were crushed, stockpiled, and sampled. This chapter describes the process and explains how PCC rubble was processed and crushed into a material sized for pavement layers. This chapter includes a description of the preparation of the PCC prior to crushing and further information on reasons why an impact style crusher was used to crush the PCC rubble.

3.1 Production of Aggregate Materials

Conventional granular base and rock aggregate materials are quarried from aggregate pits. The materials are then crushed to a specified gradation using a traditional jaw and cone crusher. In the past, the City of Saskatoon had typically employed jaw and cone crushed Portland cement concrete rubble as a low quality backfill material in local road rehabilitation systems. However, the City found that conventional jaw and cone-type crushing equipment did not provide high quality material grain size distribution, crushing production, or the adequate particle cubical shape required to use recycled concrete materials in new road construction, particularly from a structural design perspective (Berthelot et al. 2010A).

In an effort to improve the end product value of stockpiled Portland cement concrete rubble materials, the City of Saskatoon piloted the use of impact crushing technology to process rubble concrete materials to meet quality road construction material specifications. The City of Saskatoon piloted state-of-the-art closed loop impact crushing and screening equipment to process the stockpiled concrete material into high quality specified road building materials. Benefits of impact crushing technology include the ability to accommodate larger pieces of concrete, the ability to remove reinforcing steel by magnetic extraction, and the generation of cubical particle shapes with a high fracture face count (PSI Technologies 2010).

The impact crusher spread commissioned in 2009 by the City of Saskatoon is pictured in Figure 3.1. The impact crushing spread had an intergraded screening capacity to reduce fines of the final product material and a continuous magnet to pull the steel from the concrete rubble after

it was crushed. The crushing spread produced material which met the city base specifications and produced a high fracture aggregate. (Berthelot et al. 2010A).

Figure 3.1 COS Impact Crushing Spread

Figure 3.2 Excavator with Muncher Processing PCC Rubble

Due to the large size of some pieces of the PCC rubble and the deleterious material present in the stockpiles, the PCC rubble was pre-processed prior to crushing, as seen in Figure 3.2. Any pieces larger than one meter in any dimensional direction were first broken down using processing equipment that was mounted to track excavators. Excavators equipped with a jack

hammer and/or muncher processed material by breaking down rubble that was larger than the maximum size, along with the removal of non-crushable objects such as steel columns and fire hydrants, as well as the removal of rebar. The impact crushing spread was also equipped with a grizzly screening located on the feeder of the crusher which eliminated nearly all the organics from the rubble.

3.1.1 Material Sampling

With regards to recycled PCC material, this study is limited to investigating the material properties of crushed well graded (GW) PCC base materials and crushed PCC drainage rock. Figure 3.3 illustrates the four research aggregates, including conventional COS granular base and conventional COS drainage rock.

The aggregate gradations of each material were sampled directly out of the processed stockpiled materials. During the sampling process, material was taken from random locations around the pile and the material was sampled by digging into several locations of the pile and then retrieving the sample from the excavated area to eliminate any possible segregation issues. The sampling procedure followed the specifications set by ASTM D75. The samples collected were blended and a representative sample was used for both the conventional testing and mechanistic sampling to avoid any variability in the sampled material.

a) Conventional COS Granular Base

b) Recycled GW PCC Base

c) Conventional COS Drainage Rock **d) Recycled PCC Drainage Rock**

Figure 3.3 Research Aggregates

3.2 Chapter Summary

This chapter presented a discussion on the stockpiles of PCC rubble that the COS had accumulated over the past years. This chapter also reviewed the conventional crushing techniques and equipment that are used to crush conventional granular materials and how these techniques and equipment when used to crush PCC rubble, produce a material that does not meet COS base aggregate specification.

Specialized preprocessing equipment and an impact crusher are needed to produce PCC aggregates that meet COS base aggregate specifications, which were stockpiled by the COS to complete the crushing of the PCC rubble. Sampling of the conventional and PCC materials was completed by following the specification ASTM Standard D075.

CHAPTER 4 PHYSICAL PROPERTIES OF RECYCLED PORTLAND CEMENT CONCRETE AND CONVENTIONAL PIT RUN AGGREGATE MATERIALS

Physical properties such as particle size distribution and fracture count have traditionally been used to classify aggregates in road construction. This chapter presents a summary of the physical properties of City of Saskatoon (COS) recycled Portland cement concrete (PCC) and pit run granular base aggregates. Materials tested as part of this research include:

- Conventional COS granular base,
- Conventional COS drainage rock,
- Recycled PCC well graded base, and
- Recycled PCC drainage rock.

Material tests performed included aggregate gradation, coarse and fine aggregate angularity, standard Proctor compaction, California bearing ratio (CBR), United Soil Classification System (USCS), and Micro-Deval.

One sample specimen for each of the conventional tests was performed. City of Saskatoon specifications require one test to be completed for every 6000 tonnes of subbase, base and crushed rock aggregates (COS 2009B).

4.1 Grain Size Distribution of Research Aggregates

The COS specifies ASTM D6931 for gradation analysis of base and crushed rock aggregate (COS 2009B). Figure 4.1 illustrated the gradations for the COS base aggregate, conventional COS crushed rock, recycled PCC well graded base and recycled PCC drainage rock. The conventional COS granular base fell within the COS specification and was within a specified top rock size of 19 mm; however, the amount of fines was the lower limit of the COS base specification and the large rock size was on the high part of the limit. The conventional COS drainage rock also fell within the COS specifications; the conventional COS drainage rock aggregate had a top size of 25 mm.

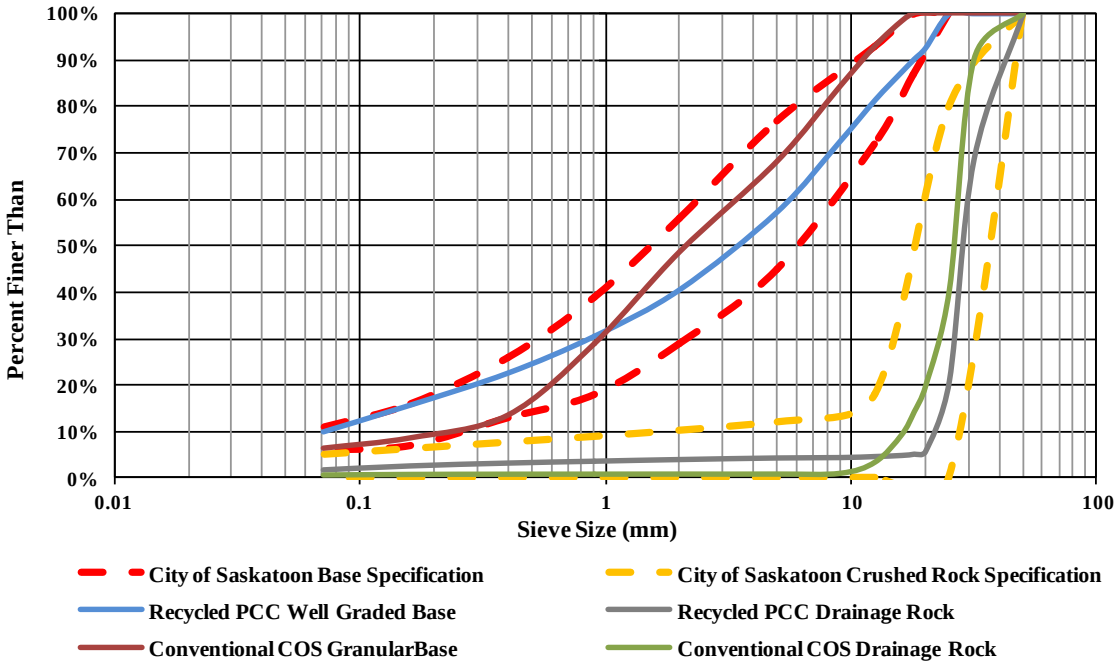

Figure 4.1 Conventional and PCC Grain Size Distributions

The recycled PCC well graded base fell within the COS granular base specification. The PCC well graded base material had a top size of 19 mm and was higher in fines as it approached the top of the upper limit of the COS specifications, as shown Figure 4.1. A higher fine content can improve the compaction of the material and reduce the compaction effort required to reach optimum density. The recycled PCC drainage rock also fell within specification. The PCC drainage rock fell towards the coarse limit of the gradation curve with very few fines. These characteristics make the material ideal for drainage rock applications.

4.2 Organic Content of Aggregates

Figure 4.2 and Figure 4.3 present the organic content for materials sized overall, and less than 5 mm for both conventional and recycled PCC materials, respectively. In both cases, no organic content was measured for the conventional COS drainage rock and the recycled PCC drainage rock due to the large top size of material. Organic material is screened off during the impact crushing process with a grizzly screening located on the feeder of the crusher. The organic content found in the conventional COS granular base was one percent for the material less than 5 mm, and 0.6 percent overall. The recycled GW PCC base material organic content

was 1.6 percent for the material less than 5 mm, and 0.8 percent overall. The COS granular base and GW PCC material met the City's specification of less than three percent organic content.

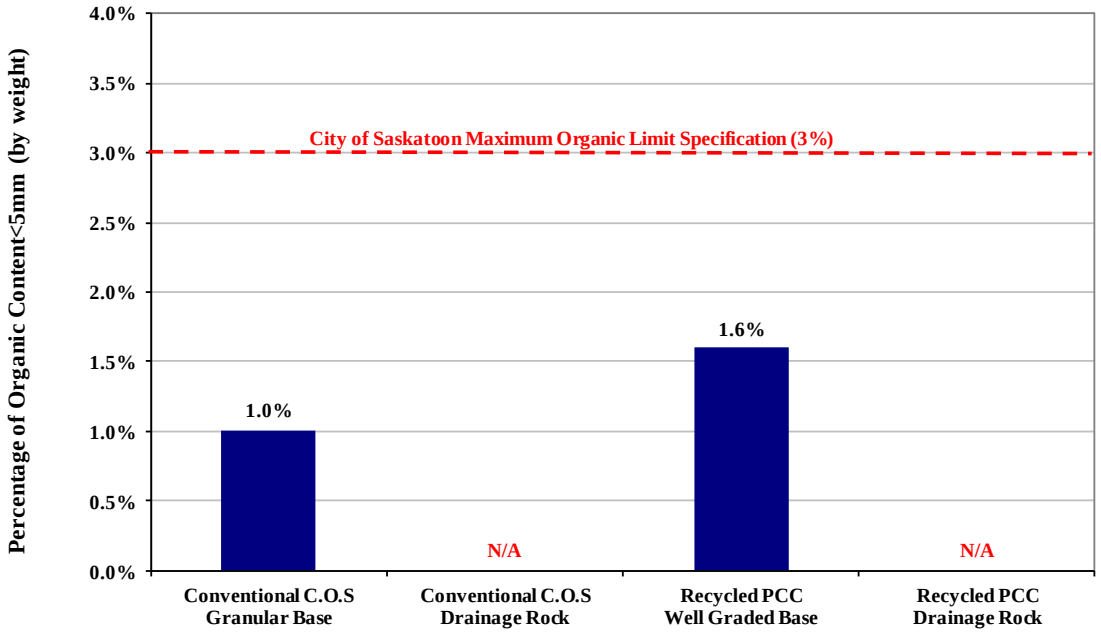

Figure 4.2 Organic Content of Conventional and PCC Materials <5 mm

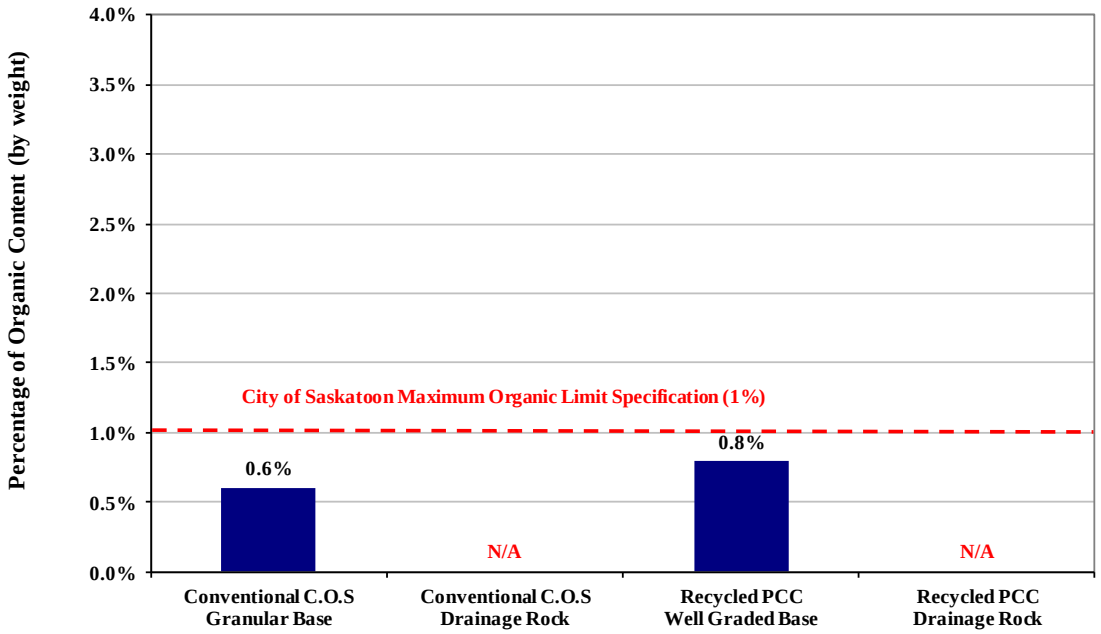

Figure 4.3 Organic Content of Conventional and PCC Material Overall

4.3 United Soil Classification System

The United Soil Classification System (USCS) was used to classify the conventional COS granular base and the PCC well graded base. The conventional COS granular base had a specific gravity of 2.66 and was classified as well graded (GW) base coarse material. The recycled PCC well graded base also was graded using the USCS classification system. The material was classified as a well graded (GW) material with a specific gravity of 2.51. Both crushed rock and PCC rock were not classified as the City does not specific a USCS classification for rock materials.

4.4 Aggregate Angularity

Conventional granular base, conventional drainage rock, recycled GW PCC base material, and recycled PCC drainage rock were characterized for both the fine and coarse aggregate angularity. The COS specifies that coarse angularity be completed on conventional granular base materials and crushed rock materials (COS 2009B). Presently, the City of Saskatoon does not test for fine aggregate angularity. Fine aggregate angularity is important because it quantifies the fine material that fills the voids between the coarse materials in the matrix of compacted material and contributes to aggregate interlock (Huber et al. 1998).

4.4.1 Coarse Aggregate Angularity

The coarse angularity was determined using the City of Saskatoon specifications and ASTM 5821. The specification states that a minimum of 50 percent of the fractured faces, measured by weight on particles greater than 5 mm in nominal dimension must be created during the crushing process (COS 2009B). Figure 4.4 compares the coarse aggregate angularity measured for recycled PCC materials to the coarse aggregate angularity measured for the conventional granular base and drainage rock materials.

The coarse angularity for the recycled PCC well graded base was 95 percent, which greatly exceeded the City's specification. The recycled PCC drainage rock coarse angularity also met COS specification with a percentage of fractured faces of 96 percent. The conventional granular base material did not meet the COS specification of greater than 50 percent fractured faces; the percentage of fractured faces that was measured was 47 percent. The conventional COS drainage rock met COS specifications and had a coarse angularity of 59 percent.

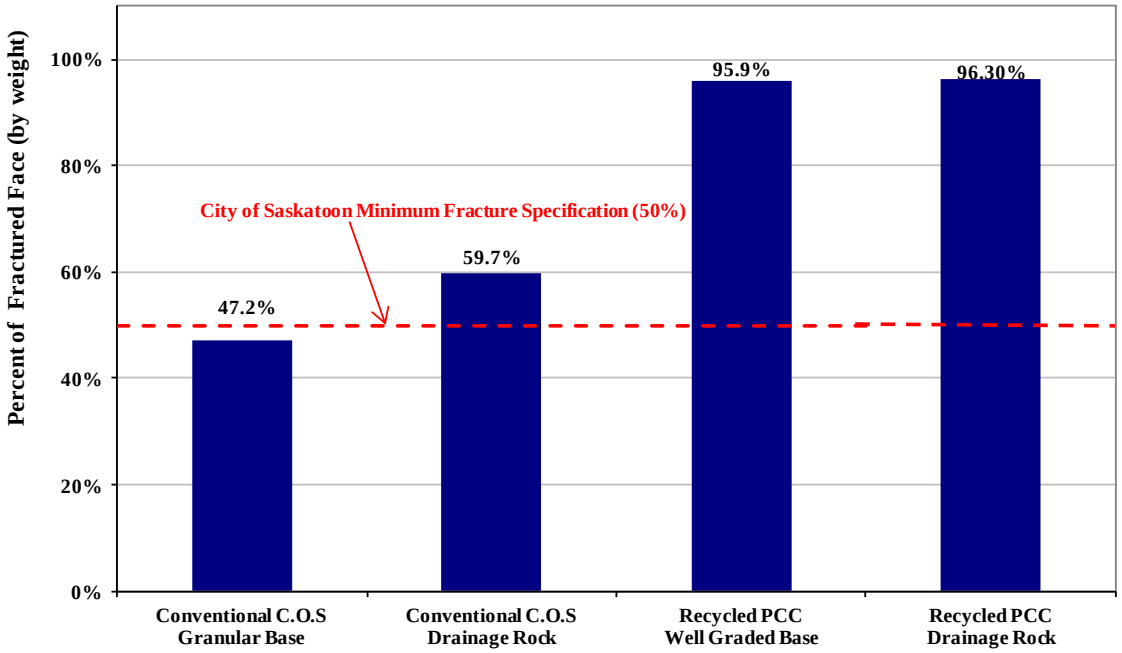

Figure 4.4 Percent Fracture Face for Conventional and Recycled Materials

The difference between the coarse fracture of PCC and conventional granular base pit run can be attributed to original source size and method of crushing. Conventional COS granular base course material and drainage rock are primarily crushed using a jaw and cone type crusher. Using this type of crushing configuration, typical jaw and cone operations have a breakdown ratio of up ten to one. With this limitation the crushers will only crush a small percentage of the aggregate, thus allowing aggregate that is smaller than the maximum size to fall through the crusher without being processed. Using the impact crusher, regardless of the size of aggregate, all the material is fed through the spinning mandrel of the crusher, therefore creating a high fracture count. Due to the nature of the impact crusher, the fractured face percentage is near 100 percent. The deviation from the perfect coarse fracture is caused by the aggregate which was originally used to construct the concrete, but has now fallen out of the concrete matrix during the crushing process. These loose pieces of aggregate tended to be a round stone with no fractures.

4.4.2 Fine Aggregate Angularity

Fine angularity was measured for the conventional COS granular base and recycled PCC well graded base. Fine aggregate angularity testing was not completed on the conventional COS drainage rock or the recycled PCC drainage rock, since there are no fines in the material at this large size.

Fine aggregate angularity is defined as the uncompacted void percentage. The void content of the material depends on the texture and shape of the fine aggregate. To provide a specification for comparison purposes, the Strategic Highway Research Program (SHRP) specification of a minimum of 45 percent uncompacted voids (by weight) was used. Figure 4.5 shows the uncompacted void percentage of both the conventional and recycled PCC research aggregates.

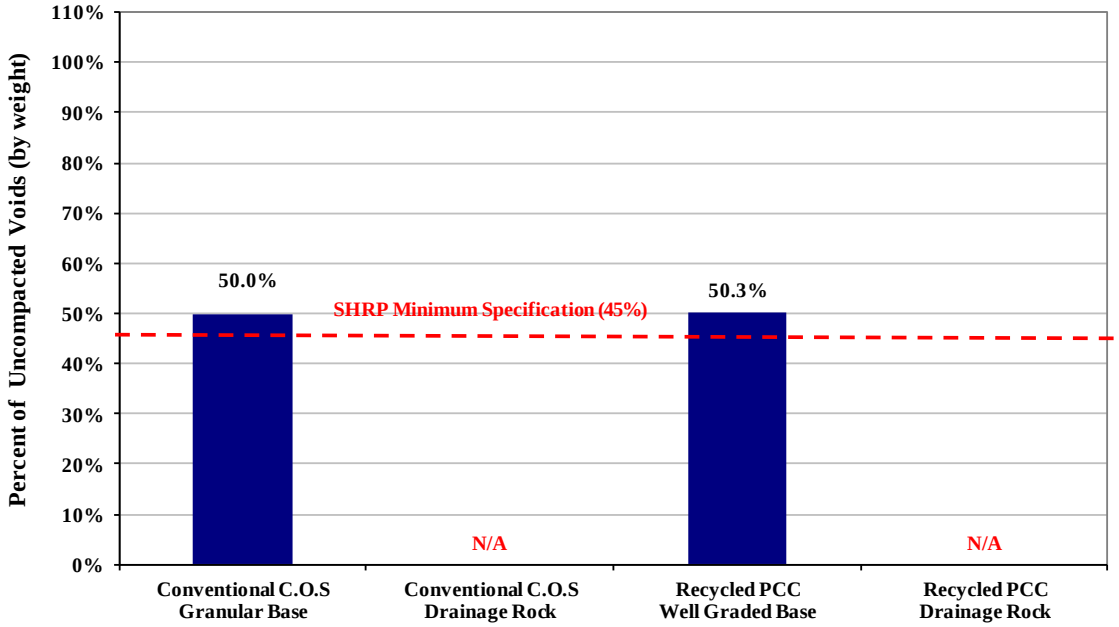

Figure 4.5 Fine Aggregate Angularity

The conventional COS granular base course material had 50 percent uncompacted voids, which met the SHRP specification. The uncompacted void percentage for the recycled PCC well graded base was calculated to be 50 percent, which also met the SHRP specification. The fines contained in the well graded PCC material were observed to be visually more angular due to the fact that the PCC material fines are primarily manufactured. However, this was not reflected in

the test results. No percent uncompacted voids were determined for the conventional and recycled drainage rock as there was little to no fines content in these materials.

4.5 Compaction of Research Materials

Two different compaction methods were used to compact the California Bearing Ratio (CBR) samples. Initially, as specified by the City of Saskatoon Base aggregate specifications the standard Proctor method was first used. A second method of compaction using the gyratory compactor was also conducted. Conventional and recycled PCC drainage rock materials were not standard Proctor compacted because the City's aggregate specifications do not specify the CBR test for rock materials.

4.5.1 Standard Proctor Compaction

Figure 4.6 illustrates the moisture-density relationship for the conventional granular base and the recycled PCC base material by impact Proctor compaction. The conventional COS granular base had a maximum dry density of 2230 kg/m^3 at 6.15 percent moisture. The recycled GW PCC base material had a maximum density of 1980 kg/m^3 at 7.2 percent moisture.

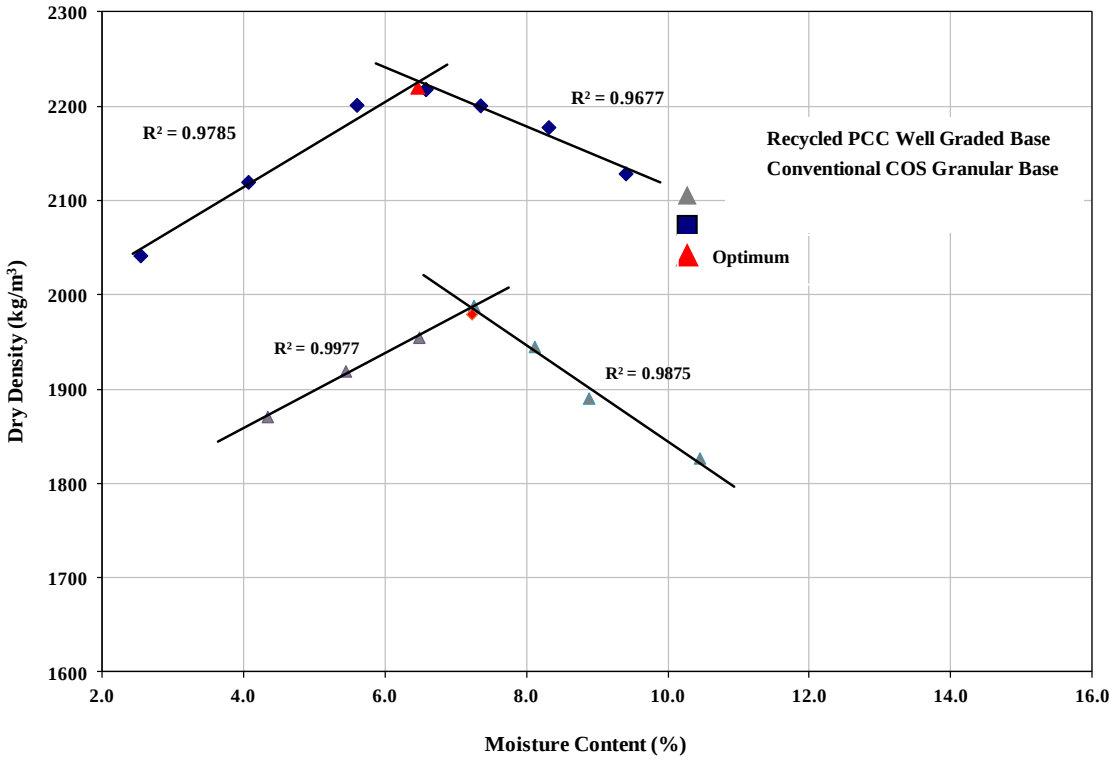

Figure 4.6 Standard Proctor Compaction Results for Base Materials

The optimum density achieved for the PCC base material was within the range observed by other researchers using the Proctor compaction method (Kuo et al. 1998, Arulrajah amd Piratheepan 2010). The optimum density range found by other researchers is from 1820 kg/m^3 to 1980 kg/m^3 at moisture percentages from 7.0 to 12.0 percent moisture for Recycled PCC well graded material with high fines. The lighter density of the recycled PCC GW material compared to the conventional COS granular base can be attributed to its reduced specific gravity (2.51 compared to 2.66).

However, observations were made that the material was not tightly compacted within the mold after the three lifts compacted according to ASTM specifications. Following ASTM specifications, the three lifts of material were compacted at 25 blows per layer per lift in an effort to obtain a maximum density. Recycled PCC GW base material resisted the compaction effort of the impact style compaction specified by the specification. During the Proctor compaction method, the method is dependent on the fines content within the material to act similar to a lubricant allowing the material particles to move around and compact as the Proctor hammer is dropping (Berthelot et al. 2002). However, with the recycled PCC well graded base evaluated in this research, the fines content was lower in that it met the City of Saskatoon base specification. Therefore, the lower amount of fines reduced the effectiveness of the Proctor type style compaction method.

4.5.2 Gyratory Compaction

The gyratory method consists of setting the gyratory to compact with a vertical stress of 600 kPa, at a gyration angle of 1.25 degrees, and to a number of gyrations of 115. The recycled PCC well graded base material and conventional granular base material were compacted using the gyratory compactor. Both specimens were compacted to a height of 150 ±5 mm.

Figure 4.7 illustrates the moisture-density relationship for the conventional granular base and the recycled PCC base material by gyratory compaction. The optimum dry density of the recycled PCC well graded base was 2230 kg/m^3 at 5.2 percent moisture content, which was an increase in density compared to the impact Proctor compaction results. The primary reason for the increase in density is the method of compaction used; gyratory compaction kneads the material into place allowing the material to interlock together.

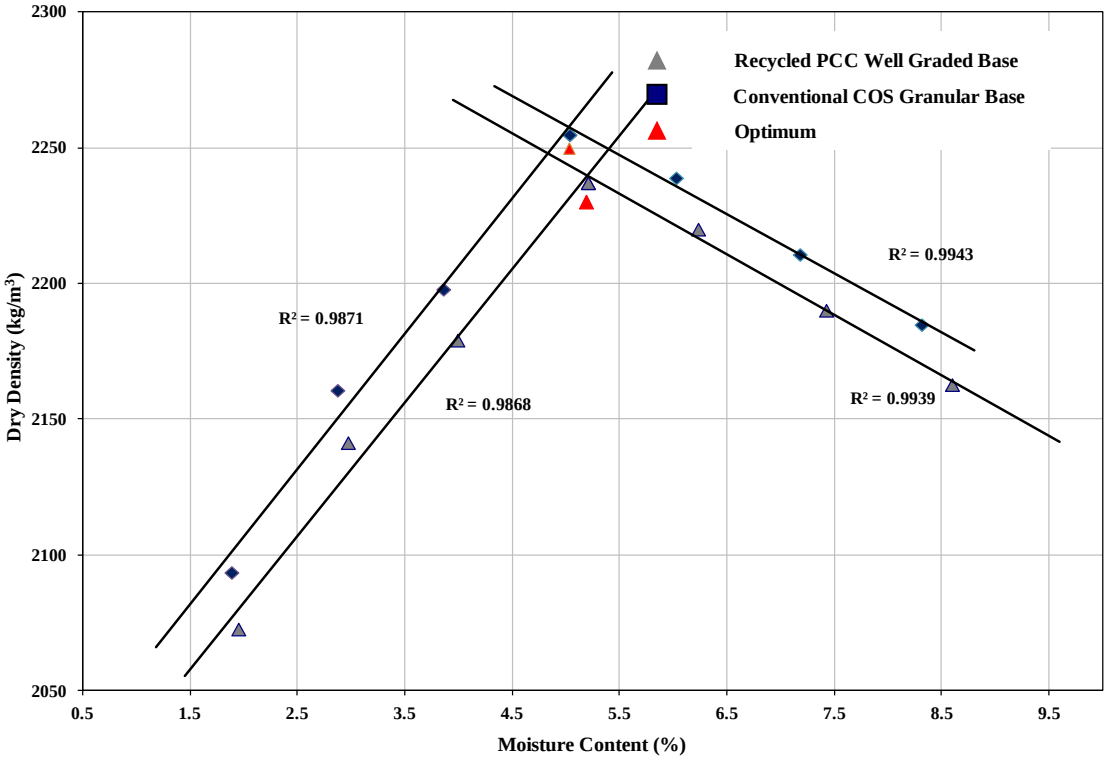

Figure 4.7 Gyratory Compaction Results for Base Materials

4.5.3 Summary of Compaction Results

Table 4.1 summarizes the maximum densities for the recycled PCC well graded base and the conventional COS granular base. The maximum density of the recycled PCC well graded base increased when gyratory compaction was used instead of Proctor compaction. When using the gyratory compaction method, the optimum density of the recycled PCC GW base material increased by approximately 11 percent. The conventional COS granular base had a minimal difference of approximately 0.9 percent in maximum density when comparing the two styles of compaction used.

Table 4.1 Summary of Compacted Dry Density Results

Research Material	Compaction Method	Results (kg/m^3)	Percent Difference (%)
Conventional COS Granular Base	Proctor	2230	0.89
	Gyratory	2250	
Recycled PCC GW Base	Proctor	1980	11.21
	Gyratory	2230	

4.6 California Bearing Ratio (CBR) Characterization

The City of Saskatoon specifies a minimum unsoaked CBR strength of 65%. Figure 4.8 illustrates the unsoaked CBR values of the conventional and PCC base aggregates, compacted using Proctor compaction and gyratory compaction.

The conventional granular base that was standard Proctor compacted had a CBR of 75 percent; the gyratory compacted granular base had a CBR value was 77 percent. There was little difference between these two CBR values. The recycled PCC well graded (GW) material that was standard Proctor compacted had a CBR of 22 percent while the gyratory compacted PCC base had a CBR value of 123 percent. The low CBR value for the Proctor compacted recycled PCC GW sample is likely due to the lower compaction density achieved using impact Proctor compaction.

Initially, when the recycled PCC GW was compacted using the standard effort Proctor method, the CBR value obtained did not meet the COS specification. However, following gyratory compaction, the recycled PCC GW base material achieved a much greater density and subsequent CBR test results. The PCC GW base material has high angularity and fracture count when compared to the conventional granular base. These two properties enable the material to have good aggregate interlock, which results in a high CBR value. The CBR value obtained for the conventional COS base course material using both Proctor compaction and gyratory compaction methods are similar. This demonstrates that both compaction methods are applicable for aggregate material compaction purposes.

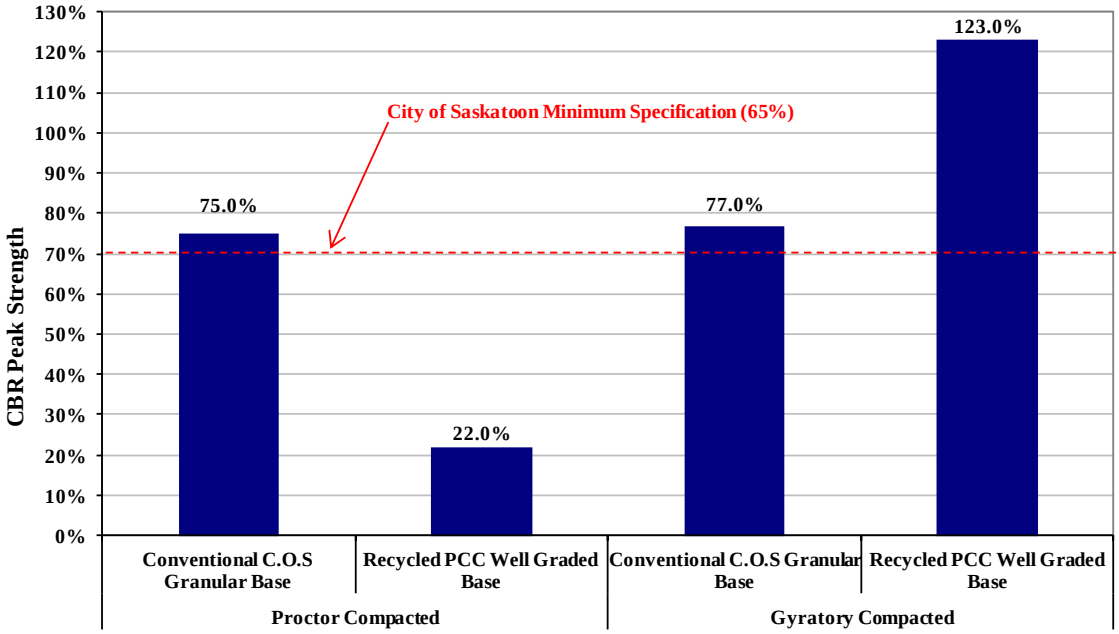

Figure 4.8 CBR Peak Strength Unsoaked Results

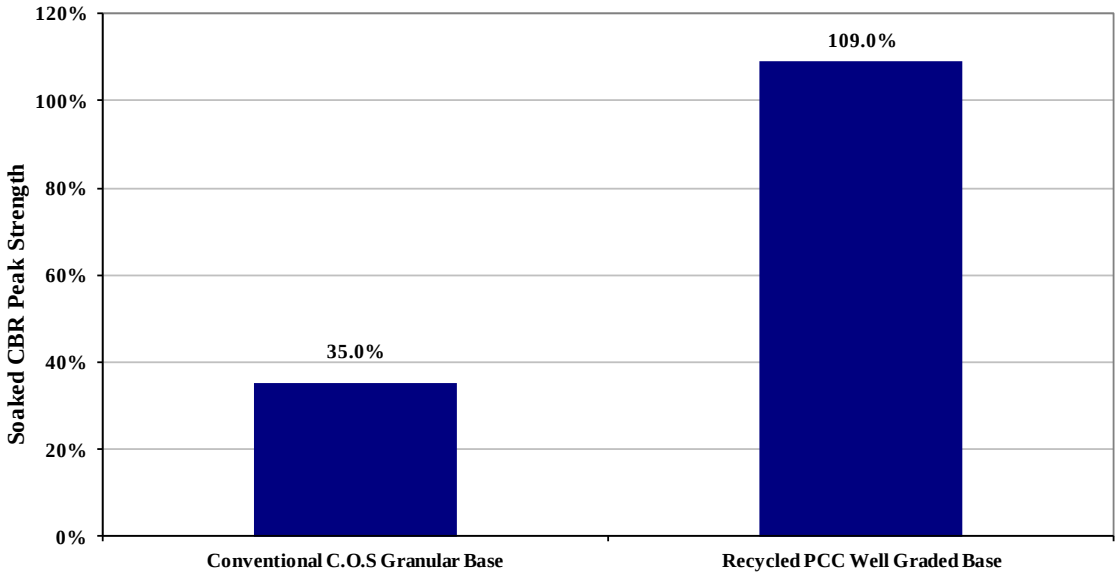

Figure 4.9 CBR Peak Strength Soaked Results, Gyratory Compacted Specimens

The City of Saskatoon does not specify an unsoaked CBR value. Figure 4.9 illustrates the unsoaked CBR values for the conventional and PCC base aggregates, compacted using gyratory compaction only. This result shows that when soaked, the recycled PCC base material has a higher CBR value compared to the conventional granular base material. The loss in strength highlights the reason why road agencies such as Ministry of Highways and Infrastructure apply

weight restrictions during periods of road structure saturation (Berthelot et al. 2009B). These results show the effect of soaked conditions on a base layer.

4.7 Micro-Deval Abrasion Resistance

The conventional COS granular base, conventional COS drainage rock, recycled PCC well graded base, and recycled PCC drainage rock were assessed using the Micro-Deval test (ASTM D7438). For both materials, samples of 1500 ±5 grams consisting of material retained on the 16.0 mm, 12.5 mm, 9.5 mm were placed in the drum followed by 5000 ± 5 grams of steel balls, and two liters of water.

Figure 4.10 illustrates the Micro-Deval test percent abrasion loss for all conventional and recycled PCC research materials. The conventional COS granular base and conventional drainage rock had good abrasion resistance with an abrasion loss of 8.7 percent, which is well below the NCHRP specification of 18 percent. Both PCC materials had a measured abrasion loss of 15.8 percent, which also fell below the NCHRP specification. The recycled PCC materials had a higher abrasion loss compared to the virgin base aggregates and rock, which may be due to the cement mortar that is present in the PCC aggregates.

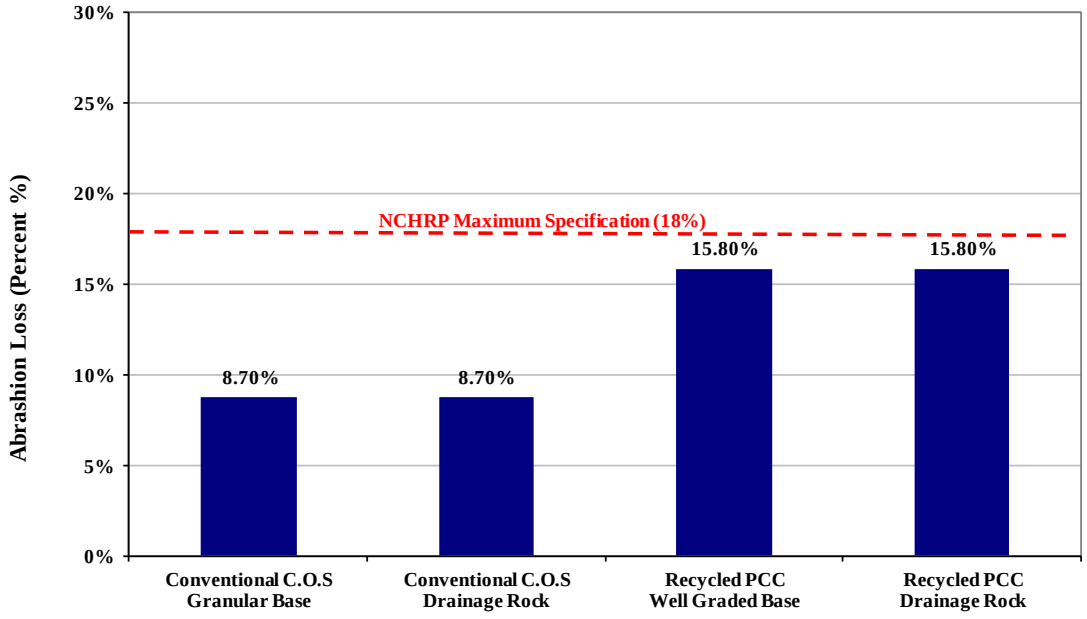

Figure 4.10 Percentage Loss of Material Due to Micro-Deval Abrasion

4.8 Chapter Summary

Based on the conventional materials characterization performed on aggregate materials considered in this study, it was found that the recycled Portland cement concrete materials can be crushed to meet conventional material specifications set by the City of Saskatoon including gradation, organic content, and aggregate angularity.

The standard Proctor compaction method was used to compact recycled PCC GW material and resulted in a low (unsoaked) CBR value that did not meet COS specification. Gyratory compaction was used to compact specimens for CBR testing, which resulted in CBR values that met City specifications for both the conventional base and recycled PCC base materials.

Fine aggregate angularity was measured due to the significance of how the fines can affect the performance of a base layer. The conventional COS granular base and PCC GW base had the same fine angularity, meeting specifications set by SHRP.

Following the Micro-Deval test, the recycled PCC materials had a higher abrasion loss compared to the virgin base aggregates and rock, which may be due to the cement mortar that is present in the PCC aggregates.

CHAPTER 5 MECHANISTIC CHARACTERIZATION OF MATERIALS

The second laboratory element of this research included mechanistic laboratory characterization of conventional COS granular base, recycled PCC drainage rock, and recycled PCC GW base material without stabilizers, as well as recycled PCC GW base material with added cement and emulsion stabilizers. The research aggregates were gyratory compacted, moist cured for 28 days, tested in the rapid triaxial test (RATT), vacuum saturated, then tested in the RATT again.

This Chapter describes the testing protocol and mechanistic material characterization of the research aggregates.

5.1 Research Aggregates

Five repeat samples of conventional COS granular base were compacted using the gyratory compactor. The conventional COS granular base was used as a baseline to compare and evaluate the different PCC materials. Five repeat samples of recycled PCC GW base material were tested using the following stabilization systems:

- Two percent cement,
- Two percent slow-setting (SS-1) emulsion,
- One percent cement with one percent SS-1 emulsion,
- Three percent cement with three percent SS-1 emulsion, and
- 1.5 percent cement with 1.5 percent SS-1 emulsion.

No stabilizers were added to the recycled PCC drainage rock because drainage rock is designed to be poorly graded for drainage purposes. Only one sample of the recycled PCC drainage rock was tested. Due to the high angularity and degree of coarseness of the large aggregate size of the material, there was a risk of rupturing the bladder of the rapid triaxial tester cell. Conventional COS drainage rock was not tested using the RATT cell due to the same concerns of rupturing the bladder.

5.2 Gyratory Shear Stress Compaction Profile of Research Aggregates

All samples were compacted using gyratory compaction. The Servopac-type gyratory compactor, which was used to compact the samples, uses the following algorithm to calculate the shear stress of the material. The equation used in the algorithm is Equation 5.1.

$$G_s = \frac{2PL}{Ah} \qquad \textbf{Equation 5.1}$$

Where:

G_s = Shear Stress (kPa)

P = Average pressure measured in gyratory actuators (N)

L = Average distance from midpoint of sample to the midpoint of actuators (m)

A = Area of the Sample (m^2)

h = Height of the sample (m)

Using the gyratory compactor, the shear stress profiles were measured for the conventional COS granular base recycled PCC well graded base and the recycled PCC drainage rock. Shear stress dissipation capability is important within the top layers of the road because stresses applied by traffic must be dissipated. The layers below are typically built with lower quality materials, resulting in lower strength and lower resistance to the applied shear stress. If the material used to build the top two layers is of lower quality material, which is what has been observed in Saskatchewan due to the depletion of aggregate reserves, the end result is the increased plastic deformation in all structural layers prior to its expected design life (Xu and Berthelot 2010).

The shear stress profiles for both the recycled PCC well graded base and the recycled PCC drainage rock can be seen in Figure 5.1. The conventional COS granular base peak shear stress was 218 kPa, after 100 gyrations. The maximum measured shear stress for the recycled PCC well graded base material was 371 kPa after 100 gyrations. The recycled PCC drainage rock had a maximum shear stress value of 429 kPa after 100 gyrations.

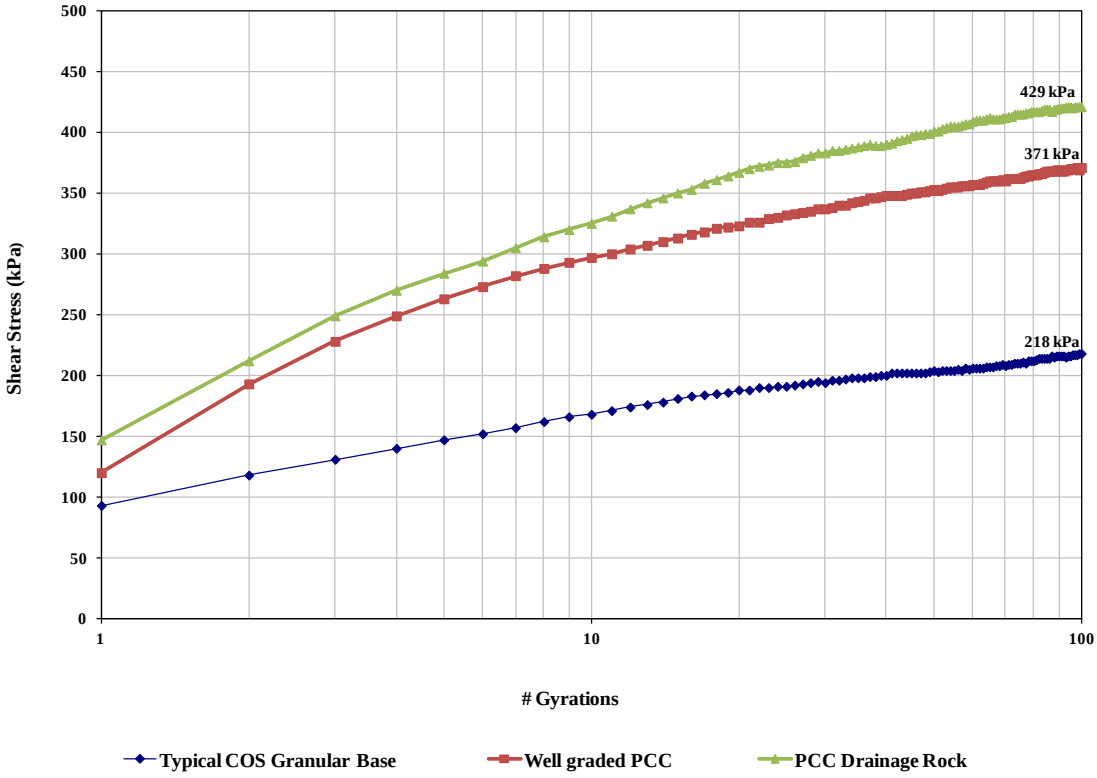

Figure 5.1 Shear Stress Measured for COS Granular Base, Well Graded PCC and PCC Drainage Rock

Using the conventional COS granular base a base line for comparison, the PCC materials offer increased shear stiffness compared to the granular base. Shear stiffness is important within the structural layers of a road, because it is within the top layers of the road in which the stresses applied by traffic must be dissipated. The layers below are typically built with lower quality materials, resulting in lower strength and lower resistance to the applied shear stress (Xu and Berthelot 2010).

5.3 Triaxial Frequency Sweep Characterization

The conventional COS granular base, recycled PCC well graded base both stabilized and unstabilized, along with the unstabilized recycled PCC drainage rock were tested mechanistically using the rapid triaxial test (RATT) cell. The COS does not have a specification for mechanistically testing aggregate materials. Testing protocols used in this research have been developed based on stress analysis across realistic field state conditions (Berthelot et al. 2005).

The mechanistic material properties determined include the dynamic modulus, Poisson's ratio, recoverable radial micro-strain, and phase angle.

5.3.1 Triaxial Frequency Sweep Testing Procedure

Gyratory samples were tested in the rapid triaxial test (RATT) apparatus in an order such that the magnitude and frequency of the axial load, as well as confinement pressures gradually increased in terms of structural damage of the sample, as listed in Table 5.1. The low stress state was applied first, the medium stress state next, followed by the high stress state and the fully reversed stress state. By increasing the magnitude of the axial load and frequency, the RATT cell simulates varying vehicle loading, such as the difference between the loadings caused by a passenger vehicle, and a primary loaded heavy truck. Varying the radial confinement pressure simulates various locations within a pavement structure. Stress state one (low) simulates loading of light traffic with gross vehicle weight of less than 8,000 kg such as passenger cars and trucks; stress state two (medium) represents vehicles up until a gross vehicle weight of 25,000 kg, such as a City bus or two axle dump truck. Stress state three (high) represents the loading experienced by vehicles with a gross vehicle weight between 25,000 kg up to 62,500 kg. An example would include a four axle cement truck or an eight axle B-train.

Loads were applied at frequencies that represent varied traffic speeds. A high frequency of 10 Hz simulates high traffic speeds and 0.5 Hz simulates low traffic speeds.

The samples were initially tested in the RATT at 20^{o}C after being moisture cured for 28 days. Following moisture cure RATT testing, the samples were vacuum saturated, and then tested in the RATT again. Vacuum saturation was conducted on the recycled PCC GW base samples. Vacuum saturation was not done on the conventional COS granular base because the samples failed during the testing prior to vacuum saturation. All the vacuum saturation testing was performed at room temperature.

Table 5.1 Triaxial Frequency Sweep Testing Stress States

Stress State	Confinement Pressure (kPa)	Maximum Dynamic Pressure (kPa)	Minimum Dynamic Pressure (kPa)	Axle Load Frequency (Hz)
1) Low	250	200	0	10
	250	200	0	5
	250	200	0	1
	250	200	0	0.5
2) Medium	250	400	0	10
	250	400	0	5
	250	400	0	1
	250	400	0	0.5
3) High	100	550	0	10
	100	550	0	5
	100	550	0	1
	100	550	0	0.5
4) Fully Reversed	250	200	-200	10
	250	200	-200	5
	250	200	-200	1
	250	200	-200	0.5

Vacuum saturating the research aggregate material samples involved removing all the entrapped air within the sample matrix by applying a vacuum source to force water into the effective pores of the coarse aggregate structure, as illustrated in Figure 5.2. The vacuum saturation procedure used in this research was similar to that of AASHTO T283. Similar procedures have been previously used by other researchers (Berthelot 2010C, Birgisson et al. 2004, Kringos et al. 2009). During the procedure, the samples were saturated under vacuum for eight hours and then allowed to drain for 16 hours before being tested again in the RATT.

Figure 5.3 illustrates an unstabilized PCC well graded specimen that failed in vacuum saturation testing. In this case, following saturation and draining of the sample, it collapsed when being removed from the saturation chamber and could not be tested further in the RATT.

Figure 5.2 Vacuum Saturation of a Recycled PCC Well Graded Base Sample

a) Specimen in Mould **b) Specimen Removed from Mould**

Figure 5.3 Unstabilized PCC Well Graded Specimen Following Vacuum Saturation

The mechanistic properties evaluated include: Dynamic Modulus (E_D); Poisson's Ratio (υ); Recoverable Radial Micro Strain ($\varepsilon_{22}=\varepsilon_{33}$); and Phase Angle ($\delta$). These RATT results provided herein are for both low and high stress states, at frequencies of 10 Hz and 0.5 Hz. All data is included in Appendix A.

The charts included in the proceeding sections include the mean values of five repeat samples tested for the conventional COS granular base, as well as the untreated and treated

recycled PCC GW base, with the error bars representing the highest and lowest value obtained out of the five samples tested. Since only one sample of recycled PCC drainage rock was tested, there are no error bars for that sample. The material property results measured at 10 Hz and 0.5 Hz at low and high stress states are presented herein.

5.4 Dynamic Modulus Results

As explained in Chapter Two, the dynamic modulus is the absolute value of the peak stress to peak strain during material testing at a given testing condition. The dynamic modulus is used to measure the stress strain relationship in material structure during an applied dynamic load also known as the stiffness of the material.

Table 5.2 presents the dynamic modulus for the research materials at both a low and high stress state across 0.5 Hz and 10 Hz loading frequencies, following moist cure and vacuum saturation. Figure 5.4 and Figure 5.5 illustrate the low and high stress states at a test frequency of 10 Hz. Figure 5.6 and Figure 5.7 illustrate the low and high stress states at a test frequency of 0.5 Hz.

A few of the general trends that were observed in the dynamic modulus data included the following:

- The dynamic modulus of the research materials increased as the testing frequency increased from 10 Hz to 0.5 Hz. Also, the dynamic modulus decreased as the stress state increased from low to high.
- Across both stress states and frequencies as well as pre and post vacuum saturation, the stabilized sample containing three percent cement had the highest stiffness.
- Across all of the research materials after the materials were vacuum saturated, the measured stiffness of the materials decreased.

Table 5.2 Dynamic Modulus Results

Dynamic Modulus	Moist Cured				Vacuum Saturated				Percent difference (%)			
	Stress State				Stress State				Stress State			
	Low		High		Low		High		Low		High	
	10 Hz	0.5 Hz	10 Hz	0.5 Hz	10 Hz	0.5 Hz	10 Hz	0.5 Hz	10 Hz	0.5 Hz	10 Hz	0.5 Hz
Granular Base												
Max (MPa)	479	491	298	0	0	0	0	0				
Min (MPa)	412	422	293	0	0	0	0	0				
Avg (MPa)	446	457	296	Failed	Failed	Failed	Failed	Failed	N/A	N/A	N/A	N/A
Drainage Rock												
Max (MPa)	0	0	0	0	0	0	0	0				
Min (MPa)	0	0	0	0	0		0	0				
Avg (MPa)	732	771	522	526	N/A	N/A	N/A	N/A	N/A	N/A	N/A	N/A
Well Graded PCC Max												
Max (MPa)	1121	1147	710	727	733	793	0	0				
Min (MPa)	886	940	569	589	619	662	0	0				
Avg (MPa)	1031	1081	632	652	676	728	Failed	Failed	34.4	32.7	N/A	N/A
2% Cement Max												
Max (MPa)	1539	1623	1094	1097	1193	1272	783	770				
Min (MPa)	1295	1387	883	910	1009	1084	694	677				
Avg (MPa)	1467	1542	995	1003	1083	1158	747	728	26.2	24.9	24.9	27.4
2% SS-1 Max												
Max (MPa)	1614	1507	1223	1006	1160	1042	779	655				
Min (MPa)	1361	1271	1042	869	847	789	665	558				
Avg (MPa)	1438	1342	1113	923	947	877	713	602	34.1	34.6	35.9	34.8
2% Cement/SS-1 Max												
Max (MPa)	1980	2045	1469	1364	1357	1360	928	828				
Min (MPa)	1641	1698	1243	1154	1085	824	756	706				
Avg (MPa)	1813	1833	1336	1240	1248	1201	853	766	31.2	34.5	36.2	38.2
3% Cement Max												
Max (MPa)	2683	2652	1984	2008	1978	2063	1424	1382				
Min (MPa)	1950	2084	1461	1502	1466	1557	997	981				
Avg (MPa)	2357	2425	1758	1765	1759	1838	1233	1194	25.4	24.2	29.9	32.4
3% SS-1 Max												
Max (MPa)	1836	1606	1514	1143	923	842	758	602				
Min (MPa)	1435	1238	1130	878	688	587	601	473				
Avg (MPa)	1576	1370	1277	984	813	686	668	539	48.4	49.9	47.7	45.2
3% Cement/SS-1												
Max (MPa)	2036	1945	1576	1364	1602	1531	1129	962				
Min (MPa)	1802	1794	1471	1295	1362	1312	1006	863				
Avg (MPa)	1936	1884	1520	1332	1465	1386	1073	890	24.3	26.4	29.4	33.2

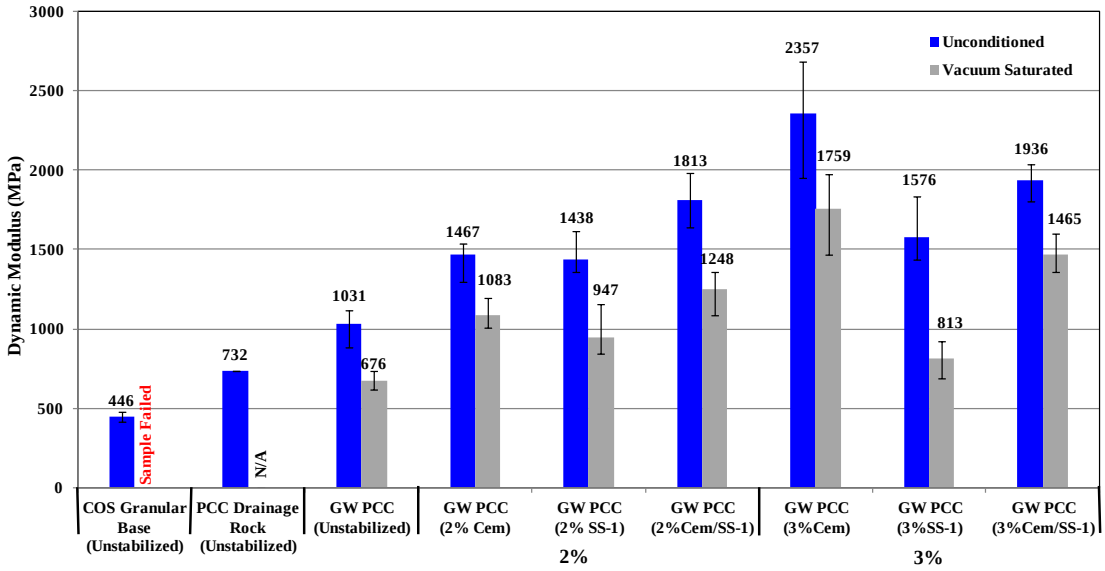

Figure 5.4 Mean Dynamic Modulus Low Stress State (σ=250kPa, Δσ=200 kPa), 10 Hz

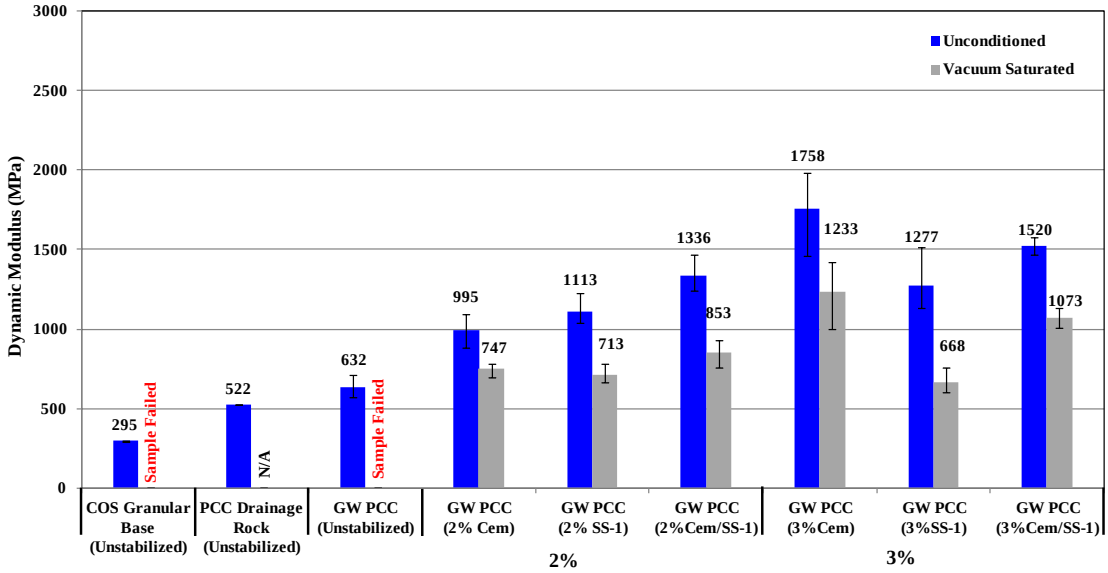

Figure 5.5 Mean Dynamic Modulus High Stress State (σ=100kPa,Δσ=550 kPa), 10 Hz

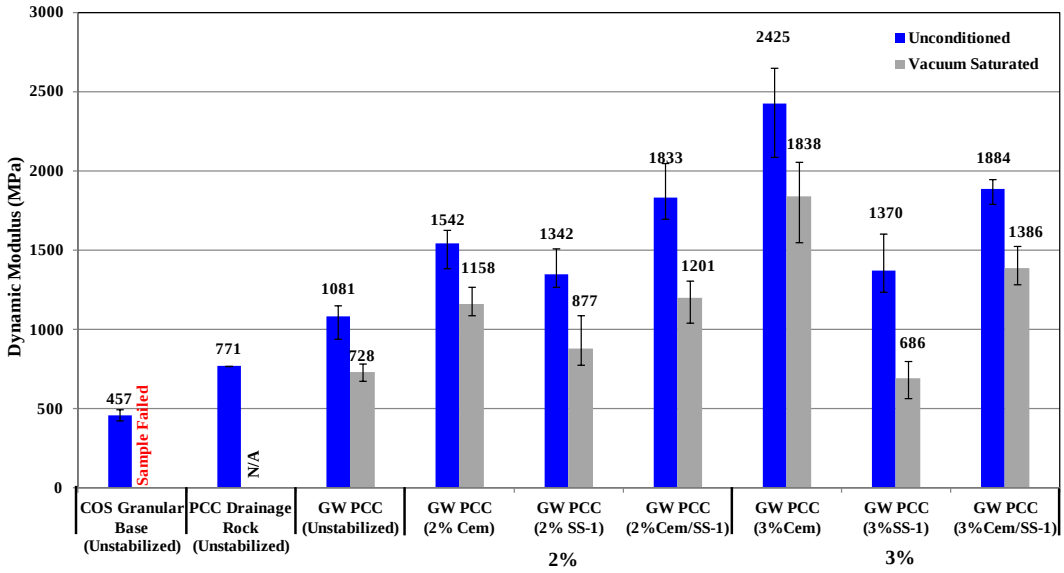

Figure 5.6 Mean Dynamic Modulus Low Stress State (σ=250kPa,Δσ=200 kPa), 0.5 Hz

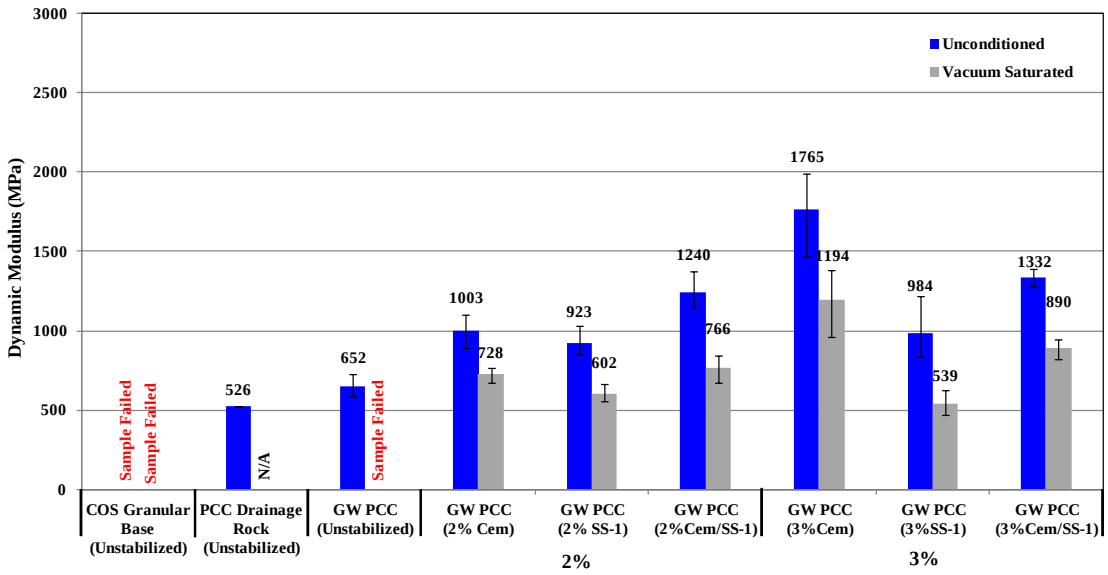

Figure 5.7 Mean Dynamic Modulus High Stress State (σ=100kPa,Δσ=550 kPa), 0.5 Hz

As seen in Figure 5.4 to Figure 5.7, the untreated recycled PCC GW base material had a considerably higher dynamic modulus when compared to the conventional COS granular base course material across two different loading frequencies and stress states under which the samples survived. As seen in Figure 5.4, in low stress state at 10 Hz, the conventional COS granular base had a mean dynamic modulus of 446 MPA which was much lower than the dynamic modulus of untreated recycled PCC GW base, which had a mean value of 1031 MPa.

The conventional COS granular base samples failed at the high stress state and a testing frequency of 0.5 Hz, prior to vacuum saturation, as seen in Figure 5.7. In comparison, the untreated recycled PCC GW base failed; however, it failed after it was vacuum saturated at the high stress state at a testing frequency of 10 Hz as seen in Figure 5.5.

In comparison, between conventional COS granular base and the PCC drainage rock, the PCC drainage rock had a higher stiffness across both testing frequencies and stress states prior to vacuum saturation. The recycled PCC drainage rock also maintained stiffness when the conventional COS granular base failed in the high stress state at a testing frequency of 0.5 Hz as seen in Figure 5.7. As seen in Figure 5.6, the recycled PCC drainage rock had a mean dynamic modulus of 771 MPa which was much higher than the conventional base, which had a mean value of 457 MPa.

When comparing the different stabilizers, not all the stabilizers performed the same. The added stabilizers did enhance the dynamic modulus values of the recycled PCC GW base when compared to the untreated recycled PCC GW base. When comparing the performance of the stabilized samples of recycled PCC GW base, the sample containing three percent cement had the highest stiffness, as seen in Figure 5.6. For example, Figure 5.6 shows the recycled PCC GW base treated with three percent cement had a mean dynamic value of 2425 MPa, which was significantly higher than the untreated recycled PCC GW base or the conventional COS granular base which had a mean stiffness of 457 MPa. However, it is shown in that same figure that the deviation of the measured values illustrated by the error bars was also a lot higher compared to the stabilized samples.

It is hypothesised that large deviations in the dynamic modulus may be attributed to an interaction between the high percentage of cement contained in the sample, and the existing amounts of cement that never hydrated contained within the recycled PCC GW base.

It was observed across both stress states and loading frequencies that the samples of recycled PCC well graded base containing three percent cement maintained the highest dynamic modulus or stiffness out of all the research materials. Some caution should be exercised if using this material in a road structure under Saskatchewan field state conditions. When a material is stabilized with too much stabilizer and becomes too stiff, the material starts to crack, therefore reducing its performance in both stiffness and survival of the freeze thaw cycles found in Saskatchewan's field state conditions (Podborochynski et al. 2011, Haichert et al. 2011). A reduction in stabilizer content will reduce the potential of cracking with a stabilized base layer and still add stiffness to the material. Over stabilizing materials is not limited to PCC material. Conventional granular base can also be over stabilized.

Overall, as seen in Figure 5.4 through Figure 5.7, adding cement stabilizers increased the stiffness of the PCC material. Through the same figures the increase of SS-1 stabilizer from two to three percent gave a minimal increase in stiffness. For example, as seen in Figure 5.5 the sample containing two percent SS-1 had a mean dynamic value of 1113 MPa and the three percent SS-1 sample had a mean value of 1336 MPa. Similar increases in stiffness were also observed for the samples containing two and three percent cement and SS-1.

After the samples were vacuum saturated, the dynamic modulus of all the samples across both stress states and loading frequencies decreased. The overall reduction of the dynamic modulus across the different materials was between 25 and 50 percent after the samples were vacuum saturated as seen in Table 5.2. However, all the stabilized recycled PCC GW samples maintained stiffness that was higher than both the untreated recycled PCC GW base and the conventional COS granular base post vacuum saturation. Figure 5.6 shows that the recycled PCC GW base with two percent SS-1 had a mean value of 877 MPa post vacuum saturation at 0.5 Hz low stress state, which was higher than unstabilized recycled PCC GW base material which had a mean value of 728 MPa at the same testing parameters. The recycled PCC GW base with the two percent SS-1 sample was stiffer than the conventional COS granular base sample, which failed. The only exception to the stabilized samples outperforming the untreated sample occurred at the low stress state, at a testing frequency of 0.5 Hz after vacuum saturation. The recycled PCC GW base containing three percent SS-1 had the lowest dynamic modulus out of all stabilized and untreated samples of recycled PCC GW base material.

5.5 Phase Angle Results

Phase angle is the phase shift in time between the applied stress and the resultant strain during a repeated load axial testing. The test is used to indicate the viscous-elastic properties of the material (Berthelot et al. 2009A, Osman 2005). In a purely elastic material the angle is 0 degrees, in a purely viscous state the phase angle is 90 degrees and phase angles between 0 and 90 degrees are viscoelastic. Phase angle has been used as an indication of the potential viscoelastic stiffness effects within a material system. Further discussion on phase angle can be found in Chapter Two.

As with dynamic modulus, the phase angle was measured during the testing of the samples with the RATT cell. Table 5.3 presents the combined phase angle for each of the research materials at both low and high stress states across 10 Hz and 0.5 Hz testing frequencies, following moist cure and vacuum saturation. Figure 5.8 and Figure 5.9 illustrate the low and high stress states at a test frequency of 10 Hz. Figure 5.10 and Figure 5.11 illustrate the low and high stress states at a test frequency of 0.5 Hz.

A few of the general trends that were observed in the phase angle data included the following:

- The phase angle of the research materials decreased as the testing frequency increased from 10 Hz to 0.5 Hz. Also the phase angle increased as the stress state increased from low to high.
- Across both stress states and frequencies as well as pre and post vacuum saturation, the stabilized sample containing three percent cement had the lowest phase angle.
- Across all of the research materials after they were vacuum saturated, the measured phase angle of the materials increased, except for the recycled PCC GW base with three percent SS-1 at high stress state and 0.5 Hz.

Table 5.3 Mean Phase Angle Results

Phase Angle	Moist Cured				Vacuum Saturated				Percent difference (%)			
	Stress State				Stress State				Stress State			
	Low		High		Low		High		Low		High	
	10 Hz	0.5 Hz	10 Hz	0.5 Hz	10 Hz	0.5 Hz	10 Hz	0.5 Hz	10 Hz	0.5 Hz	10 Hz	0.5 Hz
Granular Base												
Max (deg.)	8.6	5.1	15.2	0.0	0.0	0.0	0.0	0.0				
Min (deg.)	8.2	4.8	14.7	0.0	0.0	0.0	0.0	0.0				
Avg (deg.)	8.4	4.9	15.0	Failed	Failed	Failed	Failed	Failed	N/A	N/A	N/A	N/A
Drainage Rock												
Max (deg.)	0.0	0.0	0.0	0.0	0.0	0.0	0.0	0.0				
Min (deg.)	0.0	0.0	0.0	0.0	0.0	0.0	0.0	0.0				
Avg (deg.)	8.6	5.2	10.6	7.3	N/A	N/A	N/A	N/A	N/A	N/A	N/A	N/A
Well Graded PCC Max												
Max (deg.)	9.9	5.5	11.3	7.8	10.2	6.7	0.0	0.0				
Min (deg.)	7.7	5.0	10.2	7.1	9.4	6.1	0.0	0.0				
Avg (deg.)	8.8	5.2	10.7	7.4	9.8	6.4	Failed	Failed	10.4	18.5	N/A	N/A
2% Cement Max												
Max (deg.)	7.9	5.1	9.9	6.9	10.2	5.9	11.7	7.8				
Min (deg.)	6.1	4.5	8.6	5.8	8.5	5.0	10.9	7.4				
Avg (deg.)	7.2	4.8	9.3	6.3	9.4	5.4	11.1	7.6	23.0	11.8	16.0	17.2
2% SS-1 Max												
Max (deg.)	12.1	9.4	14.4	11.5	15.7	10.0	16.1	12.1				
Min (deg.)	11.3	8.0	13.2	10.9	13.6	8.6	14.7	11.1				
Avg (deg.)	11.7	8.8	13.8	11.3	14.5	9.5	15.5	11.7	19.1	7.0	11.4	2.6
2% Cement/SS-1 Max												
Max (deg.)	10.1	7.4	12.0	9.4	13.1	9.0	14.9	10.5				
Min (deg.)	8.3	5.0	11.0	8.5	10.5	7.0	12.9	9.8				
Avg (deg.)	9.5	6.6	11.5	9.0	11.4	7.5	13.6	10.0	16.7	12.6	15.5	10.3
3% Cement Max												
Max (deg.)	8.6	5.2	9.0	6.1	9.7	5.8	11.0	7.8				
Min (deg.)	6.1	3.8	7.8	5.6	8.1	4.6	9.6	6.7				
Avg (deg.)	6.9	4.2	8.3	5.8	8.8	5.3	10.2	7.2	22.2	19.7	19.0	19.4
3% SS-1 Max												
Max (deg.)	15.0	10.8	16.3	13.1	18.8	12.8	17.8	13.0				
Min (deg.)	11.5	10.0	14.5	12.5	14.7	10.2	17.1	12.6				
Avg (deg.)	12.9	10.3	15.4	12.9	16.7	11.2	17.5	12.7	22.3	8.3	12.2	1.2
3% Cement/SS-1												
Max (deg.)	10.6	8.2	13.2	10.8	13.4	9.3	15.3	11.4				
Min (deg.)	8.0	6.8	11.2	9.2	12.0	7.8	13.4	10.2				
Avg (deg.)	9.6	7.3	12.3	10.1	12.6	8.4	14.6	11.0	24.1	13.3	16.0	8.0

As seen in Figure 5.8 through Figure 5.11, the measured phase angles were approximately the same for the conventional COS granular base and the recycled PCC GW base under a low stress state and both testing frequencies of 10 Hz and 0.5 Hz. For example, as seen in Figure 5.8, the average measured phase angle for conventional COS granular base was 8.4 degrees, whereas the mean value of recycled PCC GW base was 8.8 degrees. When the stress state increased, the phase angle for the conventional COS granular base was higher than recycled PCC GW base at a testing frequency of 10 Hz, seen in Figure 5.9. As seen in Figure 5.11, the conventional COS granular base sample failed and the recycled PCC GW base survived and had a mean value of 7.4 degrees.

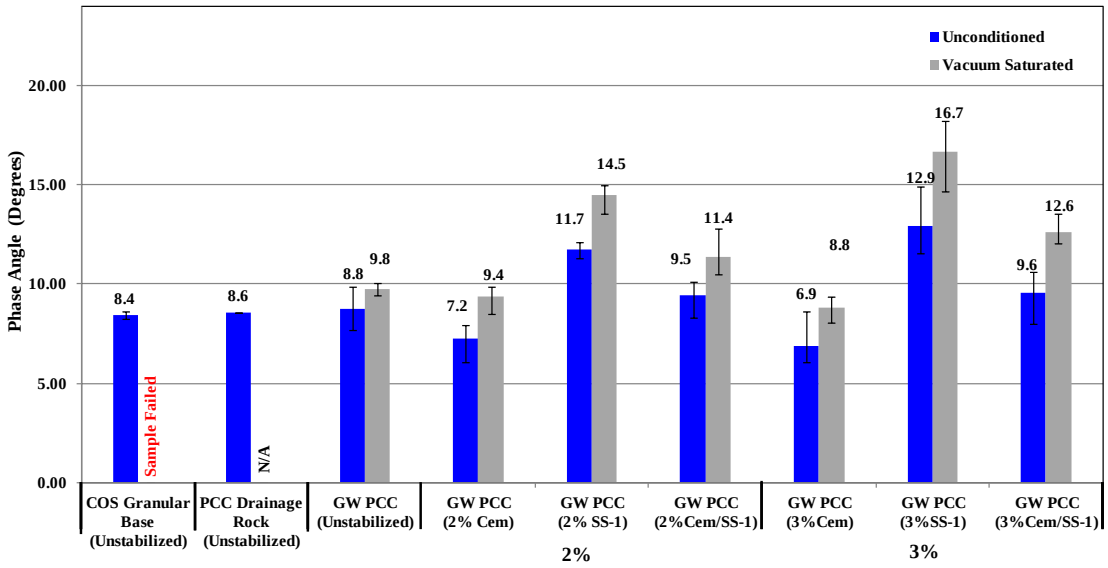

Figure 5.8 Mean Phase Angle Low Stress State (σ=250kPa, Δσ=200 kPa) at 10 Hz

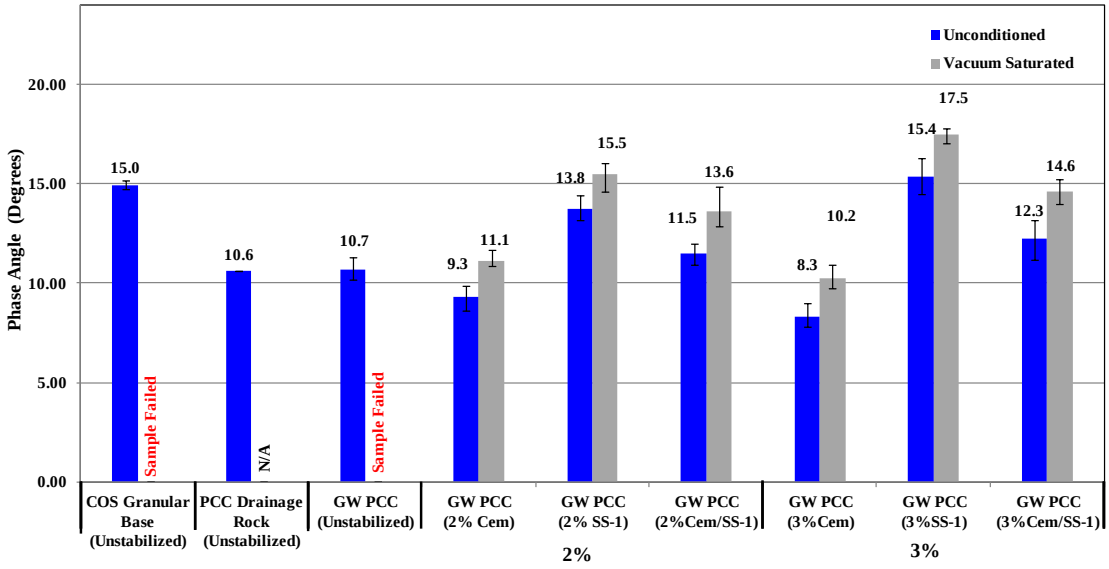

Figure 5.9 Mean Phase Angle High Stress State (σ=100kPa, Δσ=550 kPa) at 10 Hz

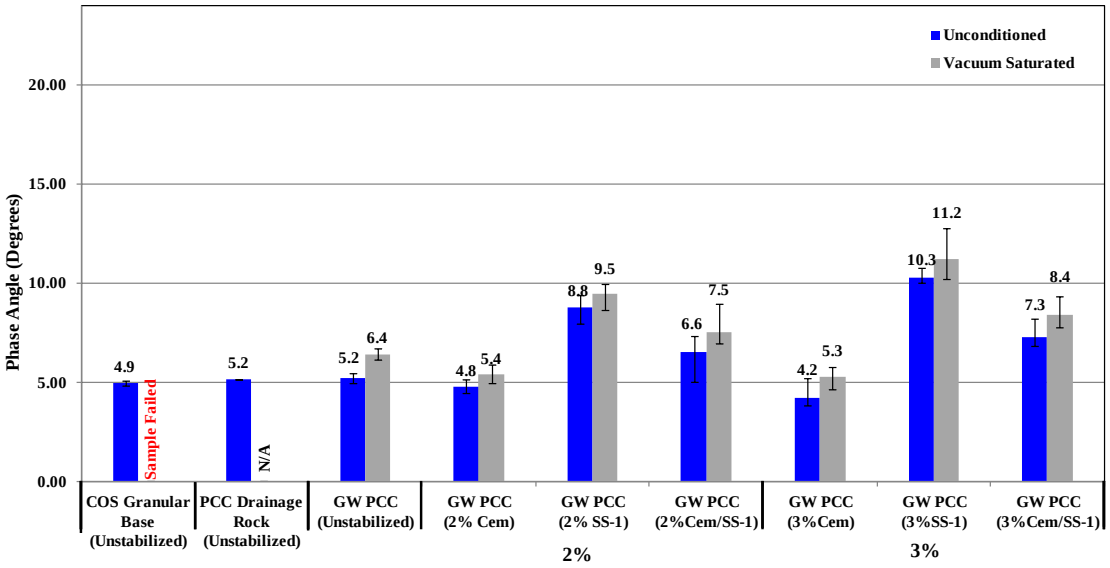

Figure 5.10 Mean Phase Angle Low Stress State (σ=250kPa, Δσ=200 kPa) at 0.5 Hz

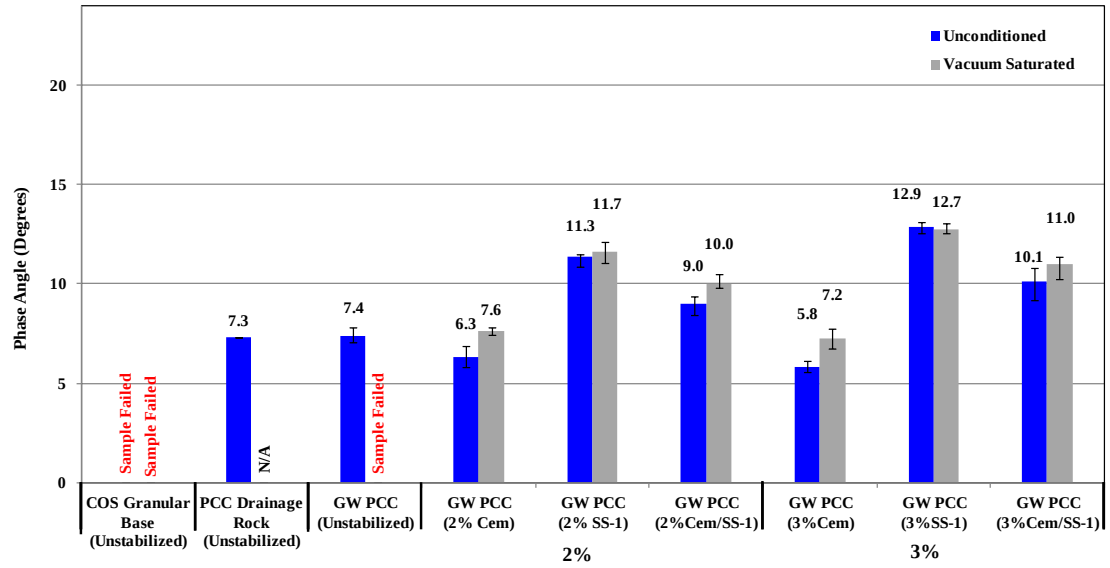

Figure 5.11 Mean Phase Angle High Stress State (σ=100kPa,Δσ=550 kPa) at 0.5 Hz

The conventional COS granular base samples failed at the high stress state and a testing frequency of 0.5 Hz, prior to vacuum saturation as seen in Figure 5.11. In comparison, the untreated recycled PCC GW base failed; however, it failed after it was vacuum saturated at the high stress state at a testing frequency of 10 Hz, as seen in Figure 5.9.

In a comparison between conventional COS granular base and the PCC drainage rock, the PCC drainage rock had a lower average phase angle across both testing frequencies at the high stress state prior to vacuum saturation. The conventional COS granular base had a slightly lower average phase angle compared to the recycled PCC drainage rock at the low stress states at both testing frequencies of 10 Hz and 0.5 Hz. As seen in Figure 5.8, the conventional COS granular base had an average phase angle of 8.4 degrees; the recycled PCC drainage rock had a phase angle value of 8.6 degrees.

When comparing the different stabilizers, not all the stabilizers performed the same. The samples of recycled PCC GW base that contained percentages of cement only had average measured phase angles that were lower than those of conventional COS granular base. As seen in Figure 5.8, the conventional COS granular base had an average phase angle of 8.4 degrees, the recycled PCC GW base sample containing two percent cement had a phase angle of 7.2 degrees, and the sample that had a cement content of three percent had a mean phase angle of 6.9 degrees.

Throughout the two stress states, the phase angle of the recycled PCC well graded base with three percent cement stayed relatively low when compared to the other samples, including the conventional COS granular base. For example, the recycled PCC GW base material containing three percent cement stabilizer had a peak phase angle of 8.3 degrees which occurred at the high stress state at a testing frequency of 10 Hz. When compared to the conventional COS granular base at the same testing frequency and stress state, the material had a mean phase angle of 15.0 degrees.

The recycled PCC GW base samples that were stabilized with only SS-1 and both cement and SS-1 had average measured phase angles that were significantly higher than the conventional COS granular base at a low stress state at both frequencies prior to vacuum saturation. As seen in Figure 5.10, the conventional COS granular base had a mean phase angle of 4.9 degrees and the samples of recycled PCC GW base stabilized with SS-1 had measured average values of 8.8 degrees and 10.3 degrees for the two and three percent SS-1 samples. However, after vacuum

saturation all of the stabilized samples of recycled PCC GW base had average phase angle values lower than conventional COS granular base.

After the samples were vacuum saturated, the phase angle of all the samples across both stress states and loading frequencies increased. As seen in Table 5.3, the percentage difference in the phase angles caused by vacuum saturation ranged from one percent to 30 percent. As seen in Figure 5.11 and Table 5.3, the phase angle of the three percent SS-1 sample was the least affected by vacuum saturation. The three percent SS-1 sample decreased from an average phase angle of 12.9 degrees to an average value of 12.7 degrees with a difference of approximately one percent.

The stabilized sample containing three percent SS-1 had the highest average measured phase angle out of all the research materials as seen in Figure 5.8 through Figure 5.11 except for the samples that failed. A high phase angle indicates that the material is stiffer or more viscous, such as the conventional COS granular base, when compared to the other research materials. The high phase angle also indicates that the conventional granular material is acting more like a viscous material. A lower phase angle as displayed by the recycled PCC GW base sample with three cement stabilizer indicates that the material is elastic, which could explain why the sample also had the highest dynamic modulus. At the applied stress states, the material is only within its elastic limits, so the material is therefore in a recoverable strain state which relates to a low phase angle as seen with the recycled PCC well graded base materials stabilized with three percent cement.

5.6 Radial Micro Strain Results

The behaviour of radial micro strain within materials is believed to be an indicator for the potential of a road material to exhibit lateral shear failure (Berthelot et al. 2010C). When evaluating the results obtained using the triaxial frequency sweep characterization, the radial micro strain of the recycled PCC well graded base materials both stabilized and untreated, recycled PCC drainage rock and conventional COS granular base was found to be highly sensitive to material type, stress state, stabilizer, and load rate.

Table 5.4 Mean Radial Micro Strain Results

Radial Micro Strain	Moist Cured				Vacuum Saturated				Percent difference (%)			
	Stress State				Stress State				Stress State			
	Low		High		Low		High		Low		High	
	10 Hz	0.5 Hz	10 Hz	0.5 Hz	10 Hz	0.5 Hz	10 Hz	0.5 Hz	10 Hz	0.5 Hz	10 Hz	0.5 Hz
Granular Base												
Max	202	197	1815	0	0	0	0	0				
Min	185	181	1617	0	0	0	0	0				
Avg	194	189	1716	Failed	Failed	Failed	Failed	Failed	N/A	N/A	N/A	N/A
Drainage Rock												
Max	0	0	0	0	0	0	0	0				
Min	0	0	0	0	0	0	0	0				
Avg	19	17	587	588	N/A	N/A	N/A	N/A	N/A	N/A	N/A	N/A
Well Graded PCC Max												
Max	65	61	750	766	113	105	0	0				
Min	41	37	518	547	79	77	0	0				
Avg	54	50	624	644	96	91	Failed	Failed	44	45	N/A	N/A
2% Cement Max												
Max	38	38	287	314	62	59	480	570				
Min	18	17	173	192	38	38	388	461				
Avg	25	24	209	235	50	46	420	499	50	48	50	53
2% SS-1 Max												
Max	32	41	201	336	84	92	519	750				
Min	21	30	166	274	47	48	393	575				
Avg	29	36	182	300	66	74	477	694	57	51	62	57
2% Cement/SS-1 Max												
Max	23	23	179	219	61	99	518	600				
Min	15	19	132	163	34	33	288	411				
Avg	19	21	152	189	41	49	371	485	54	57	59	61
3% Cement Max												
Max	13	12	62	67	20	18	153	193				
Min	9	8	33	35	13	11	89	112				
Avg	10	9	49	53	17	15	117	149	39	40	59	65
3% SS-1 Max												
Max	34	45	201	338	122	164	672	1103				
Min	22	27	106	194	61	71	440	665				
Avg	29	37	141	252	92	125	544	830	69	70	74	70
3% Cement/SS-1												
Max	20	21	119	152	31	34	245	364				
Min	17	17	86	126	23	23	171	256				
Avg	19	19	97	138	28	30	204	319	34	38	53	57

The radial micro strain was measured during the testing of the research material samples with the RATT cell. Table 5.4 presents the combined radial micro strain for each of the research materials at both low and high stress states across 10 Hz and 0.5 Hz testing frequencies, following moist cure and vacuum saturation. Figure 5.12 and Figure 5.13 illustrate the low and high stress states at a test frequency of 10 Hz. Figure 5.14 and Figure 5.15 illustrate the low and high stress states at a test frequency of 0.5 Hz.

A few of the general trends that were observed in the radial micro strain data included the following:

- The radial micro strain of the research materials increased as the testing frequency increased from 10 Hz to 0.5 Hz. Also the radial micro strain increased as the stress state increased from low to high.
- Across both stress states and frequencies, as well as pre and post vacuum saturation, the stabilized sample containing three percent cement had the lowest radial micro strain.
- Across all of the research materials after being vacuum saturated, the measured radial micro strain of the materials increased.

As shown in Figure 5.12 through Figure 5.15, the measured radial micro strain was higher for the conventional COS granular base compared to the stabilized and unstabilized recycled PCC GW base at all frequencies and stress states. For example, Figure 5.13 reveals that the average measured radial micro strain for conventional COS granular base was 1716, compared to the recycled PCC GW base which had a mean value of 624. The higher radial micro strain in the conventional base course material indicates it has a high potential for lateral shear when compared to the unstabilized recycled PCC GW base material.

The conventional COS granular base samples failed at the high stress state and a testing frequency of 0.5 Hz, prior to vacuum saturation as seen in Figure 5.15. In comparison, the untreated recycled PCC GW base failed; however, it failed after it was vacuum saturated at the high stress state at a testing frequency of 10 Hz as seen in Figure 5.13.

When evaluating the different stabilizers blended with the recycled PCC GW base, not all of the stabilizers performed the same. All of the stabilizers reduced the measured radial micro strain of the recycled PCC GW base, unlike the untreated recycled PCC GW base and the conventional COS granular base. As seen in Figure 5.14, the conventional COS granular base had an average radial micro strain of 189, the untreated recycled PCC GW base sample had an average radial micro strain of 50, and the recycled PCC GW base sample with two percent SS-1 had a radial micro strain value of 36.

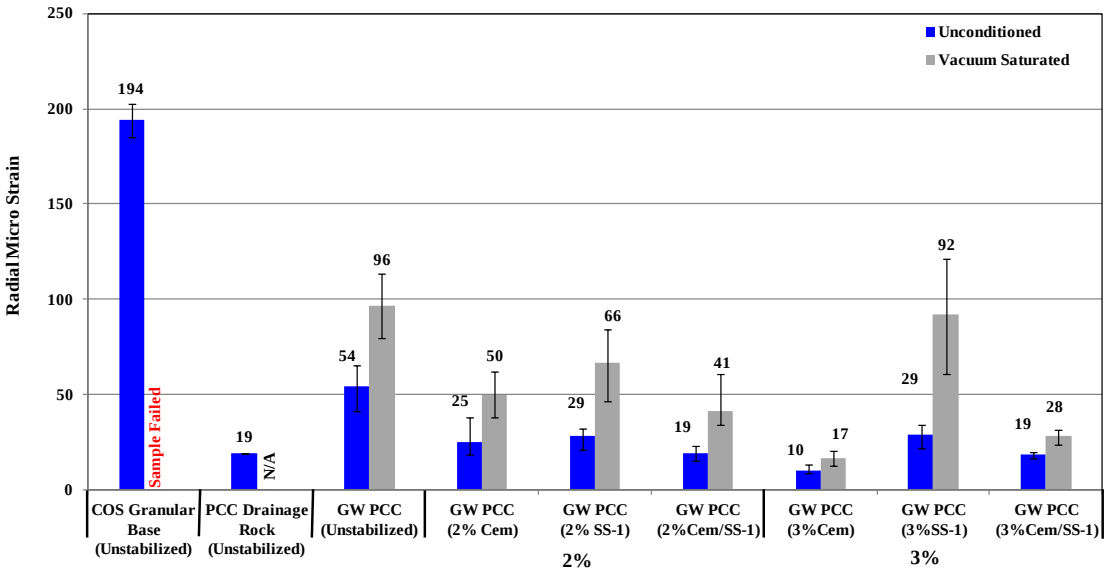

Figure 5.12 Mean Radial Micro Strain Low Stress State (σ=250kPa,Δσ=200 kPa), 10 Hz

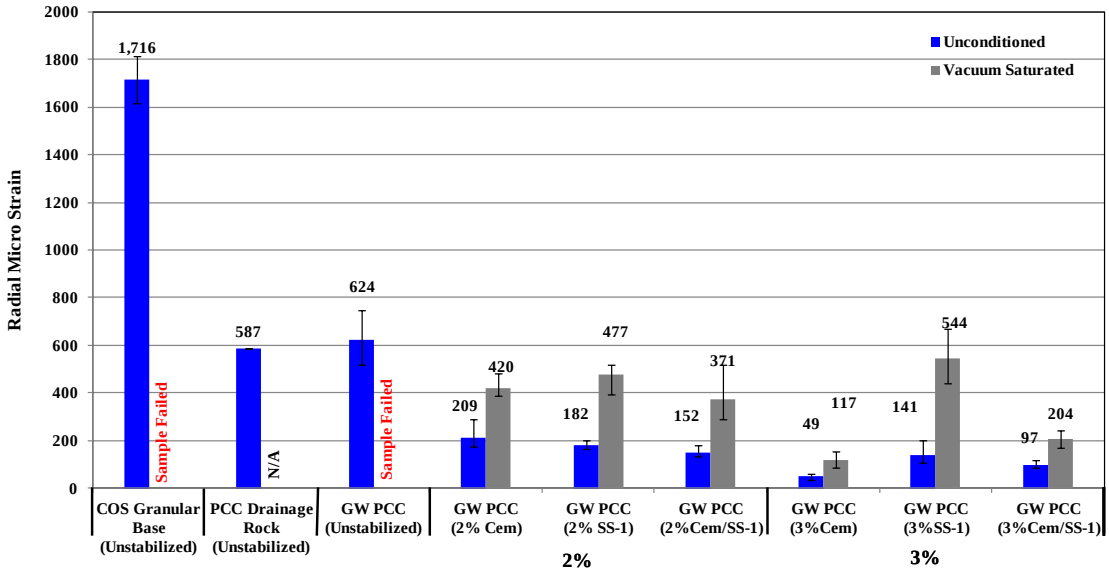

Figure 5.13 Mean Radial Micro Strain High Stress State (σ=100kPa,Δσ=550 kPa), 10 Hz

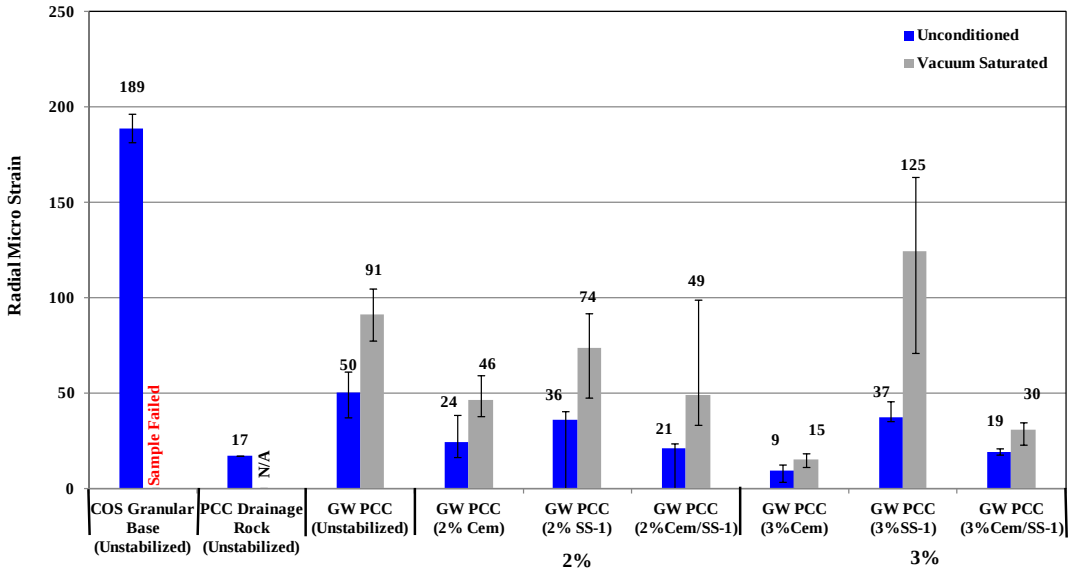

Figure 5.14 Mean Radial Micro Strain Low Stress State (σ=250kPa,Δσ=200 kPa), 0.5 Hz

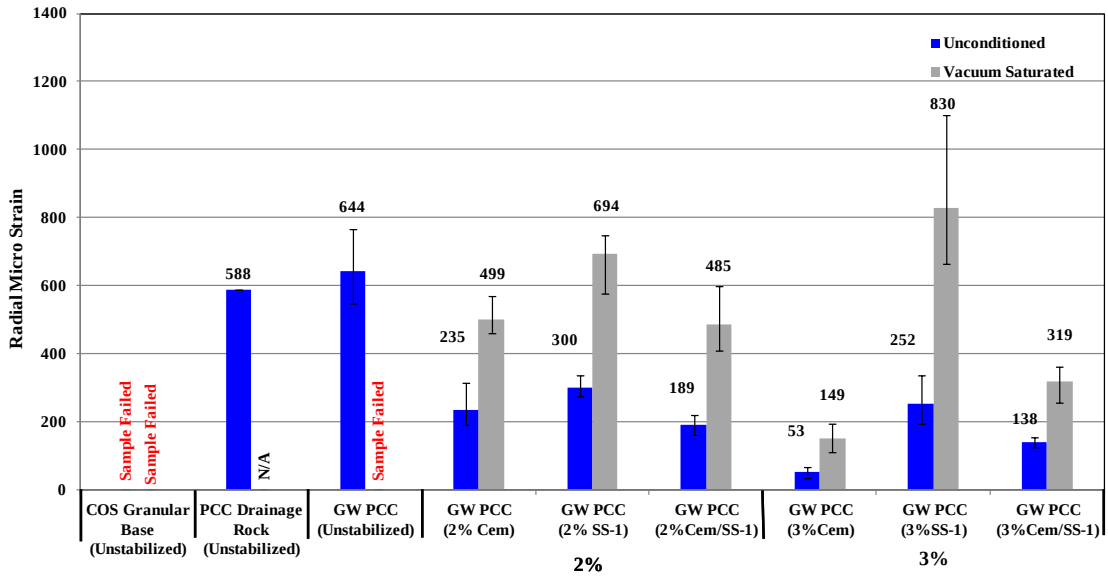

Figure 5.15 Mean Radial Micro Strain High Stress State (σ=100kPa,Δσ=550 kPa), 0.5 Hz

Throughout both stress states the radial micro strain of the recycled PCC well graded base with three percent cement stayed relatively low when compared to the other samples, including the conventional COS granular base. For example, the recycled PCC well graded base material containing three percent cement stabilizer had a peak radial micro strain value of 53 degrees which occurred at the high stress state at a testing frequency of 0.5Hz. When compared to the conventional COS granular base at the same testing frequency and stress state, the sample failed.

After the samples were vacuum saturated, the radial micro strain of all the samples across both stress states and loading frequencies increased. As seen in Table 5.4, the percentage increase in radial micro strain due to vacuum saturation ranged from approximately 51 percent to 236 percent across the different research materials. However, all the stabilized recycled PCC GW samples maintained radial micro strains that were lower than both the untreated recycled PCC GW base and the conventional COS granular base. The only exceptions were the samples of recycled PCC GW base that contained only three percent SS-1 stabilizer. As seen in Figure 5.14, the untreated recycled PCC GW base had a mean radial micro strain of 91; the three percent stabilized sample had a mean radial micro strain of 125.

5.7 Poisson's Ratio Results

Poisson's ratio is a mechanistic material characteristic which is used in road structural modeling. The material property is used to characterize the multi-axial strain behavior of a material. Poisson's ratio is used in road modeling because it is a critical material constitutive property for accurately modeling a material's behaviour within a specific road structure given the natural dependence road materials have on multi axial shear behaviour (Berthelot et al. 2010C).

Poisson's ratio was measured during the testing of the research material samples with the RATT cell. Table 5.5 presents the combined Poisson's ratio for each of the research materials at both low and high stress states across 10 Hz and 0.5 Hz testing frequencies, following moist cure and vacuum saturation. Figure 5.16 and Figure 5.17 illustrate the low and high stress states at a test frequency of 10 Hz. Figure 5.18 and Figure 5.19 illustrate the low and high stress states at a test frequency of 0.5 Hz.

Table 5.5 Mean Poisson's Ratio Results

Poisson's Ratio	Moist Cured				Vacuum Saturated				Percent difference (%)			
	Stress State				Stress State				Stress State			
	Low		High		Low		High		Low		High	
	10 Hz	0.5 Hz	10 Hz	0.5 Hz	10 Hz	0.5 Hz	10 Hz	0.5 Hz	10 Hz	0.5 Hz	10 Hz	0.5 Hz
Granular Base												
Max	0.46	0.45	1.00	0.00	0.00	0.00	0.00	0.00				
Min	0.43	0.42	0.89	0.00	0.00	0.00	0.00	0.00				
Avg	0.44	0.44	0.94	Failed	Failed	Failed	0.00	Failed	N/A	N/A	N/A	N/A
Drainage Rock												
Max	0.00	0.00	0.00	0.00	0.00	0.00	0.00	0.00				
Min	0.00	0.00	0.00	0.00	0.00	0.00	0.00	0.00				
Avg	0.15	0.14	0.80	0.80	N/A	N/A	N/A	N/A	N/A	N/A	N/A	N/A
Well Graded PCC Max												
Max	0.32	0.31	0.80	0.82	0.36	0.35	0.00	0.00				
Min	0.22	0.21	0.69	0.71	0.30	0.31	0.00	0.00				
Avg	0.28	0.27	0.73	0.76	0.33	0.33	Failed	Failed	15.15	18.18	N/A	N/A
2% Cement Max												
Max	0.25	0.27	0.47	0.52	0.32	0.33	0.62	0.70				
Min	0.14	0.14	0.32	0.36	0.21	0.22	0.54	0.61				
Avg	0.18	0.19	0.39	0.43	0.27	0.27	0.59	0.66	33.33	29.63	33.90	34.85
2% SS-1 Max												
Max	0.23	0.27	0.41	0.54	0.36	0.37	0.67	0.81				
Min	0.18	0.23	0.35	0.47	0.28	0.25	0.57	0.69				
Avg	0.21	0.24	0.38	0.51	0.31	0.32	0.63	0.76	32.26	25.00	39.68	32.89
2% Cement/SS-1 Max												
Max	0.22	0.21	0.42	0.48	0.34	0.42	0.73	0.77				
Min	0.13	0.17	0.34	0.39	0.21	0.21	0.50	0.62				
Avg	0.18	0.20	0.38	0.43	0.26	0.28	0.59	0.67	30.77	28.57	35.59	35.82
3% Cement Max												
Max	0.17	0.17	0.22	0.23	0.20	0.18	0.30	0.36				
Min	0.10	0.10	0.12	0.13	0.11	0.11	0.23	0.26				
Avg	0.12	0.11	0.16	0.17	0.15	0.14	0.26	0.32	20.00	21.43	38.46	46.88
3% SS-1 Max												
Max	0.25	0.29	0.43	0.56	0.43	0.52	0.76	0.95				
Min	0.20	0.22	0.27	0.36	0.29	0.30	0.57	0.69				
Avg	0.23	0.25	0.33	0.44	0.37	0.42	0.67	0.80	37.84	40.48	50.75	45.00
3% Cement/SS-1												
Max	0.20	0.20	0.34	0.38	0.23	0.24	0.47	0.58				
Min	0.16	0.17	0.24	0.31	0.16	0.15	0.35	0.45				
Avg	0.18	0.18	0.28	0.34	0.21	0.21	0.41	0.52	14.29	14.29	31.71	34.62

A few of the general trends that were observed in the Poisson's ratio data included the following:

- The Poisson's ratio of the research materials slightly increased as the testing frequency increased from 10 Hz to 0.5 Hz. Also there was a small increase in the Poisson's ratio as the stress state increased from low to high.
- Across the stress states and frequencies as well as pre and post vacuum saturation, the stabilized sample containing three percent cement had the lowest Poisson's ratio.
- Across all of the research materials post vacuum saturated, the measured Poisson's ratio of the materials increased.

As shown in Figure 5.16 through Figure 5.19, there was a greater increase in the measured Poisson's ratio for the conventional COS granular base compared to the recycled PCC GW base across both frequencies and stress states. For example, Figure 5.16 indicates that the average measured Poisson ratio for conventional COS granular base was 0.44, compared to the recycled PCC GW base which had a mean value of 0.28.

The conventional COS granular base samples failed at the high stress state and a testing frequency of 0.5 Hz, prior to vacuum saturation as seen in Figure 5.19. In comparison, the untreated recycled PCC GW base failed; however, it failed after it was vacuum saturated at the high stress state at a testing frequency of 10 Hz as seen in Figure 5.17.

The higher Poisson's ratio in the conventional COS granular base course material indicates that the sample is straining more in the radial direction compared to the axial direction, as opposed to the unstabilized well graded PCC material. The behavior that describes a material straining in one direction more than another direction is called orthotropic material behaviour. The material behavior causes dilation of the sample which occurred with the conventional COS granular base sample along with the other samples that had a Poisson's ratio that reached or exceeded 0.5. When a material has a higher radial strain than axial strain, or a high Poisson's ratio, it indicates that the material has a higher susceptibility to axial shear, which coincides with a higher radial micro strain shown previously for the same material at the same stress states and loading frequency.

In comparison between conventional COS granular base and the PCC drainage rock, the PCC drainage rock had a much lower average Poisson's ratio across both testing frequencies and stress states. Except for the testing parameters of high stress state at 10 Hz, the recycled PCC drainage rock had an average Poisson's ratio that was approximately two times smaller than the average measured values for conventional COS granular base. The exception, as seen in Figure 5.17, is that the conventional COS granular base had an average Poisson's ratio of 0.94, and the untreated recycled GW PCC had a value of 0.80. At a low stress state at both loading frequencies the measured Poisson's ratios for the recycled PCC drainage rock were comparable to the three percent cement recycled PCC GW base samples. Figure 5.18 indicates that the untreated recycled PCC GW base had a value of 0.14 compared to the three percent stabilized recycled PCC GW base which had a value of 0.11.

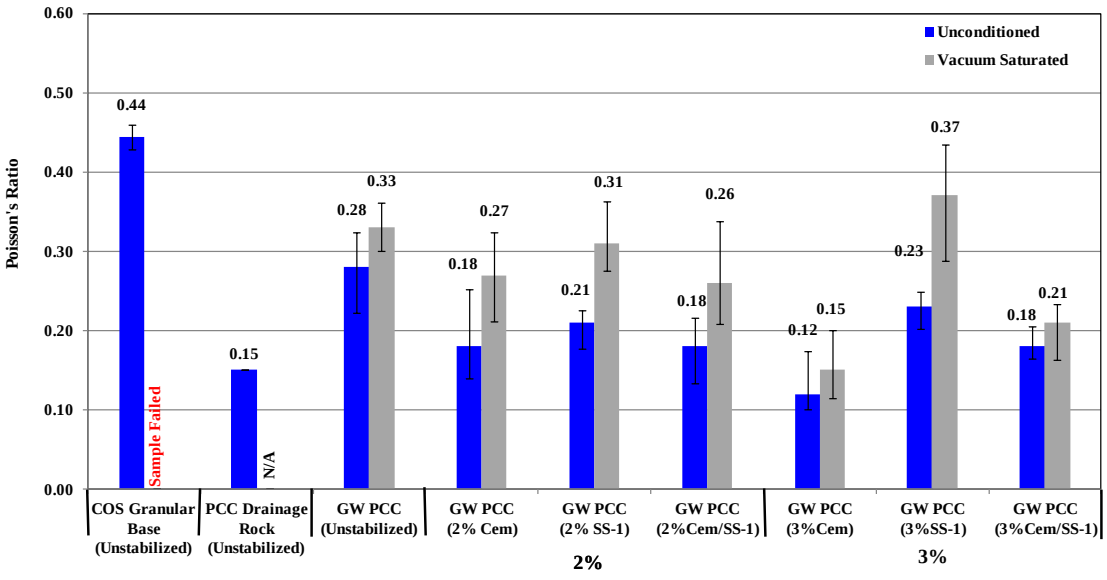

Figure 5.16 Mean Poisson's Ratio Low Stress State (σ=250kPa, Δσ=200 kPa), 10 Hz

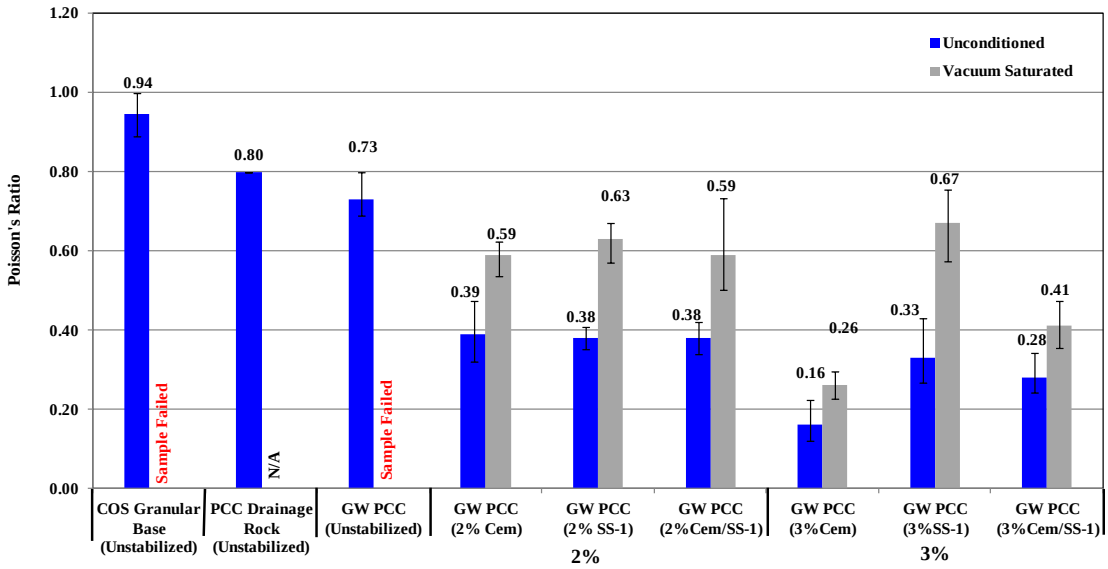

Figure 5.17 Mean Poisson's Ratio High Stress State (σ=100kPa, Δσ=550 kPa), 10 Hz

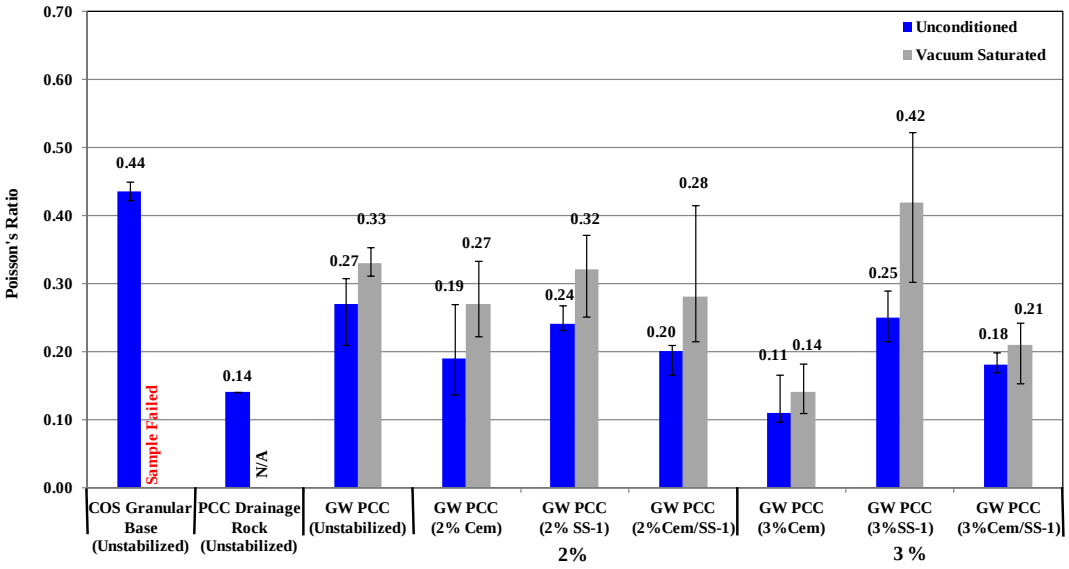

Figure 5.18 Mean Poisson's Ratio Low Stress State (σ=250kPa,Δσ=200 kPa), 0.5 Hz

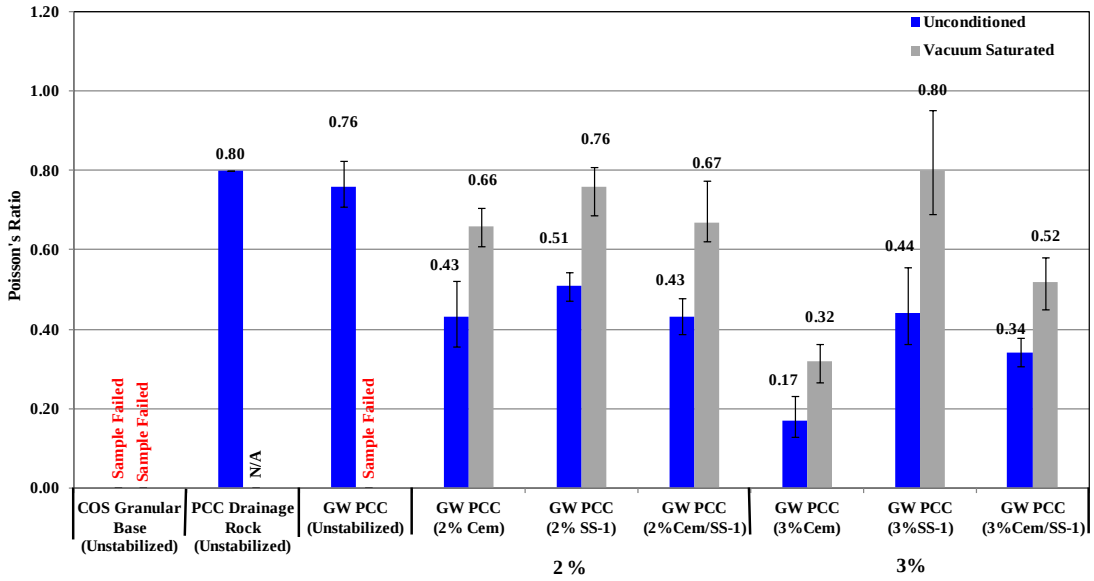

Figure 5.19 Mean Poisson's Ratio High Stress State (σ=100kPa,Δσ =550 kPa), 0.5 Hz

When comparing the different stabilizers, not all the stabilizers performed the same. All of the stabilizers reduced the measured Poisson's ratio of the recycled PCC GW base, when compared to the untreated recycled PCC GW base and the conventional COS granular base. As seen in Figure 5.17, the conventional COS granular base had an average Poisson's ratio of 0.94, the untreated recycled PCC GW base sample had an average Poisson's ratio of 0.73, and the recycled PCC GW base sample with three percent SS-1 had an average Poisson's ratio value of 0.33.

Throughout both stress states, the Poisson's ratio of the recycled PCC GW base with three percent cement stayed relatively low when compared to the other samples, including the conventional COS granular base. For example, the recycled PCC well graded base material containing three percent cement stabilizer had an average Poisson's ratio value of 0.17 which occurred at the high stress state at a testing frequency of 0.5Hz. When compared to the conventional COS granular base at the same testing frequency and stress state, the sample failed.

After the samples were vacuum saturated, the Poisson's ratio values of all the samples across both stress states and loading frequencies increased. The added moisture due to the vacuum saturation affected each of the research materials differently. Overall, the materials showed an approximate increase of the Poisson's ratio between 17 and 90 percent due to the vacuum saturation process as seen in Table 5.5. However, all the stabilized recycled PCC GW samples maintained Poisson's ratio values that were lower than those of both the untreated recycled PCC GW base and the conventional COS granular base.

RATT prior to vacuum saturation established that the Poisson's ratio of the conventional COS granular base was higher than the untreated and stabilized recycled PCC well graded base materials and the recycled PCC drainage rock. As seen in Figure 5.16 and Figure 5.18, the conventional COS granular base course material had an average Poisson's ratio of 0.44 at a testing frequency of 10 Hz and 0.5 Hz at low stress state. In comparison, the recycled PCC drainage rock had an average Poisson's ratio value of 0.15, and the recycled PCC GW base had an average Poisson's ratio of 0.28 at the same testing frequencies. Figure 5.16 and Figure 5.17 show that as the stress states increased the conventional granular base had a much greater increase in the average measured Poisson's ratio compared to all the other research materials. The substantial increase in Poisson's ratio from 0.44 to 0.94 under a testing frequency of 10Hz

was the same when the conventional COS granular base increased stress states under a testing frequency of 0.5 Hz.

5.8 Chapter Summary

Mechanistic based material characterization testing protocols were used to characterize both conventional aggregate and recycled PCC materials. The advantage of using mechanistic based characterization is that the measured material properties are not empirically-based. The RATT cell measures material properties such strains due to applied stress directly.

Shear stress was analyzedf using the gyratory compactor. The results showed that the conventional COS granular base had the lowest shear stress out of all three materials. The recycled PCC drainage rock had the highest shear stress. The highest shear stress is attributed to the larger aggregate size, compared to the well graded materials and the high angularity of the material.

Through the use of the frequency sweep characterization employed through the rapid triaxial test, untreated and stabilized recycled PCC well graded base, recycled PCC drainage rock, and conventional COS granular base were tested. The conventional COS granular base course material is highly sensitive to both stress state and moisture state. The dynamic modulus of the conventional granular base decreased as the stress states increased. The phase angle, radial micro strain and Poisson's ratio increased substantially through the three stress states. The conventional COS granular base samples failed under high stress states prior to vacuum saturation.

The untreated recycled PCC well graded material and the recycled PCC drainage rock both had a higher dynamic modulus than the conventional COS granular base. The phase angle, radial micro strain, and Poisson's ratio were also lower when compared to the conventional COS granular base material. Both PCC materials were also sensitive to the testing stress state, which was illustrated by the increase in Poisson's ratio radial micro strain and phase angle with respect to the change in stress state. The well graded PCC material initially survived the vacuum saturation but failed under the high stress state at a loading frequency of 10 Hz.

The evaluation of the recycled PCC GW base material stabilized with the different stabilizers showed that the sample containing three percent cement performed better than the

others when comparing the mechanistic properties both prior and post vacuum saturation. The three percent cement samples also showed the least sensitivity to the changing of stress states when compared to the other stabilized and non-stabilized materials.

CHAPTER 6 FIELD TEST SECTION CONSTRUCTION AND STRUCTURAL PERFORMANCE VALIDATION

Through the introduction of the "Green Street" Infrastructure Program in 2008, the City of Saskatoon along with the University of Saskatchewan investigated alternative road construction methods using recycled materials in an effort to maximize budget efforts without sacrificing quality, performance, and service life of their road infrastructure. This research considered two test sections, both of which used recycled PCC drainage rock as a structural and drainage layer within the road structure. The test sections included:

- The east bound lanes of Marquis Drive constructed by the City of Saskatoon in the summer of 2009.
- A section of North Road located in the University of Saskatchewan, constructed by PSI Technologies in the summer of 2009.

This chapter summarizes the test section layout and construction of Marquis Drive and North Road. Pre and post construction heavy weight deflectometer testing results are presented to validate the structural performance of the recycled pavement structures.

6.1 Marquis Drive Test Section

The construction limits of Marquis Drive extended from the intersection of Thatcher Avenue at km 0.000, east to the intersection of Idylwyld Drive at km 0.425 as shown in Figure 6.1.

6.1.1 Marquis Drive Pre Construction Structure

Marquis Drive had severe rutting, potholes, fatigue cracking, and longitudinal and transverse cracking before construction (Figure 6.2). Heavy traffic and substructure moisture problems were contributing factors to the structural failure of the road. Pre construction, Marquis Drive was comprised of a conventional hot mix asphalt concrete (HMAC) surface on a conventional granular base structure on top of a marginal quality subgrade as seen in Figure 6.3. The City of Saskatoon selected these two segments of Marquis Drive due to the poor pre construction structural condition of the road.

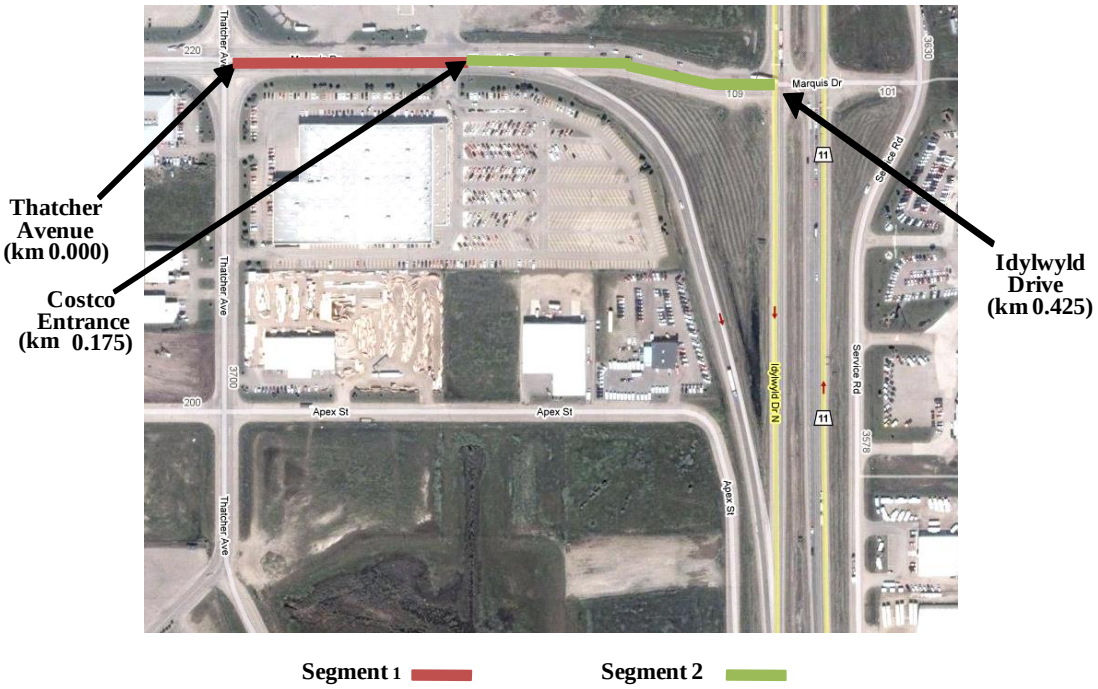

Figure 6.1 Marquis Drive Construction Limits (Google Map)

Figure 6.2 Typical Surface Condition and Structural Failure of Marquis Drive (courtesy of PSI Technologies)

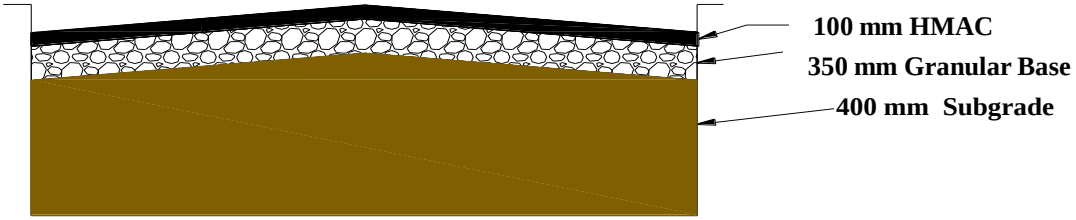

Figure 6.3 Pre Construction Cross Section of Marquis Drive

6.1.2 Marquis Drive Test Section Construction

Due to the expansion of the local heavy industrial park along Marquis Drive, including construction of two truck stops, the primary objective of rehabilitating the eastbound lanes of Marquis Drive was to increase its load carrying capacity. A key component to the City's pavement structure design was to increase the substructure and eliminate subsurface moisture problems found within the west end of the construction limits. These objectives were addressed by using the reclaimed asphalt pavement (RAP) and *in situ* material obtained by rotomixing the existing pavement structure and using this material as a structural base layer. PCC drainage rock was used as a drainage layer. Figure 6.4 illustrates Marquis Drive's post construction cross sections.

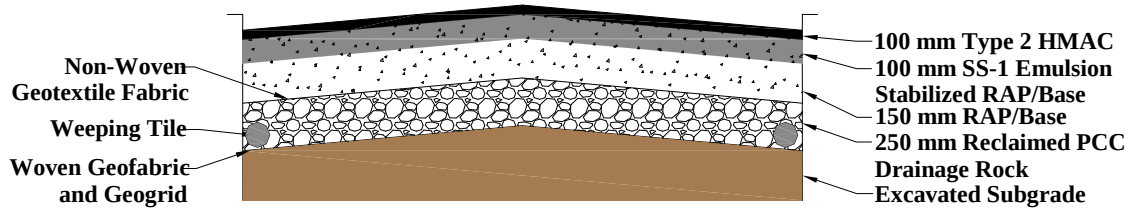

a) Marquis Drive (Segment 1 km 0.000-0.175)

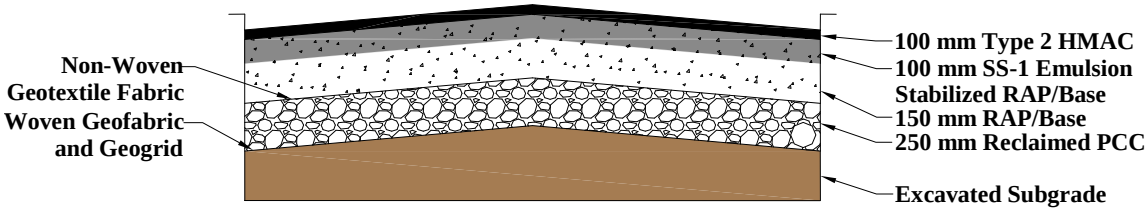

b) Marquis Drive (Segment 2 km 0.175-0.425)

Figure 6.4 Post Construction Cross Sections of Marquis Drive

Segment 1 of Marquis Drive (km 0.000 to Costco Entrance at km 0.155) was constructed with 250 mm recycled PCC drainage rock layer and weeping tile to accommodate drainage. A 250 mm layer of RAP/base material was placed on top of the PCC rock drainage layer and the top 100 mm of RAP was SS-1 emulsion stabilized.

The east end of Marquis Drive (km 0.155 to km 0.425) was constructed with 250 mm recycled PCC drainage rock with no weeping tile. A 250 mm layer of RAP/base material was placed on top of the recycled PCC drainage rock layer and the top 100 mm of RAP was two percent SS-1 emulsion stabilized. Both the west and east ends of Marquis Drive were surfaced with 100 mm of hot mix asphalt concrete (HMAC): Type 2 for the bottom lift and Type 2 HMAC with polymer modification (Type 2P) for the top lift.

Marquis Drive was reconstructed in the summer of 2009. During construction of east bound lanes of Marquis Drive, a total approximate depth of 550 mm was excavated. The top 150 mm of HMAC and COS granular base was rotomixed and stockpiled onsite as seen in Figure 6.5. The remaining 400 mm of subgrade material was excavated and hauled away.

Once the material had been milled and excavated, woven geotextile was placed on the subgrade (weeping tile was installed in Segment 1) and the recycled PCC drainage rock was then laid on top of the fabric, as seen in Figure 6.6. The recycled PCC drainage rock was placed and compacted and a non-woven geofabric was laid down, followed by the placement of the RAP material. The existing RAP which was reclaimed prior to excavation was placed and compacted, and RAP stockpiled at City of Saskatoon yards was transported to the site and placed to meet the 250 mm depth requirement. The top 100 mm of the RAP material was stabilized with SS-1 as seen in Figure 6.7 and the surface was paved with 100 mm of a City specified Type 2 HMAC as seen in Figure 6.8.

Figure 6.5 Reclaiming of the *in situ* Aggregate Material on Marquis Drive (courtesy of PSI Technologies)

Figure 6.6 Placement of the PCC Drainage Rock Layer placed on the Geo-textiles Layer (courtesy of PSI Technologies)

Figure 6.7 Rotomixing the SS-1 with the RAP Layer (courtesy of PSI Technologies)

Figure 6.8 Post Construction of Marquis Drive (courtesy of PSI Technologies)

6.1.3 Marquis Drive Test Section Quality Assurance

To measure the *in situ* structural asset condition of Marquis Drive, heavy weight deflection structural testing was used to measure the peak surface deflections. Figure 6.9 shows the heavy weight deflectometer used. The heavy weight deflection (HWD) test was used to simulate truck loading from a secondary legal load limit to a primary legal load limit plus 50 percent. The deflection criteria ranges used to evaluate the structural integrity were developed by the City of Saskatoon as specified in their asset management program. Since 2007, the City has collected HWD measurements for a number of its arterial, collector, and local roads, which COS has used to establish HWD peak surface deflection measurement thresholds. The peak surface deflection condition classification was based on the following rating categories:

- Good: < 1.0mm,
- Fair: 1.0mm to 2.0 mm, and
- Poor: >2.0mm.

Figure 6.9 Heavy Weight Deflectometer on Marquis Drive (courtesy of PSI Technologies)

Heavy weight deflectometer peak surface deflection results across Saskatchewan secondary, primary, primary plus 25 and primary plus 50 legal weight limits are summarized in Table 6.1 and Table 6.2 and illustrated in Figure 6.10 for both pre and post construction of both segments of Marquis Drive.

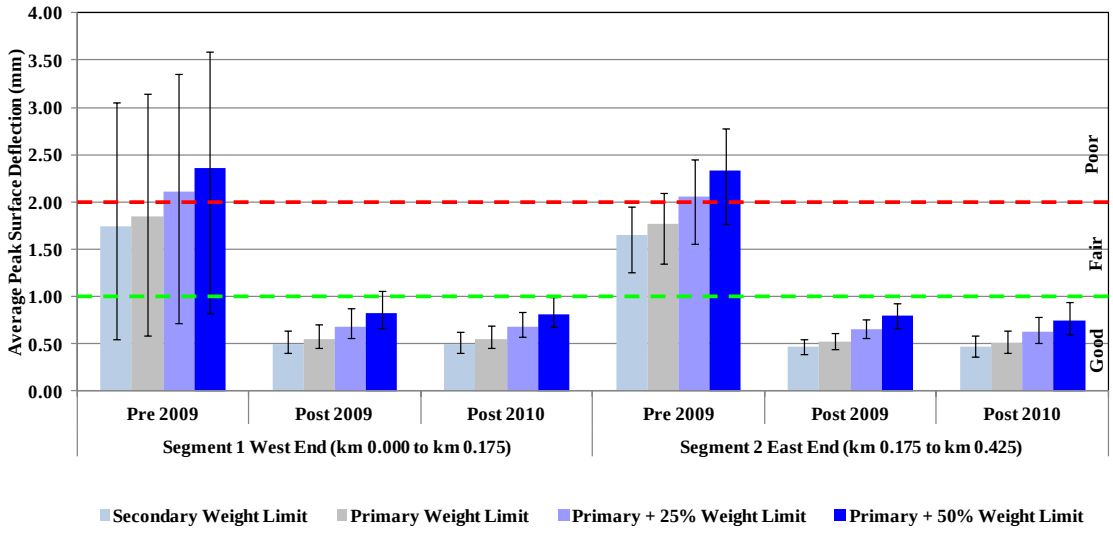

Figure 6.10 Peak Surface Deflection Summary Statistics of Marquis Drive

The deflection measurements show that pre construction, the structural layers of Marquis Drive were weak and not suitable for heavy truck traffic that travels on the road segment. Pre construction, the average peak surface deflection was greater than 1.0 mm and the measurements were variable. The variance in the pre construction deflection measurements is due to poor structural layers underneath the asphalt surface including the base, subbase and subgrade layers.

Initially, post construction structural asset management testing was completed 14 days after the final lift of HMAC was placed. The 14 day time delay was selected to ensure that there was proper curing of the stabilized base material and the HMAC had time to cool and stiffen. The following year (2010) deflections were measured in the two sections. These are also presented in Figure 6.10. Post construction deflections all met the City specification of less than 1.00 mm of deflection. The variability in the deflections across the different weight limits also decreased in both 2009 and 2010 as compared to the pre-construction deflection measurements. The City of Saskatoon was able to achieve their main objective of increasing the load carrying capacity of the road without sacrificing quality and durability.

Table 6.1 Summary of the Peak Surface Deflections with Respect to Load Spectra of Marquis Drive Segment 1

	Segment 1 - West End (km 0.000 to km 0.175)		
	Pre 2009	**Post 2009**	**Post 2010**
Peak Surface Deflection at Secondary Weight Limits			
Average (mm)	1.74	0.49	0.50
Minimum (mm)	0.53	0.39	0.41
Maximum (mm)	4.00	0.68	0.65
Standard Deviation (mm)	0.97	0.08	0.08
Coefficient of Variance (%)	55.00	17.00	16.00
5th Percentile (mm)	0.54	0.41	0.41
95th Percentile (mm)	3.05	0.64	0.63
+ Error Bar	1.31	0.15	0.13
-Error Bar	1.20	0.09	0.09
Peak Surface Deflection at Primary Weight Limits			
Average (mm)	1.85	0.55	0.55
Minimum (mm)	0.57	0.43	0.45
Maximum (mm)	4.00	0.75	0.72
Standard Deviation (mm)	0.97	0.09	0.09
Coefficient of Variance (%)	53.00	16.00	16.00
5th Percentile (mm)	0.59	0.45	0.45
95th Percentile (mm)	3.14	0.71	0.69
+ Error Bar	1.29	0.16	0.14
-Error Bar	1.26	0.10	0.09
Peak Surface Deflection at Primary +25% Weight Limits			
Average (mm)	2.11	0.68	0.68
Minimum (mm)	0.69	0.54	0.57
Maximum (mm)	4.00	0.94	0.88
Standard Deviation (mm)	1.00	0.11	0.10
Coefficient of Variance (%)	47.00	16.00	15.00
5th Percentile (mm)	0.71	0.56	0.57
95th Percentile (mm)	3.36	0.88	0.84
+ Error Bar	1.24	0.29	0.16
-Error Bar	1.40	0.12	0.11
Peak Surface Deflection at Primary +50% Weight Limits			
Average (mm)	2.36	0.82	0.81
Minimum (mm)	0.80	0.64	0.68
Maximum (mm)	4.00	1.12	1.05
Standard Deviation (mm)	1.05	0.13	0.12
Coefficient of Variance (%)	44.00	16.00	15.00
5th Percentile (mm)	0.83	0.67	0.68
95th Percentile (mm)	3.59	1.50	0.99
+ Error Bar	1.23	0.24	0.18
-Error Bar	1.53	0.15	0.13

Table 6.2 Summary of the Peak Surface Deflections with Respect to Load Spectra of Marquis Drive Segment 2

Segment 2 - East End (km 0.175 to km 0.425)			
	Pre 2009	**Post 2009**	**Post 2010**
Peak Surface Deflection at Secondary Weight Limits			
Average (mm)	1.65	0.47	0.46
Minimum (mm)	0.98	0.39	0.36
Maximum (mm)	1.96	0.57	0.60
Standard Deviation (mm)	0.24	0.05	0.08
Coefficient of Variance (%)	15.00	11.00	17.00
5th Percentile (mm)	1.25	0.40	0.37
95th Percentile (mm)	1.95	0.55	0.59
+ Error Bar	0.30	0.08	0.12
-Error Bar	0.39	0.07	0.10
Peak Surface Deflection at Primary Weight Limits			
Average (mm)	1.77	0.52	0.51
Minimum (mm)	1.05	0.43	0.40
Maximum (mm)	2.11	0.63	0.66
Standard Deviation (mm)	0.26	0.06	0.08
Coefficient of Variance (%)	15.00	11.00	16.00
5th Percentile (mm)	1.34	0.44	0.41
95th Percentile (mm)	2.10	0.61	0.64
+ Error Bar	0.33	0.09	0.13
-Error Bar	0.42	0.08	0.11
Peak Surface Deflection at Primary +25% Weight Limits			
Average (mm)	2.06	0.66	0.63
Minimum (mm)	1.22	0.54	0.50
Maximum (mm)	2.52	0.78	0.80
Standard Deviation (mm)	0.31	0.07	0.10
Coefficient of Variance (%)	15.00	10.00	15.00
5th Percentile (mm)	1.56	0.56	0.51
95th Percentile (mm)	2.45	0.76	0.79
+ Error Bar	0.39	0.11	0.16
-Error Bar	0.50	0.10	0.13
Peak Surface Deflection at Primary +50% Weight Limits			
Average (mm)	2.33	0.79	0.75
Minimum (mm)	1.38	0.65	0.59
Maximum (mm)	2.92	0.94	0.95
Standard Deviation (mm)	0.36	0.08	0.11
Coefficient of Variance (%)	15.00	10.00	14.00
5th Percentile (mm)	1.76	0.67	0.61
95th Percentile (mm)	2.78	0.92	0.94
+ Error Bar	0.45	0.13	0.19
-Error Bar	0.57	0.12	0.14

6.2 University of Saskatchewan North Road Test Section

The Green Road Project is a project created by the University of Saskatchewan to reduce greenhouse gas emissions and enhance access to city transit and environmental sustainability (U of S 2009). The two objectives of the North Road reconstruction project were to better accommodate heavy bus and construction traffic and to reduce the environmental footprint associated with reconstruction of campus roads. The construction limits of North Road are illustrated in Figure 6.11. The construction limits of North Road were from the intersection of Campus drive at km 0.000, and north to km 0.482,. The construction limits of the section were divided into three test sections of equal surface area to examine the performance of different surfacing structures. Section 1 is from km 0.000 to 0.153, Section 2 is from km 0.153 to 0.322, and Section 3 is from km 0.322 to 0.482.

6.2.1 North Road Pre Construction Structure

Pre construction, North Road was comprised of a conventional HMAC wearing surface on a conventional granular base structure, on top of subgrade material as seen in Figure 6.12. The pre construction structure of North Road was initially designed to accommodate light traffic; however, as the university expanded, traffic levels and loads did too. As seen in Figure 6.13, the road had severe rutting, potholes, fatigue cracking, and longitudinal and transverse cracking. There were also areas that showed full depth structural failures. Heavy traffic and substructure and surface moisture problems were the factors attributed to the failure of the road. At the time of construction, traffic on North Road was comprised of light and heavy vehicle traffic, including City transit buses and construction traffic. The University of Saskatchewan selected this section of North Road due to the condition of the road combined with the end objective of increasing university accessibility for bus and heavy construction traffic.

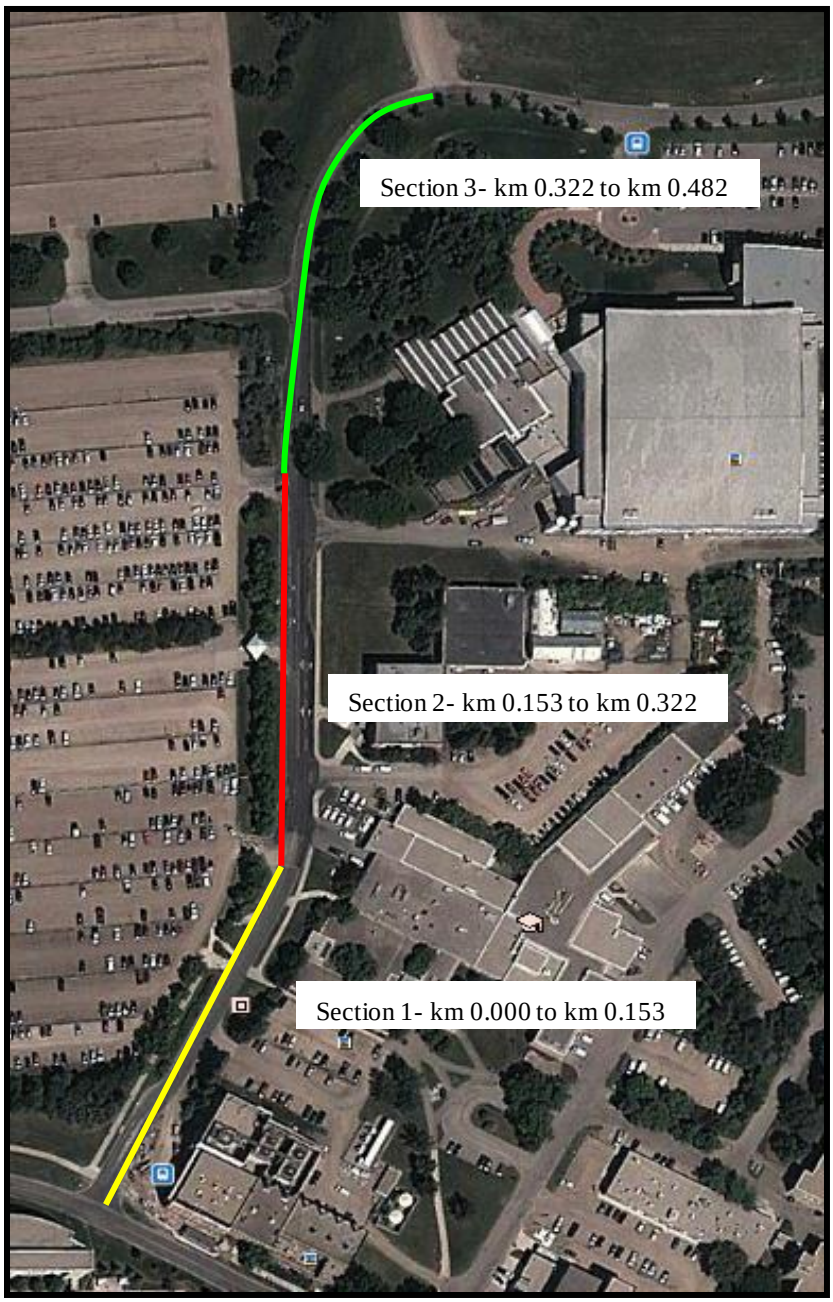

Figure 6.11 North Road Construction Limits (Google Map)

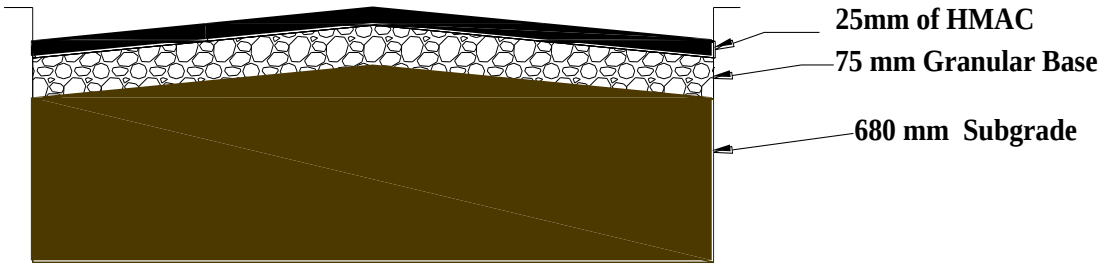

Figure 6.12 Pre Construction Cross Section of North Road

Figure 6.13 Typical Surface Distresses and Structural Failures of North Road (courtesy of PSI Technologies)

6.2.2 North Road Test Section Construction

The cross sections of each of the three segments can be seen in Figure 6.14. The structure of Section 1 (km 0.000 to km 0.153) was constructed with a surfacing structure of 80 mm of interlocking concrete paving stones, a 25 mm sand bedding layer, and a 125 mm recycled and stabilized reclaimed asphalt concrete base. Section 2 was constructed with 50 mm hot mix asphalt concrete (HMAC) over 40 mm engineered emulsion cold mix, and 140 mm recycled and cement stabilized reclaimed RAP. Section 3 was constructed with 80 mm HMAC over 150 mm

recycled and stabilized reclaimed RAP. Below each of the three sections, 250 mm of recycled PCC drainage rock was placed on top of a 300 mm layer of a sand drainage layer with weeping tile.

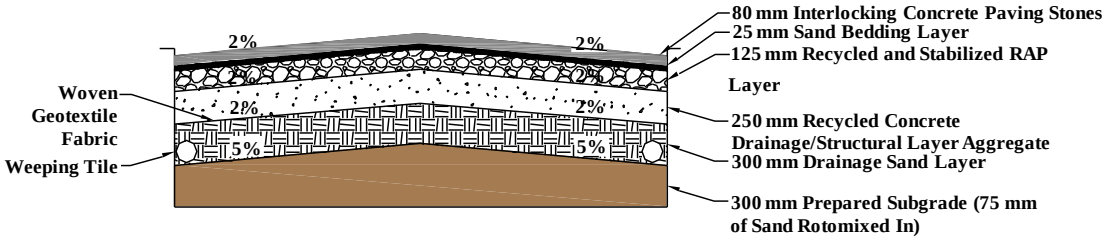

North Road Section 1 (km 0.000 to km 0.153)

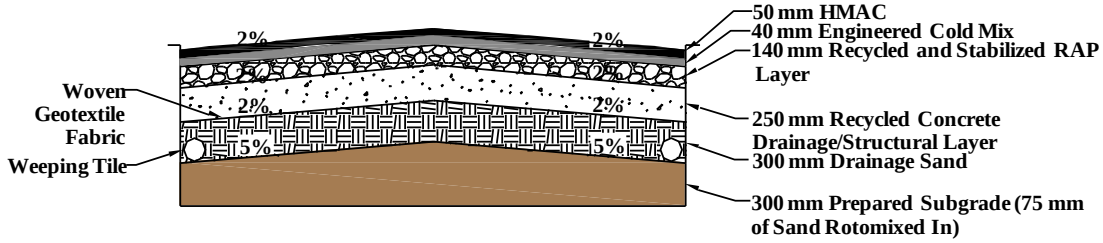

North Road Section 2 (km 0.153 to km 0.322)

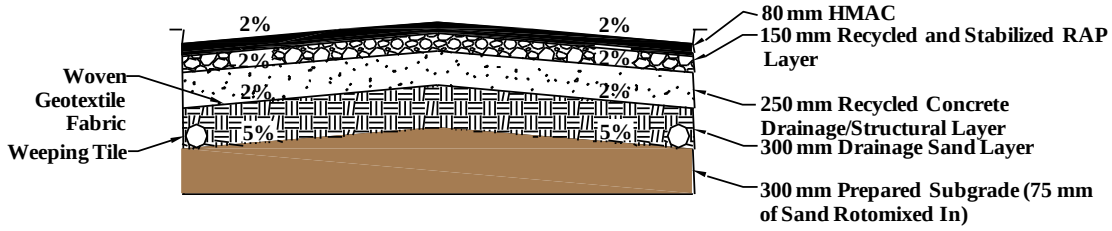

North Road Section 3 (km 0.322 to km 0.482)

Figure 6.14 Post Construction Cross Sections of North Road

During construction of North Road, a total depth of 780 mm of material was excavated (Figure 6.15). There were parts of Section 3 which were dug slightly deeper to remove saturated subgrade. HMAC and granular base was rotomixed and stockpiled onsite. Saturated base and subgrade material was excavated and hauled away.

Figure 6.15 Excavation of North Road (courtesy of PSI Technologies)

Once the material had been milled and excavated, the subgrade was rotomixed with 75 mm of sand, after which the 300 mm drainage sand layer was placed and weeping tile was installed (Figure 6.6). The woven geocloth was laid on top of the drainage sand layer followed by the recycled PCC drainage rock (Figure 6.17). Once the PCC drainage rock was placed, the reclaimed asphalt pavement (RAP) was placed over the recycled PCC drainage rock material and compacted. RAP stockpiled at City of Saskatoon yards was transported to the site and placed to meet the 125 mm, 140 mm, and 150 mm depth requirements at each of the three sections. The three segments were stabilized (Figure 6.18) using two percent SS-1 making the material into an engineered cold mix. The wearing surfaces of the second and third sections were paved with hot mix asphalt, and installation of paving stones was used as the wearing surface for first section, as seen in Figure 6.19.

Figure 6.16 Placement of the Sand Drainage Layer and Weeping Tile on North Road (courtesy of PSI Technologies)

Figure 6.17 PCC Drainage Layer Place on Woven Geocloth at North Road (courtesy of PSI Technologies)

Figure 6.18 Application of Engineered Cold Mix to Base Layer on North Road (courtesy of PSI Technologies)

Figure 6.19 North Road Section 1: Paving Stone Surface (courtesy of PSI Technologies)

6.2.3 North Road Test Section Quality Assurance

Prior to construction, non destructive structural asset management testing was completed using the HWD to measure the heavy weight deflections of the road. Post construction testing was also conducted. The same load spectra of typical commercial truck loading used on Marquis Drive was used on North Road. The load spectra included Saskatchewan secondary weight, primary weight, primary plus 25 percent and primary plus 50 percent legal axle weights. The same peak surface deflection rating system that was used on Marquis Drive was used on North Road. The surface deflections measured on North Road were rated based on the following rating criteria:

- Good: < 1.0 mm,
- Fair: 1.0mm to 2.0 mm, and
- Poor: > 2.0 mm.

Figure 6.20 illustrates and Table 6.3 through Table 6.5 list peak surface deflection measurements for each section of North Road

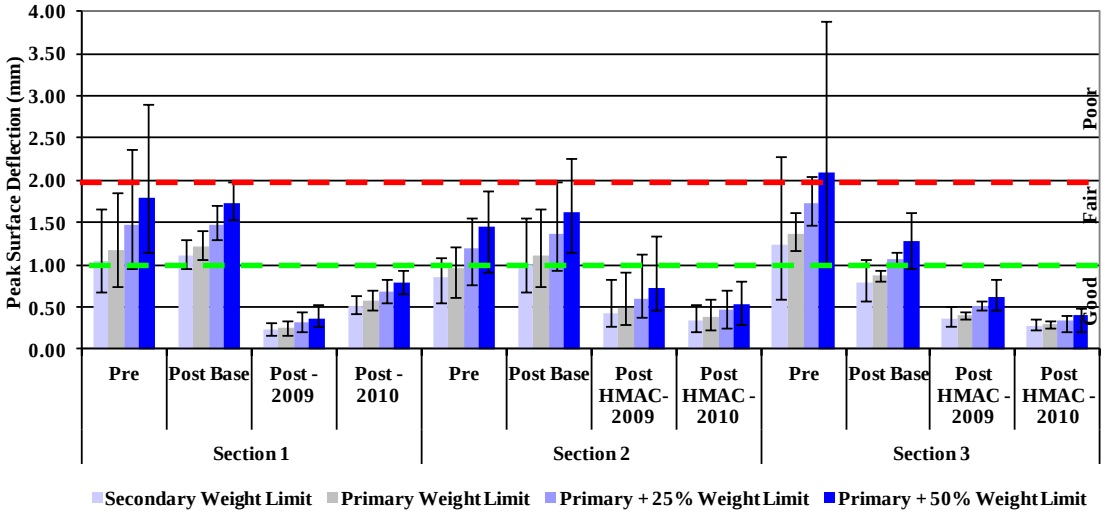

Figure 6.20 Peak Surface Deflection Summary of North Road

Table 6.3 Summary of the Peak Surface Deflections with Respect to Load Spectra of North Road Section 1

	Section 1		
	Pre 2009	Post 2009	Post 2010
Peak Surface Deflection at Secondary Weight Limits			
Average (mm)	1.05	0.22	0.52
Minimum (mm)	0.84	0.16	0.41
Maximum (mm)	2.10	0.36	0.72
Standard Deviation (mm)	0.40	0.06	0.08
Coefficient of Variance (%)	37.81	27.04	16.05
5th Percentile (mm)	0.68	0.16	0.42
95th Percentile (mm)	1.66	0.32	0.65
+ Error Bar	0.61	0.09	0.13
-Error Bar	0.37	0.06	0.10
Peak Surface Deflection at Primary Weight Limits			
Average (mm)	1.17	0.25	0.57
Minimum (mm)	0.93	0.17	0.45
Maximum (mm)	2.37	0.40	0.77
Standard Deviation (mm)	0.45	0.07	0.09
Coefficient of Variance (%)	38.31	27.41	15.57
5th Percentile (mm)	0.76	0.18	0.46
95th Percentile (mm)	1.86	0.35	0.70
+ Error Bar	0.69	0.10	0.13
-Error Bar	0.42	0.07	0.10
Peak Surface Deflection at Primary +25% Weight Limits			
Average (mm)	1.48	0.31	0.68
Minimum (mm)	1.18	0.21	0.55
Maximum (mm)	3.05	0.51	0.92
Standard Deviation (mm)	0.58	0.09	0.10
Coefficient of Variance (%)	39.40	28.26	14.57
5th Percentile (mm)	0.95	0.22	0.56
95th Percentile (mm)	2.38	0.44	0.83
+ Error Bar	0.90	0.13	0.15
-Error Bar	0.53	0.09	0.12
Peak Surface Deflection at Primary +50% Weight Limits			
Average (mm)	1.79	0.37	0.79
Minimum (mm)	1.42	0.25	0.65
Maximum (mm)	3.75	0.62	1.05
Standard Deviation (mm)	0.72	0.11	0.11
Coefficient of Variance (%)	40.33	29.01	13.82
5th Percentile (mm)	1.15	0.27	0.66
95th Percentile (mm)	2.91	0.53	0.95
+ Error Bar	1.11	0.16	0.16
-Error Bar	0.64	0.10	0.13

Table 6.4 Summary of the Peak Surface Deflections with Respect to Load Spectra of North Road Section 2

	Section 2 Pre 2009	Post 2009	Post 2010
Peak Surface Deflection at Secondary Weight Limits			
Average (mm)	0.85	0.44	0.35
Minimum (mm)	0.73	0.30	0.19
Maximum (mm)	1.22	0.98	0.58
Standard Deviation (mm)	0.17	0.21	0.13
Coefficient of Variance (%)	20.17	48.39	38.54
5th Percentile (mm)	0.56	0.27	0.21
95th Percentile (mm)	1.09	0.83	0.54
+ Error Bar	0.24	0.40	0.19
-Error Bar	0.30	0.16	0.14
Peak Surface Deflection at Primary Weight Limits			
Average (mm)	0.95	0.48	0.38
Minimum (mm)	0.81	0.34	0.21
Maximum (mm)	1.36	1.09	0.63
Standard Deviation (mm)	0.19	0.23	0.15
Coefficient of Variance (%)	20.28	48.15	38.42
5th Percentile (mm)	0.62	0.31	0.23
95th Percentile (mm)	1.22	0.92	0.59
+ Error Bar	0.27	0.44	0.21
-Error Bar	0.33	0.18	0.15
Peak Surface Deflection at Primary +25% Weight Limits			
Average (mm)	1.20	0.60	0.46
Minimum (mm)	1.00	0.42	0.23
Maximum (mm)	1.72	1.36	0.75
Standard Deviation (mm)	0.25	0.29	0.18
Coefficient of Variance (%)	20.54	47.66	0.39
5th Percentile (mm)	0.77	0.39	0.26
95th Percentile (mm)	1.55	1.14	0.71
+ Error Bar	0.36	0.53	0.25
-Error Bar	0.43	0.22	0.20
Peak Surface Deflection at Primary +50% Weight Limits			
Average (mm)	1.45	0.73	0.53
Minimum (mm)	1.20	0.51	0.25
Maximum (mm)	2.09	1.63	0.88
Standard Deviation (mm)	0.30	0.34	0.21
Coefficient of Variance (%)	20.79	47.28	0.39
5th Percentile (mm)	0.92	0.46	0.30
95th Percentile (mm)	1.89	1.35	0.82
+ Error Bar	0.44	0.63	0.29
-Error Bar	0.52	0.26	0.24

Table 6.5 Summary of the Peak Surface Deflections with Respect to Load Spectra of North Road Section 3

	Section 3		
	Pre 2009	Post 2009	Post 2010
Peak Surface Deflection at Secondary Weight Limits			
Average (mm)	1.23	0.37	0.28
Minimum (mm)	0.56	0.26	0.24
Maximum (mm)	2.42	0.57	0.40
Standard Deviation (mm)	0.63	0.09	0.05
Coefficient of Variance (%)	51.49	24.44	18.3
5^{th} Percentile (mm)	0.61	0.28	0.23
95^{th} Percentile (mm)	2.28	0.51	0.36
+ Error Bar	1.05	0.14	0.08
-Error Bar	0.62	0.09	0.05
Peak Surface Deflection at Primary Weight Limits			
Average (mm)	1.36	0.40	0.29
Minimum (mm)	1.15	0.37	0.27
Maximum (mm)	1.65	0.47	0.34
Standard Deviation (mm)	0.26	0.06	0.03
Coefficient of Variance (%)	18.95	13.82	9.19
5^{th} Percentile (mm)	1.17	0.37	0.26
95^{th} Percentile (mm)	1.61	0.46	0.33
+ Error Bar	0.25	0.05	0.04
-Error Bar	0.20	0.03	0.03
Peak Surface Deflection at Primary +25% Weight Limits			
Average (mm)	1.73	0.51	0.34
Minimum (mm)	1.45	0.46	0.15
Maximum (mm)	2.09	0.58	0.42
Standard Deviation (mm)	0.33	0.06	0.08
Coefficient of Variance (%)	19.17	12.80	22.80
5^{th} Percentile (mm)	1.47	0.46	0.22
95^{th} Percentile (mm)	2.05	0.57	0.41
+ Error Bar	0.32	0.06	0.07
-Error Bar	0.26	0.04	0.12
Peak Surface Deflection at Primary +50% Weight Limits			
Average (mm)	2.09	0.62	0.40
Minimum (mm)	0.91	0.44	0.09
Maximum (mm)	4.00	0.94	0.50
Standard Deviation (mm)	1.10	0.14	0.12
Coefficient of Variance (%)	52.60	22.90	30.60
5^{th} Percentile (mm)	0.98	0.47	0.21
95^{th} Percentile (mm)	3.90	0.84	0.49
+ Error Bar	1.80	0.22	0.09
-Error Bar	1.11	0.15	0.19

Post construction, all three sections had deflections of no greater than 0.50 mm which is rated as good based on the rating criterion, immediately following construction in 2009. As seen in Figure 6.20, the results measured in 2010 from Section 1 were 50 percent higher than the values measured in 2009, and the values in Section 2 and Section 3 were 22 to 25 percent lower. The difference in deflections from Section 1 through Section 3 is still below an average of 1.00 mm deflection. From the data it can also been seen that variability in the deflections was reduced following construction.

6.3 Application of Three Dimensional Modeling to Predict Road Performance

Currently the City of Saskatoon uses conventional granular materials and follows the Saskatchewan Highways modified California Bearing Ratio (CBR) Shell Design Curve when designing a new road structure (SMHI 2009). When using the CBR design curves, the CBR curves determine the thickness of hot mix asphalt concrete, conventional granular base and the subbase layer thicknesses. The thicknesses of each of the layers are based on the *in situ* CBR of the subgrade. However, using this design method does not account for change in climatic effects, traffic levels including heavy truck traffic, or the use of other materials such as recycled PCC materials. Shell curve design method is empirically based, and is built on the "layered linear elastic primary response of the road structure indirectly; using the vertical compressive stress and strain at the top of the subgrade as the limiting factors for permanent deformation of the subgrade and horizontal tensile strain at the bottom of the asphalt layer for rutting" (Berthelot et al. 2011). Other design methods commonly used by other jurisdictions are explained in Chapter Two.

The implementation or use of alternative building materials within COS road structures cannot proceed without the alternative designs procedure, which accepts the use of innovative building materials. With the advancements in technology and research, a mechanistic based road design model has been developed to overcome the disadvantages of conventional road structural design methods currently employed. The mechanistic road model used to calculate the primary response principals related to long term pavement performance is called (PSIPave3D^{TM}). The model incorporates road layer thicknesses, load spectra, climatic conditions and mechanistic material properties into the design of the road. Given the previous inputs, the stress strain behavior of the road structure is spatially calculated using the finite element method and the

latest advancements in computational mechanics (Soares 2005). With the input of mechanistic material properties and road geometry the model can be used to predict and verify field performance. In order to validate the output of the model, peak surface deflections can be compared between the model predicted output and those measured by the HWD testing performed in the field.

In this research, one section from both the Marquis Drive and the North Road test sections were inputted into the road model and then compared using the HWD data collected post construction of both the test sections. The structural layers from section two of North Road, and section one of Marquis Drive as seen in Figure 6.21 and Figure 6.22 were input in the PSIPave3D^{TM} road modeling program. The strains modeled for each road structure are based on a four tire single axle loaded at primary weight limits.

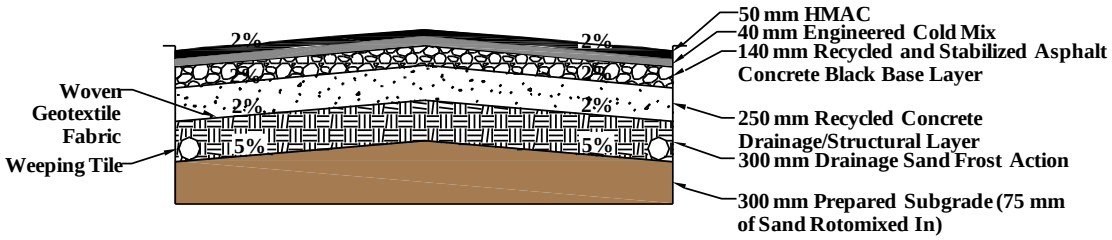

Figure 6.21 North Road Section 2 Cross Section (km 0.153 to km 0.322)

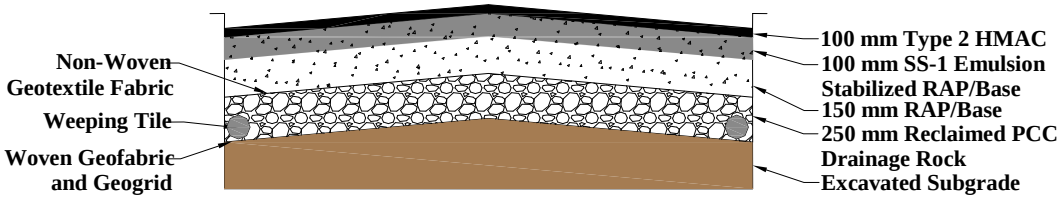

Figure 6.22 Marquis Drive Segment 1 Cross Section (km 0.000 to km 0.175)

6.3.1 Model Validation Using Peak Surface Deflections

As seen in Figure 6.23, Figure 6.24 and Table 6.6, the HWD deflections from Section 2 of North Road and Segment 1 of Marquis Drive post construction were plotted, along with the output of the model. The deflection measured using the HWD for Section 2 of North Road across the load spectrum ranged from 0.35 mm under secondary weight up until 0.53 mm under primary weight plus 50 percent. In comparison the deflection ranges for the Section 2 in North Road using the road modeling program ranged from 0.32 mm under the secondary weight to up to 0.54 mm under primary plus 50 percent. The difference in the deflection measurements made by the HWD and the road model was a maximum of eight percent.

The post construction deflections measured by the HWD and the road model for Segment 1 of Marquis Drive are also shown in Table 6.6 and Figure 6.24. The deflection measures using the HWD for Segment 1 of Marquis Drive across the load spectrum ranged from 0.50 mm under secondary weight up until 0.81 mm under primary weight plus 50 percent. In comparison, the deflection ranges for the Segment 1 in Marquis Drive using the road modeling program ranged from 0.51 mm under the secondary weight up until 0.86 mm under primary plus 50 percent. The difference in the deflection measurements made by the HWD and the road model was a maximum of six percent.

In addition to road deflections, PSIPave3D^{TM} is also able to predict the normal and shear strain results of a road structure which can be used to predict the fatigue cracking and structural rutting of a road structure. Currently, many jurisdictions use the American Association of State Transport (AASHTO) design manual. The AASHTO design manual is an observed performance statistically correlated to tensile strain at the bottom of the HMAC layer and the vertical compressive strain at the top of subgrade to forecast fatigue cracking and structural rutting of a road structure (AASHTO 2002, Berthelot et al. 2011).

Table 6.6 Peak Deflection Comparison (Post 2010)

Test Section	Testing Weight	HWD Deflections (mm)	Model Deflections (mm)	Percent Difference (%)
North Road	Secondary	0.35	0.32	8.6
	Primary	0.38	0.36	5.3
	Primary+25%	0.46	0.45	2.2
	Primary+50%	0.53	0.56	5.7
Marquis Drive	Secondary	0.50	0.47	6.4
	Primary	0.55	0.52	5.8
	Primary+25%	0.68	0.69	1.4
	Primary+50%	0.81	0.80	1.3

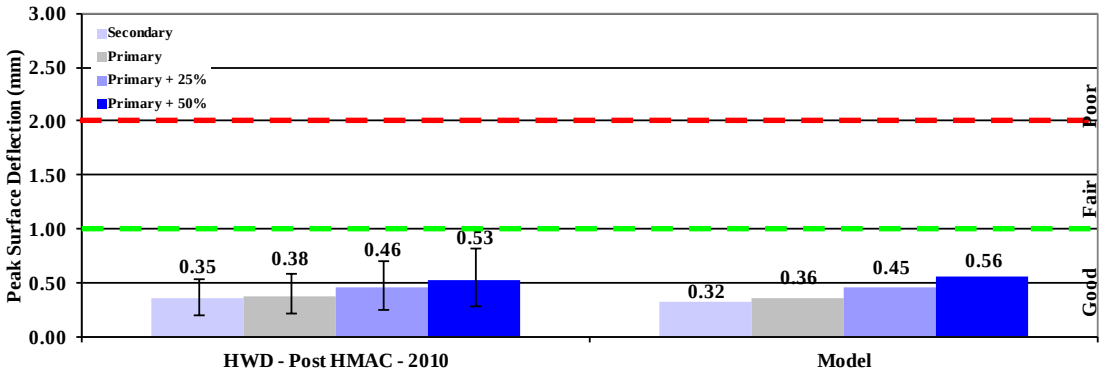

Figure 6.23 North Road Section 2 Peak Surface Deflection Profiles Comparison (Post 2010)

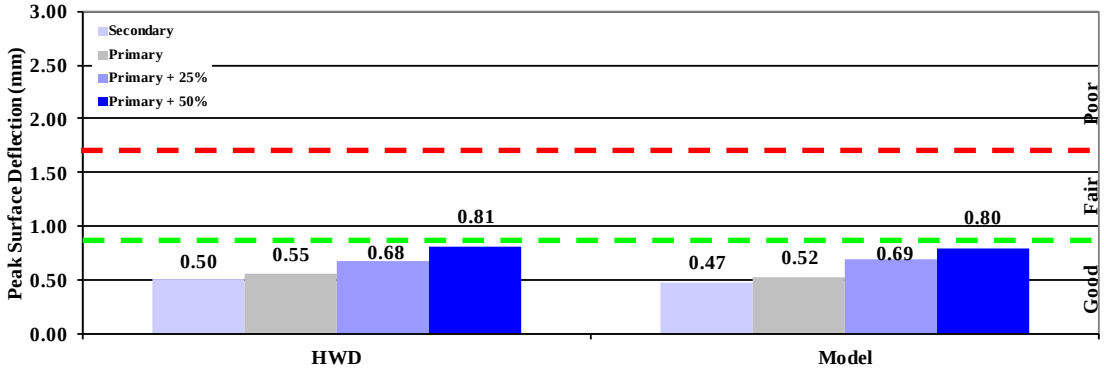

Figure 6.24 Marquis Drive Segment 1 Peak Surface Deflection Profiles Comparison (Post 2010)

6.3.2 Model Calculated Peak Strains for Post Construction Test Sections

The PSIPave3D^{TM} model was used to predict different strain components found within the road structures analyzed. The model is also able to produce strain profiles with the purpose of visually identifying weak areas in the structure. Table 6.7 lists the peak vertical compressive strain, the peak horizontal tensile strain, and the peak shear strain in both Marquis Drive Section 2 and North Road Section 1 for both the drainage layer and the subgrade layer, post construction.

Table 6.7 Peak Strains in Drainage and Subgrade Layers under Primary Weight Limit (Post 2010)

Test Section	Peak Vertical Compressive Strain		Peak Horizontal Tensile Strain		Peak Shear Strain	
	Drainage Layer	Subgrade	Drainage Layer	Subgrade	Drainage Layer	Subgrade
Marquis Drive Segment 1	48	200	28	54	76	174
North Road Section 2	39	112	10	37	50	98

Figure 6.25 illustrates the vertical strain contours for both Marquis Drive Segment 1 and North Road Section 2. As seen in Figure 6.25, the highest vertical strain was contained within the top structural layers of the road structure for both the test sections modeled. When designing a road structure, whether using a road model or the shell design curves, it is ideal to have the highest compressive strains dissipated in the top layers of road structure since the material used is of higher quality, higher stiffness and strength.

Figure 6.26 presents the peak vertical strain in each of these layers, for each test section. As seen in Figure 6.26, North Road test section had lower vertical compressive strains when compared to Marquis Drive test section.

Figure 6.27 illustrates the horizontal strain contour profiles for both test sections under primary weight limits. Figure 6.28 compares the peak horizontal strain in the drainage and subgrade layers. As seen in Figure 6.27, the high horizontal strain, which is illustrated by the red colouring, extends into the subgrade for both sections.

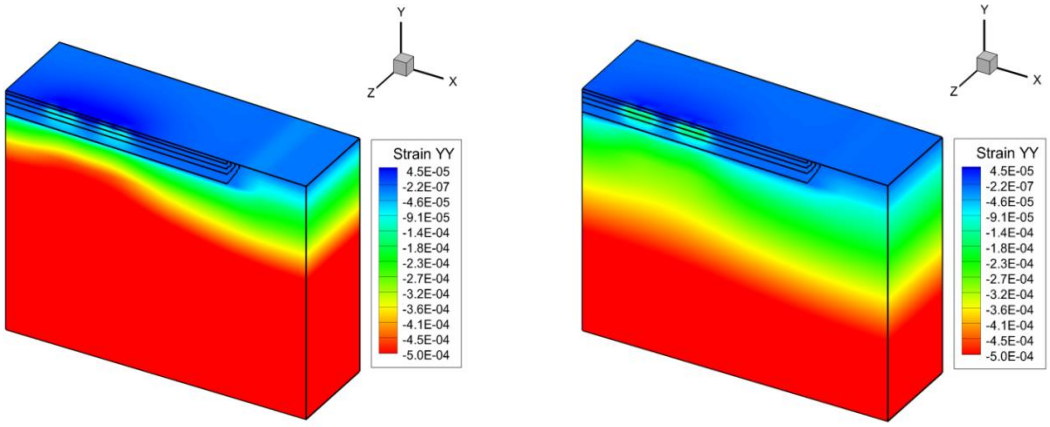

a) Marquis Drive Segment 1 **b) North Road Section 2**

Figure 6.25 Vertical Strain under Primary Weight Limit

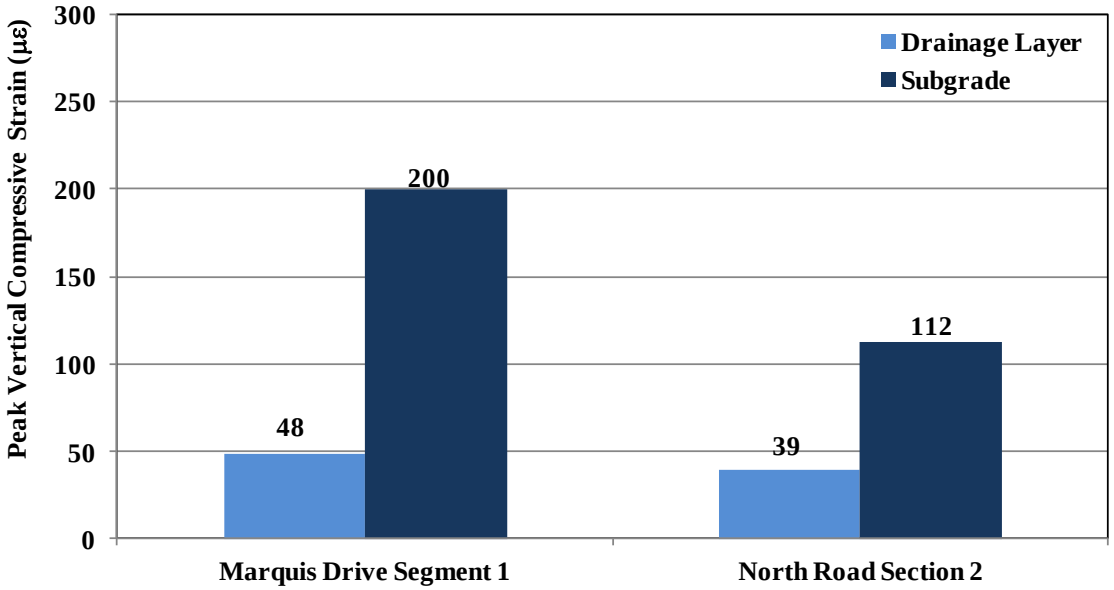

Figure 6.26 Peak Vertical Compressive Strain in Drainage and Subgrade Layers under Primary Weight Limit

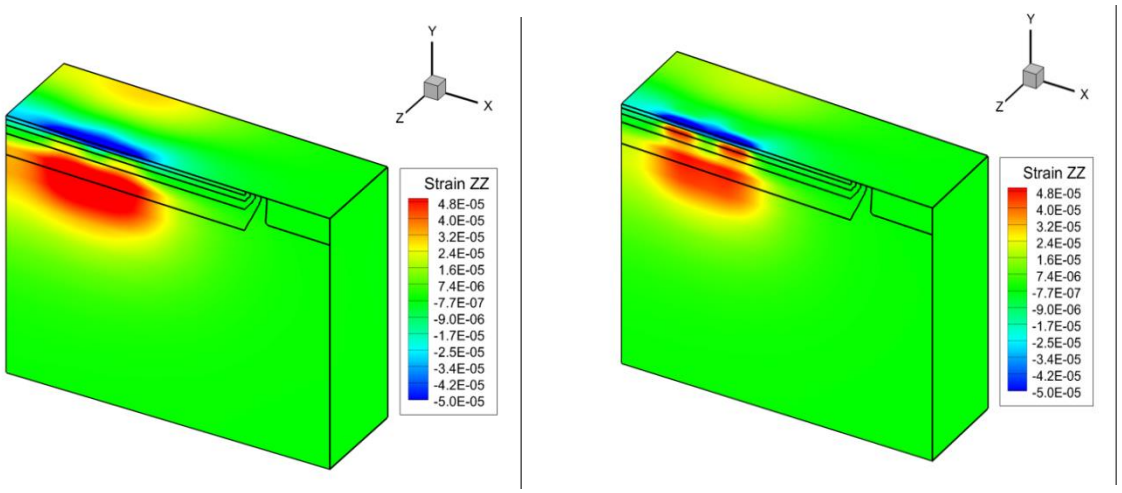

a) Marquis Drive Segment 1 **b) North Road Section 2**

Figure 6.27 Horizontal Strain Profiles under Primary Weight

As seen in Figure 6.28, the North Road test section had lower horizontal strains when compared to the Marquis Drive test section. As with the vertical compressive strains, the horizontal strains found in the drainage layers of both test sections were reduced, compared with those in the subgrade layers.

Figure 6.29 illustrates the shear strain contour profiles for both test sections under primary weight limits. Figure 6.30 illustrates the peak shear strain in each drainage and subgrade layer of each test section.

Shear strain is an important component because structural failure within a road structure is typically associated with high shear strains induced by traffic loading. This correlates to the fact that road materials are weaker in shear, with higher shear strains often present in a road structure's subgrade. The shear strain profiles also indicate that these two road structures are subgrade dependant, in that the shear strain is not contained within the top three layers. In comparing the two test sections the North Road test section had lower shear strains than the Marquis Drive test section, which can be seen in Figure 6.29. The reason that the shear strains are larger in the Marquis Drive test section is because the subgrade is much wetter compared to the North Road section.

Road models are becoming an important tool that road designers can use to evaluate road designs before construction starts, which is becoming important when road budgets need to be

maximized. Through the road deflections taken from one section of both North Road and Marquis Drive, PSIPave3D^{TM} accurately correlated to HWD data. Through the road model, strain profiles were generated, illustrating the behavior of each of road structure layers under traffic loading.

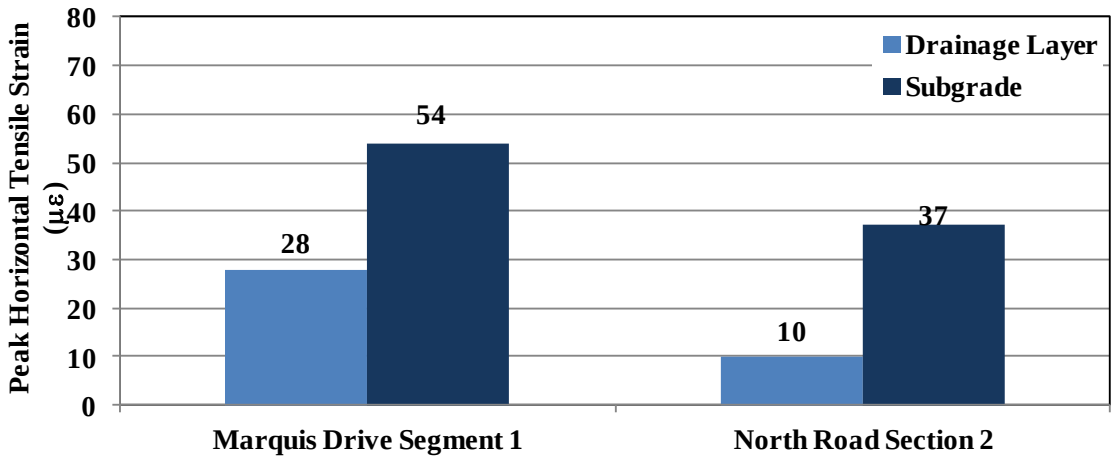

Figure 6.28 Peak Horizontal Tensile Strain in Drainage Layer and Subgrade Layers under Primary Weight

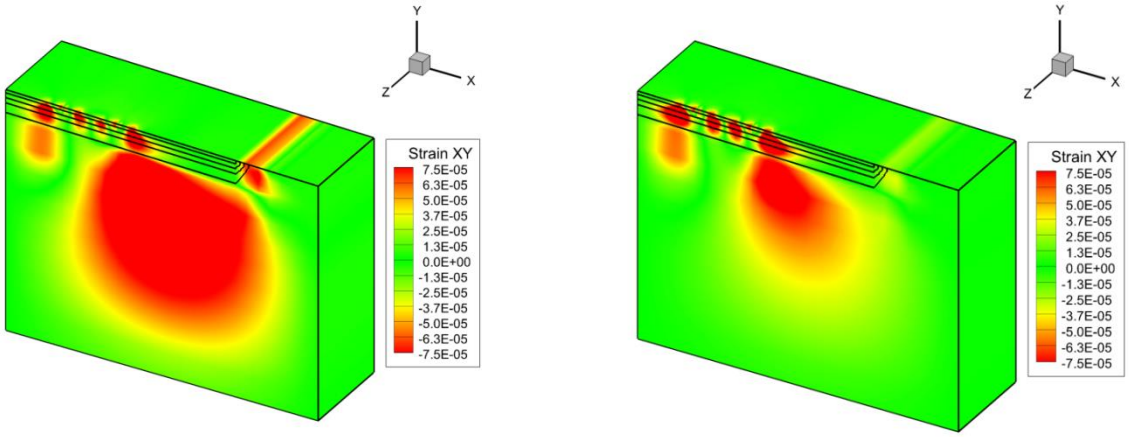

a) Marquis Drive Segment 1 **b) North Road Section 2**

Figure 6.29 Shear Strain Profiles under Primary Weight

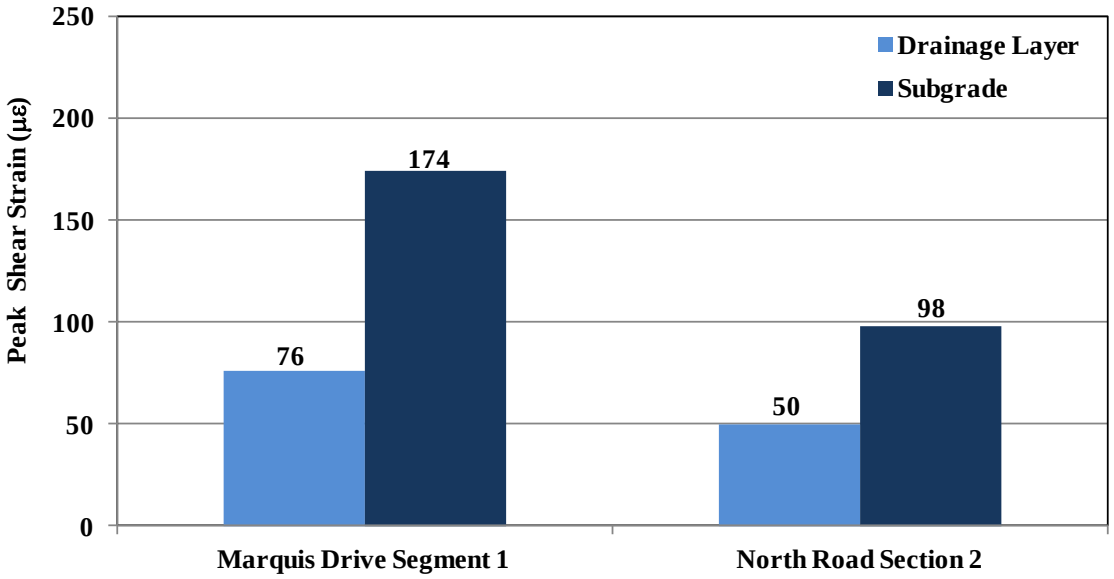

Figure 6.30 Peak Shear Strain in Drainage and Subgrade Layers

6.4 Chapter Summary

Alternative road construction methods using recycled materials were investigated by the City of Saskatoon and the University of Saskatchewan. Both test sections included in this research incorporated crushed PCC rock as a drainage layer in road reconstruction. Both Marquis Drive and North Road had reduced peak surface deflection measured using a non-destructive heavy weight deflectometer post construction. After construction, Marquis Drive Segment 1 had an average surface peak deflection of 0.55 mm and North Road Section 1 had an average peak surface deflection of 0.25 mm.

Using the HWD deflection data collected at both test sections, a finite element model (PSIPave3D^{TM}) was used to predict different strain components found within the road structures. Both the vertical compressive strains and the horizontal strains found in the drainage layers of both test sections were reduced. The road model also demonstrated the strain behaviour of City of Saskatoon subgrades. Also, the model-predicted peak surface deflections were comparable to those measured in the field.

CHAPTER 7 ECONOMIC COMPARISON

The laboratory component of this research has shown that using crushed Portland cement concrete (PCC) in a pavement structure is technically feasible. PCC drainage rock was used in two City of Saskatoon test sections, demonstrating construction feasibility. However, to consider crushed PCC as a base course or drainage rock alternative, costs associated with using the recycled concrete material must be comparable or better than the conventional aggregate materials currently used by the City of Saskatoon. This chapter discusses the following costs:

- Test section material capital costs;
- Test section material haul costs;
- Landfill cost savings; and
- City of Saskatoon road rehabilitation aggregate supply annual cost.

7.1.1 Test Section Material Capital Costs

The capital costs used in this research are one-time expenses associated with construction of the test sections and include material costs only. Labour, equipment and placement costs are not included. Figure 7.1 compares the total capital costs associated with the construction of the Marquis Drive and North Road test sections using recycled granular materials and conventional granular materials. Table 7.1 and Table 7.2 detail the capital costs based on present day material costs for each material component: hot mix asphalt concrete (HMAC), base material, drainage rock, geotextiles, and stabilizers. The authors experience and industry personnel were consulted to determine material costs used in the cost estimate. Also, the prices of the material include delivery to site.

The rehabilitation of Marquis Drive using recycled materials had an approximate cost of $440,500 or $144 per m^2. Had Marquis Drive been constructed using virgin aggregates for the base layer and drainage rock, the rehabilitation would have cost approximately $530,000 or $173 per m^2. The rehabilitation of North Road using recycled materials was approximately $493,000 or $134 per m^2. Had North Road been constructed using virgin aggregate for the base layer and drainage rock, the rehabilitation would have cost approximately $568,500 or $155 per m^2.

The City of Saskatoon and University of Saskatchewan saved 17 percent or \$29 per m^2, and 15 percent or \$21 per m^2 in capital costs, respectively, by using recycled materials in lieu of conventional road building materials. These reduced costs demonstrate the economic feasibility of using PCC drainage rock in a pavement structure.

PCC drainage rock is less expensive than conventional drainage rock primarily due to reduced transportation costs. The costs associated with processing and crushing the PCC rock and the conventional materials are approximately the same. However, the recycled materials are crushed within City limits and have haul distances from the City limits. Virgin aggregates are crushed outside of City limits and have haul distances up to 100 km (Berthelot et al. 2007). For example, virgin aggregate is hauled 80 kilometres from Wakaw, Saskatchewan to Saskatoon. Recycled PCC materials are hauled from Nicholson Yard or the landfill within the City of Saskatoon. For example, the haul distance for Nicholson Yard to Marquis Drive was 20 km.

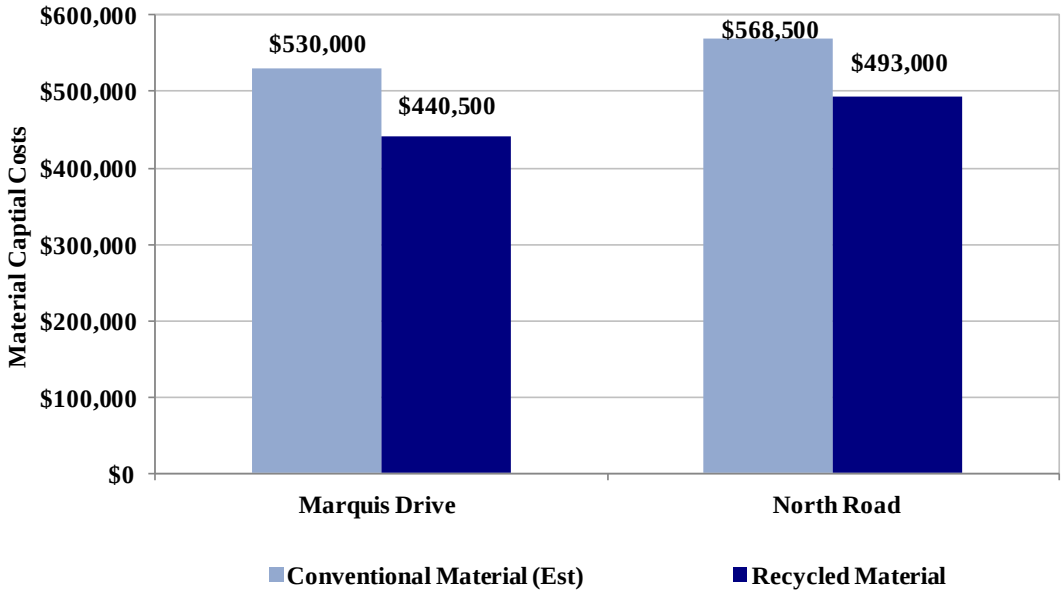

Figure 7.1 Capital Construction Costs for both Marquis Drive and North Road

Table 7.1 Material Costs for Marquis Drive Test Section

a) Recycled Materials

Material Type	Material Costs ($/m2)	Material Costs ($/tonne)	Quantity used (m^2)	Quantity used (tonnes)	Total Costs ($)
PCC Drainage Rock	-	15	-	2450	36,750.00
RAP/BASE	-	15	-	1010	15,150.00
Stabilizer (2%)	-	750	-	20	15,150.00
Geotextile	2	-	3060	-	6,120.00
HMAC	120	-	3060	-	367,200.00
Total					**$440,500.00**

b) Conventional Materials Est

Material Type	Material Costs ($/m2)	Material Costs ($/tonne)	Quantity used (m^2)	Quantity used (tonnes)	Total Costs ($)
COS Drainage Rock	-	35	-	2550	89,250.00
COS Granular Base	-	27	-	2480	66,960.00
Geotexile	2	-	3060	-	6,120.00
HMAC	120	-	3060	-	367,200.00
Total					**$530,000.00**

Table 7.2 Material Costs for North Road Test Section

a) Recycled Materials

Material Type	Material Costs ($/m2)	Material Costs ($/tonne)	Quantity used (m^2)	Quantity used (tonnes)	Total Costs ($)
RAP/BASE	-	15	-	300	4,500.00
Sand	-	10	-	3000	30,000.00
PCC Drainage Rock	-	15	-	2100	31,500.00
Stabilizer (2%)	-	250	-	6	1,500.00
Geotextile	2	-	3668	-	7,336.00
HMAC	90	-	2368	-	213,120.00
Paving Stone	120	-	1300	-	156,000.00
Engineered Coldmix	40	-	1216	-	48,640.00
Total					**$493,000.00**

b) Conventional Materials Est

Material Type	Material Costs ($/m2)	Material Costs ($/tonne)	Quantity used (m^2)	Quantity used (tonnes)	Total Costs ($)
Sand	-	10	-	3000	30,000.00
COS Drainage Rock	-	35	-	2350	82,250.00
COS Granular Base	-	27	-	1150	31,050.00
Geotextile	2	-	3668	-	7,336.00
HMAC	90	-	2368	-	213,120.00
Paving Stone	120	-	1300	-	156,000.00
Engineered Coldmix	40	-	1216	-	48,640.00
Total					**$568,500.00**

7.1.2 Test Section Haul Costs

The transportation haul costs are the total costs required to haul the material from the crushing site to the construction site. The transportation costs were calculated for the two test sections that were mentioned in this research. The costs associated with hauling aggregates to the construction sites in 2009 are provided in Table 7.3. The following assumptions were used in the calculations:

- For virgin aggregate (base and rock), the average round trip between the two test sections to Wakaw, Saskatchewan is 195 km.
- For recycled aggregates (base and drainage rock), the average round trip between the two test sections to Nicholson Yard is 23 km
- The cost of hauling the PCC material to Nicholson Yard is considered negligible since the concrete material would be hauled a short distance within the City or to the landfill for disposal.

The average trucking rate for a 35 tonne truck is 0.20 cents per tonne/km.

The cost to transport conventional granular base to both of the test sections in 2009 is estimated to be $71,000. The cost to transport conventional drainage rock in 2009 is estimated to be $96,000. The cost to transport recycled PCC aggregate to the test sections from the Nicholson yard is estimated to be $14,000. As seen in Table 7.3 there is a cost savings of approximately $82,000 in transportation in using recycled PCC drainage rock compared to conventional drainage rock for both test sections.

Table 7.3 Transportation Costs of Conventional Aggregates

Material Type	Cost for Transportation ($/Tonne)	Quantities used in Table 7.1 and 7.2 (Tonne)	Total Cost ($)
Conventional COS Granular Base	19.50	3,630	$71,000
Conventional Drainage Rock	19.50	4,900	$96,000
Recycled PCC Drainage Drainage Rock	3.00	4,550	$14,000

7.1.3 Landfill Cost Savings

There are additional cost savings that may be considered when comparing the use of recycled Portland cement concrete (PCC) material to conventional material. The cost of disposing solid waste in 2009 at the City of Saskatoon landfill was approximately $65/tonne (COS 2009A, COS 2011). Since then, it has increased to $95/tonne (COS 2013).

A total of 4,550 tonnes of PCC rubble was used in Marquis Drive and North Road test sections. Had this material been disposed of in the City landfill, the cost would have been $292,750 or $44 per m^2 based on 2009 tipping fees. Based on the recent cost increase, it would have cost upwards of $430,000 to dispose of the 4,550 tonnes of PCC rubble in the landfill (COS 2013).

7.2 Annual City of Saskatoon Road Rehabilitation Aggregate Supply Cost

The City of Saskatoon uses quantities of granular base and drainage rock in road rehabilitation projects every year. From 2009 to 2011, the City's annual consumption of granular base and conventional drainage rock has consistently increased (Guenther 2010). Table 7.4 lists and Figure 7.2 illustrates quantities of granular base and drainage rock the City consumed in 2009, 2010, and 2011. Capital costs are also provided. The cost of virgin granular base and drainage rock materials increased incrementally from 2009 to 2011. No increase in PCC cost is listed because the material was only used by the City in 2009.

Table 7.4 City of Saskatoon Aggregate Consumption for Road Rehabilitation Project

Year	Consumed tonnes	Material Type	$/tonnes	Total Cost
2009	2,000	COS Drainage Rock	30	$60,000
	25,000	COS Granular Base	19	$475,000
2010	3,000	COS Drainage Rock	32	$96,000
	30,000	COS Granular Base	24	$720,000
2011	5,000	COS Drainage Rock	35	$175,000
	40,000	COS Granular Base	27	$1,080,000
2009 PCC Material	5,000	PCC Drainage Rock	15	$75,000
	40,000	PCC Well graded Base	15	$600,000

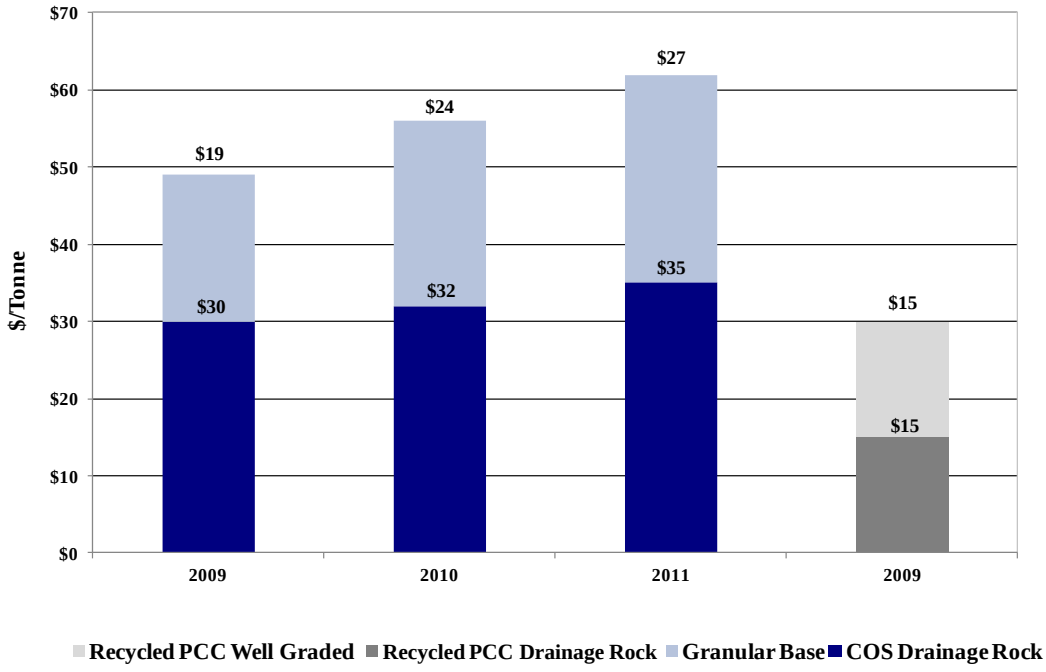

Figure 7.2 Budget of Aggregate Used by City of Saskatoon

Aggregate sustainability is becoming more of an issue as the province, including the towns and cities, continues to grow. As new construction and rehabilitation increase so does the demand for quality aggregates. In 2011, the City used 40,000 tonnes of base aggregate for road rehabilitation, at a cost of $27 per tonne. This cost the City $1,080,000 dollars.

7.3 Chapter Summary

The costs associated with the construction of both test sections using recycled materials were significantly lower when compared to using conventional materials. The cost savings were approximately $89,000 dollars or $29 per m^2 for the Marquis Drive project and $75,800 or $21 per m^2 for the North Road project in capital costs. As the local conventional aggregate sources have been consumed, the transportation costs of transporting conventional aggregates are continuing to increase. If recycled PCC materials are used within the road structure, the transportation costs are minimized since the material is processed within the city limits.

The COS is saving significant money by recycling the PCC rubble instead of putting it in the landfill. The city saves in two ways; the first includes not paying a tipping fee for the PCC material, as well as saving valuable space at the landfill. The demand, limited supply of

conventional aggregates and increased transportation costs are causing the price to steadily increase. By using the recycled PCC materials in road construction, the city and provincial road agencies are able to save the non-renewable resource for when it is needed or when its physical and mechanistic properties are superior to recycled PCC materials, and maximize their budgets by using PCC where conventional materials are not needed.

CHAPTER 8 CONCLUSIONS

The City of Saskatoon relies on conventional granular material for the construction and rehabilitation of its road infrastructure system. Portland cement concrete (PCC) rubble provides an alternative aggregate source that can be processed and used as aggregate within multiple layers in a road structural system. The hypothesis of this research was that crushed Portland cement concrete is technically feasible as a granular base course and drainage layer to be used in City of Saskatoon road structures.

The goal of this research was to validate the use of crushed Portland cement concrete rubble in City of Saskatoon road structures. Sub-objectives of this research were to compare PCC material properties to those of conventional granular materials under realistic field state conditions, and to validate the economic feasibility of using recycled PCC material within City of Saskatoon road structures through test section design and field test section structural performance.

8.1 Summary of Results

Conventional laboratory testing showed that the well graded Portland cement concrete (PCC) base material and the PCC drainage rock met the aggregate specifications for the City of Saskatoon. Once the material met the City specifications, the conventional City of Saskatoon granular base, the recycled well graded (GW) PCC base material, and the recycled PCC drainage rock were mechanistically characterized as part of the first objective.

With respect to the first objective of comparing PCC material properties to those of conventional granular material under realistic field state conditions, the following observations can be made:

- The conventional COS granular base samples failed under the high stress state under a testing frequency of 0.5 Hz prior to vacuum saturation. Following vacuum saturation, the recycled PCC GW failed under high stress state at a testing frequency of 10 Hz. All other recycled PCC GW specimens survived vacuum saturation.
- The cement and/or SS-1 emulsion stabilized PCC GW base material and the PCC drainage rock samples survived all RATT stress states and frequencies, prior to vacuum saturation testing.

- The dynamic modulus of the research materials increased as the testing frequencies increased from 10 Hz to 0.5 Hz. The dynamic modulus also decreased as the stress state increased from low to high.
- The recycled PCC drainage rock, the recycled PCC GW base, and the stabilized PCC GW base had dynamic moduli ranging from 39 to 82 percent higher than the conventional COS granular base depending on the material and testing parameters used.
- Some caution should be used if the stabilized PCC with three percent cement is used as a structural layer. The material may be too stiff or brittle to survive the freeze thaw action found in Saskatchewan field state conditions.
- Overall, the phase angles of the research materials decreased as the testing frequency increased. The phase angles also increased as the stress state increased from low to high.
- The phase angles for the PCC materials were similar to the measured values of the conventional COS granular base at testing parameters of low stress state at both testing frequencies. However, after the stress state increased the conventional COS granular base phase angles increased by 44 percent when compared to the phase angles for the PCC materials.
- Poisson's ratio values for the research materials showed very little dependence on the change of testing frequency or the increase from 10 Hz to 0.5 Hz. However, there was a greater increase in Poisson's ratio when the stress state increased from low to high. The conventional COS granular base and the recycled PCC drainage rock showed the greatest Poisson's ratio of an approximate increase of 67 percent.

With respect to the second objective of validating the economic feasibility of using recycled PCC material within City of Saskatoon road structures through test section design and field test section structural performance, the following observations can be made:

- Recycled PCC drainage rock was used as both a structural layer and a drainage layer within the road structures in both test sections and no specialized construction equipment was needed to construct the test sections including the PCC drainage layer.

- Using non-destructive heavy weight deflectometer measurements, both test sections met the City's peak deflection thresholds for secondary weight up until primary plus 50 percent both post construction and one year later.
- The City of Saskatoon and University of Saskatchewan saved between $21 per m^2 and $29 per m^2 by using the recycled aggregate materials compared to using conventional materials.

Additional observations that can be made after completing this research project include:

- The utilization of other conventional material tests such as fine aggregate angularity and the Micro-Deval test is needed if recycled PCC materials are used in construction.
- The use of mechanistic testing allows engineers to design road structures based on actual material data for the specified field state conditions instead of empirically based material tests such as the California Bearing Ratio and its use in the Shell design curves. The use of mechanistic material properties then allows the engineer to input the material properties into a road modeling program.
- By utilizing new mechanistic based road modeling software, engineers are able to evaluate the performance of a road structure, including the use of unconventional materials prior to construction of the road structure.

8.2 Conclusions

The hypothesis of this research was that crushed Portland cement concrete is technically feasible as a granular base course and drainage layer to be used in City of Saskatoon road structures.

Through conventional material testing it was proven that recycled PCC drainage rock and recycled PCC GW base met the City of Saskatoon crushed rock and the base aggregate specification. It was also shown that conventional base aggregate material tests, including standard Proctor compaction and CBR testing, are not designed for unconventional aggregate material such as recycled PCC GW base. Given the empirical nature of CBR test, triaxial frequency sweep characterization of the PCC materials was complete and compared against conventional COS granular base.

Mechanistic materials' characterization of the recycled PCC drainage rock, as well as the unstabilized and stabilized recycled PCC GW base, resulted in PCC materials that were high quality and outperformed conventional COS granular across different stress states and testing frequencies. The construction and good performance of two test sections built by the City of Saskatoon and the University of Saskatchewan using recycled PCC drainage rock as both a structural layer and a drainage layer showed that using PCC material is an economic solution that does not compromise the strength and performance of the road structure.

8.3 Future Research

This research found that if the City of Saskatoon implements the use of recycled PCC in its road structures, aggregate resources will be conserved; budget funding allocations will be optimized; and the structural capacity of urban roads will be improved. To further enhance the potential for implementing PCC rubble materials into urban road construction, future research should include the construction and analysis of a City of Saskatoon urban road test section using recycling PCC GW base aggregate in the base layer of the road structure and the quantification of environmental benefits of using recycled PCC materials in road construction.

Conventional material testing proved that the recycled PCC GW base met the COS base aggregate specifications. Mechanistic material characterization also showed that the material has better material properties than conventional COS granular base. However, a field test section needs to be completed to determine and validate recycled well graded PCC material as a base layer in COS field state conditions.

Although the environmental benefits of using PCC materials were discussed in this research, they were not quantified. There are new environmental models that can evaluate different construction processes, and identify which process is creating the smallest footprint in the environment.

LIST OF REFERENCES

AASHTO. 2002. Compaction of Bituminous Mixture by Means of the Gyratory Compactor. American Association of State Highway and Transportation Officials Provisional Standards.

Abdo, A., Bayomy, F., Masad, E., Santi, M. 2006. Evaluation of Aggregate Structure Stability Using the Superpave Gyratory Compactor. Transportation Research Board Annual Conference, Washington, D.C. USA.

ACPA. 2008. Concrete Pavement Technology Series. Available from http://www.pavement.com/Concrete_Pavement/Technical/Fundamentals/Reconstructing_and_Recycling.asp. [Accessed on Dec 23 2011]

Anthony, A. 2007. Effects of Manufactured Fine Aggregate on Physical and Mechanistic Properties of Saskatchewan Asphalt Concrete. M.Sc. Thesis, Department of Civil and Geological Engineering, University of Saskatchewan.

Arulrajah, A. and Piratheepan, J. 2010. Geotechnical Characteristics of Recycled Crushed Concrete. Faculty of Engineering and Industrial Science, Swinburne University of Technology, Hawthorn, Australia.

ASTM C 131-06. 2011. Standard test Method for Resistance to Degradation of Small Size Course Aggregate by Abrasion and Impact in the Los Angeles Machine. Annual Book of ASTM Standards, American Society for Testing and Materials .

ASTM C 1252. 2010. Standard Method for Uncompacted Void Content of Fine Aggregate – Method A. Annual Book of ASTM Standards, American Society for Testing and Materials.

ASTM D 075. 2010. Standard Method for Sampling Aggregates. Annual Book of ASTM Standards, American Society for Testing and Materials, 2010.

ASTM D 0698. 2007. Standard Test Method of Laboratory Compaction Characteristics of Soil Using Standard Effort. Annual Book of ASTM Standards, American Society for Testing and Materials.

ASTM D 1557. 2009. Standard Test Method for Laboratory Compacted Characteristics of Soil Using Modified Effort. Annual Book of ASTM Standards, American Society for Testing and Materials

ASTM D 1883. 2011. Standard Test Method for CBR (California Bearing Ratio) of Laboratory Compacted Soil. Annual Book of ASTM Standards, American Society for Testing and Materials.

ASTM D 2974. 2012. Standard Test Method for Moisture, Ash, and Organic Matter of Peat and Other Organic Soils. Annual Book of ASTM Standards, American Society for Testing and Materials.

ASTM D 3282. 2011. Standard Practice for Classification of Soils and Soil-Materials. Annual Book of ASTM Standards, American Society for Testing and Materials

ASTM D 3387. 2012 Standard Practice for Compaction and Shear properties of Bituminous mixtures by means of U.S. Corps of Engineers Gyratory Testing Machine. Annual Book of ASTM Standards, American Society for Testing and Materials.

ASTM D 5821. Standard Test Method for Determining the Percentage of Fractured Particles in Course Aggregate. Annual Book of ASTM Standards, American Society for Testing and Materials.

ASTM D 6913. 2009 Standard Test Method for Particle-Size Distribution (Gradation). Annual Book of ASTM Standards, American Society for Testing and Materials.

ASTM D 6928. 2011. Standard Test Method for Resistance of Course Aggregate to Degradation by Abrasion in the Micro-Deval Apparatus. Annual Book of ASTM Standards, American Society for Testing and Materials.

ASTM D 7115. 2011. Standard Test Method Gyratory Measurement of Super pave Gyratory Compactor Internal Angle of Gyration. Annual Book of ASTM Standards, American Society for Testing and Materials.

ASTM D 7428. 2011. Standard Test Method for Resistance of Fine Aggregate to Degradation Annual Book of ASTM Standards, American Society for Testing and Materials.

Beale, J. and Zhanping, Y. 2008. Determining the Specific Gravity of Coarse Aggregates utilizing Vacuum Saturation Approach. Department of Civil and Environmental Engineering, Michigan Technological University, Michigan United States.

Berthelot, C., Soares, R., Haichert, R., Podborochynski, D., Guenther, D., and Kelln, R. 2011. Modeling the Structural Response of Urban Sub-Surface Drainage Systems. Transportation Research Board 91st Annual Meeting Compendium of Papers. Transportation Research Board of the National Academies, Washington, D.C.

Berthelot, C.F., Haichert, R., Taylor, B. 2010A. Crushing and Processing Reclaimed Concrete for the City of Saskatoon Rehabilitation of Road Structure. Transportation Association of Canada (TAC), Annual Conference. Halifax, Canada.

Berthelot, C.F., Haichert, R., Podborochynski, D., Taylor, B., Guenther, D. 2010B. Mechanisitic Laboratory Evaluation and Field Construction of Recycled Concrete Materials for Use in Road Substructures. Transportation Research Record: Journal of the Transportation Research Board of the National Academies, Washington, D.C. USA. Vol.2167, pp:41-52.

Berthelot, C.F., Haichert, R., Anthony, A. 2010C. Triaxial Frequency Sweep Mechanistic-Climatic Properties of Lime Treated Asphalt Mixes in Saskatchewan. Canadian Technical Asphalt Association (CTAA), Annual Conference. Edmonton, Canada.

Berthelot, C.F., Podborochynski, D., Fair, J, Marjerison, B., 2009A. Field Investigation of Granular Base Rehabilitation Project Incorporating a Woven Geotextile Separation Layer, Sand, and Cement Stabilization. Canadian Journal of Civil Engineering. Ottawa, Canada. Vol.36 No.1, pp:14-25.

Berthelot, C.F., Podborochynski, D., Berthelot, J., Prang, C., 2009B. Mechanistic Design and Structural Evaluation of Time Sensitive Urban Full Depth Strengthening Projects Transportation Association of Canada (TAC), Annual Conference. Vancouver, Canada.

Berthelot, C.F., Taylor, B., Stuber, E., Prang, C., Marjerison, C. 2009C. Use of Structural Asset Management to Evaluate Road Substructure Drainage Systems. Transportation Research Record: Journal of the Transportation Research Board of the National Academies, Washington, D.C. USA. No.2101, pp:44-52.

Berthelot, C.F., Podborochynski, D., Marjerison, B. 2009D. A Saskatchewan Field Case Study of Triaxial Frequency Sweep Characterization to Predict Failure of a Granular Base across Increasing Fines Content and Traffic Speed Applications. American Society of Civil Engineering, Journal of Transportation Engineering. Reston, USA. Vol. 135, No.11, pp:907-914.

Berthelot, C.F., Haichert, R., Podborochynski, D., Taylor,B., Guenther, D. 2008. Use of Recycled Asphalt Concrete and Portland Cement Concrete in Road Substructure. Transportation Research Board 87th Annual Meeting Compendium of Papers. Transportation Research Board of the National Academies, Washington, D.C.

Berthelot, C.F., Marjerison, B., Houston, G., McCaig, J., Warrener, S., Gorlick, R. 2007. Mechanistic Comparison of Cement and Bituminous-Stabilized Granular Base Systems. Transportation Research Board 86th Annual Meeting Compendium of Papers. Transportation Research Board of the National Academies, Washington, D.C.

Berthelot, C.F. 2007. CE 867 Pavement Management Systems II Class Notes. Department of Civil and Geological Engineering, University of Saskatchewan.

Berthelot, C.F., Scullion, T., Luhr, D. 2005. Investigation of Cement Modification of Granular Base and Subbase Materials using Triaxial Frequency Sweep Characterization. Transportation Research Board 84th Annual Meeting Compendium of Papers. Transportation Research Board of the National Academies, Washington, D.C.

Berthelot, C.F., Allen, D., Searcy, C. 2003. Method for Performing Accelerated Characterization of Viscoelastic Constitutive Behaviour of Asphalt Concrete. Journal of Materials in Civil Engineering. American Society of Civil Engineers. Vol.15, No.5, pp:496-505.

Berthelot, C.F., and Gerbrandt, R. 2002. Cold In Place Recycling and Full Depth Strengthening of Expansive Subgrade Soils using Cementitious Waste Products in Northern Climates. Transportation Research Record: Journal of the Transportation Research Board of the National Academies, Washington, D.C. USA. No. 1787, pp. 3-12.

Berthelot, C.F. 1999. Mechanisitic Modeling of Saskatchewan Specific Pavement Studies 9A Asphalt Concrete Pavements. Ph.D. dissertation. Texas A&M University.

Bigl, S, Berg, R, 1996. Modeling of MN/Road Test Sections with the CRREL mechanistic Pavement Design Procedure. US ARMY CORPS of Engineers. Minnesota.

Birgisson, B., Roque, R., Page, G., 2004. Performance Based Fracture Criterion for Evaluation of Moisture Susceptibility in Hotmix Asphalt. Transportation Research Record, No. 1891, pp. 55-61.

Brown, E.R., Kandhall, P.S., Zhang, J. 2004. Performance Testing for Hot-M<ix Asphalt., Transportation Research Board of the National Academies Transportation Research Circular No. E-C068, Washington, DC. pp:85-106.

British Standards. 2011. BS EN 1097 Part 1: Tests for mechanical and physical properties of aggregates-determination of resistance to wear. Annual Book of BS EN Standards, British European Standards.

Butcher, M., 1998. Determining Gyratory Compaction Characteristics Using Servopac Gyratory Compactor. Transportation Research Record Transportation Research Board of the National Academies, Washington, D.C. USA.. Vol. 1630, No.98, pp:1-14

Caterpillar. 2006. Introduction to Soil Stabilization and Understanding the Basics of Soil Stabilization. Institute of Aggregate Research, Michigan University, USA.

Cement Association of Canada, 2003. Where is Construction Waste Management Today? Available from: http://www.cement.ca/images/stories/Concrete Recycling December 2003.pdf. [Accessed on Nov 23 2010]

City of Camrose. 2011. Recycling Concrete. Available from: http://www.camrose.ca/ index.aspx?NID=227. [Accessed on Nov 23 2010]

City of Saskatoon (COS). 2011. City of Saskatoon 2011 Operating and Capital Budgets. Available from: http://www.saskatoon.ca/DEPARTMENTS/Corporate%20Services/ Office%20of%20the%20Finance%20Branch/Documents/Business%20Lines%20Operating%20Capital%20Combined.pdf. [Accessed on May 09 2012]

City of Saskatoon (COS), 2009A. City of Saskatoon 2009 Annual Report, Available from:http://www.saskatoon.ca/DEPARTMENTS/Corporate%20Services/ Office%20of%20the%20Finance%20Branch/Documents/2009%20Annual%20Financial%20Report.pdf. [Accessed on May 09 2012]

City of Saskatoon (COS), 2009B. City of Saskatoon Aggregate Specifications. Available from:http://www.saskatoon.ca/DEPARTMENTS/Infrastructure%20Services/ Construction%20and%20Design/Construction%20Services/Project%20Management%20Group/ Documents/AGGREGATE_Dec22_2010.pdf. [Accessed on May 09 2012]

Chan, D, and Poon, C, 2005. Feasible Use of Recycled Concrete Aggregates and Crushed Clay Brick as Unbound Road Sub-base. Department of Civil and Structural Engineering, The Hong Kong Polytechnic University, Hung Hom, Kowloon, Hong Kong.

Chini, A., Kuo, S., Armaghani, J. 2001. Test of Recycled Concrete Aggregate in Accelerated Test Track. Journal of Transportation Engineering. Vol.127 No.6.

Crockford, W., Berthelot, C., Tritt, B., Sinadinos, C. 2002. Rapid Triaxial Test. Asphalt Paving Technology: Association of Asphalt Paving Technologists – Proceedings of the Technical Sessions, Vol.71, pp. 712-724.

Erkens, S., Liu, X., Scarpas, A., 2002. 3D Finite Element Model for Asphalt Concrete Response Simulation. International Journal of Geomechanics, Vol.2, No.3. pp:305-330.

FHWA. 2007. Long-Life Concrete Pavements in Europe and Canada. FHWA-PL-07-027. Federal Highway Administration. Washington, D.C.

FHWA. 2008. Recycled Concrete Aggregate. Available from: http://www.fhwa.dot.gov/pavement/recycling/rca.cfm. [Accessed on Nov 29 2010]

FHWA. 2010. Precast Concrete Pavement Systems. Available from: http://www.fhwa.dot.gov/hfi/innovations/PDFS/precast.pdf. [Accessed on Dec 29, 2011]

Frondiston, Y., 1977. Waste Concrete as Aggregate for new Concrete. Journal of the American Concrete Institute, Vol.74, No.8, pp:373-376. Farrington Hills, Michigan.

Guenther, D. 2010. Senior Project Engineer, City of Saskatoon. Personal Correspondence.

Guenther, D., Haichert, R., Foth, M., Berthelot, C. 2010 Effects of Fines on Structural Capacity of Urban Base Course Materials. Transportation Research Board 89th Annual Meeting Compendium of Papers. Transportation Research Board of the National Academies, Washington, D.C.

Graymont Cement. 2010. Website. Available from: http://www.graymont.com/ applications_soil.shtml.[Accessed on Dec 23 2010]

Haddock, J. 2000. Superpave Aggregate. Asphalt, Vol.15, No.2, pp:14-16.

Haichert, R., Kelln, R., Berthelot, C., Guenther, D. 2011. Cement Stabilization of Conventional Granular Base and recycled Crushed Portland Cement Concrete. Transportation Research Board 90th Annual Meeting Compendium of Papers. Transportation Research Board of the National Academies, Washington, D.C.

Hansen, T. 1992. Recycling of Demolished Concrete and Masonary. Rilen Report 6, Spon Press, United Kingdom.

Hansen, T. 1985. Recycled Aggregates and Recycled Aggregate Concrete Second State-of-the-Art Report Developments, 1945-1985. Building Materials Laboratory, Technical University of Denmark, Lyngby, Denmark.

Holtz, R.D., and Kovacs, W.D. 1981. An Introduction to Geotechnical Engineering. Editors Newmark, N.M. and Hall, W.J., Prentice-Hall, Englewood Cliffs, New Jersey.

Horvath, A, 2003. Life-Cycle Environmental and Economic Assessment of Using Recycled Material for Asphalt Pavements. University of California Transportation Center Technical Report.

Holicim Ltd. 2010. Available from: http://www.holicim.com/. [Accessed on Nov 29 2010]

Huber, G.A., Jones, C, Messersmith, P. 1998. Contribution of Fine Aggregate Angularity and Particle Shape to Superpave Mixture Performance. Transportation Research Record: Journal of the Transportation Research Board of the National Academies, Washington, D.C. USA. No.1609, pp:28-35.

Huber, G.A. 1996. Development of the Superpave Gyratory Compactor. The Superpave Asphalt Research Program, The University of Texas in Austin. Available from: http://www.utexas.edu/research/superpave/articles/gyr_hist.html. [Accessed on May 09 2012]

ICPI. 2010. Sustainability of using Paving Stones as a Road Surface. Available from: http://www.icpi.org/node/352. [Accessed on Dec 30 2010]

Karlsson, R., and Isacsson, U. 2006. Material-Related Aspects of Asphalt Recycling State-of-the-Art. Journal of Materials in Civil Engineering. Vol.18, No.1, pp:81-92.

Kazmierowski, T., and Marks, P. 1999. Development of Cement-Treated Open Graded Drainage Layer Placement Techniques in Ontario, Canada. Transportation Research Record: Journal of the Transportation Research Board of the National Academies, Washington, D.C. USA. No.1673, pp:16-22.

Kelly, T. 1998. Crushed Cement Concrete Substitution for Construction Aggregates-A Materials Flow Analysis. U.S Department of the Interior Technical Report.

Kringos, N., Azari, H., Scarpas, A. 2009. Identification of Moisture-Conditioning-Related Parameters Causing Variability in Modified Lottman Test. Transportation Research Board 88th Annual Meeting Compendium of Papers. Transportation Research Board of the National Academies, Washington, D.C.

Little, D., and Nair, S. 2009. Recommended Practice for Stabilization of Subgrade Soils and Base Materials. Texas Transportation Institute, Texas A&M University, Texas, USA.

Limbachiya,M., Leelawat, T., Dihir R., 2000. Use of Recycled Concrete in High Strength Concrete. Journal of Materials and Structures. Vol.33, No.9, pp:574-580.

Lytton, R. 2000. Determining Gyratory Compaction Characteristics Using Servopac Gyratory Compactor. Transportation Research Record: Journal of the Transportation Research Board of the National Academies, Washington, D.C. USA. No.1519, pp:89-97.

Malsev, M., Radonjanin, V., Marinkovic, S. 2010. Recycled Concrete as Aggregate for Structural Concrete Production, Journal of Sustainability. Available from: http://www.mdpi.com/Journal/Sustainability. [Accessed on Dec 23 2011]

NAPA. 2007. Recycling Hot-mix Asphalt Pavements. National Asphalt Pavement Association.

NCHRP. 2001. Performance-Related Tests of Aggregate for Use in Unbound Pavement Layers. Report 453 Transportation Research Board. Washington D.C., USA.

Nixon, P, 1978. Recycled concrete as an aggregate for concrete. Journal of Materials and Structures, Springer, Netherlands. Vol.11, No.5, pp:371-378.

Nixon, P, 1976. The use of materials from Demolition in Construction. Journal of Materials and Structures, Springer Netherlands. Vol.2, No.4, pp:276-283.

Ooi, P.S.K., Rajabipour, F., Shafaatian, A., and S. Joo. 2011. Forensic Investigation of a Distressed Pavement Supported on a Base Course Containing Recycled Concrete Aggregate. Transportation Research Record: Journal of the Transportation Research Board of the National Academies, Washington, D.C. USA. No.2253, pp:22-31.

Osman, A., 2005. Evaluation of the Mechanistic Emperical Pavement Design Guide (NCHRP 1-37A). National Research Council Canada. Vol. UR 3002.1.

Pellinen, T., and Witczak, M 2002. Use of Stiffness of Hot-mix Asphalt as a Simple Preformance Test. Transportation Research Record: Journal of the Transportation Research Board of the National Academies, Washington, D.C. USA. No.1789, pp:80-90.

Ping, W., Leonard, M., Zenghai, Y. 2003. Laboratory Simulation of Field Compaction Characteristics (Phase I). Department of Civil and Environmental Engineering, Florida A&M University. Tallahassee F.L.

Podborochynski, D., Wandzura, C., Berthelot, C., Kelln, R. 2011. Crushed Reclaimed Asphalt Pavement (RAP) and Portland Cement Concrete (PCC) Aggregate Material Stabilization. Transportation Research Board 90th Annual Meeting Compendium of Papers. Transportation Research Board of the National Academies, Washington, D.C.

PSI Technologies. 2010. Sustainable “Green Street” Road Rehabilitation using Recycled Asphaltic Concrete, Portland Cement Concrete and other Waste Rubble Materials, Final Report. Saskatoon, Saskatchewan

Rao, A., Jha, K., Misra, S. 2006. Use of Aggregates from Recycled Construction and Demolition Waste in Concrete, Department of Civil Engineering, IIT Kanpur, Kanpur, Indian.

Raducanu, C. 2002. Evaluation of Mechanical Breakdown of Hot Mix Aggregates using Gyratory Compactor. M.Sc. thesis, Department of Civil and Geological Engineering, University of Saskatochewan.

Rangaraju, P, Edlinski, J,2008. Comparative Evaluation of Micro-Deval Abrasion Test with Other Toughness/Abrasion Resistance and Soundness Tests. Journal of Materials in Civil Engineering. Vol.20, No.5: 343-351.

Rathje, E, Rauch, A, Trejo, D, 2006. Evaluation of Crushed Concrete and Recycled Asphalt Pavement as Backfill for Mechanically Stabilized Earth Walls. University of Texas Department of Transportation Technical Report.

Roberts, F.L., Kandhal, P.S., Brown, E.R., Lee, D., Kennedy, T.W. 1996. Hot Mix Asphalt Materials, Mixture Design and Construction, 2nd Edition. NAPA Education Foundation, Lanham, Maryland.

Saskatchewan Ministry of Highways and Infrastructure (SMHI). 2001-A. Aggregate Management Strategy Review. Final Report, Project Services Group, Saskatchewan Highways and Transportation.

Saskatchewan Ministry of Highways and Infrastructure (SMHI). 2009. Surfacing Manual.

Kuo, S-S., Mahgoub, H.S., Nazef, A. 1998. Investigation of Recycled Concrete made with Limestone Aggregate for a Base Course in Flexible Pavement. Transportation Research Record: Journal of the Transportation Research Board of the National Academies, Washington, D.C. USA. No.1787, pp:99-108.

Snyder, M., and Bruinsma, J. 1996. Determining Gyratory Compaction Characteristics Using Servopac Gyratory Compactor. Transportation Research Record: Journal of the Transportation Research Board of the National Academies, Washington, D.C. USA. No.1519, pp:51-58.

Soares, R. Finite Element Analysis of the Mechanics of Viscoelastic Asphalt Pavements Subjected to Varying Tire Configurations. M.Sc. thesis, University of Nebraska, Lincoln, Nebraska.

Sorensen, J. 2010. Leed Helps Jump Start Interest in Concrete rRcycling. Journal of Commerce. Available from: http://www.journalofcommerce.com/article/ id40842/concrete. [Accessed on Nov 29 2010]

Sotil, A., Kaloush, K.E, Witczak, M.W. 2004. Reduced Confined Dynamic Modulus Testing Protocol for Asphalt Mixtures. Transportation Research Board 83rd Annual Meeting Compendium of Papers. Paper No. 04-5180.

Staton, J, 2006. Absorption Capacity of Course Aggregates for Portland Cement Concrete. Michigan Department of Transportation, Construction and Technology Division Technical Report,

Statistics Canada, 2012. Available from: http://www.statcan.gc.ca/start-debut-eng.html. [Accessed on Mar 01 2012]

Stone City USA, 2010, Available from: http://www.stonecityusa.com/bulk-a-bagged-materials [Accessed on Mar 09 2010]

Thomas, L., Berthelot, C.**,** and Taylor, B. Oct 14-18, 2007. Mechanistic Based ESALs for Urban Pavement Systems. Transportation Association of Canada (TAC) Annual Conference. Saskatoon, Canada.

Thomas, L. Mechanistic Based ESALs for Urban Pavements. M.Sc. thesis, Department of Civil and Geological Engineering, University of Saskatchewan.

Transport Canada. 2009. Available from: http://www.tc.gc.ca/eng/programs/environment-utsp-greencommutinginitiatives-880.htm. [Accessed on Jan 02 2011]

University of Saskatchewan. 2009. Available from: http://facilities.usask.ca/sustainability/whatcampusisdoing/. [Accessed on Dec 23 2010]

Weiland, C.D., and Muench, S.T. 2010. Life Cycle Assessment of Portland Cement Concrete Interstate Highway Rehabilitation and Replacement. Washington State Department of Transportation.

White, T., Haddock, J., Rismantojo, E. 2006. National Cooperative Highway Research Program Report 557 Aggregate Tests for Hot-Mix Asphalt Mixtures Used in Pavements. Washington, D.C.

White, T., Nourreldin, S., Harris, D. 2008. Evaluation of Long-Term Performance of Pavement Drainage Layers on I-469 in Indiana. Transportation Research Record: Journal of the Transportation Research Board of the National Academies, Washington, D.C. USA. No.2048, pp:77-84.

Williamson, G, Weyers, R, 2007. Vacuum Saturated Absorption as Aggregate Durability Indicator. American Concrete Institute, Technical Paper, Vol.104, Issue 3, pp:77-84.

Woosung, K. 2006. Resilient Modulus and Strength of Base Course. University of Minnesota, Minneapolis.

Xu, J. 2008. Mechanistic Evaluation of Granular Base Stabilization Systems in Saskatchewan. M.Sc. thesis, Department of Civil and Geological Engineering, University of Saskatchewan.

Xu, J., and Berthelot, C. 2010. Mechanistic Road Upgrade Structural Design Evaluation Using Rapid Triaxial Frequency Sweep Testing and Linear Elastic Modeling. Canadian Journal of Civil Engineering. NRC Research Press. Ottawa, Canada. Vol.37, No.12, pp:1572-1580.

Appendix A Mechanistic Material Results (RATT) for all Stress States

Table A.1 Conventional COS Granular Base, Moist Cured

Conventional COS Granular Base , Moist Cured

Sample ID	Material Property	Low Stress State Stress State #1				Medium Stress State Stress State #2				High Stress State Stress State #3				Fully Reversed Stress State Stress State #4			
		10 Hz	5 Hz	1 Hz	0.5 Hz	10 Hz	5 Hz	1 Hz	0.5 Hz	10 Hz	5 Hz	1 Hz	0.5 Hz	10 Hz	5 Hz	1 Hz	0.5 Hz
Sample A	Dynamic Modulus (MPa)	479	480	488	491	446	448	458	465	295	Sample Failed	Sample Failed	Sample Failed	Sample Failed	Sample Failed	Sample Failed	Sample Failed
	Phase Angle (degrees)	8.63	6.85	5.34	5.06	10.89	9.12	7.22	6.79	15.21	Sample Failed	Sample Failed	Sample Failed	Sample Failed	Sample Failed	Sample Failed	Sample Failed
	Radial Micro-Strain	185	190	186	181	542	551	533	516	1815	Sample Failed	Sample Failed	Sample Failed	Sample Failed	Sample Failed	Sample Failed	Sample Failed
	Poisson's Ratio	0.46	0.47	0.46	0.45	0.62	0.63	0.62	0.61	1.00	Sample Failed	Sample Failed	Sample Failed	Sample Failed	Sample Failed	Sample Failed	Sample Failed
Sample B	Dynamic Modulus (MPa)	412	413	419	422	412	420	428	432	295	Sample Failed	Sample Failed	Sample Failed	Sample Failed	Sample Failed	Sample Failed	Sample Failed
	Phase Angle (degrees)	8.23	6.77	5.21	4.83	10.27	8.75	7.23	6.71	14.72	Sample Failed	Sample Failed	Sample Failed	Sample Failed	Sample Failed	Sample Failed	Sample Failed
	Radial Micro-Strain	202	200	195	197	517	519	510	502	1617	Sample Failed	Sample Failed	Sample Failed	Sample Failed	Sample Failed	Sample Failed	Sample Failed
	Poisson's Ratio	0.43	0.42	0.41	0.42	0.55	0.55	0.55	0.55	0.89	Sample Failed	Sample Failed	Sample Failed	Sample Failed	Sample Failed	Sample Failed	Sample Failed
Sample C	Dynamic Modulus (MPa)	462	464	476	468	431	439	451	458	298	Sample Failed	Sample Failed	Sample Failed	Sample Failed	Sample Failed	Sample Failed	Sample Failed
	Phase Angle (degrees)	8.54	6.83	5.31	5.03	10.79	9.07	7.22	6.78	15.03	Sample Failed	Sample Failed	Sample Failed	Sample Failed	Sample Failed	Sample Failed	Sample Failed
	Radial Micro-Strain	186	190	186	182	534	548	529	513	1812	Sample Failed	Sample Failed	Sample Failed	Sample Failed	Sample Failed	Sample Failed	Sample Failed
	Poisson's Ratio	0.46	0.47	0.46	0.45	0.61	0.62	0.61	0.59	0.97	Sample Failed	Sample Failed	Sample Failed	Sample Failed	Sample Failed	Sample Failed	Sample Failed
Sample D	Dynamic Modulus (MPa)	430	432	439	445	427	429	435	439	293	Sample Failed	Sample Failed	Sample Failed	Sample Failed	Sample Failed	Sample Failed	Sample Failed
	Phase Angle (degrees)	8.32	6.79	5.24	4.86	10.37	8.80	7.23	6.73	14.90	Sample Failed	Sample Failed	Sample Failed	Sample Failed	Sample Failed	Sample Failed	Sample Failed
	Radial Micro-Strain	202	200	195	196	525	522	513	505	1620	Sample Failed	Sample Failed	Sample Failed	Sample Failed	Sample Failed	Sample Failed	Sample Failed
	Poisson's Ratio	0.43	0.42	0.41	0.42	0.56	0.56	0.56	0.56	0.91	Sample Failed	Sample Failed	Sample Failed	Sample Failed	Sample Failed	Sample Failed	Sample Failed
Sample E	Dynamic Modulus (MPa)	446	451	455	456	429	434	443	449	Sample Failed	Sample Failed	Sample Failed	Sample Failed	Sample Failed	Sample Failed	Sample Failed	Sample Failed
	Phase Angle (degrees)	8.43	6.81	5.26	4.94	10.58	8.94	7.23	6.75	Sample Failed	Sample Failed	Sample Failed	Sample Failed	Sample Failed	Sample Failed	Sample Failed	Sample Failed
	Radial Micro-Strain	194	195	190	189	530	535	521	509	Sample Failed	Sample Failed	Sample Failed	Sample Failed	Sample Failed	Sample Failed	Sample Failed	Sample Failed
	Poisson's Ratio	1.04	1.04	1.04	1.02	1.00	1.01	1.02	1.02	Sample Failed	Sample Failed	Sample Failed	Sample Failed	Sample Failed	Sample Failed	Sample Failed	Sample Failed

Table A.2 Recycled PCC Drainage Rock, Moist Cured

Recycled PCC Drainage Rock, Moist Cured

Sample ID	Material Property	Low Stress State Stress State #1				Medium Stress State Stress State #2				High Stress State Stress State #3				Fully Reversed Stress State Stress State #4			
		10 Hz	5 Hz	1 Hz	0.5 Hz	10 Hz	5 Hz	1 Hz	0.5 Hz	10 Hz	5 Hz	1 Hz	0.5 Hz	10 Hz	5 Hz	1 Hz	0.5 Hz
Sample A	Dynamic Modulus (MPa)	732	738	743	771	725	720	720	733	522	521	518	526	358	356	342	343
	Phase Angle (degrees)	11.76	9.89	8.15	7.96	13.62	11.80	10.37	9.83	16.81	14.41	12.74	12.31	17.35	164.69	166.17	166.71
	Radial Micro-Strain	100	99	99	95	245	254	256	250	695	720	731	720	496	501	519	510
	Poisson's Ratio	0.38	0.37	0.37	0.37	0.46	0.46	0.46	0.46	0.68	0.69	0.69	0.69	0.45	0.45	0.45	0.44

Table A.3 Recycle PCC GW Untreated, Moist Cured

Sample ID	Material Property	Low Stress State Stress State #1				Medium Stress State Stress State #2				High Stress State Stress State #3				Fully Reversed Stress State Stress State #4			
		10 Hz	5 Hz	1 Hz	0.5 Hz	10 Hz	5 Hz	1 Hz	0.5 Hz	10 Hz	5 Hz	1 Hz	0.5 Hz	10 Hz	5 Hz	1 Hz	0.5 Hz
Sample A	Dynamic Modulus (MPa)	479	480	488	491	446	448	458	465	295	Sample Failed	Sample Failed	Sample Failed	Sample Failed	Sample Failed	Sample Failed	Sample Failed
	Phase Angle (degrees)	8.63	6.85	5.34	5.06	10.89	9.12	7.22	6.79	15.21	Sample Failed	Sample Failed	Sample Failed	Sample Failed	Sample Failed	Sample Failed	Sample Failed
	Radial Micro-Strain	185	190	186	181	542	551	533	516	1815	Sample Failed	Sample Failed	Sample Failed	Sample Failed	Sample Failed	Sample Failed	Sample Failed
	Poisson's Ratio	0.46	0.47	0.46	0.45	0.62	0.63	0.62	0.61	1.00	Sample Failed	Sample Failed	Sample Failed	Sample Failed	Sample Failed	Sample Failed	Sample Failed
Sample B	Dynamic Modulus (MPa)	412	413	419	422	412	420	428	432	295	Sample Failed	Sample Failed	Sample Failed	Sample Failed	Sample Failed	Sample Failed	Sample Failed
	Phase Angle (degrees)	8.23	6.77	5.21	4.83	10.27	8.75	7.23	6.71	14.72	Sample Failed	Sample Failed	Sample Failed	Sample Failed	Sample Failed	Sample Failed	Sample Failed
	Radial Micro-Strain	202	200	195	197	517	519	510	502	1617	Sample Failed	Sample Failed	Sample Failed	Sample Failed	Sample Failed	Sample Failed	Sample Failed
	Poisson's Ratio	0.43	0.42	0.41	0.42	0.55	0.55	0.55	0.55	0.89	Sample Failed	Sample Failed	Sample Failed	Sample Failed	Sample Failed	Sample Failed	Sample Failed
Sample C	Dynamic Modulus (MPa)	462	464	476	468	431	439	451	458	298	Sample Failed	Sample Failed	Sample Failed	Sample Failed	Sample Failed	Sample Failed	Sample Failed
	Phase Angle (degrees)	8.54	6.83	5.31	5.03	10.79	9.07	7.22	6.78	15.03	Sample Failed	Sample Failed	Sample Failed	Sample Failed	Sample Failed	Sample Failed	Sample Failed
	Radial Micro-Strain	186	190	186	182	534	548	529	513	1812	Sample Failed	Sample Failed	Sample Failed	Sample Failed	Sample Failed	Sample Failed	Sample Failed
	Poisson's Ratio	0.46	0.47	0.46	0.45	0.61	0.62	0.61	0.59	0.97	Sample Failed	Sample Failed	Sample Failed	Sample Failed	Sample Failed	Sample Failed	Sample Failed
Sample D	Dynamic Modulus (MPa)	430	432	439	445	427	429	435	439	293	Sample Failed	Sample Failed	Sample Failed	Sample Failed	Sample Failed	Sample Failed	Sample Failed
	Phase Angle (degrees)	8.32	6.79	5.24	4.86	10.37	8.80	7.23	6.73	14.90	Sample Failed	Sample Failed	Sample Failed	Sample Failed	Sample Failed	Sample Failed	Sample Failed
	Radial Micro-Strain	202	200	195	196	525	522	513	505	1620	Sample Failed	Sample Failed	Sample Failed	Sample Failed	Sample Failed	Sample Failed	Sample Failed
	Poisson's Ratio	0.43	0.42	0.41	0.42	0.56	0.56	0.56	0.56	0.91	Sample Failed	Sample Failed	Sample Failed	Sample Failed	Sample Failed	Sample Failed	Sample Failed
Sample E	Dynamic Modulus (MPa)	446	451	455	456	429	434	443	449	Sample Failed	Sample Failed	Sample Failed	Sample Failed	Sample Failed	Sample Failed	Sample Failed	Sample Failed
	Phase Angle (degrees)	8.43	6.81	5.26	4.94	10.58	8.94	7.23	6.75	Sample Failed	Sample Failed	Sample Failed	Sample Failed	Sample Failed	Sample Failed	Sample Failed	Sample Failed
	Radial Micro-Strain	194	195	190	189	530	535	521	509	Sample Failed	Sample Failed	Sample Failed	Sample Failed	Sample Failed	Sample Failed	Sample Failed	Sample Failed
	Poisson's Ratio	0.44	0.44	0.43	0.44	0.59	0.59	0.58	0.57	Sample Failed	Sample Failed	Sample Failed	Sample Failed	Sample Failed	Sample Failed	Sample Failed	Sample Failed

Table A.4 Recycled PCC GW 2% Cement, Moist Cured

Recycled PCC GW 2% Cement, Moist Cured

Sample ID	Material Property	Low Stress State Stress State #1				Medium Stress State Stress State #2				High Stress State Stress State #3				Fully Reversed Stress State Stress State #4			
		10 Hz	5 Hz	1 Hz	0.5 Hz	10 Hz	5 Hz	1 Hz	0.5 Hz	10 Hz	5 Hz	1 Hz	0.5 Hz	10 Hz	5 Hz	1 Hz	0.5 Hz
Sample A	Dynamic Modulus (MPa)	1479	1457	1495	1532	1399	1412	1434	1459	986	980	987	992	578	579	581	584
	Phase Angle (degrees)	7.72	6.04	4.89	4.93	8.41	6.74	5.75	5.60	9.13	8.05	6.73	6.38	9.85	8.40	172.93	173.14
	Radial Micro-Strain	27	27	25	26	75	75	78	80	212	227	235	242	206	206	204	201
	Poisson's Ratio	0.20	0.20	0.19	0.20	0.27	0.27	0.28	0.29	0.39	0.41	0.42	0.44	0.30	0.30	0.30	0.30
Sample B	Dynamic Modulus (MPa)	1295	1323	1358	1387	1257	1267	1303	1336	883	890	898	910	483	489	488	494
	Phase Angle (degrees)	7.94	6.01	5.46	4.47	8.58	7.18	6.22	6.22	9.88	8.27	7.26	6.88	10.46	9.17	172.00	172.24
	Radial Micro-Strain	38	38	36	38	104	105	103	100	287	300	311	314	311	306	306	303
	Poisson's Ratio	0.25	0.26	0.24	0.27	0.34	0.34	0.33	0.33	0.47	0.49	0.51	0.52	0.38	0.38	0.38	0.38
Sample C	Dynamic Modulus (MPa)	1539	1544	1599	1623	1475	1464	1491	1510	1020	1012	1013	1020	616	624	620	627
	Phase Angle (degrees)	6.83	4.94	4.27	4.45	8.81	7.22	5.63	5.73	9.67	8.36	6.87	6.42	9.56	8.30	172.87	173.00
	Radial Micro-Strain	21	19	20	17	55	54	57	58	199	217	228	232	166	166	166	162
	Poisson's Ratio	0.16	0.15	0.16	0.14	0.21	0.20	0.21	0.22	0.38	0.40	0.42	0.42	0.26	0.26	0.26	0.26
Sample D	Dynamic Modulus (MPa)	1492	1491	1521	1545	1435	1442	1461	1492	994	987	990	996	586	587	578	584
	Phase Angle (degrees)	7.63	6.97	4.65	5.13	8.01	6.72	5.78	5.35	9.36	7.74	6.39	6.09	10.15	8.31	173.01	173.19
	Radial Micro-Strain	18	20	24	21	64	63	62	61	173	183	191	196	164	162	165	162
	Poisson's Ratio	0.14	0.15	0.18	0.16	0.24	0.23	0.23	0.23	0.32	0.33	0.34	0.36	0.24	0.24	0.24	0.24
Sample E	Dynamic Modulus (MPa)	1528	1584	1607	1622	1516	1528	1558	1571	1094	1095	1090	1097	663	666	662	668
	Phase Angle (degrees)	6.09	5.98	4.38	4.79	7.50	6.25	5.82	5.13	8.64	7.27	6.34	5.82	9.21	7.85	173.22	173.48
	Radial Micro-Strain	21	23	20	20	69	65	70	65	174	185	192	192	164	165	168	167
	Poisson's Ratio	0.17	0.18	0.16	0.16	0.27	0.25	0.27	0.26	0.36	0.37	0.38	0.38	0.27	0.28	0.28	0.28

Table A.5 Recycled PCC GW 2% Cement, Vacuum Saturated

Recycled PCC GW 2% Cement, Vacuum Saturated

Sample ID	Material Property	Low Stress State Stress State #1				Medium Stress State Stress State #2				High Stress State Stress State #3				Fully Reversed Stress State Stress State #4			
		10 Hz	5 Hz	1 Hz	0.5 Hz	10 Hz	5 Hz	1 Hz	0.5 Hz	10 Hz	5 Hz	1 Hz	0.5 Hz	10 Hz	5 Hz	1 Hz	0.5 Hz
Sample A	Dynamic Modulus (MPa)	1009	1013	1055	1084	1109	1105	1127	1147	763	745	732	733	453	452	441	443
	Phase Angle (degrees)	8.64	6.46	5.73	4.96	9.33	7.48	6.21	5.82	11.66	9.80	8.21	7.73	11.82	10.15	171.50	171.83
	Radial Micro-Strain	50	51	51	48	121	127	127	124	401	437	469	484	314	318	321	313
	Poisson's Ratio	0.26	0.26	0.27	0.26	0.35	0.36	0.36	0.36	0.57	0.60	0.63	0.65	0.36	0.36	0.36	0.35
Sample B	Dynamic Modulus (MPa)	1018	1051	1081	1111	1042	1051	1068	1088	694	686	677	677	390	390	384	386
	Phase Angle (degrees)	9.80	8.12	6.24	5.88	9.64	7.71	6.60	6.50	11.16	9.72	8.21	7.84	12.20	10.55	171.03	171.37
	Radial Micro-Strain	62	62	60	59	146	153	152	151	480	519	554	570	411	417	420	414
	Poisson's Ratio	0.32	0.33	0.33	0.33	0.40	0.41	0.41	0.41	0.62	0.66	0.68	0.70	0.41	0.41	0.40	0.40
Sample C	Dynamic Modulus (MPa)	1112				1156	1163	1174	1194	756	746	737	737	455	457	449	452
	Phase Angle (degrees)	9.94				9.71	8.37	6.64	6.40	10.92	9.38	7.80	7.59	11.61	8.15	171.64	172.00
	Radial Micro-Strain	52				126	126	131	123	428	474	500	517	327	328	325	320
	Poisson's Ratio	0.30				0.37	0.37	0.39	0.37	0.61	0.65	0.67	0.70	0.38	0.38	0.37	0.36
Sample D	Dynamic Modulus (MPa)	1081	1107	1142	1164	1125	1123	1141	1159	739	730	725	725	429	426	416	418
	Phase Angle (degrees)	8.48	7.05	5.32	5.40	9.18	7.62	6.68	6.27	10.88	9.23	7.82	7.43	11.80	10.08	171.48	171.85
	Radial Micro-Strain	38	44	42	38	109	112	110	110	388	423	453	461	276	281	282	278
	Poisson's Ratio	0.21	0.25	0.24	0.22	0.31	0.32	0.31	0.32	0.54	0.57	0.60	0.61	0.30	0.30	0.30	0.29
Sample E	Dynamic Modulus (MPa)	1193	1221	1228	1272	1192	1197	1200	1218	783	777	767	770	474	472	462	464
	Phase Angle (degrees)	10.16	7.93	6.27	5.31	9.30	7.63	6.55	6.22	10.98	9.44	7.93	7.56	11.68	10.04	171.52	171.85
	Radial Micro-Strain	46	47	44	41	125	124	120	119	402	432	454	463	317	319	321	314
	Poisson's Ratio	0.28	0.29	0.27	0.26	0.38	0.38	0.36	0.37	0.59	0.62	0.64	0.65	0.38	0.38	0.37	0.37

Table A.6 Recycled PCC GW 2% SS-1, Moist Cured

Recycled PCC GW 2% SS-1, Moist Cured

Sample ID	Material Property	Low Stress State Stress State #1				Medium Stress State Stress State #2				High Stress State Stress State #3				Fully Reversed Stress State Stress State #4			
		10 Hz	5 Hz	1 Hz	0.5 Hz	10 Hz	5 Hz	1 Hz	0.5 Hz	10 Hz	5 Hz	1 Hz	0.5 Hz	10 Hz	5 Hz	1 Hz	0.5 Hz
Sample A	Dynamic Modulus (MPa)	1388	1347	1284	1272	1449	1394	1291	1262	1083	1037	935	902	713	675	585	555
	Phase Angle (degrees)	11.99	10.12	8.93	9.35	12.32	11.25	10.09	10.05	13.62	12.51	11.69	11.45	15.51	165.48	166.19	166.48
	Radial Micro-Strain	27	30	33	36	71	75	92	97	175	200	255	288	144	162	203	218
	Poisson's Ratio	0.19	0.20	0.22	0.23	0.27	0.26	0.30	0.31	0.36	0.38	0.43	0.47	0.26	0.28	0.30	0.31
Sample B	Dynamic Modulus (MPa)	1388	1369	1299	1298	1378	1315	1234	1231	1042	1006	909	869	659	645	561	536
	Phase Angle (degrees)	12.13	10.14	9.82	8.80	13.93	12.39	10.93	10.16	14.42	12.62	11.83	11.51	16.05	165.46	166.29	166.53
	Radial Micro-Strain	32	33	38	41	79	86	96	104	180	202	260	297	151	166	211	231
	Poisson's Ratio	0.23	0.23	0.25	0.27	0.28	0.29	0.30	0.32	0.35	0.37	0.43	0.47	0.25	0.27	0.30	0.31
Sample C	Dynamic Modulus (MPa)	1361	1344	1282	1271	1402	1350	1273	1250	1072	1022	920	886	681	641	556	533
	Phase Angle (degrees)	11.29	10.27	9.13	8.47	12.56	11.19	10.38	9.84	13.87	12.58	11.70	11.40	15.60	165.65	166.50	166.65
	Radial Micro-Strain	32	33	41	39	85	91	106	112	201	233	300	336	173	194	234	251
	Poisson's Ratio	0.22	0.22	0.27	0.25	0.31	0.31	0.34	0.35	0.40	0.44	0.50	0.54	0.30	0.31	0.33	0.34
Sample D	Dynamic Modulus (MPa)	1437	1434	1378	1363	1505	1460	1364	1340	1145	1097	990	953	730	693	601	570
	Phase Angle (degrees)	11.95	9.80	9.15	9.37	12.83	11.53	10.10	10.06	13.71	12.56	11.60	11.50	15.56	165.49	166.05	166.46
	Radial Micro-Strain	30	32	37	34	80	86	97	104	190	214	275	306	177	194	237	254
	Poisson's Ratio	0.22	0.23	0.26	0.24	0.31	0.32	0.33	0.35	0.41	0.43	0.50	0.53	0.33	0.34	0.36	0.37
Sample E	Dynamic Modulus (MPa)	1614	1593	1508	1507	1579	1523	1419	1394	1223	1165	1047	1006	780	732	633	605
	Phase Angle (degrees)	11.30	9.45	8.86	7.98	12.08	11.16	9.98	9.76	13.17	12.11	11.39	10.88	14.96	165.97	166.78	167.00
	Radial Micro-Strain	21	27	27	30	79	81	91	97	166	193	246	274	145	162	203	216
	Poisson's Ratio	0.18	0.22	0.20	0.23	0.32	0.31	0.32	0.34	0.38	0.41	0.47	0.50	0.28	0.30	0.32	0.33

Table A.7 Recycled PCC GW 2% SS-1, Vacuum Saturated

Recycled PCC GW 2% SS-1, Vacuum Saturated

Sample ID	Material Property	Low Stress State Stress State #1				Medium Stress State Stress State #2				High Stress State Stress State #3				Fully Reversed Stress State Stress State #4			
		10 Hz	5 Hz	1 Hz	0.5 Hz	10 Hz	5 Hz	1 Hz	0.5 Hz	10 Hz	5 Hz	1 Hz	0.5 Hz	10 Hz	5 Hz	1 Hz	0.5 Hz
Sample A	Dynamic Modulus (MPa)	899	884	844	848	949	909	848	837	670	638	584	571	Sample Failed	Sample Failed	Sample Failed	Sample Failed
	Phase Angle (degrees)	15.66	13.57	10.79	9.96	14.88	12.79	10.88	10.54	15.91	14.22	12.64	12.10	Sample Failed	Sample Failed	Sample Failed	Sample Failed
	Radial Micro-Strain	65	73	76	77	164	186	215	221	503	579	702	746	Sample Failed	Sample Failed	Sample Failed	Sample Failed
	Poisson's Ratio	0.30	0.33	0.32	0.33	0.40	0.43	0.46	0.46	0.63	0.68	0.75	0.78	Sample Failed	Sample Failed	Sample Failed	Sample Failed
Sample B	Dynamic Modulus (MPa)	848	833	799	797	1003	977	923	910	690	661	608	592	Sample Failed	Sample Failed	Sample Failed	Sample Failed
	Phase Angle (degrees)	14.69	12.64	10.73	9.87	14.37	12.44	10.73	10.11	16.06	14.52	12.76	11.92	Sample Failed	Sample Failed	Sample Failed	Sample Failed
	Radial Micro-Strain	84	84	91	92	156	165	179	182	519	570	661	697	Sample Failed	Sample Failed	Sample Failed	Sample Failed
	Poisson's Ratio	0.36	0.36	0.37	0.37	0.40	0.41	0.41	0.42	0.67	0.70	0.73	0.75	Sample Failed	Sample Failed	Sample Failed	Sample Failed
Sample C	Dynamic Modulus (MPa)	981	933	909	911	1009	963	888	894	759	719	656	635	Sample Failed	Sample Failed	Sample Failed	Sample Failed
	Phase Angle (degrees)	13.74	11.79	10.13	9.05	13.93	12.44	10.56	10.28	15.12	13.67	11.83	11.50	Sample Failed	Sample Failed	Sample Failed	Sample Failed
	Radial Micro-Strain	63	71	74	73	168	186	220	217	468	539	648	699	Sample Failed	Sample Failed	Sample Failed	Sample Failed
	Poisson's Ratio	0.32	0.33	0.34	0.34	0.44	0.45	0.49	0.49	0.66	0.72	0.78	0.81	Sample Failed	Sample Failed	Sample Failed	Sample Failed
Sample D	Dynamic Modulus (MPa)	847	823	792	789	869	795	713	685	665	637	580	558	Sample Failed	Sample Failed	Sample Failed	Sample Failed
	Phase Angle (degrees)	14.93	12.80	10.54	9.81	14.70	13.34	11.39	11.01	15.86	14.35	12.33	11.64	Sample Failed	Sample Failed	Sample Failed	Sample Failed
	Radial Micro-Strain	74	77	82	79	198	242	305	330	499	572	695	750	Sample Failed	Sample Failed	Sample Failed	Sample Failed
	Poisson's Ratio	0.32	0.32	0.33	0.32	0.44	0.49	0.55	0.57	0.62	0.67	0.73	0.76	Sample Failed	Sample Failed	Sample Failed	Sample Failed
Sample E	Dynamic Modulus (MPa)	1160	1122	1058	1042	1151	1102	1034	1015	779	740	677	655	Sample Failed	Sample Failed	Sample Failed	Sample Failed
	Phase Angle (degrees)	13.55	12.07	9.22	8.63	13.22	11.52	9.93	9.41	14.65	13.22	11.40	11.07	Sample Failed	Sample Failed	Sample Failed	Sample Failed
	Radial Micro-Strain	47	44	49	48	122	133	150	156	393	452	538	575	Sample Failed	Sample Failed	Sample Failed	Sample Failed
	Poisson's Ratio	0.28	0.25	0.26	0.25	0.36	0.37	0.39	0.40	0.57	0.62	0.67	0.69	Sample Failed	Sample Failed	Sample Failed	Sample Failed

Table A.8 Recycled PCC GW 2% Cement/SS-1, Moist Cured

Recycled PCC GW 2% Cement/SS-1, Moist Cured

Sample ID	Material Property	Low Stress State Stress State #1				Medium Stress State Stress State #2				High Stress State Stress State #3				Fully Reversed Stress State Stress State #4			
		10 Hz	5 Hz	1 Hz	0.5 Hz	10 Hz	5 Hz	1 Hz	0.5 Hz	10 Hz	5 Hz	1 Hz	0.5 Hz	10 Hz	5 Hz	1 Hz	0.5 Hz
Sample A	Dynamic Modulus (MPa)	1896	1892	1886	1861	1812	1776	1743	1737	1321	1282	1227	1210	788	766	716	712
	Phase Angle (degrees)	10.13	8.49	7.21	6.90	11.93	10.15	8.20	8.05	11.54	10.51	9.29	9.21	12.87	11.44	169.61	170.01
	Radial Micro-Strain	21	22	24	22	65	69	73	73	170	183	205	216	183	190	202	204
	Poisson's Ratio	0.20	0.21	0.23	0.21	0.30	0.31	0.32	0.32	0.42	0.43	0.46	0.48	0.36	0.37	0.37	0.37
Sample B	Dynamic Modulus (MPa)	1641	1692	1685	1698	1710	1727	1703	1715	1316	1292	1243	1229	807	798	747	740
	Phase Angle (degrees)	9.57	8.37	6.30	7.34	11.03	9.52	8.79	7.47	11.99	10.43	9.48	9.30	12.76	11.39	169.62	170.01
	Radial Micro-Strain	16	18	19	19	55	58	62	57	137	144	162	172	124	130	144	145
	Poisson's Ratio	0.13	0.16	0.16	0.17	0.24	0.25	0.26	0.25	0.34	0.34	0.37	0.39	0.25	0.26	0.27	0.27
Sample C	Dynamic Modulus (MPa)	1721	1761	1755	1756	1671	1662	1645	1657	1243	1219	1167	1154	721	709	663	658
	Phase Angle (degrees)	9.88	8.86	7.06	7.35	10.98	9.17	8.09	8.12	11.93	10.68	9.59	9.36	12.92	11.39	169.56	169.75
	Radial Micro-Strain	21	23	24	23	76	76	81	75	179	192	212	219	186	189	202	204
	Poisson's Ratio	0.19	0.21	0.21	0.21	0.32	0.32	0.33	0.31	0.42	0.43	0.45	0.46	0.34	0.34	0.34	0.34
Sample D	Dynamic Modulus (MPa)	1827	1804	1829	1807	1787	1775	1772	1770	1330	1307	1255	1241	803	785	742	736
	Phase Angle (degrees)	9.35	7.89	6.37	6.15	9.73	8.50	7.72	7.43	11.06	9.74	8.93	8.45	11.83	10.62	170.41	170.84
	Radial Micro-Strain	107	109	108	109	217	222	225	225	401	414	437	442	494	505	536	538
	Poisson's Ratio	0.22	0.21	0.20	0.21	0.27	0.26	0.28	0.27	0.35	0.37	0.38	0.40	0.32	0.32	0.32	0.33
Sample E	Dynamic Modulus (MPa)	1980	2010	1972	2045	1961	1943	1936	1938	1469	1430	1383	1364	886	871	830	818
	Phase Angle (degrees)	8.32	7.51	6.60	5.04	10.11	8.52	7.68	7.19	10.96	9.44	8.48	8.64	11.55	10.38	170.47	170.79
	Radial Micro-Strain	15	18	15	19	50	52	53	55	132	141	155	163	135	138	144	143
	Poisson's Ratio	0.15	0.18	0.15	0.20	0.25	0.25	0.26	0.27	0.36	0.37	0.39	0.41	0.30	0.30	0.30	0.30

Table A.9 Recycled PCC GW 2% Cement/SS-1, Vacuum Saturated

Recycled PCC GW 2% Cement/SS-1, Vacuum Saturated

Sample ID	Material Property	Low Stress State Stress State #1				Medium Stress State Stress State #2				High Stress State Stress State #3				Fully Reversed Stress State Stress State #4			
		10 Hz	5 Hz	1 Hz	0.5 Hz	10 Hz	5 Hz	1 Hz	0.5 Hz	10 Hz	5 Hz	1 Hz	0.5 Hz	10 Hz	5 Hz	1 Hz	0.5 Hz
Sample A	Dynamic Modulus (MPa)	1202	1192	1190	1208	1260	1249	1215	1226	859	823	776	757	495	480	446	441
	Phase Angle (degrees)	10.59	9.04	7.70	7.44	11.53	9.72	8.66	8.20	13.61	12.36	10.28	9.79	14.61	167.08	168.95	169.42
	Radial Micro-Strain	34	38	34	38	93	100	103	105	342	388	449	478	275	288	312	317
	Poisson's Ratio	0.21	0.23	0.20	0.23	0.30	0.32	0.32	0.33	0.55	0.59	0.64	0.66	0.34	0.35	0.35	0.35
Sample B	Dynamic Modulus (MPa)	1273	1268	1270	1282	1235	1210	1190	1197	844	812	769	756	510	497	466	461
	Phase Angle (degrees)	10.50	8.60	8.14	6.98	11.88	10.55	9.15	8.57	13.45	12.02	10.63	10.12	14.52	167.11	168.79	169.12
	Radial Micro-Strain	35	36	36	33	121	124	129	124	376	417	463	477	286	290	306	311
	Poisson's Ratio	0.23	0.23	0.23	0.21	0.38	0.38	0.38	0.37	0.59	0.62	0.65	0.66	0.37	0.36	0.36	0.36
Sample C	Dynamic Modulus (MPa)	1085	987	839	824	1118	1028	893	834	756	739	712	706	227	Sample Failed	Sample Failed	Sample Failed
	Phase Angle (degrees)	13.10	11.54	9.40	8.99	12.95	11.48	10.06	9.78	14.89	13.06	10.96	10.51	18.80	Sample Failed	Sample Failed	Sample Failed
	Radial Micro-Strain	61	73	88	99	146	175	224	262	518	554	592	600	665	Sample Failed	Sample Failed	Sample Failed
	Poisson's Ratio	0.34	0.37	0.37	0.42	0.42	0.46	0.50	0.55	0.73	0.75	0.77	0.77	0.39	Sample Failed	Sample Failed	Sample Failed
Sample D	Dynamic Modulus (MPa)	1357	1324	1328	1360	1337	1320	1288	1285	876	842	793	781	492	480	454	447
	Phase Angle (degrees)	11.56	9.60	7.35	7.11	11.50	9.69	8.37	8.19	13.20	11.74	10.19	9.85	14.51	167.29	168.89	169.29
	Radial Micro-Strain	43	42	43	38	97	103	109	109	334	378	431	459	320	331	346	348
	Poisson's Ratio	0.30	0.28	0.29	0.27	0.34	0.35	0.35	0.35	0.55	0.59	0.62	0.65	0.40	0.40	0.39	0.39
Sample E	Dynamic Modulus (MPa)	1323	1318	1306	1331	1359	1351	1326	1321	928	896	849	828	542	526	497	493
	Phase Angle (degrees)	11.02	9.17	7.66	7.00	11.34	9.76	8.28	7.86	12.90	11.46	10.09	9.81	14.21	167.45	169.07	169.44
	Radial Micro-Strain	34	34	34	37	87	91	97	94	288	332	386	411	274	283	302	300
	Poisson's Ratio	0.23	0.23	0.23	0.25	0.31	0.31	0.32	0.31	0.50	0.55	0.60	0.62	0.37	0.38	0.38	0.37

Table A.10 Recycled PCC GW 3% Cement, Moist Cured

Recycled PCC GW 3% Cement, Moist Cured

Sample ID	Material Property	Low Stress State Stress State #1				Medium Stress State Stress State #2				High Stress State Stress State #3				Fully Reversed Stress State Stress State #4			
		10 Hz	5 Hz	1 Hz	0.5 Hz	10 Hz	5 Hz	1 Hz	0.5 Hz	10 Hz	5 Hz	1 Hz	0.5 Hz	10 Hz	5 Hz	1 Hz	0.5 Hz
Sample A	Dynamic Modulus (MPa)	2295	2273	2309	2421	2274	2312	2313	2358	1747	1749	1741	1755	1131	1145	1129	1148
	Phase Angle (degrees)	6.59	5.47	5.03	3.82	8.16	6.70	5.76	5.05	8.76	7.29	6.15	6.11	8.72	7.41	173.61	173.79
	Radial Micro-Strain	9	10	10	8	25	26	26	25	49	51	51	51	43	44	47	44
	Poisson's Ratio	0.10	0.12	0.12	0.10	0.14	0.15	0.15	0.15	0.16	0.16	0.16	0.16	0.12	0.13	0.13	0.13
Sample B	Dynamic Modulus (MPa)	2566	2530	2690	2652	2449	2441	2464	2503	1924	1892	1894	1890	1297	1293	1274	1279
	Phase Angle (degrees)	6.19	5.14	3.37	3.82	7.16	5.88	5.38	5.17	7.89	7.02	5.87	5.80	8.05	7.04	173.99	174.35
	Radial Micro-Strain	13	11	15	12	36	34	35	32	62	62	67	67	60	62	65	62
	Poisson's Ratio	0.17	0.15	0.20	0.17	0.23	0.21	0.22	0.20	0.22	0.22	0.23	0.23	0.20	0.20	0.21	0.20
Sample C	Dynamic Modulus (MPa)	2683	2648	2664	2634	2617	2579	2620	2619	1984	1983	1998	2008	1432	1436	1434	1448
	Phase Angle (degrees)	6.80	6.78	4.55	4.39	9.44	7.23	6.12	5.65	7.80	6.50	5.97	5.58	8.34	6.99	174.17	174.21
	Radial Micro-Strain	10	11	10	8	16	17	22	20	33	35	35	35	24	24	26	23
	Poisson's Ratio	0.13	0.15	0.13	0.10	0.10	0.11	0.14	0.13	0.12	0.13	0.01	0.13	0.08	0.09	0.09	0.08
Sample D	Dynamic Modulus (MPa)	1950	2010	2060	2084	1978	2015	2053	2087	1461	1468	1482	1502	888	906	896	909
	Phase Angle (degrees)	8.61	6.55	4.34	5.23	9.43	7.64	5.47	5.91	8.97	7.47	6.45	6.03	9.31	7.82	173.50	173.51
	Radial Micro-Strain	10	9	12	10	26	25	27	28	50	55	55	57	52	53	54	53
	Poisson's Ratio	0.10	0.09	0.12	0.10	0.13	0.13	0.14	0.15	0.14	0.15	0.15	0.16	0.12	0.12	0.12	0.12
Sample E	Dynamic Modulus (MPa)	2293	2251	2268	2332	2219	2227	246	2292	1675	1662	1661	1669	1064	1060	1046	1053
	Phase Angle (degrees)	6.06	5.10	4.29	3.87	7.59	5.88	5.15	5.18	8.05	6.97	6.14	5.63	8.33	7.22	173.90	174.41
	Radial Micro-Strain	9	7	8	9	25	24	28	27	50	50	55	54	46	49	49	49
	Poisson's Ratio	0.10	0.08	0.09	0.10	0.14	0.13	0.16	0.16	0.16	0.15	0.17	0.17	0.12	0.13	0.13	0.13

Table A.11 Recycled PCC GW 3% Cement, Vacuum Saturated

Recycled PCC GW 3% Cement, Vacuum Saturated

Sample ID	Material Property	Low Stress State Stress State #1				Medium Stress State Stress State #2				High Stress State Stress State #3				Fully Reversed Stress State Stress State #4			
		10 Hz	5 Hz	1 Hz	0.5 Hz	10 Hz	5 Hz	1 Hz	0.5 Hz	10 Hz	5 Hz	1 Hz	0.5 Hz	10 Hz	5 Hz	1 Hz	0.5 Hz
Sample A	Dynamic Modulus (MPa)	1798	1813	1835	1876	1819	1826	1818	1825	1272	1250	1235	1232	764	766	749	759
	Phase Angle (degrees)	9.68	8.15	6.41	4.97	9.97	7.92	6.37	6.01	9.96	8.23	7.07	6.89	10.57	9.01	172.48	172.67
	Radial Micro-Strain	15	12	11	15	34	35	40	38	100	108	119	130	96	97	99	97
	Poisson's Ratio	0.14	0.11	0.10	0.15	0.16	0.16	0.18	0.18	0.24	0.25	0.27	0.29	0.18	0.19	0.19	0.19
Sample B	Dynamic Modulus (MPa)	1909	1892	1913	1972	1941	1961	1957	1956	1424	1407	1379	1382	883	875	854	856
	Phase Angle (degrees)	8.24	6.69	5.60	5.17	8.12	7.18	6.20	5.62	9.61	8.22	7.11	6.74	10.34	8.89	172.54	172.84
	Radial Micro-Strain	20	24	18	18	43	47	46	45	104	111	123	127	118	118	121	119
	Poisson's Ratio	0.20	0.23	0.18	0.18	0.21	0.23	0.22	0.22	0.28	0.29	0.31	0.32	0.26	0.26	0.26	0.26
Sample C	Dynamic Modulus (MPa)	1978	2034	2039	2063	1962	1932	1936	1945	1357	1332	1305	1299	878	871	852	853
	Phase Angle (degrees)	8.05	5.88	5.14	4.63	9.62	8.19	6.68	6.04	10.02	8.85	7.47	7.08	10.78	9.17	172.07	172.52
	Radial Micro-Strain	13	12	10	11	31	32	32	36	89	97	104	112	73	73	75	73
	Poisson's Ratio	0.13	0.12	0.10	0.11	0.16	0.15	0.16	0.17	0.23	0.24	0.25	0.26	0.16	0.16	0.16	0.16
Sample D	Dynamic Modulus (MPa)	1466	1468	1493	1557	1487	1482	1503	1530	997	983	978	981	558	556	546	547
	Phase Angle (degrees)	9.68	7.26	6.32	5.80	9.31	8.19	7.08	6.59	10.96	9.71	8.14	7.78	11.91	10.22	171.29	171.74
	Radial Micro-Strain	15	17	19	14	44	46	50	49	153	169	184	193	179	176	178	175
	Poisson's Ratio	0.11	0.13	0.14	0.11	0.17	0.17	0.19	0.19	0.29	0.31	0.33	0.35	0.25	0.25	0.24	0.24
Sample E	Dynamic Modulus (MPa)	1644	1649	1697	1721	1652	1655	1665	1681	1116	1095	1084	1076	632	633	620	624
	Phase Angle (degrees)	8.40	6.63	5.75	5.73	10.97	8.64	6.71	6.45	10.65	9.05	7.81	7.68	11.47	9.75	171.63	172.22
	Radial Micro-Strain	19	16	18	17	46	45	47	48	141	158	176	185	151	146	150	145
	Poisson's Ratio	0.16	0.13	0.15	0.15	0.20	0.19	0.20	0.20	0.30	0.32	0.35	0.36	0.24	0.23	0.23	0.23

Table A.12 Recycled PCC GW 3% SS-1, Moist Cured

Recycled PCC GW 3% SS-1, Moist Cured

Sample ID	Material Property	Low Stress State Stress State #1				Medium Stress State Stress State #2				High Stress State Stress State #3				Fully Reversed Stress State Stress State #4			
		10 Hz	5 Hz	1 Hz	0.5 Hz	10 Hz	5 Hz	1 Hz	0.5 Hz	10 Hz	5 Hz	1 Hz	0.5 Hz	10 Hz	5 Hz	1 Hz	0.5 Hz
Sample A	Dynamic Modulus (MPa)	1536	1475	1355	1327	1576	1505	1355	1318	1249	1167	1021	968	860	793	656	612
	Phase Angle (degrees)	12.42	11.91	10.53	10.01	13.96	12.73	11.80	11.14	15.35	14.13	13.17	12.74	16.92	164.06	164.67	164.97
	Radial Micro-Strain	31	33	36	38	72	77	93	100	141	163	215	243	127	143	189	205
	Poisson's Ratio	0.24	0.25	0.24	0.26	0.29	0.29	0.32	0.33	0.33	0.35	0.40	0.43	0.27	0.29	0.31	0.32
Sample B	Dynamic Modulus (MPa)	1440	1395	1252	1238	1452	1374	1222	1182	1130	1069	928	878	796	733	596	551
	Phase Angle (degrees)	14.95	12.59	11.66	10.80	15.21	13.38	12.09	11.35	16.29	14.68	13.37	13.07	17.86	162.27	164.02	164.44
	Radial Micro-Strain	33	38	40	42	77	87	105	112	151	180	249	287	126	148	203	225
	Poisson's Ratio	0.24	0.27	0.25	0.27	0.29	0.30	0.32	0.33	0.32	0.36	0.42	0.46	0.25	0.27	0.30	0.31
Sample C	Dynamic Modulus (MPa)	1435	1394	1296	1265	1505	1413	1283	1239	1141	1078	946	904	781	718	587	545
	Phase Angle (degrees)	13.64	11.81	10.88	10.36	14.43	12.94	11.55	11.48	16.22	14.51	13.27	12.95	18.32	162.98	163.91	164.28
	Radial Micro-Strain	34	36	40	45	85	90	113	121	201	230	304	338	161	184	245	273
	Poisson's Ratio	0.25	0.25	0.26	0.29	0.33	0.32	0.36	0.38	0.43	0.46	0.52	0.56	0.32	0.33	0.36	0.38
Sample D	Dynamic Modulus (MPa)	1635	1601	1480	1415	1712	1616	1441	1382	1350	1263	1090	1027	959	872	720	664
	Phase Angle (degrees)	11.53	11.53	11.10	10.02	12.82	12.02	11.52	11.04	14.57	13.50	12.86	12.54	16.53	164.33	165.00	165.23
	Radial Micro-Strain	25	24	28	30	56	62	72	81	106	120	170	194	97	110	145	164
	Poisson's Ratio	0.21	0.19	0.21	0.22	0.25	0.25	0.26	0.28	0.27	0.28	0.34	0.36	0.23	0.24	0.26	0.27
Sample E	Dynamic Modulus (MPa)	1836	1810	1660	1606	1887	1795	1615	1529	1514	1414	1231	1143	1057	977	805	743
	Phase Angle (degrees)	12.16	11.36	10.61	10.22	13.21	12.40	11.77	11.74	14.51	13.50	13.04	13.10	15.95	164.72	165.00	165.10
	Radial Micro-Strain	22	22	26	27	51	60	70	76	106	125	170	198	97	108	147	157
	Poisson's Ratio	0.20	0.20	0.22	0.22	0.24	0.27	0.28	0.29	0.30	0.33	0.38	0.41	0.26	0.27	0.30	0.29

Table A.13 Recycled PCC GW 3% SS-1, Vacuum Saturated

Recycled PCC GW 3%Cement/ SS-1, Vacuum Saturated

Sample ID	Material Property	Low Stress State Stress State #1				Medium Stress State Stress State #2				High Stress State Stress State #3				Fully Reversed Stress State Stress State #4			
		10 Hz	5 Hz	1 Hz	0.5 Hz	10 Hz	5 Hz	1 Hz	0.5 Hz	10 Hz	5 Hz	1 Hz	0.5 Hz	10 Hz	5 Hz	1 Hz	0.5 Hz
Sample A	Dynamic Modulus (MPa)	1510	1476	1440	1407	1555	1483	1401	1378	1090	1001	909	874	570	546	496	489
	Phase Angle (degrees)	13.44	12.28	9.04	8.33	12.46	11.03	9.73	9.17	15.04	12.76	11.55	11.07	16.22	165.49	167.14	167.73
	Radial Micro-Strain	30	31	37	34	76	80	92	94	228	270	334	364	232	248	274	278
	Poisson's Ratio	0.23	0.23	0.27	0.24	0.30	0.30	0.32	0.33	0.46	0.50	0.55	0.58	0.33	0.34	0.34	0.34
Sample B	Dynamic Modulus (MPa)	1362	1346	1291	1315	1513	1477	1401	1385	1103	1027	921	883	625	589	526	509
	Phase Angle (degrees)	12.03	10.36	8.59	8.28	12.58	11.00	9.28	9.21	14.53	13.11	11.47	11.24	16.25	165.48	167.50	168.00
	Radial Micro-Strain	23	23	26	23	62	66	72	75	171	207	267	303	188	198	225	230
	Poisson's Ratio	0.16	0.16	0.17	0.15	0.24	0.25	0.25	0.26	0.35	0.39	0.45	0.49	0.30	0.30	0.30	0.30
Sample C	Dynamic Modulus (MPa)	1484	1428	1329	1312	1538	1446	1333	1282	1036	974	889	863	574	477	225	198
	Phase Angle (degrees)	13.30	11.48	9.12	9.32	12.97	11.47	9.77	9.32	15.25	13.57	11.94	11.40	17.15	164.82	166.58	168.27
	Radial Micro-Strain	30	31	34	34	71	76	87	92	245	281	328	352	221	258	361	394
	Poisson's Ratio	0.23	0.22	0.23	0.23	0.28	0.28	0.29	0.30	0.47	0.50	0.53	0.55	0.32	0.31	0.20	0.20
Sample D	Dynamic Modulus (MPa)	1368	1381	1343	1364	1441	1442	1383	1380	1006	973	894	869	598	578	522	510
	Phase Angle (degrees)	12.07	10.51	9.06	8.22	13.12	11.22	9.69	9.36	14.80	13.16	11.42	11.10	16.06	165.75	167.38	167.99
	Radial Micro-Strain	31	32	31	33	69	73	79	83	203	236	295	322	209	224	247	251
	Poisson's Ratio	0.22	0.23	0.21	0.23	0.25	0.27	0.27	0.29	0.38	0.42	0.48	0.51	0.31	0.33	0.33	0.32
Sample E	Dynamic Modulus (MPa)	1602	1586	1504	1531	1623	1583	1512	1484	1129	1073	994	962	670	638	578	567
	Phase Angle (degrees)	12.29	9.62	8.35	7.79	11.82	10.46	8.92	8.71	13.39	12.13	10.73	10.24	14.87	166.70	168.34	168.83
	Radial Micro-Strain	25	26	28	28	59	64	69	66	176	199	235	256	182	191	211	214
	Poisson's Ratio	0.21	0.21	0.21	0.22	0.25	0.26	0.26	0.25	0.37	0.39	0.43	0.45	0.31	0.31	0.31	0.31

Table A.14 Recycled PCC GW 3% Cement/SS-1, Moist Cured

Recycled PCC GW 3% Cement/SS-1, Moist Cured

Sample ID	Material Property	Low Stress State Stress State #1				Medium Stress State Stress State #2				High Stress State Stress State #3				Fully Reversed Stress State Stress State #4			
		10 Hz	5 Hz	1 Hz	0.5 Hz	10 Hz	5 Hz	1 Hz	0.5 Hz	10 Hz	5 Hz	1 Hz	0.5 Hz	10 Hz	5 Hz	1 Hz	0.5 Hz
Sample A	Dynamic Modulus (MPa)	1802	1831	1798	1794	1886	1867	1800	1806	1471	1431	1328	1295	958	916	819	800
	Phase Angle (degrees)	10.61	8.97	7.01	7.09	11.44	9.92	9.08	8.45	12.61	11.61	10.78	10.57	13.88	167.16	168.33	168.47
	Radial Micro-Strain	19	18	21	20	41	47	51	54	91	104	129	145	95	105	122	128
	Poisson's Ratio	0.18	0.17	0.19	0.18	0.20	0.22	0.23	0.24	0.25	0.27	0.31	0.34	0.23	0.24	0.25	0.26
Sample B	Dynamic Modulus (MPa)	2003	1960	1949	1927	1943	1939	1864	1861	1498	1450	1346	1311	987	963	868	840
	Phase Angle (degrees)	10.16	8.97	7.98	8.22	11.81	10.37	9.61	8.32	13.17	12.03	11.01	10.83	14.24	167.25	167.90	168.05
	Radial Micro-Strain	19	20	19	20	42	47	48	53	86	99	114	129	89	96	114	117
	Poisson's Ratio	0.20	0.20	0.19	0.19	0.21	0.23	0.22	0.25	0.24	0.26	0.28	0.31	0.22	0.23	0.25	0.25
Sample C	Dynamic Modulus (MPa)	2036	1943	1917	1945	1994	1921	1854	1850	1576	1492	1392	1364	1065	1010	899	878
	Phase Angle (degrees)	10.01	9.36	8.02	7.05	10.84	9.93	9.08	8.34	12.38	11.66	10.42	10.28	13.56	167.64	168.87	168.81
	Radial Micro-Strain	20	17	17	17	44	46	51	53	100	110	129	137	91	98	112	115
	Poisson's Ratio	0.20	0.17	0.16	0.17	0.23	0.23	0.24	0.25	0.30	0.30	0.33	0.34	0.24	0.25	0.25	0.25
Sample D	Dynamic Modulus (MPa)	1929	1918	1868	1886	1945	1905	1834	1837	1503	1452	1361	1336	971	928	848	827
	Phase Angle (degrees)	9.16	8.97	8.09	7.20	10.71	9.67	8.89	8.57	11.98	10.84	10.24	9.79	13.30	167.87	168.99	169.55
	Radial Micro-Strain	17	17	17	19	44	43	45	49	89	98	118	126	91	97	110	116
	Poisson's Ratio	0.16	0.16	0.16	0.18	0.22	0.21	0.21	0.23	0.25	0.26	0.29	0.31	0.22	0.23	0.24	0.24
Sample E	Dynamic Modulus (MPa)	1912	1872	1844	1870	1993	1909	1848	1844	1553	1464	1374	1356	899	871	796	782
	Phase Angle (degrees)	7.97	6.92	6.60	6.81	10.18	9.16	8.21	7.74	11.18	10.60	9.47	9.19	12.53	168.78	169.79	170.12
	Radial Micro-Strain	18	18	18	21	50	46	50	53	119	130	145	152	119	123	141	142
	Poisson's Ratio	0.18	0.17	0.17	0.20	0.25	0.22	0.23	0.24	0.34	0.35	0.36	0.38	0.27	0.27	0.28	0.28

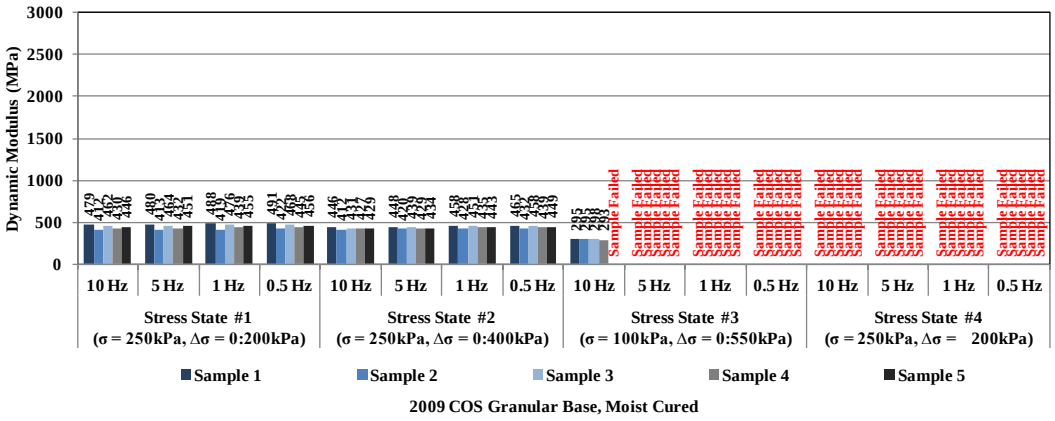

Figure A.1 Dynamic Modulus Results of Conventional COS Granular Base, Moist Cured

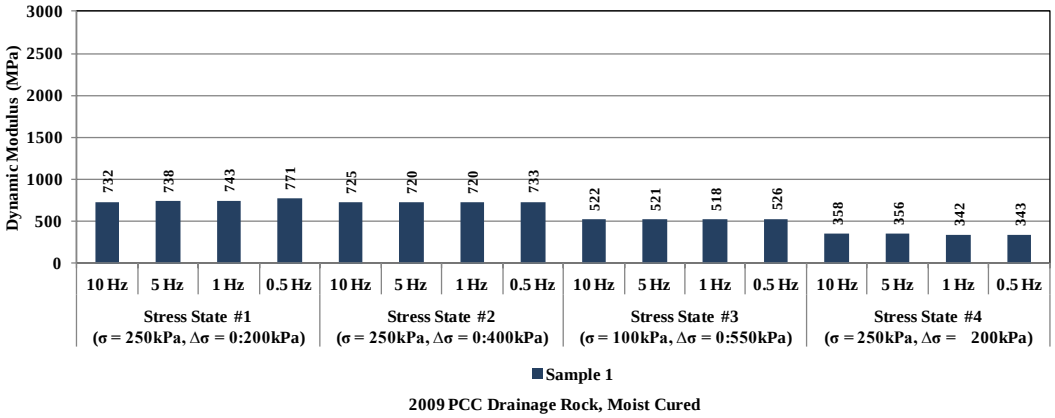

Figure A.2 Dynamic Modulus Results of Recycled PCC Drainage Rock, Moist Cured

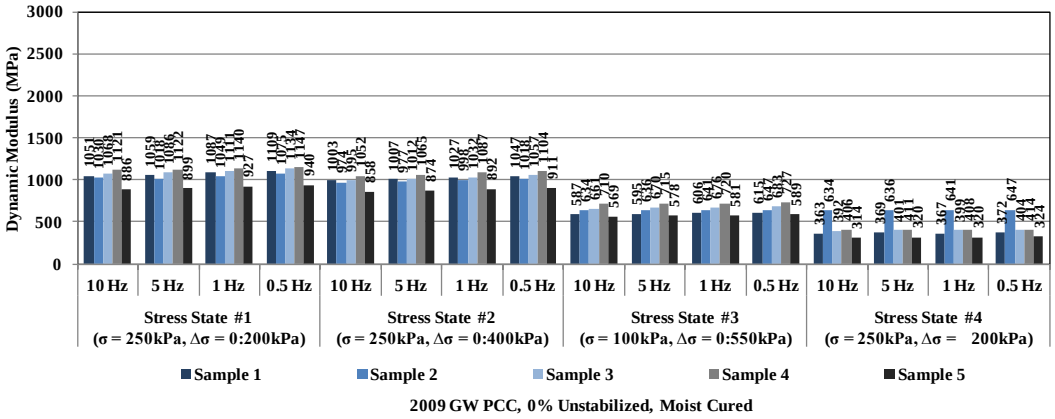

Figure A.3 Dynamic Modulus Results of Recycled PCC GW Base Untreated, Moist Cured

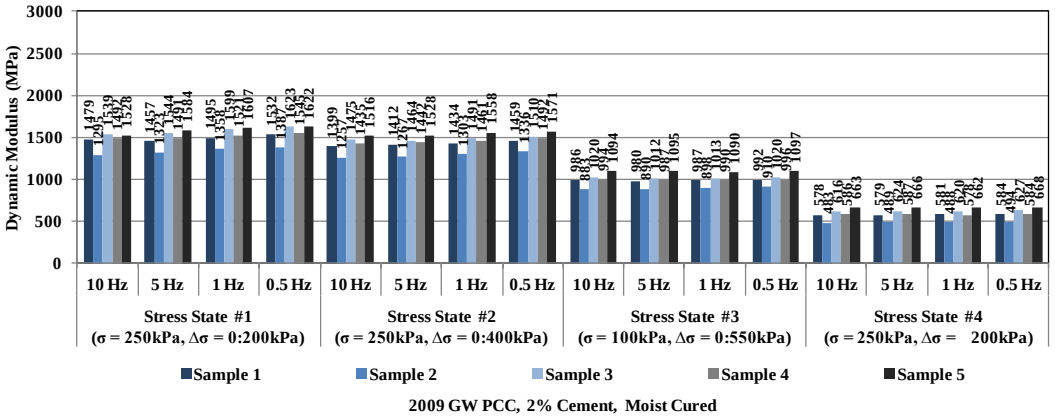

Figure A.4 Dynamic Modulus Results of Recycled PCC GW Base 2% Cement, Moist Cured

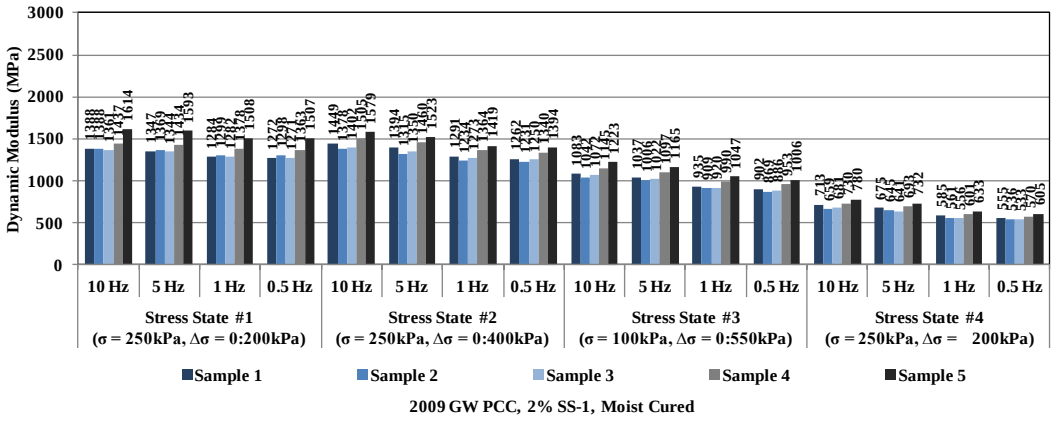

Figure A.5 Dynamic Modulus Results of Recycled PCC GW Base 2% SS-1, Moist Cured

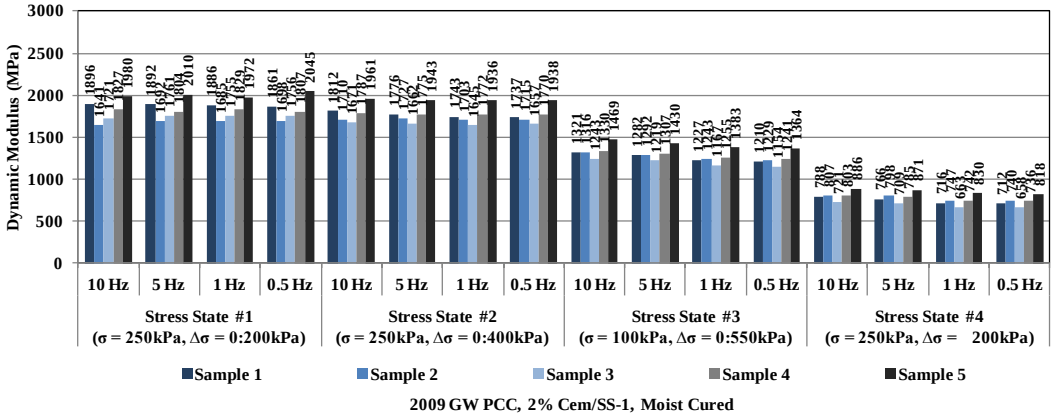

Figure A.6 Dynamic Modulus Results of Recycled PCC GW Base 2% Cement/SS-1, Moist Cured

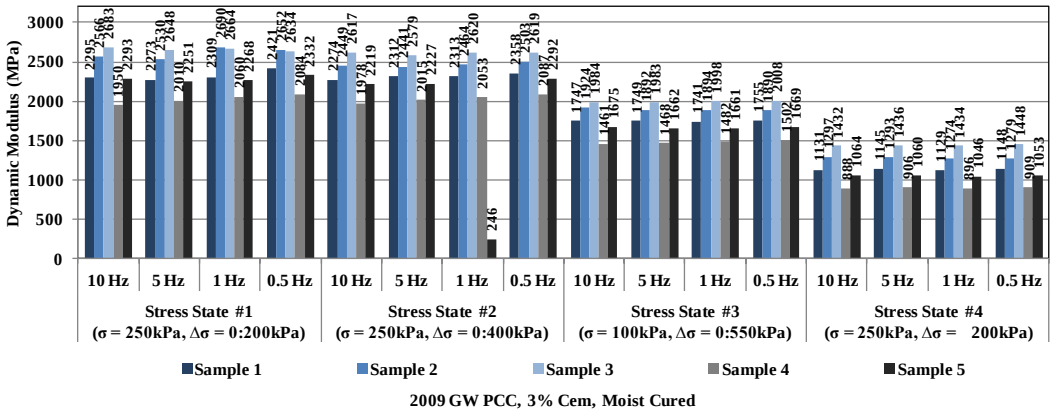

Figure A.7 Dynamic Modulus Results of Recycled PCC GW Base 3% Cement, Moist Cured

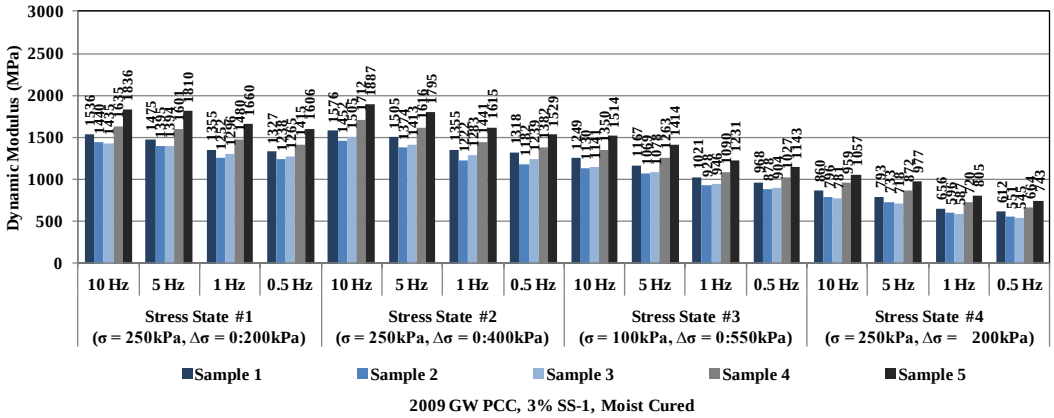

Figure A.8 Dynamic Modulus Results of Recycled PCC GW Base 3% Cement, Moist Cured

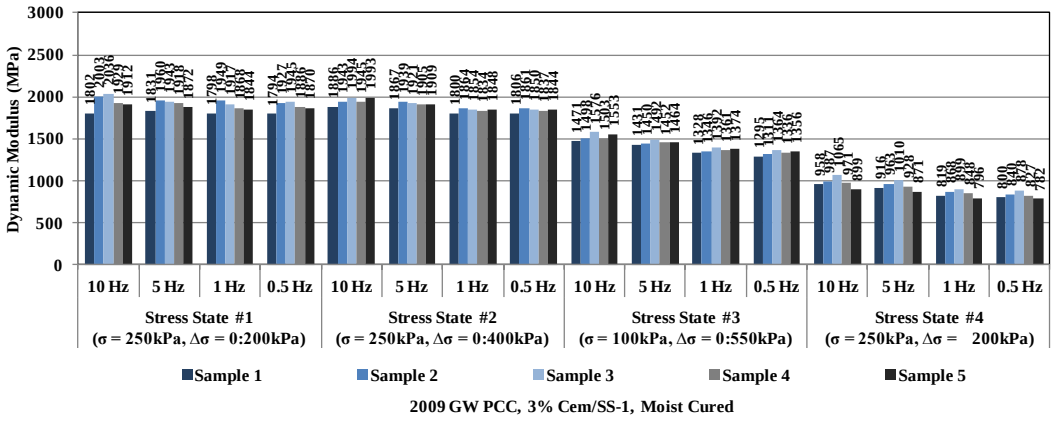

Figure A.9 Dynamic Modulus Results of Recycled PCC GW Base 3% Cement/SS-1, Moist Cured

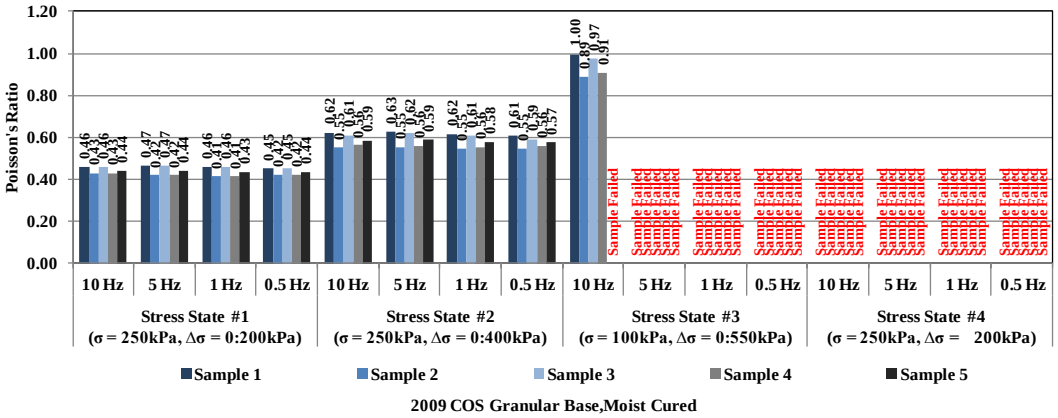

Figure A.10 Poisson's Ratio Results of COS Granular Base, Moist Cured

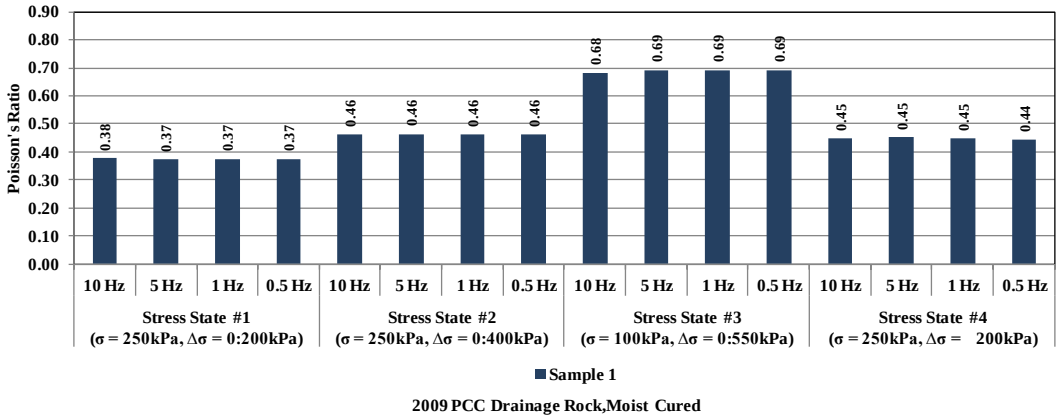

Figure A.11 Poisson's Ratio Results of Recycled PCC Drainage Rock, Moist Cured

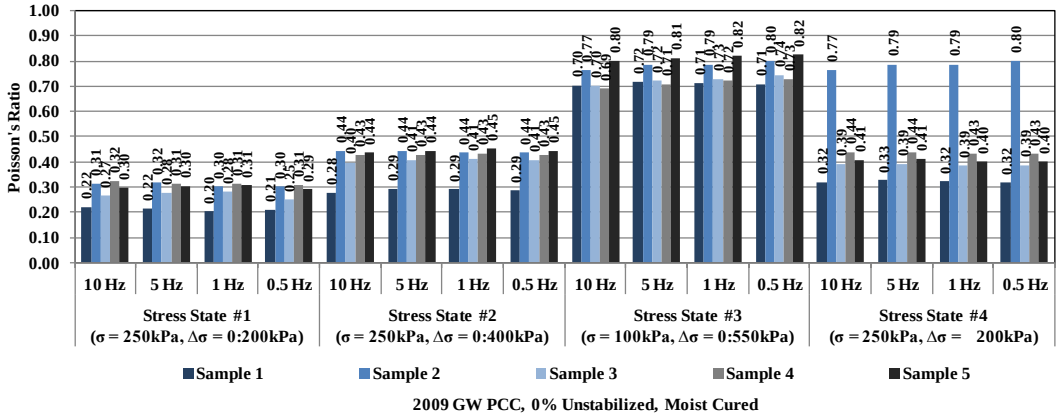

Figure A.12 Poisson's Ratio Results of Recycled PCC GW base Untreated, Moist Cured

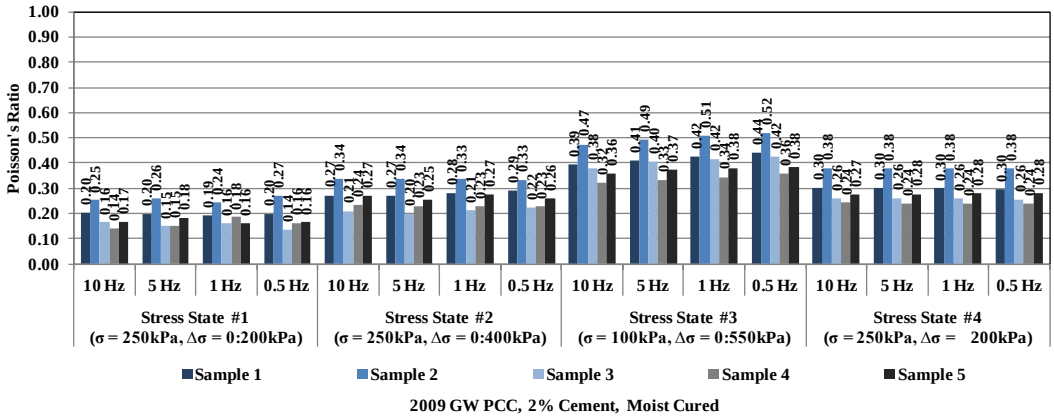

Figure A.13 Poisson's Ratio Results of Recycled PCC GW Base 2% Cement, Moist Cured

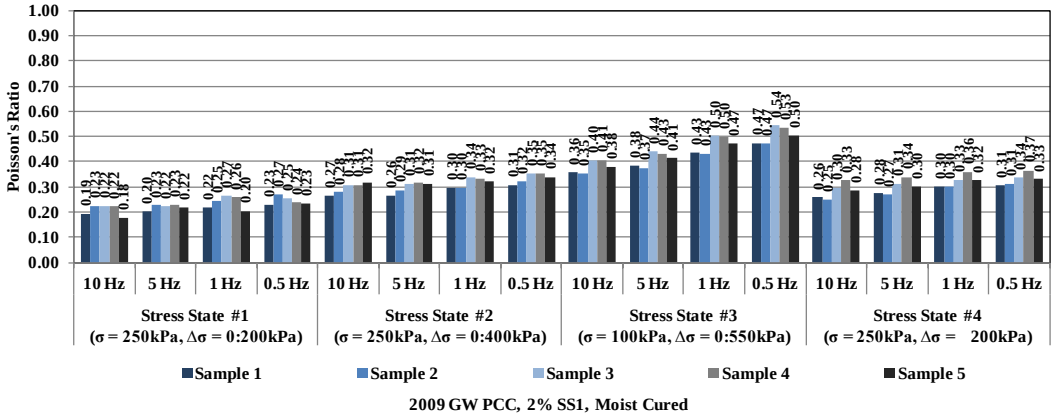

Figure A.14 Poisson's Ratio Results of Recycled PCC GW Base 2% SS-1, Moist Cured

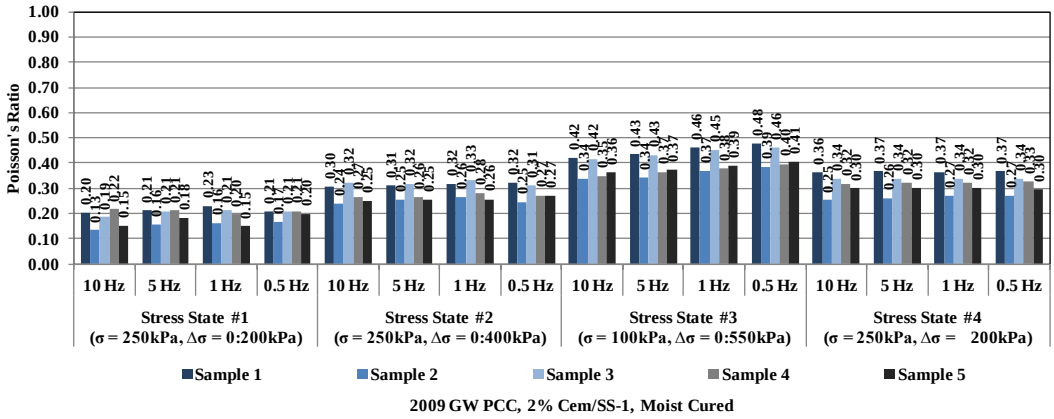

Figure A.15 Poisson's Ratio Results of Recycled PCC GW Base 2% Cement/SS-1, Moist Cured

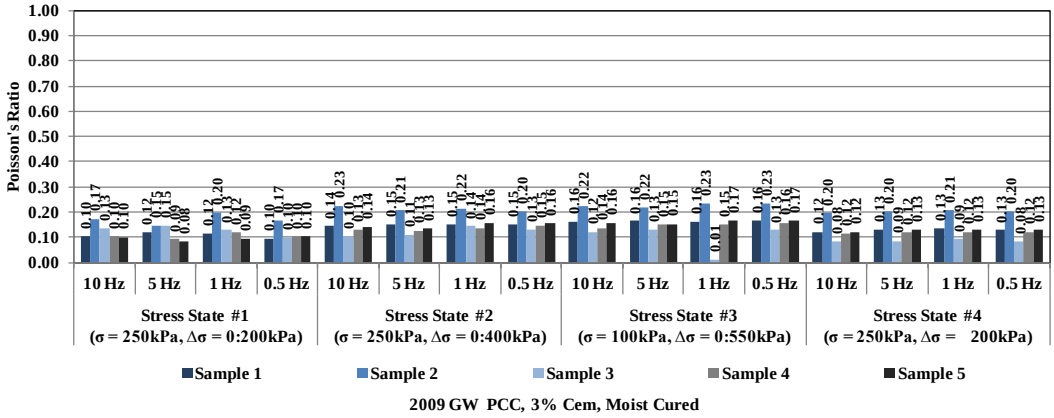

Figure A.16 Poisson's Ratio Results of Recycled PCC GW Base 3% Cement, Moist Cured

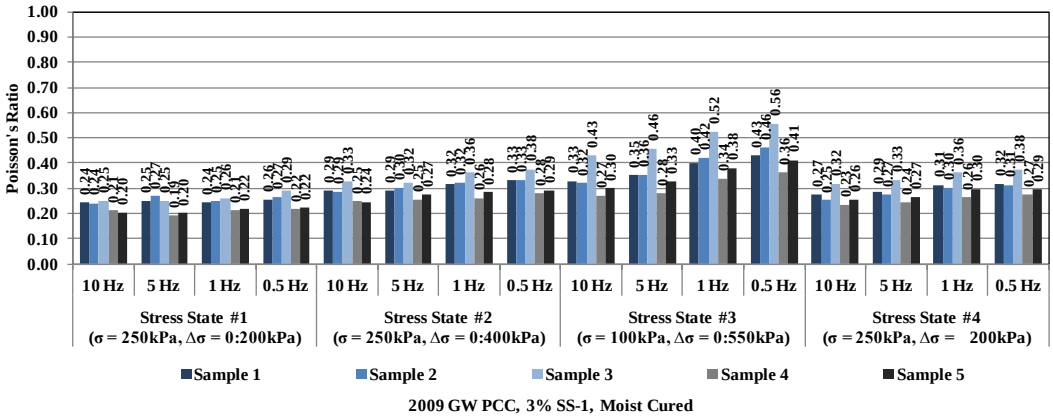

Figure A.17 Poisson's Ratio Results of Recycled PCC GW Base 3% SS-1, Moist Cured

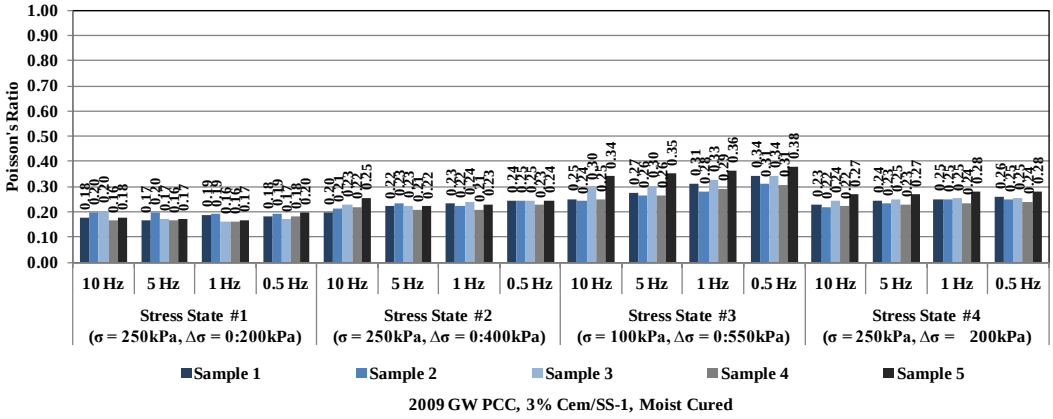

Figure A.18 Poisson's Ratio Results of Recycled PCC GW Base 3% Cement/SS-1, Moist Cured

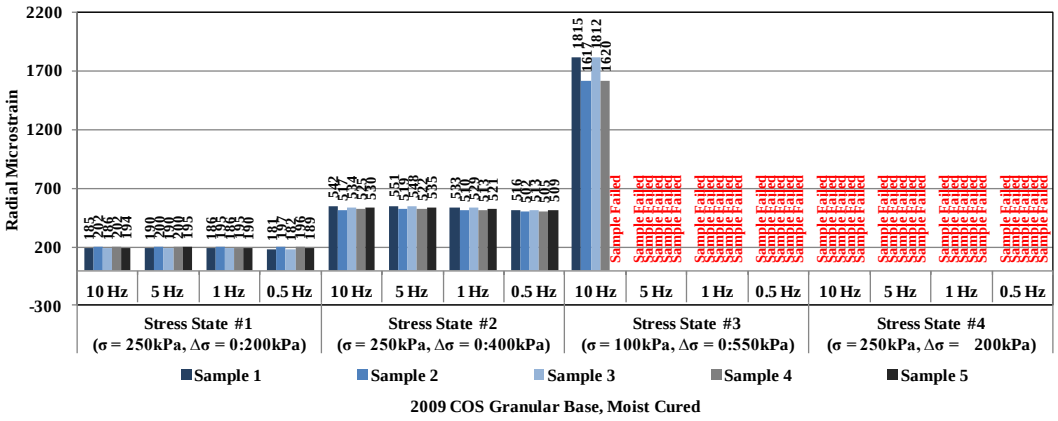

Figure A.19 Radial Micro Strain Results of COS Granular Base, Untreated Moist Cured

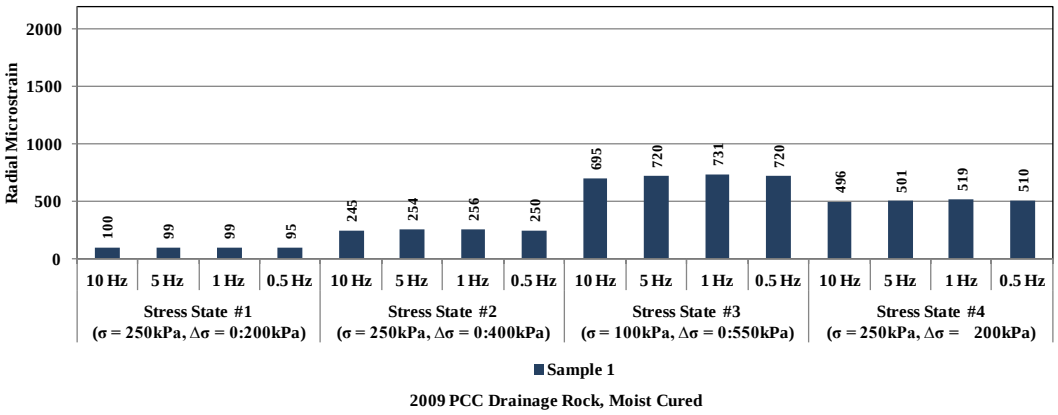

Figure A.20 Radial Micro Strain Results of Recycled PCC Drainage Rock, Moist Cured

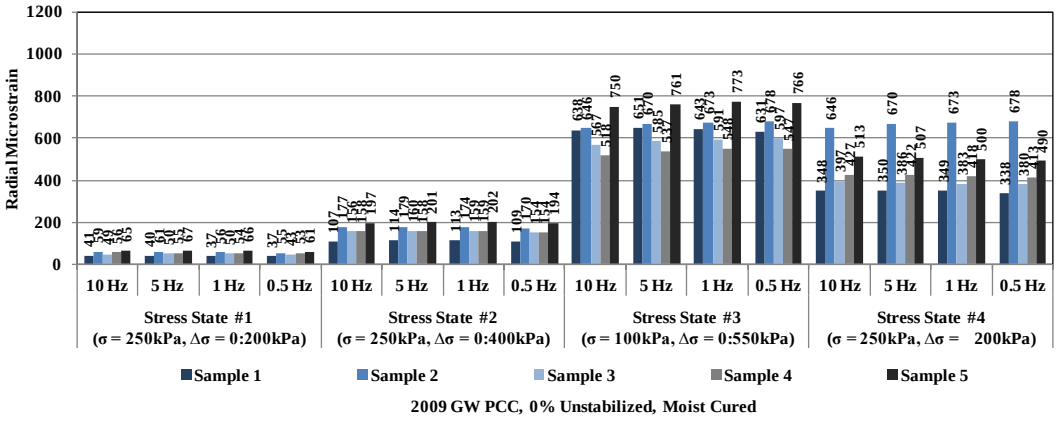

Figure A.21 Radial Micro Strain Results of Recycled PCC GW Base Untreated Moist Cured

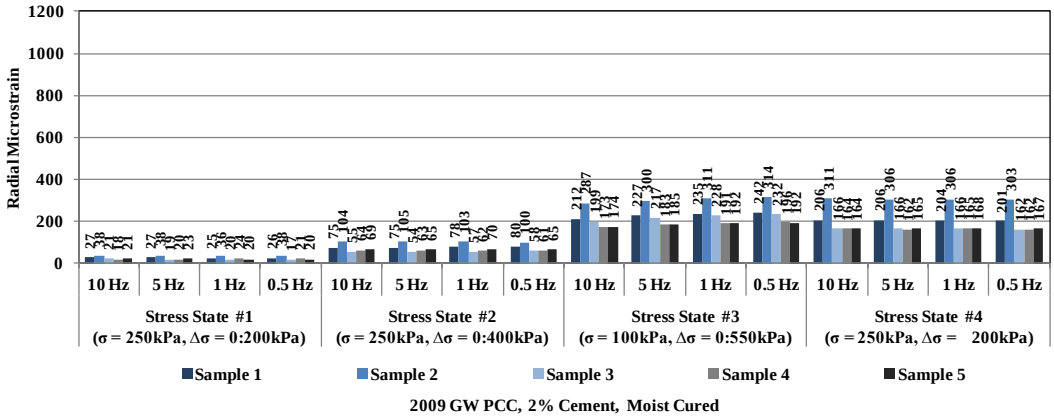

Figure A.22 Radial Micro Strain Results of Recycled PCC GW Base 2% Cement, Moist Cured

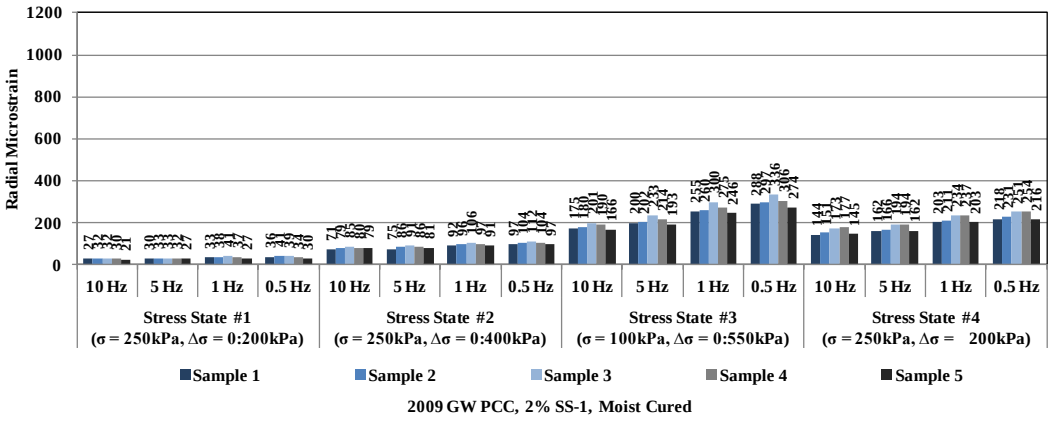

Figure A.23 Radial Micro Strain Results of Recycled PCC GW Base 2% SS-1, Moist Cured

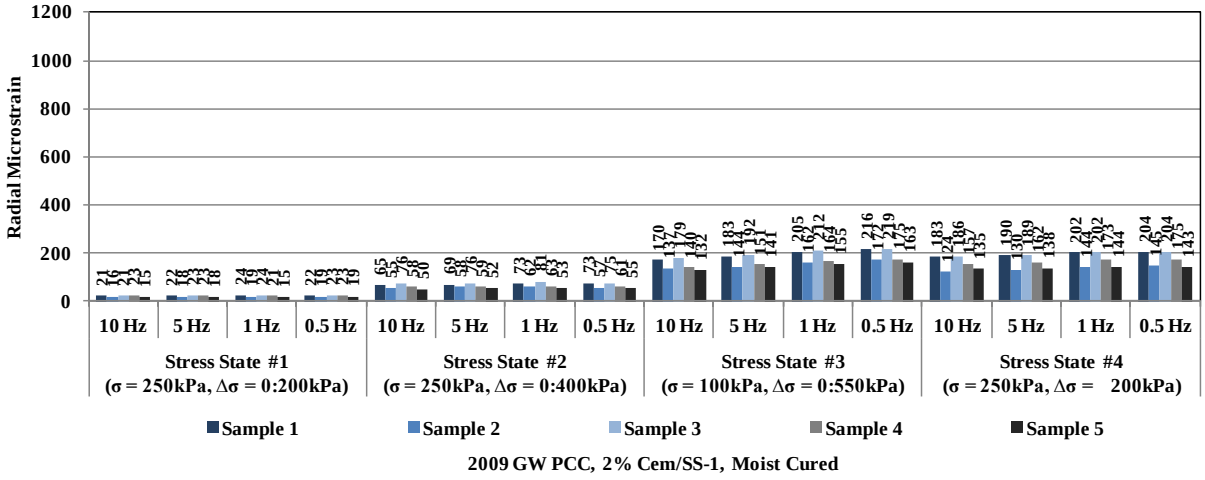

Figure A.24 Radial Micro Strain Results of Recycled PCC GW Base 2% Cement/SS-1, Moist Cured

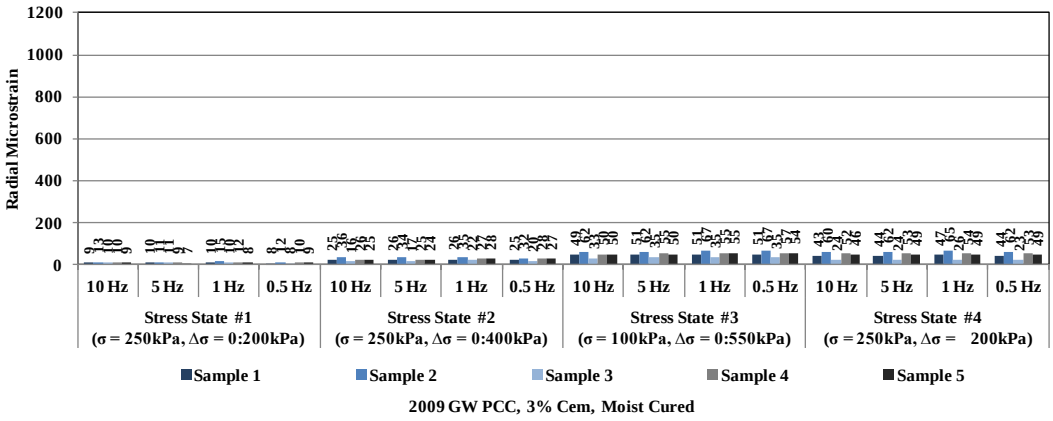

Figure A.25 Radial Micro Strain Results of Recycled PCC GW Base 3% Cement, Moist Cured

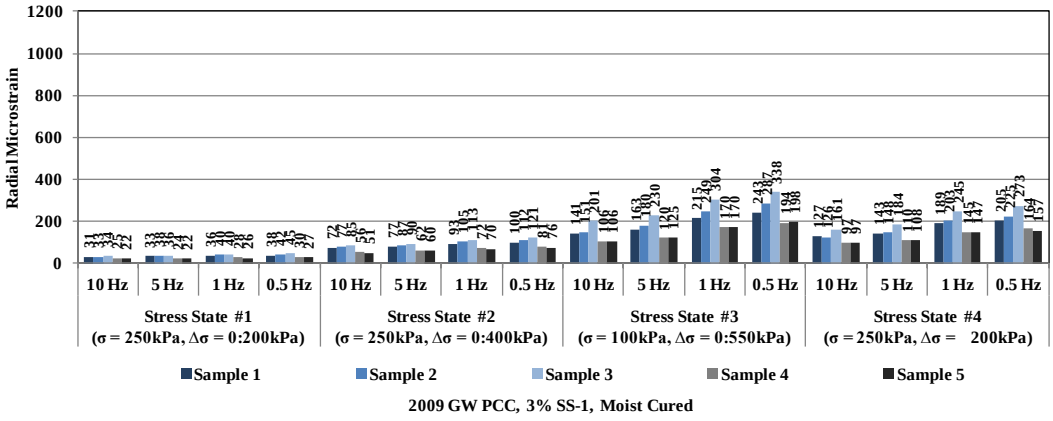

Figure A.26 Radial Micro Strain Results of Recycled PCC GW Base 3% SS-1, Moist Cured

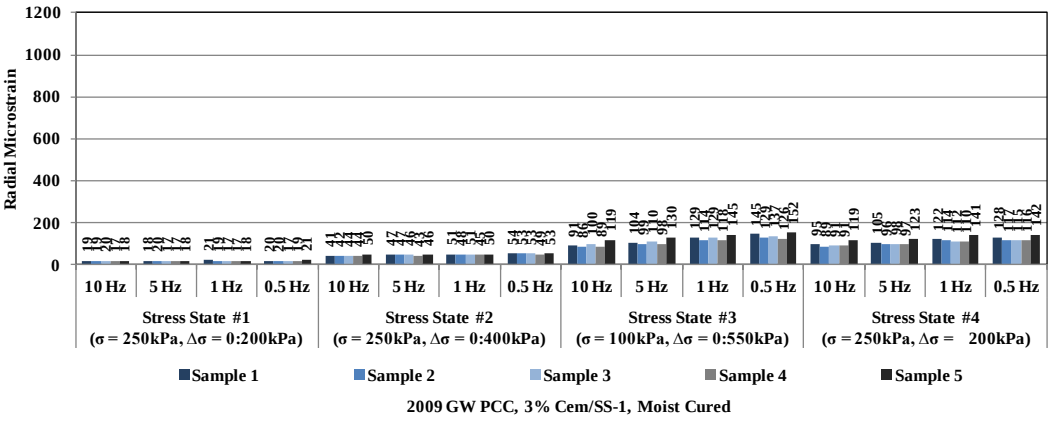

Figure A.27 Radial Micro Strain Results of Recycled PCC GW Base 3% Cement/SS-1, Moist Cured

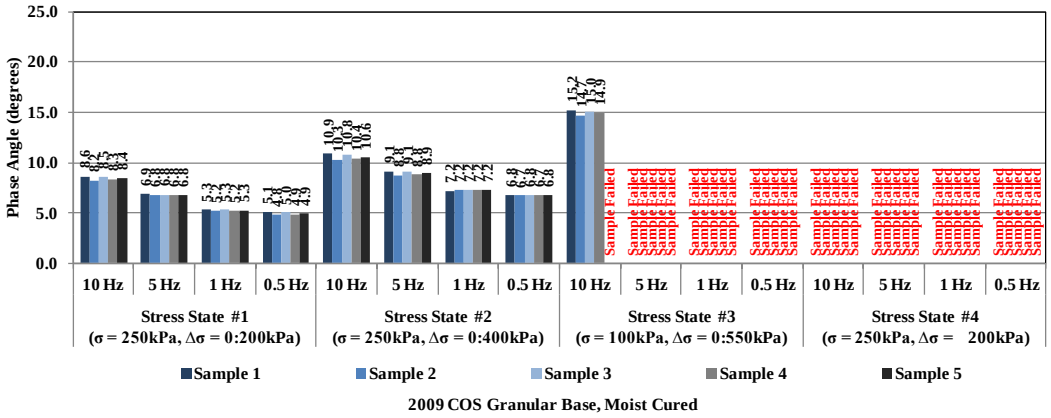

Figure A.28 Phase Angle Results of COS Granular Base, Moist Cured

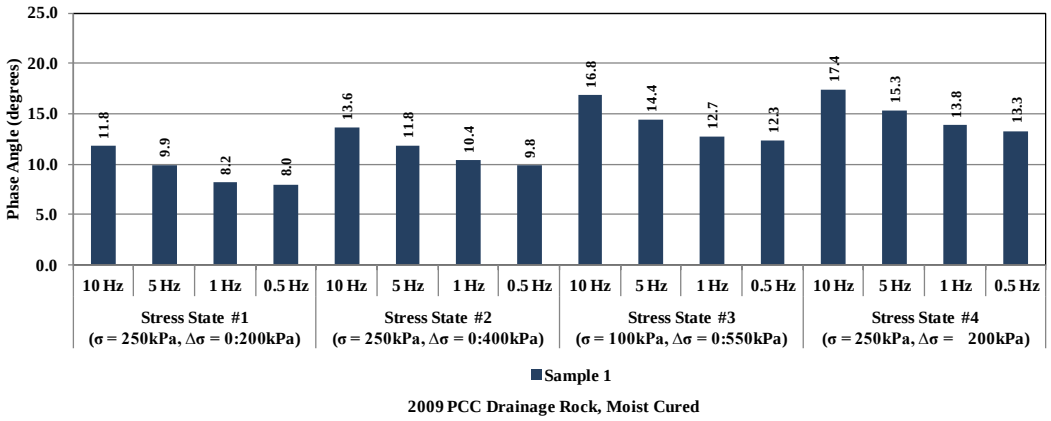

Figure A.29 Phase Angle Results of Recycled PCC Drainage Rock, Moist Cured

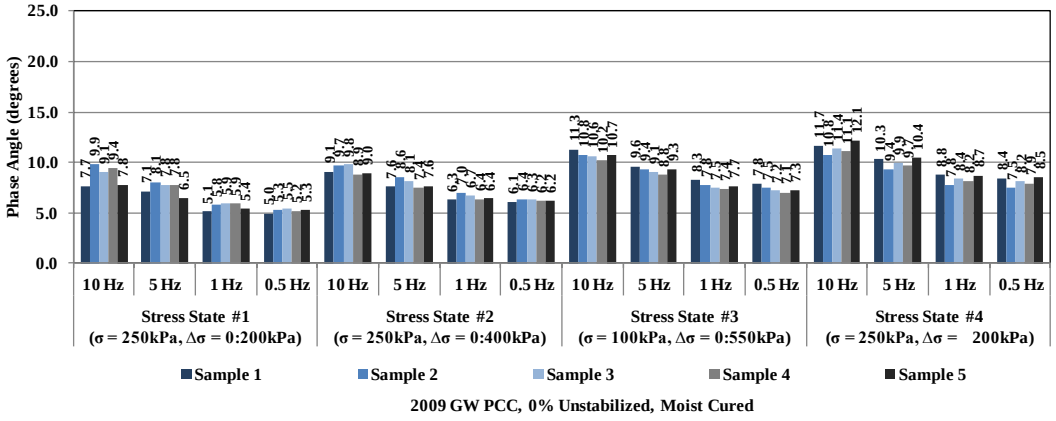

Figure A.30 Phase Angle Results of Recycled PCC GW Base Untreated, Moist Cured

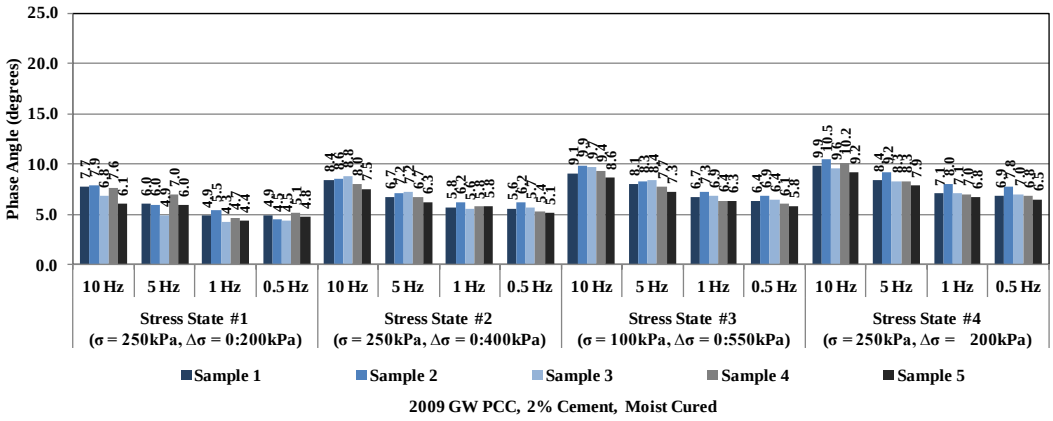

Figure A.31 Phase Angle Results of Recycled PCC GW Base 2% Cement, Moist Cured

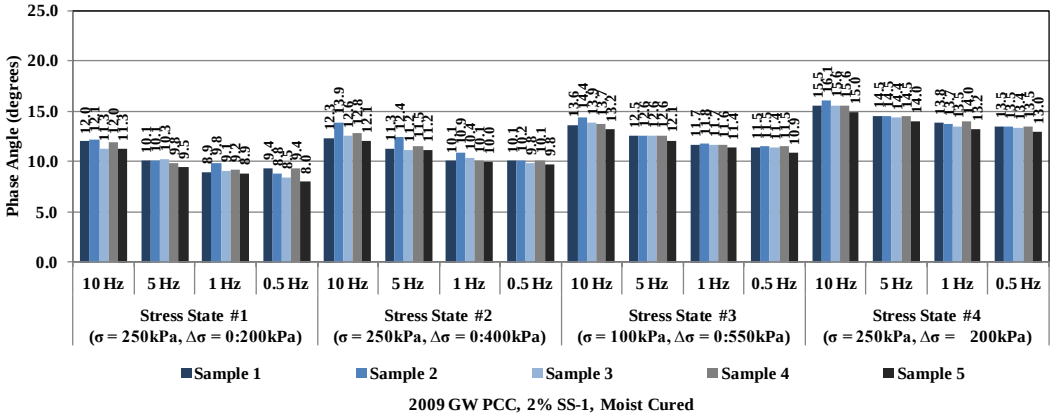

Figure A.32 Phase Angle Results of Recycled PCC GW Base 2% SS-1, Moist Cured

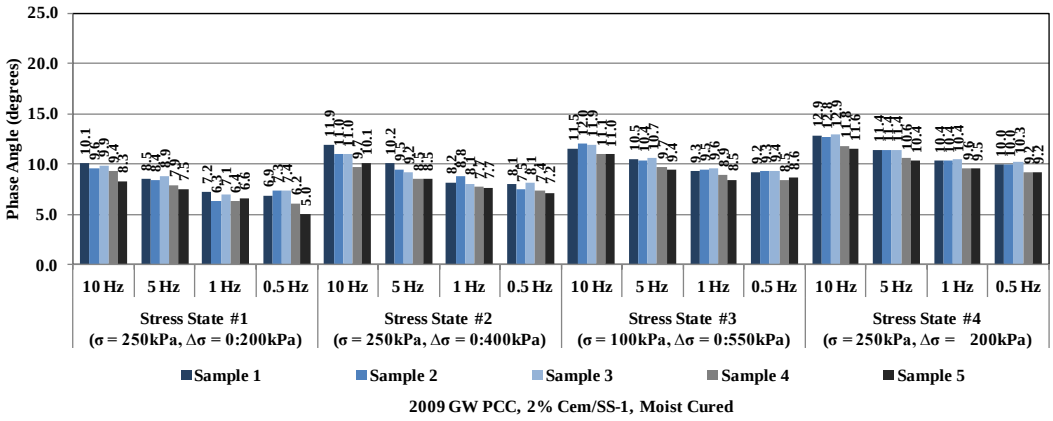

Figure A.33 Phase Angle Results of Recycled PCC GW Base 2% Cement/SS-1, Moist Cured

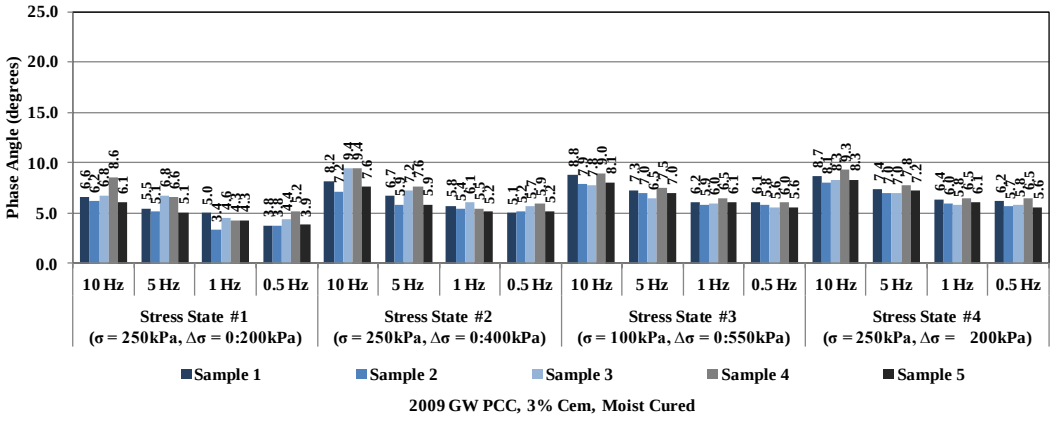

Figure A.34 Phase Angle Results of Recycled PCC GW Base 3% Cement, Moist Cured

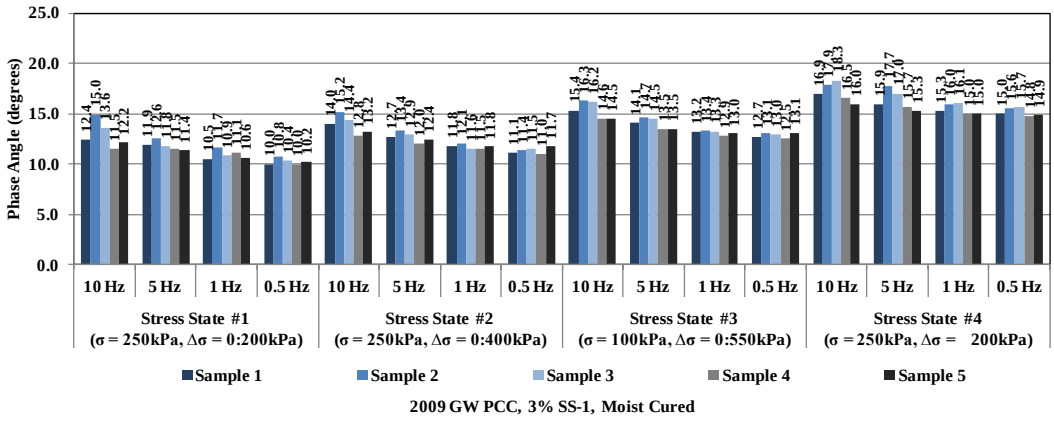

Figure A.35 Phase Angle Results of Recycled PCC GW Base 3% SS-1, Moist Cured

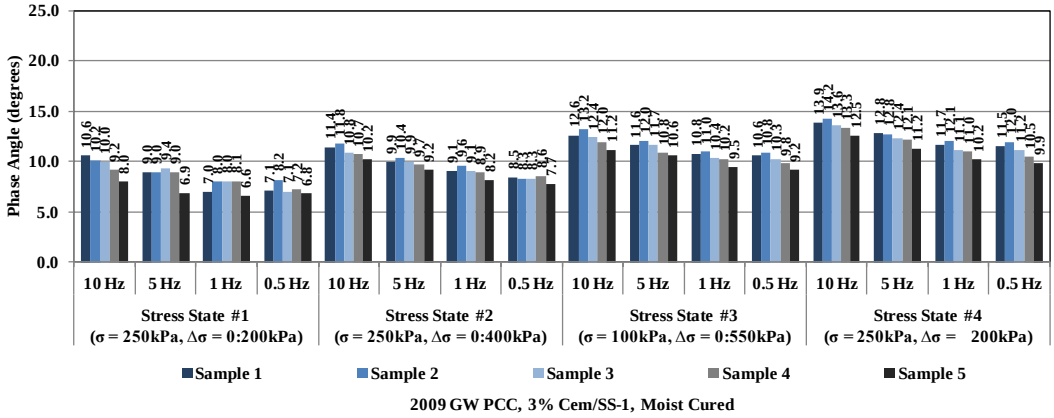

Figure A.36 Phase Angle Results of Recycled PCC GW Base 3% Cement/ SS-1, Moist Cured

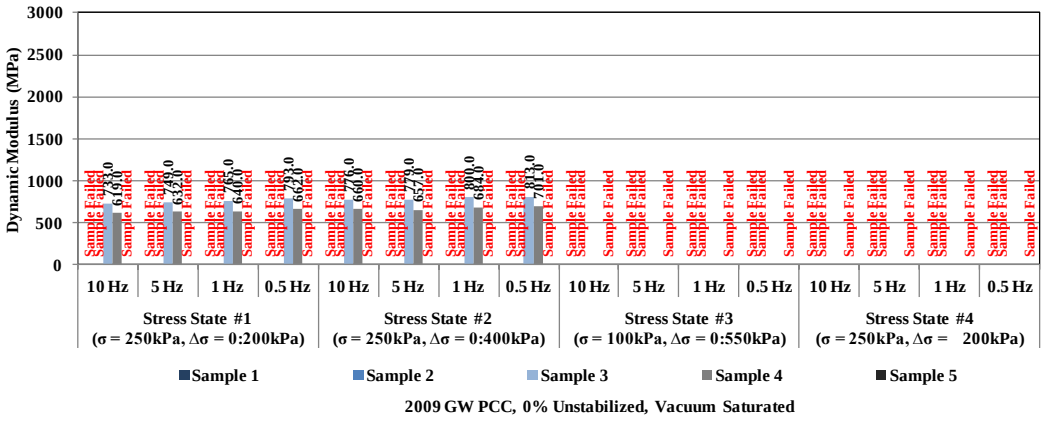

Figure A.37 Dynamic Modulus Results of Recycled PCC GW Base Untreated, Vacuum Saturated

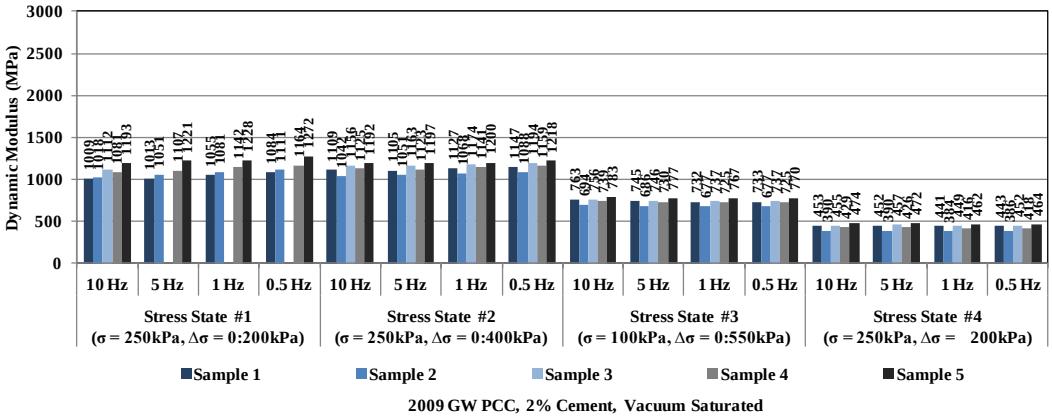

Figure A.38 Dynamic Modulus Results of Recycled PCC GW Base 2% Cement, Vacuum Saturated

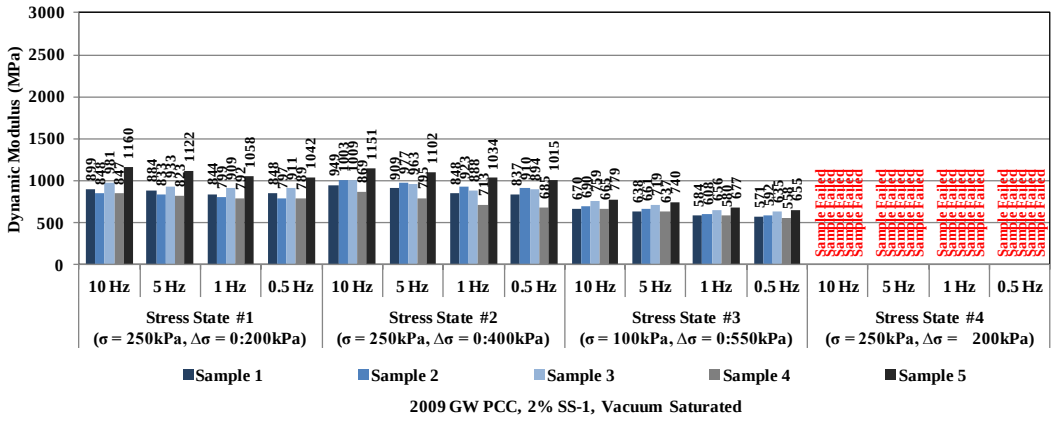

Figure A.39 Dynamic modulus Results of Recycled PCC GW Base 2% SS-1, Vacuum Saturated

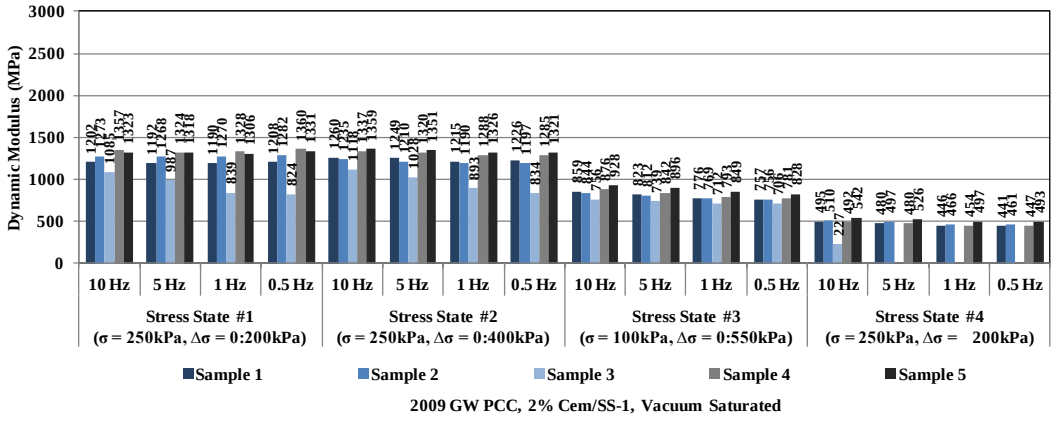

Figure A.40 Dynamic Modulus Results of Recycled PCC GW Base 2%Cement/SS-1, Vacuum Saturated

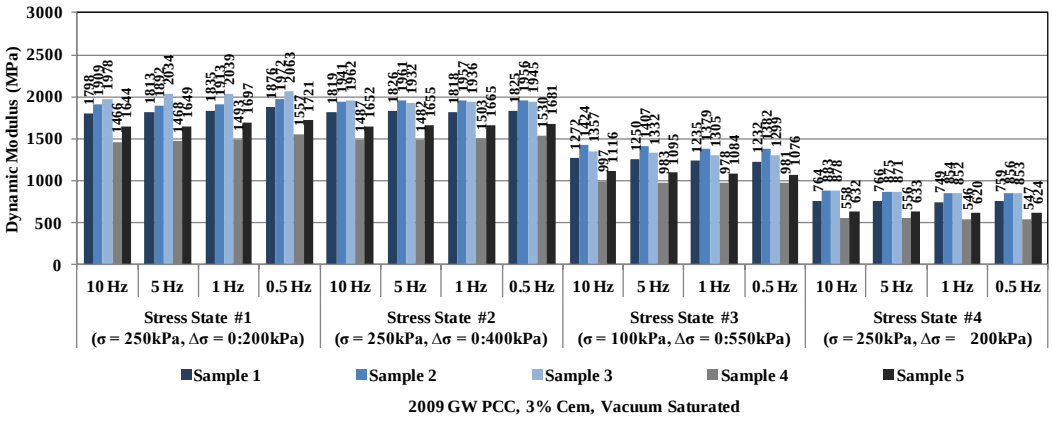

Figure A.41 Dynamic Modulus Results of Recycled PCC GW Base 3% Cement, Vacuum Saturated

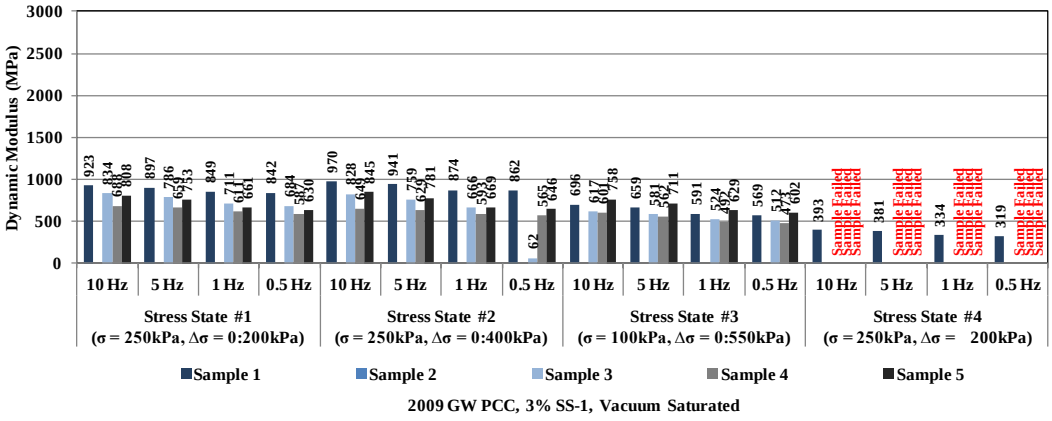

Figure A.42 Dynamic Modulus Results of Recycled PCC GW Base 3% SS-1, Vacuum Saturated

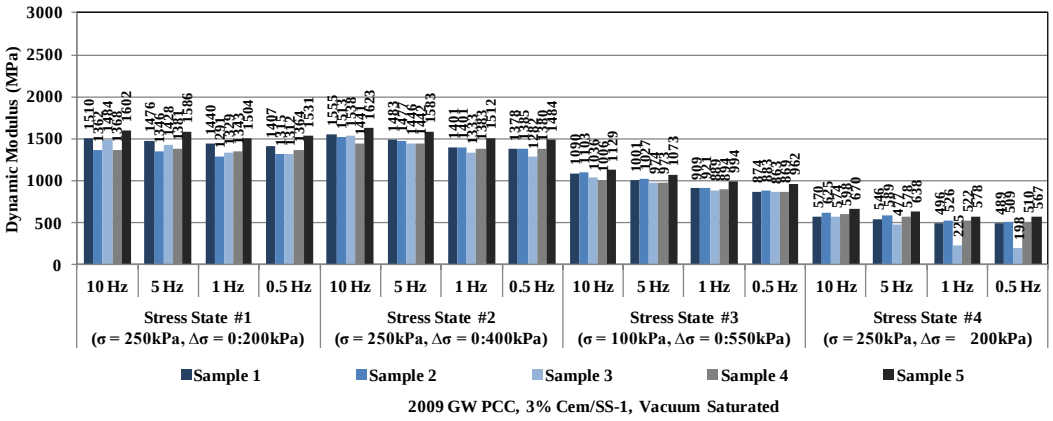

Figure A.43 Dynamic Modulus Results of Recycled PCC GW Base 3% Cement/SS-1 Vacuum Saturated

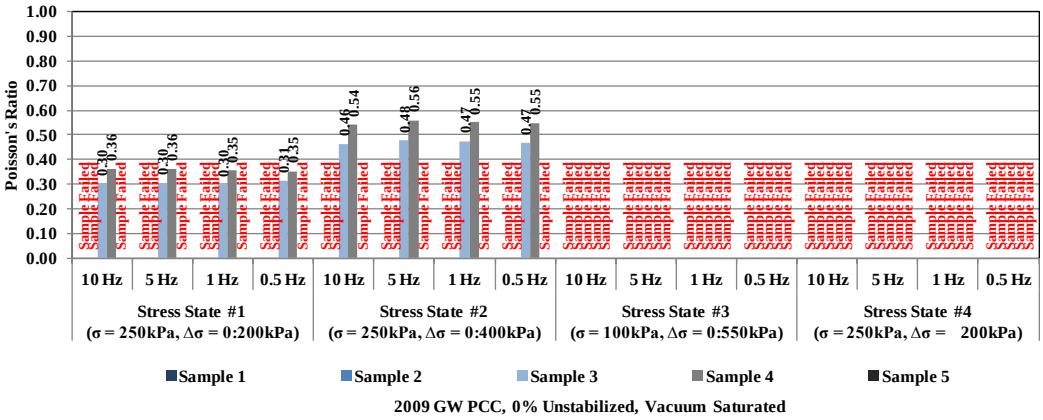

Figure A.44 Poisson's Ratio Results of Recycled PCC GW Base Untreated, Vacuum Saturated

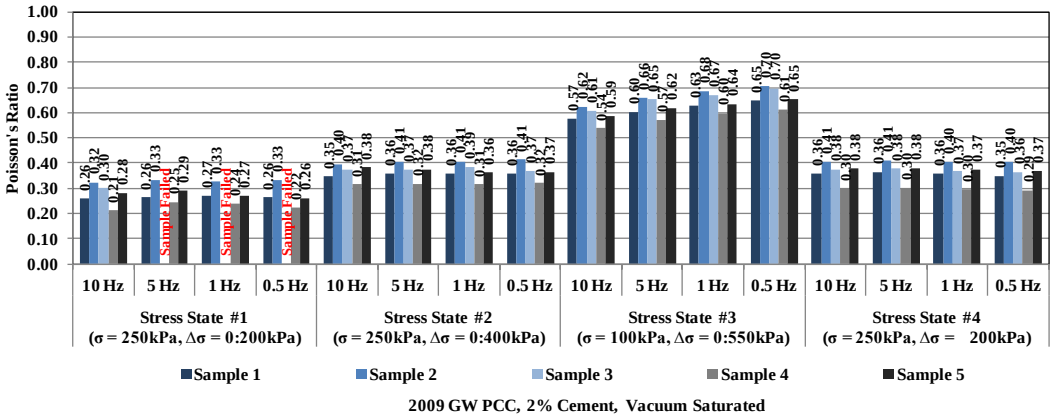

Figure A.45 Poisson's Ratio Results of Recycled PCC GW Base 2% Cement, Vacuum Saturated

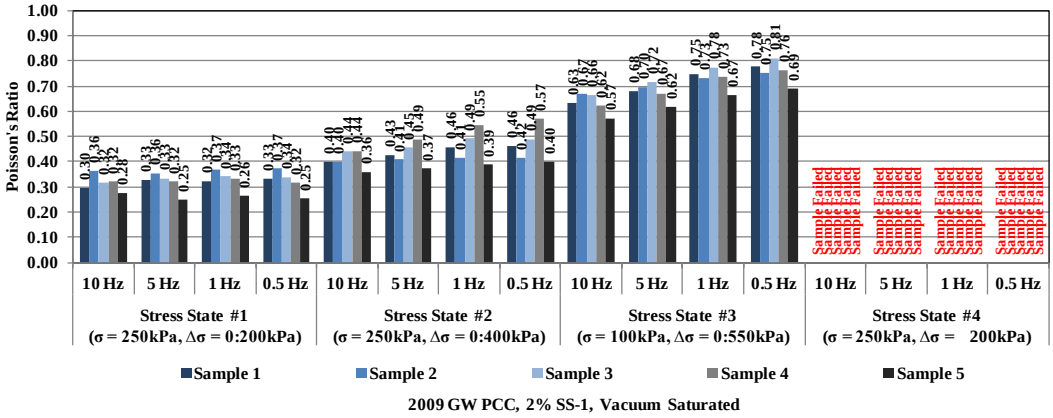

Figure A.46 Poisson's Ratio Results of Recycled PCC GW Base 2% SS-1, Vacuum Saturated

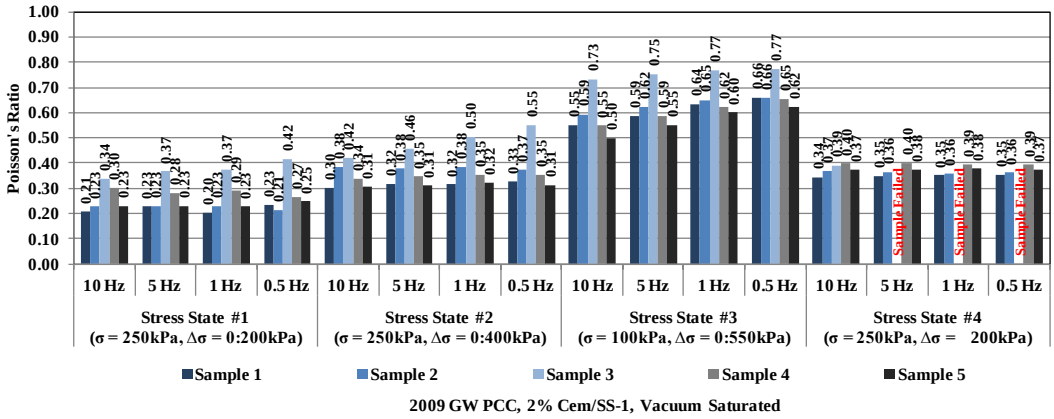

Figure A.47 Poisson's Ratio Results of Recycled PCC GW Base 2% Cement/ SS-1, Vacuum Saturated

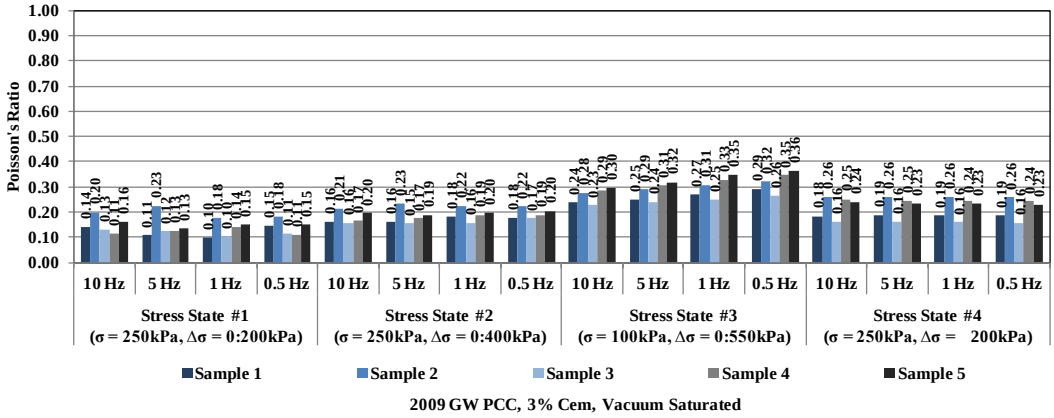

Figure A.48 Poisson's Ratio Results of Recycled PCC GW base 3% Cement, Vacuum Saturated

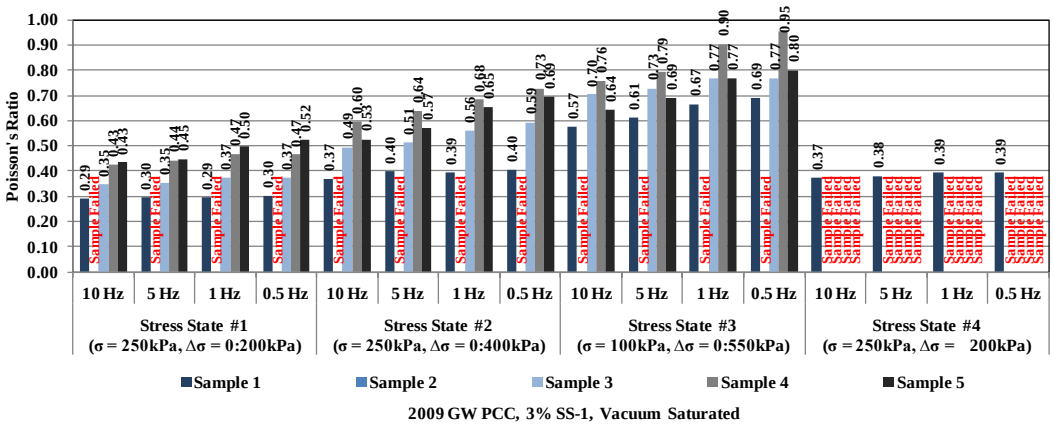

Figure A.49 Poisson's Ratio Results of Recycled PCC GW Base 3% SS-1, Vacuum Saturated

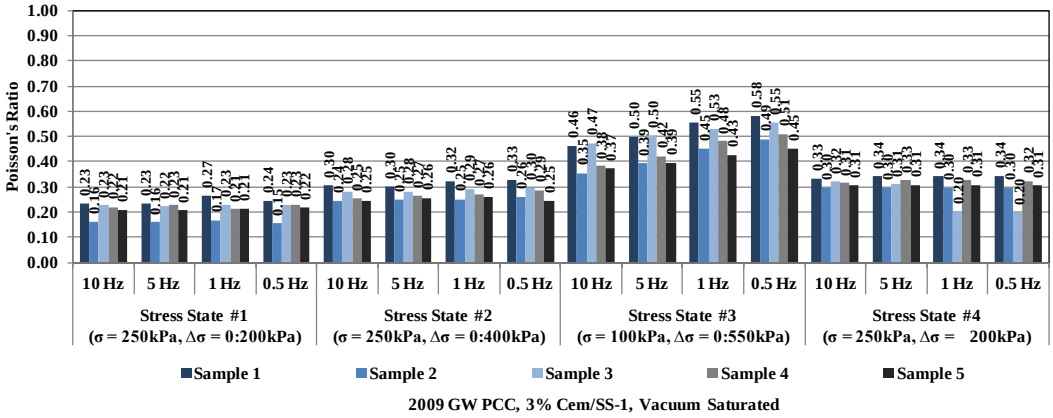

Figure A.50 Poisson's Ratio Results of Recycled PCC GW Base 3% Cement/SS-1, Vacuum Saturated

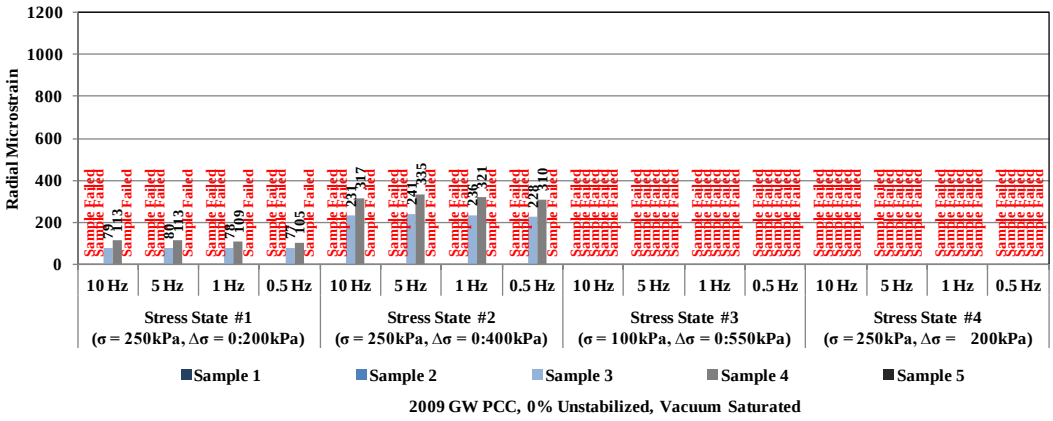

Figure A.51 Radial Micro Strain Results of Recycled PCC GW Base Untreated, Vacuum Saturated

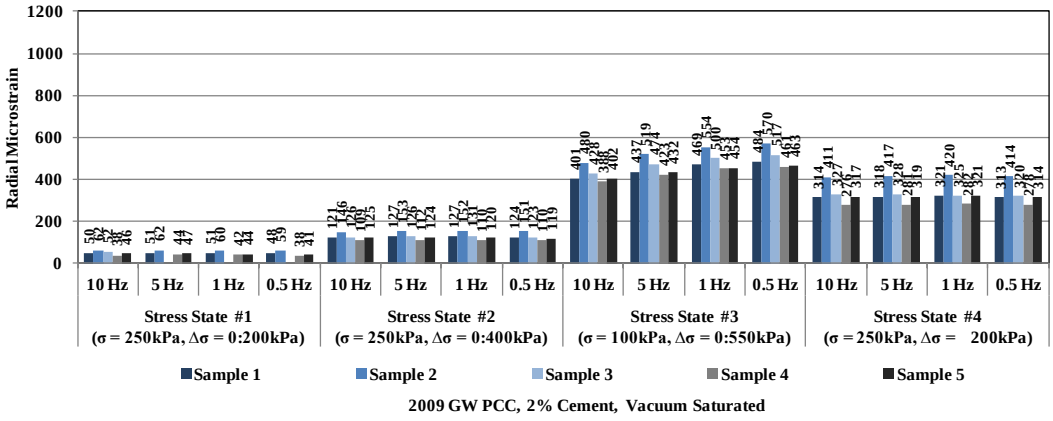

Figure A.52 Radial Micro Strain Results of Recycled PCC GW Base 2% Cement, Vacuum Saturated

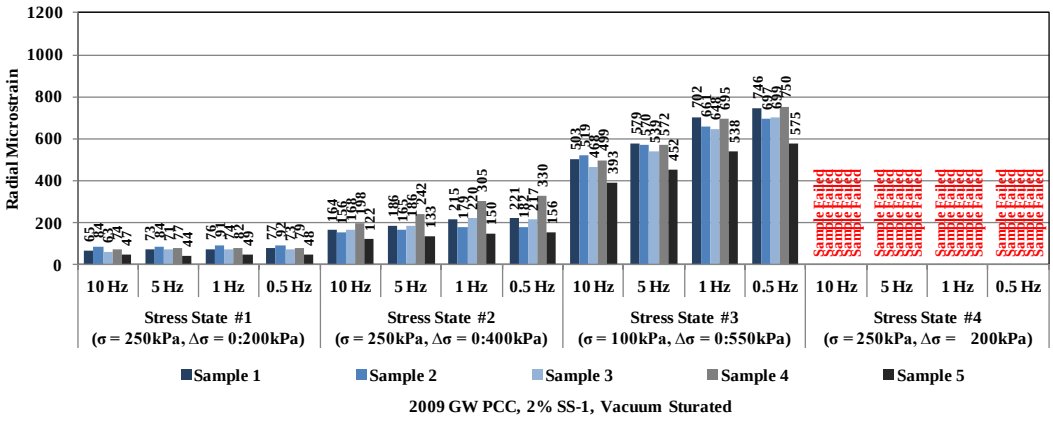

Figure A.53 Radial Micro Strain Results of Recycled PCC GW Base 2% SS-1, Vacuum Saturated

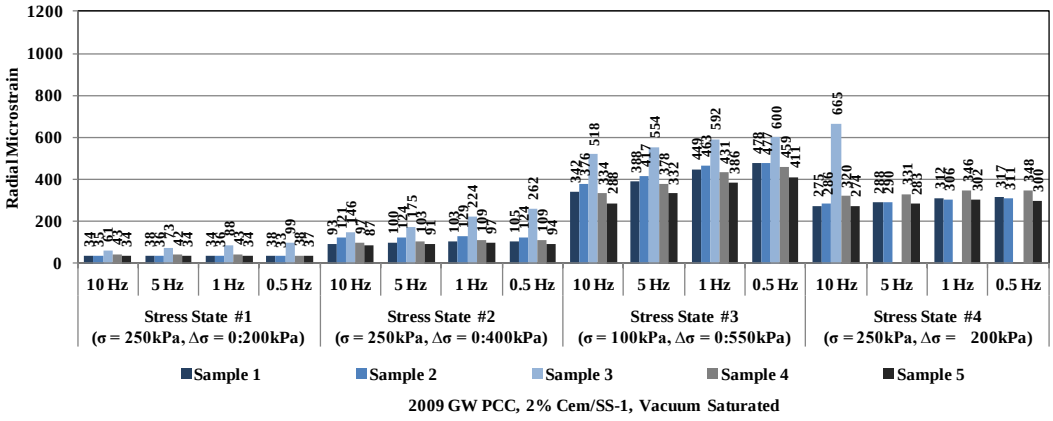

Figure A.54 Radial Micro Strain Results of Recycled PCC GW Base 2% Cement/ SS-1, Vacuum Saturated

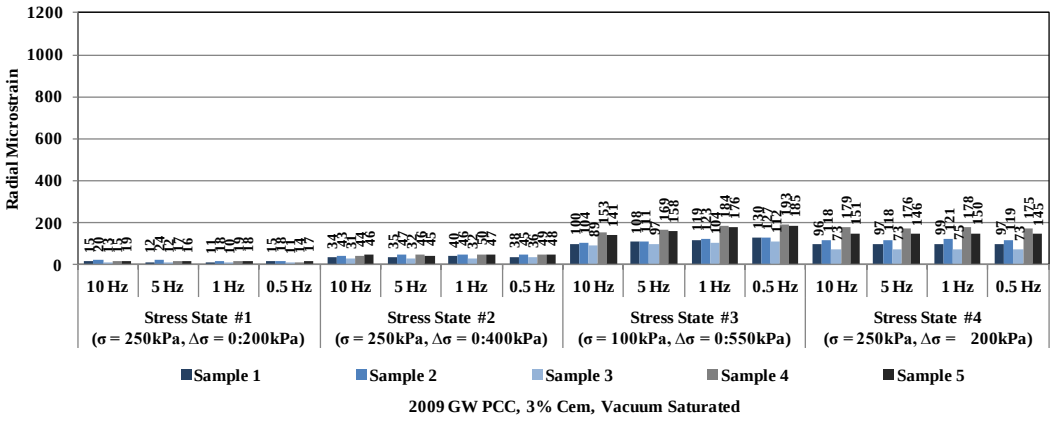

Figure A.55 Radial Micro Strain Results of Recycled PCC GW Base 3% Cement, Vacuum Saturated

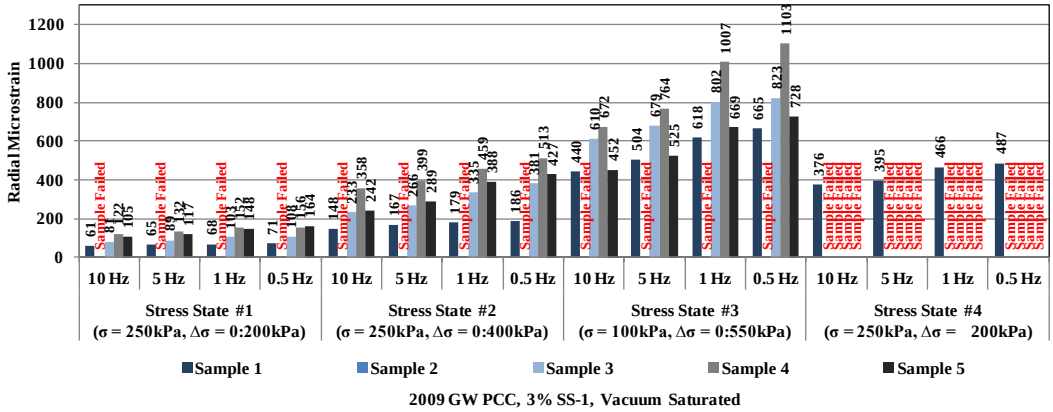

Figure A.56 Radial Micro Strain Results of Recycled PCC GW Base 3% SS-1, Vacuum Saturated

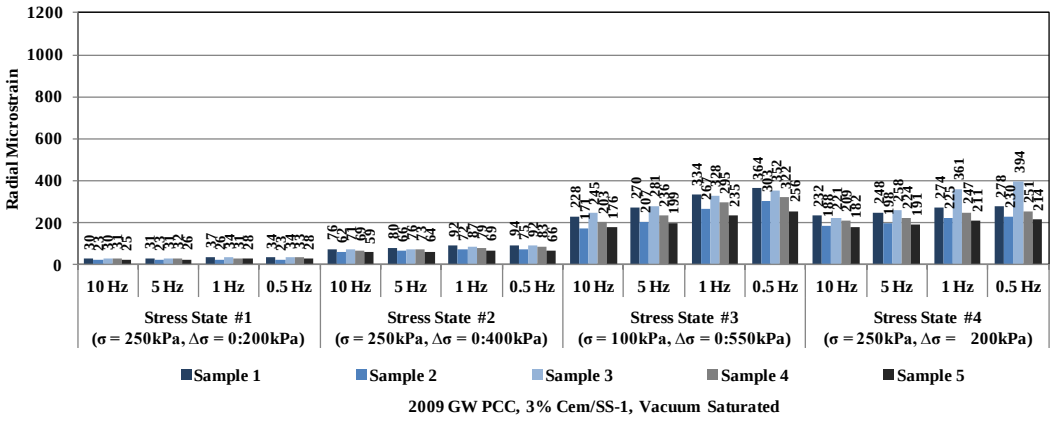

Figure A.57 Radial Micro Strain Results of Recycled PCC GW Base 3% Cement/SS-1, Vacuum Saturated

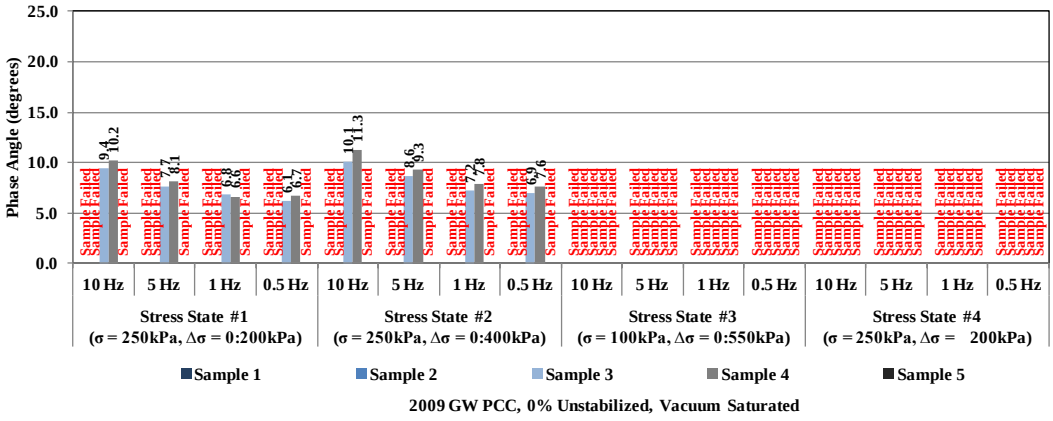

Figure A.58 Phase Angle Results of Recycled PCC GW Base Untreated, Vacuum Saturated

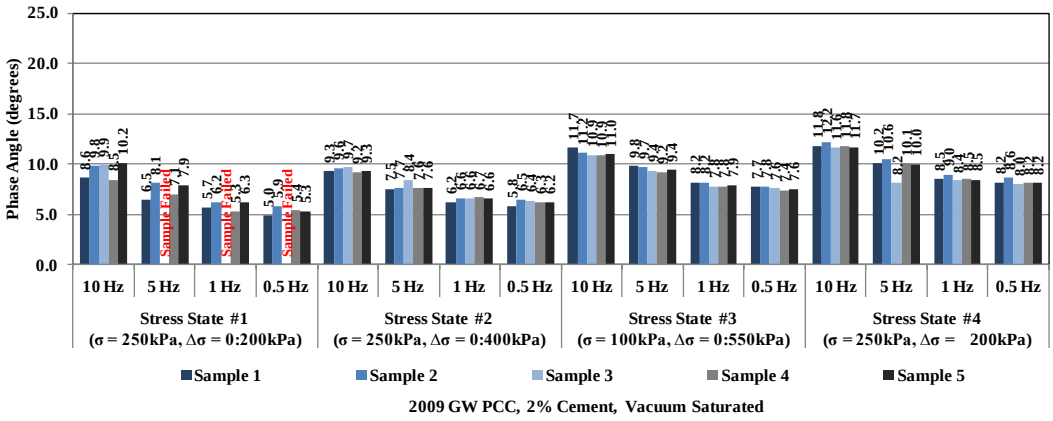

Figure A.59 Phase Angle Results of Recycled PCC GW Base 2% Cement, Vacuum Saturated

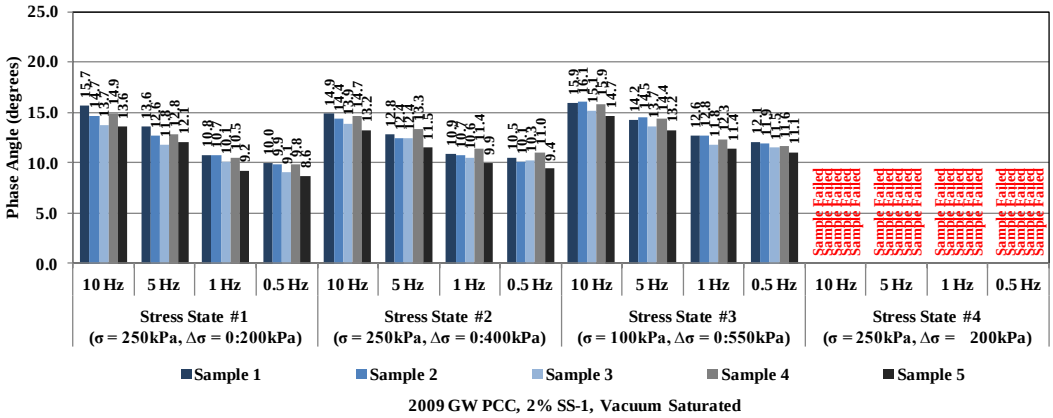

Figure A.60 Phase Angle Results of Recycled PCC GW Base 2% SS-1, Vacuum Saturated

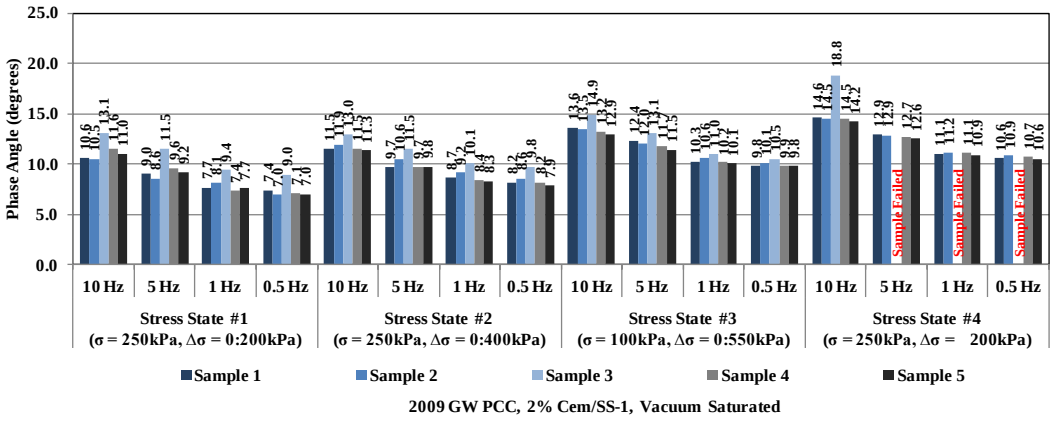

Figure A.61 Phase Angle Results of Recycled PCC GW Base 2% Cement/SS-1, Vacuum Saturated

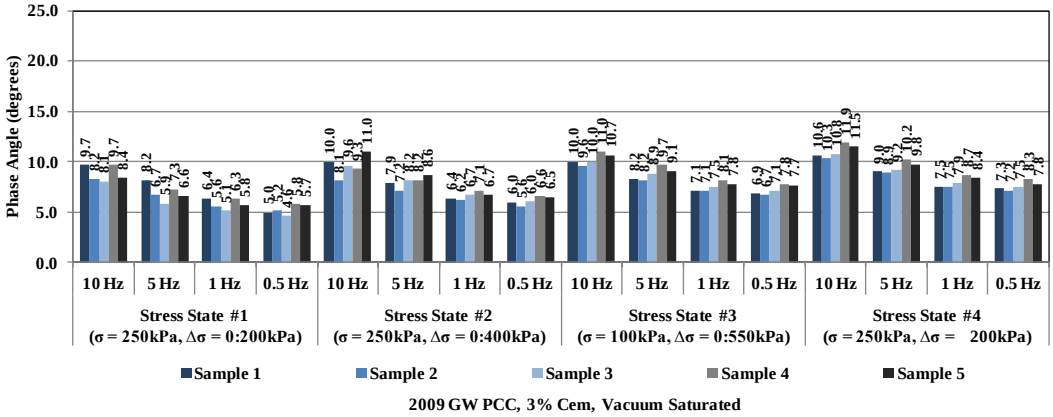

Figure A.62 Phase Angle Results of Recycled PCC GW Base 3% Cement, Vacuum Saturated

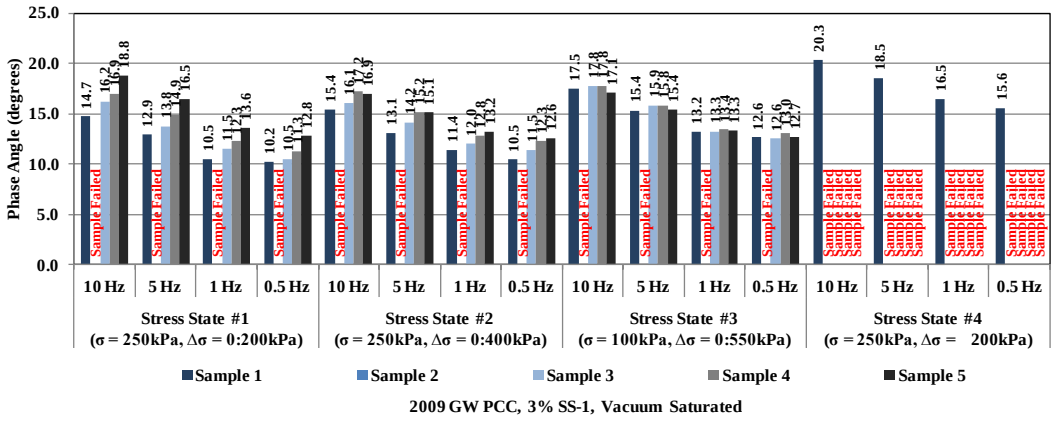

Figure A.63 Phase Angle Results of Recycled PCC GW Base 3%SS-1, Vacuum Saturated

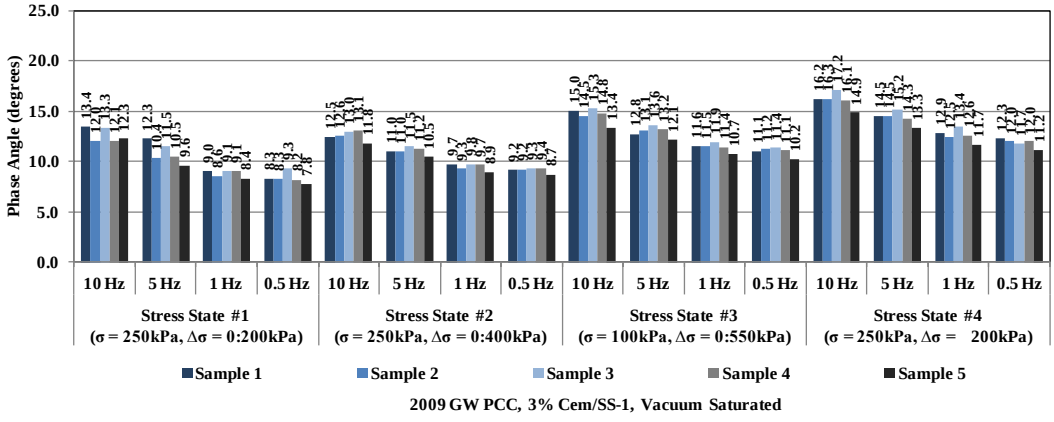

Figure A.64 Phase Angle Results of Recycled PCC GW Base 3% Cement/SS-1, Vacuum Saturated